

European Journal of Breast Health

REVIEWS

Breast Reduction

Sally H. Goudreau et al.; *Texas, USA*

Breast Cancer Treatment

Burcu Altıparmak Güleç and Fatma Yurt; *İzmir, Turkey*

Oncoplastic Breast Surgery

Nuh Zafer Cantürk et al.; *Kocaeli, Tekirdağ, Turkey*

AJCC 8th Edition: Summary

Haoling Zhu and Başak E. Doğan; *Dallas, Texas*

ORIGINAL ARTICLES

Granulomatous Mastitis and Antibiotics

Meagan S. Williams et al.; *Washington, USA*

3D-CRT and IMRT Breast Plan Evaluation

Samuel Adeneye et al.; *Lagos, Asaba, Nigeria*

COVID-19 and Breast Cancer

Aysun Dauti Işıklar et al.; *İstanbul, Turkey*

Breast Papillary Neoplasms

Ayşe Nur Uğur Kılınç et al.; *Konya, Turkey*

MRI Findings of Nipple Malignancies

Almila Coşkun Bilge et al.; *Ankara, Turkey*

Liposomal Doxorubicine in Breast Cancer Cells

Melek Aydın et al.; *İzmir, Turkey*

A Novel First-Line Treatment for Idiopathic Granulomatous Mastitis in Pregnant Women

Osman Toktas and Nurşen Toprak; *Van, Turkey*

CASE REPORTS

Fibroepithelial Breast Tumors in BWS

Ayşenur Oktay et al.; *İzmir, Turkey, Kabul, Afghanistan*

Myeloid Sarcoma of the Breast

Ecenur Varol et al.; *Kocaeli, Turkey*

Editor-in-Chief

Vahit ÖZMEN, Turkey

Editor

Atilla SORAN, USA



Turkish Federation of Breast Diseases Societies

European Journal of Breast Health
is the official journal of the
**Turkish Federation of Breast
Diseases Societies**

Société
Internationale
de Sénologie  Senologic
International
Society

Global Federation of Breast Healthcare Societies

SIS is the official supporter of the
European Journal of Breast Health



EUROPEAN JOURNAL OF BREAST HEALTH

European Journal of Breast Health

Société
Internationale
de Sénologie  Senologic
International
Society

Global Federation of Breast Healthcare Societies

SIS is the official supporter of the
European Journal of Breast Health



TMHDF

European Journal of Breast Health
is the official journal of the
**Turkish Federation of Breast Diseases
Societies**

Contact

Department of General Surgery,
İstanbul University İstanbul Faculty of
Medicine, C Service Çapa / İstanbul
Phone&Fax : + 90 212 534 02 10

Editor-in-Chief

Vahit Özmen, MD, FACS 


Istanbul University İstanbul Faculty of Medicine, İstanbul, Turkey

Editor

Atilla Soran 

University of Pittsburgh, Magee-Womens Hospital, Pittsburgh, PA, USA

Associate Editors

Alexander Mundinger 

*Marienhospital Osnabrück,
Osnabrück, Germany*

Banu Arun 

*The University of Texas MD Anderson
Cancer Center, Houston, TX, USA*

Başak E. Doğan 

*University of Texas Southwestern
Medical Center, Texas, USA*

Erkin Arıbal 

*Acıbadem Mehmet Ali Aydınlar
University, Acıbadem Altunizade
Hospital, İstanbul, Turkey*

Fatma Aktepe 

Professor of Pathology, İstanbul Turkey

Güldeniz Karadeniz Çakmak 

*Zonguldak Bülent Ecevit University
School of Medicine, Zonguldak,
Turkey*

Gürsel Soybir 

*Memorial Etiler Medical Center,
İstanbul, Turkey*

Ismail Jatoi 

*University of Texas Health Science
Center, Texas, USA*

Nuran Beşe 

*Acıbadem Research Institute of
Senology, Acıbadem University, İstanbul,
Turkey*

Osman Zekioğlu 

*Ege University School of Medicine, İzmir,
Turkey*

Tibor Tot 

*Head of Laboratory Medicine, The
University of Uppsala and Dalarna,
Uppsala, Sweden*

Didier Verhoeven 

*Department of Medical Oncology
University of Antwerp*

Biostatistics Editors

Biröl Topçu

*Namık Kemal University School of
Medicine, Tekirdağ, Turkey*

Efe Sezgin

*İzmir Advanced Technology Institute,
Department of Food Engineering*

Editing Manager

Enago

European Journal of Breast Health indexed
in PubMed Central, Web of Science-Emerging
Sources Citation Index, TUBITAK ULAKBIM TR
Index, Embase, EBSCO, CINAHL.



Galenos Publishing House
Owner and Publisher
Derya Mor
Erkan Mor

Publication Coordinator
Burak Sever

Web Coordinators
Fuat Hocalar
Turgay Akpınar

Graphics Department
Ayda Alaca
Çiğdem Birinci
Gülşah Özgül

Finance Coordinator
Sevinç Çakmak

Project Coordinators

Aysel Balta
Duygu Yıldırım
Gamze Aksoy
Gülşah Akın
Hatice Sever
Melike Eren
Meltem Acar
Özlem Çelik Çekil
Pınar Akpınar
Rabia Palazoğlu

Research&Development

Melisa Yiğitoğlu
Nihan Karamanlı

Digital Marketing Specialist
Seher Altundemir

Publisher Contact

Address: Molla Gürani Mah. Kaçamak Sk. No: 21/1
34093 İstanbul, Turkey
Phone: +90 (212) 621 99 25 Fax: +90 (212) 621 99 27
E-mail: info@galenos.com.tr/yayin@galenos.com.tr
Web: www.galenos.com.tr
Publisher Certificate Number: 14521

Online Publication Date: June 2021
E-ISSN: 2587-0831

International scientific journal published quarterly.

Editorial Advisory Board

Alexandru Eniu

Cancer Institute, Cluj-Napoca, Romania

Ayşegül Şahin

The University of Texas MD Anderson Cancer Center, Houston, TX, USA

Barbara Lynn Smith

Massachusetts General Hospital, Boston, MA, USA

Bekir Kuru

Ondokuz Mayıs University School of Medicine, Samsun, Turkey

David Atallah

Department of Obstetrics and Gynecology, Hotel Dieu de France University Hospital, Saint Joseph University, Beirut, Lebanon

Edward Sauter

Breast and Gynecologic Cancer Research Group, Division of Cancer Prevention, National Cancer Institute, Maryland, USA

Eisuke Fukuma

Breast Center, Kameda Medical Center, Kamogawa, Chiba, Japan

Eli Avisar

Division of Surgical Oncology, Miller School of Medicine University of Miami, Florida, USA

Gianluca Franceschini

Fondazione Policlinico Universitario Agostino Gemelli, IRCCS Catholic University, Rome, Italy

Hasan Karanlık

Istanbul University Oncology Institute, Istanbul, Turkey

Hideko Yamauchi

St. Luke's International Hospital, Tokyo, Japan

Jules Sumkin

Department of Radiology, University of Pittsburgh, USA

Kandace McGuire

VCU School of Medicine, VCU Massey Cancer Center, Richmond, VA, USA

Kevin S. Hughes

Harvard Medical School, Boston, MA, USA

Lisa A. Newman

University of Michigan, Comprehensive Cancer Center, Michigan, USA

Luiz Henrique Gebrim

Department of Mastology, Federal University of Sao Paulo, Sao Paulo, Brazil

Maurício Magalhães Costa

Americas Medical City Breast Center, Rio de Janeiro, Brasil

Neslihan Cabioğlu

Istanbul University Istanbul Faculty of Medicine, Istanbul, Turkey

Ronald Johnson

University of Pittsburgh, Magee-Womens Hospital, Pittsburgh, PA, USA

Schlomo Schneebaum

Department of Surgery, Breast Health Center, Tel-Aviv Sourasky Medical Center, Tel-Aviv, Israel

Seigo Nakamura

Showa University School of Medicine, Tokyo, Japan

Tadeusz Pienkowski

Medical University of Gdansk, Gdansk, Poland

Aims and Scope

The European Journal of Breast Health (Eur J Breast Health) is an international, scientific, open access periodical published by independent, unbiased, and double-blinded peer-review principles journal. It is the official publication of the Turkish Federation of Breast Diseases Societies, and the Senologic International Society (SIS) is the official supporter of the journal.

The European Journal of Breast Health is published quarterly in January, April, July, and October. The publication language of the journal is English.

EJBH aims to be a comprehensive, multidisciplinary source and contribute to the literature by publishing manuscripts with the highest scientific level in the fields of research, diagnosis, and treatment of all breast diseases; scientific, biologic, social and psychological considerations, news and technologies concerning the breast, breast care and breast diseases.

The journal publishes original research articles, reviews, letters to the editor, brief correspondences, meeting reports, editorial summaries, observations, novel ideas, basic and translational research studies, clinical and epidemiological studies, treatment guidelines, expert opinions, commentaries, clinical trials and outcome studies on breast health, biology and all kinds of breast diseases, and very original case reports that are prepared and presented according to the ethical guidelines.

TOPICS within the SCOPE of EJBH concerning breast health, breast biology and all kinds of breast diseases:

Epidemiology, Risk Factors, Prevention, Early Detection, Diagnosis and Therapy, Psychological Evaluation, Quality of Life, Screening, Imaging Management, Image-guided Procedures, Immunotherapy, molecular Classification, Mechanism-based Therapies, Carcinogenesis, Hereditary Susceptibility, Survivorship, Treatment Toxicities, and Secondary Neoplasms, Biophysics, Mechanisms of Metastasis, Microenvironment, Basic and Translational Research, Integrated Treatment Strategies, Cellular Research and Biomarkers, Stem Cells, Drug Delivery Systems, Clinical Use of Anti-therapeutic Agents, Radiotherapy, Chemotherapy, Surgery, Surgical Procedures and Techniques, Palliative Care, Patient Adherence, Cosmesis, Satisfaction and Health Economic Evaluations.

The target audience of the journal includes specialists and medical professionals in surgery, oncology, breast health and breast diseases.

The editorial and publication processes of the journal are shaped in accordance with the guidelines of the International Committee of Medical Journal Editors (ICMJE), World Association of Medical Editors (WAME), Council of Science Editors (CSE), Committee on Publication Ethics (COPE), European Association of Science Editors (EASE), and National Information Standards Organization (NISO). The journal conforms with the Principles of Transparency and Best Practice in Scholarly Publishing (doaj.org/bestpractice).

The European Journal of Breast Health indexed in PubMed Central, Web of Science-Emerging Sources Citation Index, TUBITAK ULAKBIM TR Index, Embase, EBSCO, CINAHL.

Submission Fee

The European Journal of Breast Health (Eur J Breast Health) has an open access to all articles published by itself and provides online free access as soon as it is published in the journal. We have published our journal for more than 15 years without any requests from you. But today, European Journal of Breast Health has had to charge you a low fee (50\$) at the time of application to cover its increasing costs for services.

Open Access Policy

This journal provides immediate open and free access to its content on the principle that making research freely available to the public supports a greater global exchange of knowledge.

Open Access Policy is based on the rules of the Budapest Open Access Initiative (BOAI) <http://www.budapestopenaccessinitiative.org/>. By "open access" to peer-reviewed research literature, we mean its free availability on the public internet, permitting any users to read, download, copy, distribute, print, search, or link to the full texts of these articles, crawl them for indexing, pass them as data to software, or use them for any other lawful purpose, without financial, legal, or technical barriers other than those inseparable from gaining access to the internet itself. The only constraint on reproduction and distribution, and the only role for copyright in this domain, should be to give authors control over the integrity of their work and the right to be properly acknowledged and cited.

This work is licensed under a Creative Commons Attribution-NonCommercial-NoDerivatives 4.0 (CC BY-NC-ND) International License.

CC BY-NC-ND: This license allows reusers to copy and distribute the material in any medium or format in unadapted form only, for noncommercial purposes only, and only so long as attribution is given to the creator.

CC BY-NC-ND includes the following elements:

BY – Credit must be given to the creator

NC – Only noncommercial uses of the work are permitted

ND – No derivatives or adaptations of the work are permitted

Please contact the publisher for your permission to use requests.

Contact: info@eurjbreasthealth.com

All expenses of the journal are covered by the Turkish Federation of Breast Diseases Societies and the Senologic International Society (SIS). Potential advertisers should contact the Editorial Office. Advertisement images are published only upon the Editor-in-Chief's approval.

Statements or opinions expressed in the manuscripts published in the journal reflect the views of the author(s) and not the opinions of the Turkish Federation of Breast Diseases Societies, editors, editorial board, and/or publisher; the editors, editorial board, and publisher disclaim any responsibility or liability for such materials.

All published content is available online, free of charge at www.eurjbreasthealth.com.

Turkish Federation of Breast Diseases Societies holds the international copyright of all the content published in the journal.



Editor in Chief: Prof. Vahit ÖZMEN

Address: Department of General Surgery, İstanbul University İstanbul Faculty of Medicine, Çapa, İstanbul

Phone : +90 (212) 534 02 10

Fax : +90 (212) 534 02 10

E-mail : editor@eurjbreasthealth.com

Web : www.eurjbreasthealth.com

Publisher: Galenos Yayınevi

Address: Molla Gürani Mah. Kaçamak Sok. 21/1 Fındıkzade, Fatih, İstanbul, Turkey

Phone : +90 (212) 621 99 25

E-mail : info@galenos.com.tr

Web : www.galenos.com.tr/en

The European Journal of Breast Health (Eur J Breast Health) is an international, open access, online-only periodical published in accordance with the principles of independent, unbiased, and double-blinded peer-review.

The journal is owned by Turkish Federation of Breast Diseases Societies and affiliated with Senologic International Society (SIS), and it is published quarterly on January, April, July, and October. The publication language of the journal is English. The target audience of the journal includes specialists and medical professionals in general surgery and breast diseases.

The editorial and publication processes of the journal are shaped in accordance with the guidelines of the International Council of Medical Journal Editors (ICMJE), the World Association of Medical Editors (WAME), the Council of Science Editors (CSE), the Committee on Publication Ethics (COPE), the European Association of Science Editors (EASE), and National Information Standards Organization (NISO). The journal conforms to the Principles of Transparency and Best Practice in Scholarly Publishing (doaj.org/bestpractice).

Originality, high scientific quality, and citation potential are the most important criteria for a manuscript to be accepted for publication. Manuscripts submitted for evaluation should not have been previously presented or already published in an electronic or printed medium. The journal should be informed of manuscripts that have been submitted to another journal for evaluation and rejected for publication. The submission of previous reviewer reports will expedite the evaluation process. Manuscripts that have been presented in a meeting should be submitted with detailed information on the organization, including the name, date, and location of the organization.

Manuscripts submitted to the European Journal of Breast Health will go through a double-blind peer-review process. Each submission will be reviewed by at least two external, independent peer reviewers who are experts in their fields in order to ensure an unbiased evaluation process. The editorial board will invite an external and independent editor to manage the evaluation processes of manuscripts submitted by editors or by the editorial board members of the journal. The Editor in Chief is the final authority in the decision-making process for all submissions.

An approval of research protocols by the Ethics Committee in accordance with international agreements (World Medical Association Declaration of Helsinki "Ethical Principles for Medical Research Involving Human Subjects," amended in October 2013, www.wma.net) is required for experimental, clinical, and drug studies and for some case reports. If required, ethics committee reports or an equivalent official document will be requested from the authors. For manuscripts concerning experimental research on humans, a statement should be included that shows that written informed consent of patients and volunteers was obtained following a detailed explanation of the procedures that they may undergo. For studies carried out on animals, the measures taken to prevent pain and suffering of the animals should be stated clearly. Information on patient consent, the name of the ethics committee, and the ethics committee approval number should also be stated in the Materials and Methods section of the manuscript. It is the authors' responsibility to protect the patients' anonymity carefully. For photographs that may reveal the identity of the patients, signed releases of the patient or their legal representative should be enclosed.

All submissions are screened by a similarity detection software (iThenticate by CrossCheck).

In the event of alleged or suspected research misconduct, e.g., plagiarism, citation manipulation, and data falsification/fabrication, the Editorial Board will follow and act in accordance with COPE guidelines.

Each individual listed as an author should fulfill the authorship criteria recommended by the International Committee of Medical Journal Editors

(ICMJE - www.icmje.org). The ICMJE recommends that authorship be based on the following 4 criteria:

1. Substantial contributions to the conception or design of the work; or the acquisition, analysis, or interpretation of data for the work; AND
2. Drafting the work or revising it critically for important intellectual content; AND
3. Final approval of the version to be published; AND
4. Agreement to be accountable for all aspects of the work in ensuring that questions related to the accuracy or integrity of any part of the work are appropriately investigated and resolved.

In addition to being accountable for the parts of the work he/she has done, an author should be able to identify which co-authors are responsible for specific other parts of the work. In addition, authors should have confidence in the integrity of the contributions of their co-authors.

All those designated as authors should meet all four criteria for authorship, and all who meet the four criteria should be identified as authors. Those who do not meet all four criteria should be acknowledged in the title page of the manuscript.

The European Journal of Breast Health requires corresponding authors to submit a signed and scanned version of the Copyright Transfer and Acknowledgement of Authorship Form (available for download through www.eurjbreasthealth.com) during the initial submission process in order to act appropriately on authorship rights and to prevent ghost or honorary authorship. If the editorial board suspects a case of "gift authorship," the submission will be rejected without further review. As part of the submission of the manuscript, the corresponding author should also send a short statement declaring that he/she accepts to undertake all the responsibility for authorship during the submission and review stages of the manuscript.

European Journal of Breast Health requires and encourages the authors and the individuals involved in the evaluation process of submitted manuscripts to disclose any existing or potential conflicts of interests, including financial, consultant, and institutional, that might lead to potential bias or a conflict of interest. Any financial grants or other support received for a submitted study from individuals or institutions should be disclosed to the Editorial Board. To disclose a potential conflict of interest, the ICMJE Potential Conflict of Interest Disclosure Form should be filled in and submitted by all contributing authors. Cases of a potential conflict of interest of the editors, authors, or reviewers are resolved by the journal's Editorial Board within the scope of COPE and ICMJE guidelines.

The Editorial Board of the journal handles all appeal and complaint cases within the scope of COPE guidelines. In such cases, authors should get in direct contact with the editorial office regarding their appeals and complaints. When needed, an ombudsperson may be assigned to resolve cases that cannot be resolved internally. The Editor in Chief is the final authority in the decision-making process for all appeals and complaints.

When submitting a manuscript to the European Journal of Breast Health, authors accept to assign the copyright of their manuscript to Turkish Federation of Breast Diseases Societies. If rejected for publication, the copyright of the manuscript will be assigned back to the authors. European Journal of Breast Health requires each submission to be accompanied by a Copyright Transfer and Acknowledgement of Authorship Form (available for download at www.eurjbreasthealth.com). When using previously published content, including figures,

Instructions to Authors

tables, or any other material in both print and electronic formats, authors must obtain permission from the copyright holder. Legal, financial and criminal liabilities in this regard belong to the author(s).

Statements or opinions expressed in the manuscripts published in European Journal of Breast Health reflect the views of the author(s) and not the opinions of the editors, the editorial board, or the publisher; the editors, the editorial board, and the publisher disclaim any responsibility or liability for such materials. The final responsibility in regard to the published content rests with the authors.

Submission Fee

The European Journal of Breast Health (Eur J Breast Health) has an open access to all articles published by itself and provides online free access as soon as it is published in the journal. We have published our journal for more than 15 years without any requests from you. But today, your journal has had to charge you a low fee (50\$) at the time of application to cover its increasing costs for services.

The services provided in this context are the provision of systems for editors and authors, editorial work, provision of article designs, the establishment of indexing links, provision of other publishing services and support services.

You can take a look at the unbiased article evaluation process here. If you find a problem with the open access status of your article or licensing, you can contact editor@eurjbresthealth.com

After your submission to the Eur J Breast Health evaluation system, the submission fees are collected from you or through your fund provider, institution or sponsor.

Eur J Breast Health regularly reviews the fees of submission fees and may change the fees for submission fees. When determining the costs for Eur J Breast Health submission fees, it decides according to the following developments.

- Quality of the journal,
- Editorial and technical processes of the journal,
- Market conditions,
- Other revenue streams associated with the journal

You can find the submission fees fee list here.

Article type	Price
Original articles	\$50
Editorial comment	Free of charge
Review article (No application fee will be charged from invited authors)	\$50
Case report	\$50
Letter to the editor	Free of charge
Images in clinical practices	Free of charge
Current opinion	Free of charge
Systematic review	\$50

When and How do I pay?

After the article is submitted to the Eur J Breast Health online evaluation system, an email regarding payment instructions will be sent to the corresponding author.

The editorial review process will be initiated after the payment has been made for your article.

After the article is submitted, you need to make your payment to the account number below. While making the submission fee, please indicate your article ID in the payment description section.

Account no/IBAN: TR49 0011 1000 0000 0098 1779 82 (TL)

TR17 0011 1000 0000 0098 5125 29 (USD)

TR73 0011 1000 0000 0098 5125 88 (EUR)

Account name: Meme Hastalıkları Dernekleri Federasyonu İktisadi İşletmesi

Branch code (QNB Finans Bank Cerrahpaşa): 1020

Swift code: FNNBTRISOPS

NOTE: All authors must pay the bank wire fee additionally. Otherwise, the deducted amount of the submission fee is requested from the author.

If you believe payment instructions are not in your email contact us: payment@eurjbresthealth.com

MANUSCRIPT PREPARATION

The manuscripts should be prepared in accordance with ICMJE-Recommendations for the Conduct, Reporting, Editing, and Publication of Scholarly Work in Medical Journals (updated in December 2019 - <http://www.icmje.org/icmje-recommendations>). Authors are required to prepare manuscripts in accordance with the CONSORT guidelines for randomized research studies, STROBE guidelines for observational original research studies, STARD guidelines for studies on diagnostic accuracy, PRISMA guidelines for systematic reviews and meta-analysis, ARRIVE guidelines for experimental animal studies, and TREND guidelines for non-randomized public behaviour.

Manuscripts can only be submitted through the journal's online manuscript submission and evaluation system, available at www.eurjbresthealth.com. Manuscripts submitted via any other medium will not be evaluated.

Manuscripts submitted to the journal will first go through a technical evaluation process where the editorial office staff will ensure that the manuscript has been prepared and submitted in accordance with the journal's guidelines. Submissions that do not conform to the journal's guidelines will be returned to the submitting author with technical correction requests.

Authors are required to submit the following:

- Copyright Transfer and Acknowledgement of Authorship Form, and
- ICMJE Potential Conflict of Interest Disclosure Form (should be filled in by all contributing authors)

during the initial submission. These forms are available for download at www.eurjbresthealth.com.

Preparation of the Manuscript

Title page: A separate title page should be submitted with all submissions, and this page should include:

- The full title of the manuscript as well as a short title (running head) of no more than 50 characters,
- Name(s), affiliations, and highest academic degree(s) of the author(s),

- Grant information and detailed information on the other sources of support,
- Name, address, telephone (including the mobile phone number) and fax numbers, and email address of the corresponding author,
- Acknowledgment of the individuals who contributed to the preparation of the manuscript but who do not fulfill the authorship criteria.

Abstract: An English abstract should be submitted with all submissions except for Letters to the Editor. The abstract of Original Articles should be structured with subheadings (Objective, Materials and Methods, Results, and Conclusion). Please check Table 1 below for word count specifications.

Keywords: Each submission must be accompanied by a minimum of three to a maximum of six keywords for subject indexing at the end of the abstract. The keywords should be listed in full without abbreviations. The keywords should be selected from the National Library of Medicine, Medical Subject Headings database (<https://www.nlm.nih.gov/mesh/MBrowser.html>).

Key Points: All submissions except letters to the editor should be accompanied by 3 to 5 "key points" which should emphasize the most noteworthy results of the study and underline the principle message that is addressed to the reader. This section should be structured as itemized to give a general overview of the article. Since "Key Points" targeting the experts and specialists of the field, each item should be written as plain and straightforward as possible.

Manuscript Types

Original Articles: This is the most important type of article since it provides new information based on original research. The main text of original articles should be structured with "Introduction", "Materials and Methods", "Results", "Discussion and Conclusion" subheadings. Please check Table 1 for the limitations for Original Articles.

Statistical analysis to support conclusions is usually necessary. Statistical analyses must be conducted in accordance with international statistical reporting standards (Altman DG, Gore SM, Gardner MJ, Pocock SJ. Statistical guidelines for contributors to medical journals. *Br Med J* 1983; 7; 1489-93). Information on statistical analyses should be provided with a separate subheading under the Materials and Methods section, and the statistical software that was used during the process must be specified.

Units should be prepared in accordance with the International System of Units (SI).

Editorial Comments: Editorial comments aim to provide a brief critical commentary by reviewers with expertise or with high reputation in the topic of the research article published in the journal. Authors are selected and invited by the journal to provide such comments. Abstract, Keywords, and Tables, Figures, Images, and other media are not included.

Review Articles: Reviews prepared by authors who have extensive knowledge on a particular field and whose scientific background has been translated into a high volume of publications with a high citation potential are welcomed. These authors may even be invited by the journal. Reviews should describe, discuss, and evaluate the current level of knowledge of a topic in clinical practice and should guide future studies. The main text should contain Introduction, Clinical and Research Consequences, and Conclusion sections. Please check Table 1 for the limitations for Review Articles.

Case Reports: There is limited space for case reports in the journal and reports on rare cases or conditions that constitute challenges in diagnosis and treatment, those offering new therapies or revealing knowledge not included in the literature, and interesting and educative case reports are accepted for publication. The text should include "Introduction", "Case Presentation", "Discussion and Conclusion" subheadings. Please check Table 1 for the limitations for Case Reports.

Letters to the Editor: This type of manuscript discusses important parts, overlooked aspects, or lacking parts of a previously published article. Articles on subjects within the scope of the journal that might attract the readers' attention, particularly educative cases, may also be submitted in the form of a "Letter to the Editor." Readers can also present their comments on the published manuscripts in the form of a "Letter to the Editor." Abstract, Keywords, and Tables, Figures, Images, and other media should not be included. The text should be unstructured. The manuscript that is being commented on must be properly cited within this manuscript.

Images in Clinical Practices: Our journal accepts original high-quality images related to the cases that we come across during clinical practices, that cite the importance or infrequency of the topic, make the visual quality stand out and present important information that should be shared in academic platforms. Titles of the images should not exceed 10 words. Images can be signed by no more than 3 authors. Figure legends are limited to 200 words, and the number of figures is limited to 3. Video submissions will not be considered.

Current Opinion: Current Opinion provides readers with a commentary of either recently published articles in the European Journal of Breast Health or some other hot topic selected articles. Authors are selected and invited by the journal for such commentaries. This type of article contains three main sections titled as Background, Present Study, and Implications. Authors are expected to describe the background of the subject/study briefly, critically discuss the present research, and provide insights for future studies.

Table 1. Limitations for each manuscript type

Type of manuscript	Word limit	Abstract word limit	Reference limit	Table limit	Figure limit
Original Article	3500	250 (Structured)	30	6	7 or total of 15 images
Review Article	5000	250	50	6	10 or total of 20 images
Case Report	1000	200	15	No tables	10 or total of 20 images
Letter to the Editor	500	No abstract	5	No tables	No media
Current Opinion	300	No abstract	5	No tables	No media

Tables

Tables should be included in the main document, presented after the reference list, and they should be numbered consecutively in the order they are referred to within the main text. A descriptive title must be placed above the tables. Abbreviations used in the tables should

Instructions to Authors

be defined below the tables by footnotes (even if they are defined within the main text). Tables should be created using the "insert table" command of the word processing software, and they should be arranged clearly to provide easy reading. Data presented in the tables should not be a repetition of the data presented within the main text but should be supporting the main text.

Figures and Figure Legends

Figures, graphics, and photographs should be submitted as separate files (in TIFF or JPEG format) through the submission system. The files should not be embedded in a Word document or the main document. When there are figure subunits, the subunits should not be merged to form a single image. Each subunit should be submitted separately through the submission system. Images should not be labeled (a, b, c, etc.) to indicate figure subunits. Thick and thin arrows, arrowheads, stars, asterisks, and similar marks can be used on the images to support figure legends. Like the rest of the submission, the figures too should be blind. Any information within the images that may indicate an individual or institution should be blinded. The minimum resolution of each submitted figure should be 300 DPI. To prevent delays in the evaluation process, all submitted figures should be clear in resolution and large in size (minimum dimensions: 100 × 100 mm). Figure legends should be listed at the end of the main document.

All acronyms and abbreviations used in the manuscript should be defined at first use, both in the abstract and in the main text. The abbreviation should be provided in parentheses following the definition.

When a drug, product, hardware, or software program is mentioned within the main text, product information, including the name of the product, the producer of the product, and city and the country of the company (including the state if in USA), should be provided in parentheses in the following format: "Discovery St PET/CT scanner (General Electric, Milwaukee, WI, USA)"

All references, tables, and figures should be referred to within the main text, and they should be numbered consecutively in the order they are referred to within the main text.

Limitations, drawbacks, and the shortcomings of original articles should be mentioned in the Discussion section before the conclusion paragraph.

References

While citing publications, preference should be given to the latest, most up-to-date publications. If an ahead-of-print publication is cited, the DOI number should be provided. Authors are responsible for the accuracy of references. Journal titles should be abbreviated in accordance with the journal abbreviations in Index Medicus/ MEDLINE/PubMed. All authors should be listed if an article has six or less authors; it should not be represented by "et al." in articles. Arabic numbers in parentheses. References published in PubMed should have a PMID: xxxxxx at the end of it, which should be stated in parenthesis. The reference styles for different types of publications are presented in the following examples.

Journal Article: Little FB, Koufman JA, Kohut RI, Marshall RB. Effect of gastric acid on the pathogenesis of subglottic stenosis. *Ann Otol Rhinol Laryngol* 1985; 94:516-519. (PMID: 4051410)

Book Section: Suh KN, Keystone JS. Malaria and babesiosis. Gorbach SL, Barlett JG, Blacklow NR, editors. *Infectious Diseases*. Philadelphia: Lippincott Williams; 2004.p.2290-308.

Books with a Single Author: Sweetman SC. *Martindale the Complete Drug Reference*. 34th ed. London: Pharmaceutical Press; 2005.

Editor(s) as Author: Huizing EH, de Groot JAM, editors. *Functional reconstructive nasal surgery*. Stuttgart-New York: Thieme; 2003.

Conference Proceedings: Bengissson S, Sothemin BG. Enforcement of data protection, privacy and security in medical informatics. In: Lun KC, Degoulet P, Piemme TE, Rienhoff O, editors. *MEDINFO 92. Proceedings of the 7th World Congress on Medical Informatics*; 1992 Sept 6-10; Geneva, Switzerland. Amsterdam: North-Holland; 1992. pp.1561-5.

Scientific or Technical Report: Cusick M, Chew EY, Hoogwerf B, Agrón E, Wu L, Lindley A, et al. Early Treatment Diabetic Retinopathy Study Research Group. Risk factors for renal replacement therapy in the Early Treatment Diabetic Retinopathy Study (ETDRS), Early Treatment Diabetic Retinopathy Study *Kidney Int*: 2004. Report No: 26.

Thesis: Yılmaz B. Ankara Üniversitesindeki Öğrencilerin Beslenme Durumları, Fiziksel Aktiviteleri ve Beden Kitle İndeksleri Kan Lipidleri Arasındaki İlişkiler. H.Ü. Sağlık Bilimleri Enstitüsü, Doktora Tezi. 2007.

Manuscripts Accepted for Publication, Not Published Yet: Slots J. The microflora of black stain on human primary teeth. *Scand J Dent Res*. 1974.

Epub Ahead of Print Articles: Cai L, Yeh BM, Westphalen AC, Roberts JP, Wang ZJ. Adult living donor liver imaging. *Diagn Interv Radiol*. 2016 Feb 24. doi: 10.5152/dir.2016.15323. [Epub ahead of print].

Manuscripts Published in Electronic Format: Morse SS. Factors in the emergence of infectious diseases. *Emerg Infect Dis* (serial online) 1995 Jan-Mar (cited 1996 June 5): 1(1): (24 screens). Available from: URL: <http://www.cdc.gov/ncidod/EID/cid.htm>.

REVISIONS

When submitting a revised version of a paper, the author must submit a detailed "Response to the reviewers" that states point by point how each issue raised by the reviewers has been covered and where it can be found (each reviewer's comment, followed by the author's reply and line numbers where the changes have been made) as well as an annotated copy of the main document. Revised manuscripts must be submitted within 30 days from the date of the decision letter. If the revised version of the manuscript is not submitted within the allocated time, the revision option may be cancelled. If the submitting author(s) believe that additional time is required, they should request this extension before the initial 30-day period is over.

Accepted manuscripts are copy-edited for grammar, punctuation, and format. Once the publication process of a manuscript is completed, it is published online on the journal's webpage as an ahead-of-print publication before it is included in its scheduled issue. A PDF proof of the accepted manuscript is sent to the corresponding author, and their publication approval is requested within 2 days of their receipt of the proof.

Editor in Chief: Prof. Vahit ÖZMEN

Address: Department of General Surgery, İstanbul University İstanbul Faculty of Medicine, Çapa, İstanbul

Phone : +90 (212) 534 02 10

Fax : +90 (212) 534 02 10

E-mail : editor@eurjbreasthealth.com

Web : www.eurjbreasthealth.com

Publisher: Galenos Yayınevi

Address: Molla Gürani Mah. Kaçamak Sok. 21/1 Fındıkzade, Fatih, İstanbul, Turkey

Phone : +90 (212) 621 99 25

E-mail : info@galenos.com.tr

Web : www.galenos.com.tr

REVIEWS

- 206** **Multimodality Review of Imaging Features Following Breast Reduction Surgery**
Sally H. Goudreau, Meghan A. Woughter, Stephen J. Seiler
- 214** **Treatment with Radiopharmaceuticals and Radionuclides in Breast Cancer: Current Options**
Burcu Altıparmak Güleç, Fatma Yurt
- 220** **Oncoplastic Breast-Conserving Surgery According to Tumor Location**
Nuh Zafer Cantürk, Turgay Şimşek, Sibel Özkan Gürdal
- 234** **American Joint Committee on Cancer's Staging System for Breast Cancer, Eighth Edition: Summary for Clinicians**
Haoling Zhu, Başak E. Doğan

ORIGINAL ARTICLES

- 239** **Treatment of Granulomatous Mastitis: Is There a Role for Antibiotics?**
Meagan S. Williams, Adelaide H. McClintock, Lori Bourassa, Mary B. Laya
- 247** **Evaluation of Three-Dimensional Conformal Radiotherapy and Intensity Modulated Radiotherapy Techniques for Left Breast Post-Mastectomy Patients: Our Experience in Nigerian Sovereign Investment Authority-Lagos University Teaching Hospital Cancer Center, South-West Nigeria**
Samuel Adeneye, Michael Akpochafor, Bolanle Adegboyega, Adewumi Alabi, Nusirat Adedewe, Adedayo Joseph, Omolara Fatiregun, Akintayo Omojola, Abe Adebayo, Esther Oluwadara
- 253** **How Do Breast Cancer Patients Present Following COVID-19 Early Peak in a Breast Cancer Center in Turkey?**
Aysun Dauti Işıklar, Cem Deniz, Aykut Soyder, Nilgün Göldoğan, Ebru Yılmaz, Gül Başaran
- 258** **Results of Excision of Unknown Papillary Neoplasms Detected on Core Biopsy**
Ayşe Nur Uğur Kılınç, Zeynep Bayramoğlu, Yaşar Ünlü, Nahide Baran, Ayşegül Altunkeser, Nergis Aksoy, Mehmet Ali Eryılmaz, Elif Nur Öztürk Yıldırım
- 265** **Breast and Malignant Tumor Invasion of the Nipple-Areola Complex**
Almila Coşkun Bilge, Hale Aydın, Işıl Esen Bostancı, Özge Tanışman, Diba Saygılı Öz
- 274** **Evaluation of Liposomal and Microbubbles Mediated Delivery of Doxorubicin in Two-Dimensional (2D) and Three-Dimensional (3D) Models for Breast Cancer**
Melek Aydın, Ekrem Özdemir, Zekiye Altun, Sevgi Kılıç, Safiye Aktaş
- 283** **Treatment Results of Intralesional Steroid Injection and Topical Steroid Administration in Pregnant Women with Idiopathic Granulomatous Mastitis**
Osman Toktas, Nurşen Toprak

Contents

CASE REPORTS

288 **Fibroepithelial Breast Tumors in a Teenager with Beckwith-Wiedemann Syndrome: A Case Report and Review of Literature**

Ayşenur Oktay, Habib Ahmad Esmat, Özge Aslan

292 **Breast Recurrence of Acute Myeloid Leukemia After Bone Marrow Transplantation: A Case Report About Myeloid Sarcoma of the Breast**

Ecenur Varol, Umay Kiraz, Sertaç Ata Güler, Çiğdem Vural, Zafer Gülbaş, Nihat Zafer Utkan

ERRATUM

296 Erratum



Multimodality Review of Imaging Features Following Breast Reduction Surgery

Sally H. Goudreau¹, Meghan A. Woughter², Stephen J. Seiler¹

¹Department of Radiology, UT Southwestern Medical Center, Texas, USA

²Department of Radiology, Radiology Partners, Texas, USA

ABSTRACT

Reduction mammoplasty is a common surgical procedure that removes a significant portion of the breast, and the resulting changes to the breast parenchyma are frequently seen on breast imaging studies. Any radiologist who interprets breast imaging studies must be able to recognize these changes in order to avoid unnecessary recall from screening and/or breast biopsy. The surgical techniques used in reduction mammoplasty are discussed in order to provide relevant background information for understanding the resulting imaging features. These imaging characteristics are presented for the most common breast imaging modalities, including mammography, ultrasound, and magnetic resonance imaging. Additionally, tips for distinguishing malignancy from postsurgical change are provided, as are potential pitfalls in imaging interpretation. To avoid unnecessary patient morbidity, it is critical to differentiate between the classic, benign imaging appearance of the breast after reduction mammoplasty and findings that indicate a potential malignancy.

Keywords: Breast cancer, breast imaging, breast reconstruction, mastopexy

Cite this article as: Goudreau SH, Woughter MA, Seiler SJ. Multimodality Review of Imaging Features Following Breast Reduction Surgery. Eur J Breast Health 2021; 17(3): 206-213

Key Points

- All reduction procedures involve the removal and displacement of varying amounts of parenchymal tissue and skin, largely from the inferior breast.
- This tissue and skin removal alters the normal distribution of fibroglandular tissue and can result in architectural distortion, focal asymmetries, and regions of fat necrosis with or without dystrophic calcifications.
- Fat necrosis may be difficult to interpret by ultrasound interrogation alone. A spot tangential mammographic view may assist in the visualization of internal fat within the mass to elench the diagnosis of fat necrosis.
- Preoperative imaging with mammography is recommended to assess for occult malignancy for average-risk women 40 years of age and older as well as women of any age who are at high-risk of developing breast cancer.

Introduction

Reduction mammoplasty is a common non-oncologic surgical procedure that accounts for 18% of all breast surgeries (1). In patients with symptomatic macromastia, the surgery aims to remove excess fat, glandular tissue, and skin from the breast to create a smaller, more aesthetically pleasing breast shape (2). Moreover, chronic back, neck, or shoulder pain, kyphosis, chronic intertrigo involving the inframammary folds, limitation of physical activity, or other problems associated with overly large breasts are common indications. Following reduction surgery, preoperative symptoms have been shown to be significantly reduced (3). In addition, some patients have reduction mammoplasty to improve symmetry following a contralateral partial mastectomy or total mastectomy with reconstruction. Several similar surgical techniques are used to alleviate patient symptoms while producing aesthetically pleasing results. Disruption of breast tissue following these surgical procedures can appear perplexing to those who are unfamiliar with these classic changes. Once the technical aspects of these procedures are conceptualized, the imaging appearance of the breast frequently becomes apparent. Even an experienced interpreting radiologist may have difficulty distinguishing between postsurgical changes after reduction mammoplasty and the imaging appearance of malignancy on occasion. Ultimately, if malignancy is suspected, a biopsy will be required for a definitive histopathologic diagnosis.

Corresponding Author:

Sally H. Goudreau; sally.goudreau@utsouthwestern.edu

Received: 22.01.2021

Accepted: 16.03.2021

Surgical techniques

There are several reduction mammoplasty techniques available, the majority of which involve removing parenchymal tissue and skin from the inferior breast while elevating the nipple-areolar complex (NAC). The most common surgical techniques for reduction mammoplasty involve a circumferential incision around the NAC, followed by a vertical incision extending to the inframammary fold, resulting in a keyhole scar (Figure 1a). This technique enables superior repositioning of the NAC as well as removal and repositioning/lifting of the inferior breast tissue (mastopexy). By using this keyhole skin flap pattern, the conical breast shape is preserved because the skin flaps are opposed, resulting in a skin brassiere. To achieve an aesthetic result, the NAC can be transposed with the underlying ducts and vascular pedicle intact using the inferior pedicle technique (Figure 1b) or transplanted with a full-thickness free nipple-areolar graft. With the inferior pedicle technique, the blood supply to the nipple and areola originates from the relatively large surface of the inframammary fold, which contributes to the preservation of nipple, areola, and skin sensations (4). Because it has a lower risk of NAC avascular necrosis than NAC transposition, free nipple-areolar graft transplantation is more common in women with large, pendulous breasts and those past childbearing age (5). The resulting post-reduction skin scar usually has a keyhole or lollipop appearance, with a subtle periareolar scar, a vertical scar extending inferiorly from the nipple to the inframammary fold, and a transverse scar curving along the fold (Figure 1c).

Breast reduction can also be accomplished solely through liposuction. This is the least invasive technique, resulting in only minor volume reduction and omitting the benefit of mastopexy. There are some non-specific imaging findings associated with this technique, such as developing asymmetries in regions where fat has been removed. Obtaining a history of the plastic surgical intervention would be beneficial in avoiding a biopsy of the new imaging finding, which would otherwise be required.

Mammography

Architectural distortion

When evaluating architectural distortion in the breast, the presence of surgical clips is often the first indication that a patient has had a prior surgical procedure, though this does not always mean reduction mammoplasty. While some surgical clips are left behind in reduced breasts, most surgeons do not. When mammographically evaluating what is thought to be postsurgical architectural distortion, the clinical history is confirmatory.

All reduction procedures involve the removal and displacement of varying amount amounts of parenchymal tissue and skin, which alters the normal distribution of fibroglandular tissue and can result in focal asymmetries (Figure 2a). In one early study of post-reduction mammographic changes, these asymmetries developed in roughly half of the women postoperatively, either persisting or gradually decreasing over time (6). With the appropriate clinical history and knowledge of this typical mammographic appearance, unnecessary recall from screening and/or biopsy can be avoided.

During reduction mammoplasty, most breast tissue is usually excised from the inferior aspect of the breast. The remaining tissue is gathered together, often with rearrangement. This technique produces a distinctive pattern of architectural distortion that appears

swirled or with an upward sweeping configuration (Figure 2b) (5). Mammographically, such inferior pole changes are evident in nearly all patients (6, 7).

Typical post-reduction scar patterns also include fibrotic bands that run parallel to the skin scar line and are easier to identify in non-anatomic orientations. Vertical scarring is common in the inferior breast, and

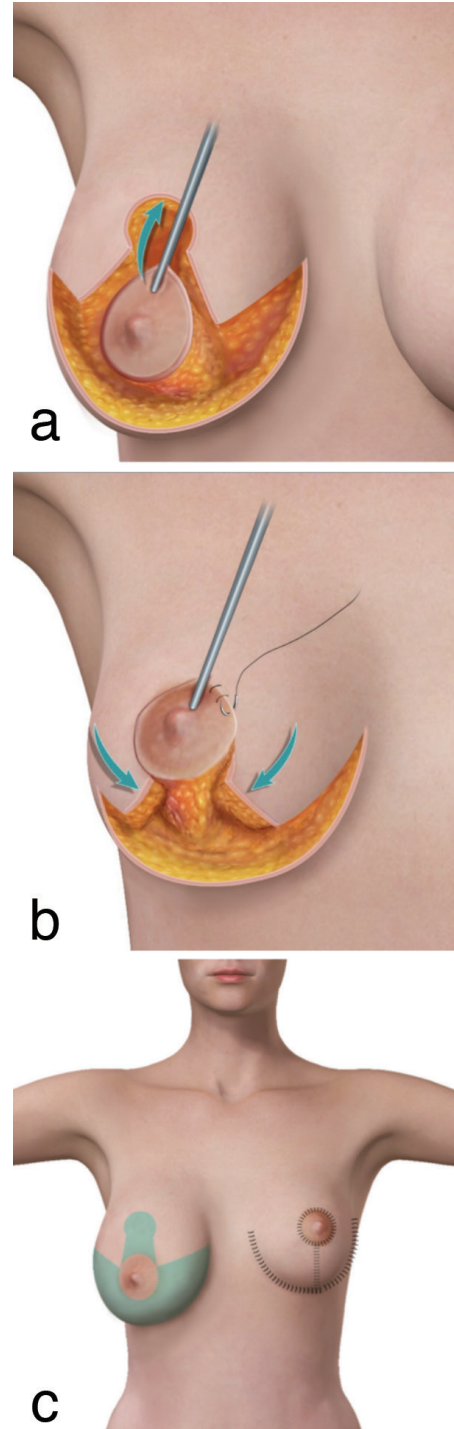


Figure 1. Surgical incisions for reduction mammoplasty. **(a)** An incision is made around the nipple areolar complex along with a vertical incision extending to a curvilinear inframammary fold incision. **(b)** The breast tissue is removed inferiorly, and the nipple is transposed superiorly, maintaining the vascular pedicle. **(c)** Appearance of the breast before (right breast) and after (left breast) reduction mammoplasty using the keyhole technique

transversely oriented scars can be seen posteriorly in the breast (8). This non-anatomic scarring pattern may result in linear bands that mammographically resemble skin folds (Figure 2c). These bands can be subtle, thinning over time and becoming difficult to distinguish

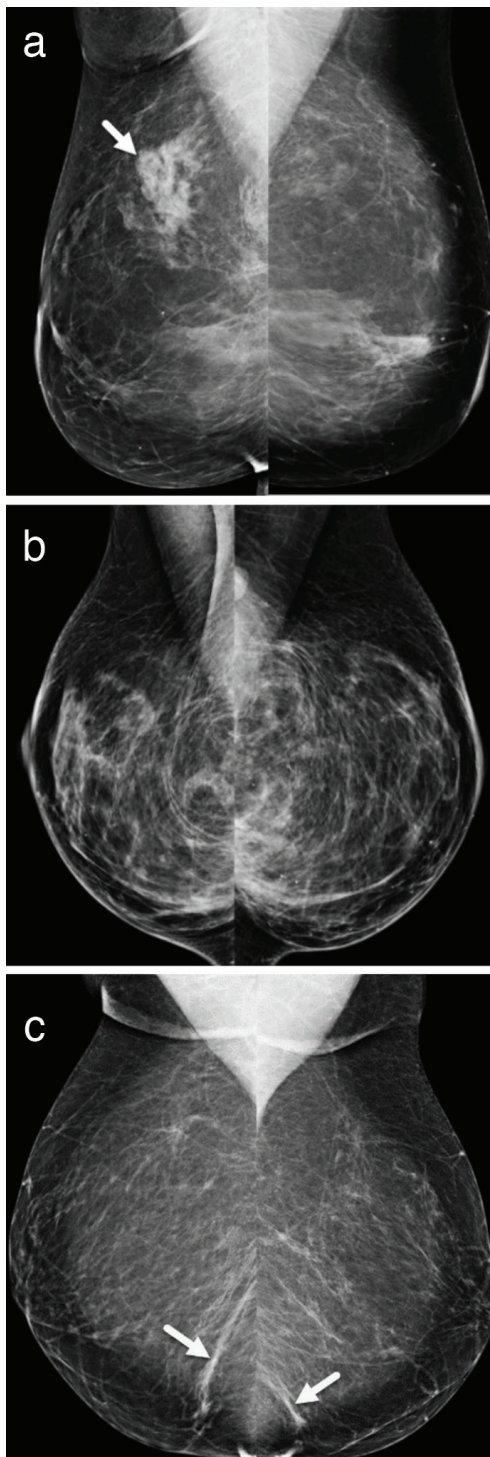


Figure 2. Rearrangement of the fibroglandular breast tissue after reduction mammoplasty. **(a)** Bilateral mediolateral oblique digital mammographic images show asymmetric tissue in the right posterior superior breast resulting from tissue rearrangement following mammoplasty. **(b)** Bilateral mediolateral oblique digital mammograms show the characteristic sweeping oblique parenchymal pattern seen after breast reduction. **(c)** Bilateral mediolateral oblique digital mammograms demonstrate non-anatomic post-reduction linear fibrotic bands which mimic skin folds (arrows)

from normal breast parenchyma. Parenchymal bands, which can extend from the chest wall to the NAC, can also be relatively thick. The most common cause of non-malignant architectural distortion is postsurgical scarring. However, as with any type of breast surgery, parenchymal surgical scarring should diminish or stabilize over time. New or increasing architectural distortion, even scarred regions, is suspicious and warrants further investigation (Figure 3).

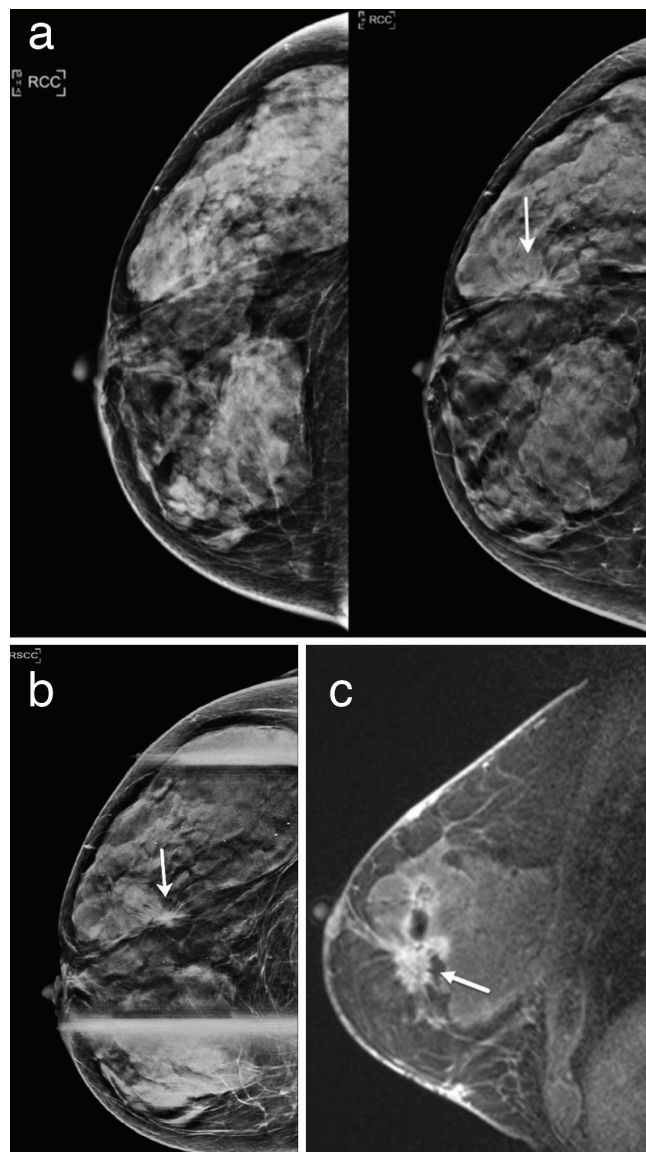


Figure 3. Malignancy developing in a reduction scar. **(a)** Sequential right craniocaudal images taken one year apart as part of screening examinations in a 57-year-old woman demonstrate interval development of architectural distortion at the reduction scar (arrow). **(b)** Craniocaudal right spot compression image taken as part of a diagnostic work-up shows persistent architectural distortion (arrow). Sonography at that time was non-contributory, only revealing scarring in the area of concern. Stereotactic core biopsy of the architectural distortion (not shown) confirmed invasive ductal carcinoma. **(c)** Enhanced MRI was subsequently performed to evaluate the extent of disease which demonstrated extensive multifocal/multicentric abnormal enhancement, including the area of developing architectural distortion (arrow) seen on this sagittal image of the right breast

MRI: Magnetic resonance imaging

Changes of the NAC

Mastopexy is used in various types of reduction mammoplasty procedures, with the NAC being relocated superiorly, as seen on the mediolateral oblique views. To create a better periareolar scar, permanent suture material may be used to secure the nipple complex (Figure 4). Along the periareolar margin, scarring with or without calcifications may be visible (9). Danikas et al. (7) demonstrated that these periareolar alterations can be seen on mammography in 85% of women postoperatively.

Calcifications and fat necrosis

Benign calcifications are a common postoperative mammographic finding, though they appear later than other mammographic features. According to one study, calcifications were found in only 3% of mammograms performed within the first 12 months after reduction, compared to 53% of mammograms performed 24 months or later after surgery (6). Furthermore, skin calcifications with lucent centers are more common at anastomotic sites.

Breast reduction surgery usually entails extensive manipulation of the breast parenchyma. Fat necrosis is caused by major trauma to an area of adipose tissue, which results in cellular death of the adipocytes and the subsequent appearance of residual oil/fat material and dystrophic calcification. As a result, fat necrosis is often encountered postoperatively and is a common cause of palpable abnormality in the postoperative breast (10). Because of internal fat at the palpable site that correlates well with the clinical history, a new palpable area of fat necrosis is often easily diagnosed mammographically, whereas the corresponding sonographic appearance can be indeterminate and potentially suspicious (Figure 5).

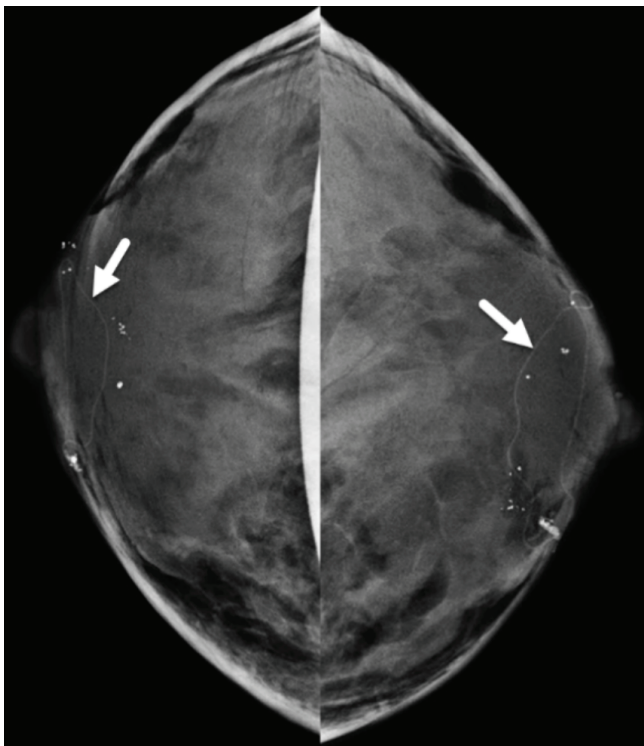


Figure 4. Mammographic appearance of the nipple areolar complex after reduction mammoplasty. Permanent sutures are seen (arrows) in the peri-areolar regions on bilateral craniocaudal digital mammographic images

Breast surgery frequently results in areas of benign fat necrosis manifesting as oil cysts. These masses are well-defined, are round or oval in shape, and contain fat, with or without rim calcification (5, 11). Oil cysts of varying sizes are seen in nearly 20% of patients and may resolve or shrink in size over time (7). As a result of oil cysts, dystrophic calcifications can develop. These calcifications may be difficult to interpret accurately at first, but they frequently coarsen over time.

Fat necrosis can also manifest as a nonspecific mass or a focal architectural distortion with or without calcifications. Moreover, postoperative changes and fat necrosis can easily be attributed to fat-containing masses with or without associated coarse or rim calcifications. However, dystrophic calcifications associated with fat necrosis that appear in the early postoperative stage infrequently may have a questionable morphology and/or distribution (12). The risk of malignancy is still very low in these cases, and calcifications associated with fat necrosis should gradually evolve, assuming a more classic dystrophic appearance and confirming the benign etiology (12). Therefore, reporting these calcifications in the Breast Imaging Reporting and Database System 3 (BI-RADS 3) category (0% to $\leq 2\%$ likelihood of malignancy) with a recommendation for a short-

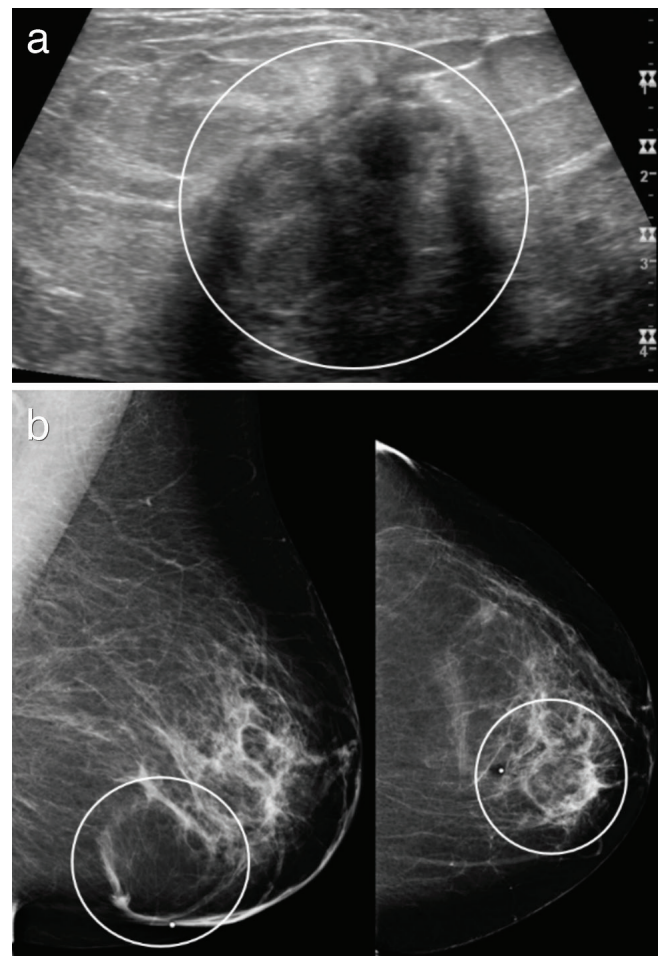


Figure 5. Post-reduction fat necrosis presenting as an area of palpable concern. (a) Sonography shows a nonspecific, solid, irregularly shaped heterogeneous mass (circle) in the region of a new, palpable lump. (b) Left mediolateral oblique and craniocaudal digital mammogram images subsequently performed demonstrate post-reduction changes with a fatty mass (circles) in the 7:00 position, confirming benign fat necrosis

term close interval follow-up to document morphologic stability is appropriate. Stereotactic biopsy should be reserved for cases that do not show early morphology and/or distribution of fat necrosis, or for cases that become suspicious after a short interval of follow-up.

Sonography

Physical examination of the breast, along with sonography, will reveal the typical scarring pattern associated with prior reduction mammoplasty. A periareolar skin scar (which may be very subtle), an inframammary fold scar, and a radially oriented scar in the 6 o'clock position will all be visible patterns. Depending on the type of surgical procedure performed, patients may have a variable combination of these scars.

The appearance of post-reduction fat necrosis on imaging varies greatly depending on its stage of evolution, particularly with sonography. Sonography is frequently used to investigate new palpable findings; however, fat necrosis is can be difficult to interpret with ultrasound alone. If the etiology of a palpable mass cannot be determined after an initial ultrasound interrogation, a spot tangential mammographic view can be obtained easily in order to visualize fat within the mass (Figure 6). One of the most useful features in classifying the mass as benign fat necrosis is the discovery of internal fat.

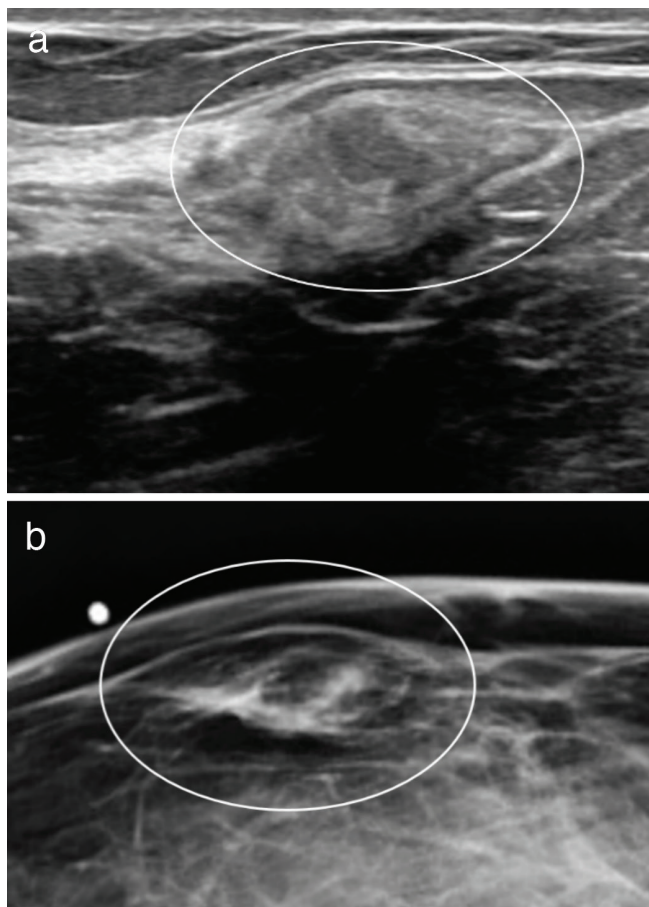


Figure 6. A palpable mass seen sonographically is confirmed to be fat necrosis with mammography. **(a)** Sonographic image shows an irregularly shaped, heterogeneous mass (circle) at the site of a patient's palpable abnormality after reduction mammoplasty. **(b)** Corresponding spot tangential digital mammogram of the palpable finding demonstrates a fat containing mass (circle), confirming fat necrosis

Furthermore, architectural distortion can occur anywhere within the breast parenchyma in post-reduction patients if significant tissue rearrangement has occurred. Sonographically, this distortion appears as vague hypoechogenicity, disruption of the normal fascial planes, and posterior acoustic shadowing, which is most prominent in the inferior breast and inframammary fold region. This sonographic appearance may be identical to cancer, necessitating a biopsy.

Magnetic resonance imaging

Because of its high sensitivity and negative predictive value of malignancy, breast magnetic resonance imaging is a valuable diagnostic tool for detecting breast cancer. There are a number of distinct post-reduction mammoplasty findings seen with magnetic resonance imaging (13).

Signal voids corresponding to suture material and/or surgical clips are seen in a linear fashion along the inframammary fold, encircle the NAC, and may be scattered throughout the breast parenchyma (Figure 7a). Similarly, post-contrast imaging can easily detect dermal scarring and keloids around the NAC, inframammary fold, and 6 o'clock radiant (Figure 7b). During surgery, fibroglandular tissue is rearranged, resulting in architectural distortion, parenchymal bands (Figure 7c), and islands of breast tissue (Figure 7d) similar to those seen on mammography. The imaging characteristics of these islands should be similar to other areas of benign fibroglandular tissue found in the breast.

Fat necrosis can occur anywhere in the reconstructed breast, but it is most common along the inferior aspect of the breast, where distortion is most common. Fat necrosis produces an isointense signal to the rest of the fatty breast tissue, with varying degrees of rim enhancement depending on its current stage of evolution and the degree of inflammation and granulation tissue. Although a thin enhancing rim is common with fat necrosis, a thickened and irregular enhancing rim that can be mistaken for malignancy may be present. The kinetic analysis of fat necrosis is nonspecific, encompassing both benign and malignant enhancement patterns (13). T1-weighted images with and without fat saturation are frequently used to determine the presence of fat within a mass or area of architectural distortion, assisting in the confirmation of the presence of benign fat necrosis (Figure 8). Fat necrosis may also be characterized by enhancing internal thin septations. The T1 signal from fat necrosis is typically isointense to other fats in the breast; however, fat necrosis may sometimes appear to have a slightly darker T1 signal due to hemosiderin deposition or chronic inflammatory changes. Mammographic correlation is recommended because the presence of oil cysts or coarse calcifications within the region of interest may provide further supporting evidence of fat necrosis.

Cancer detection

Prior to undergoing elective reduction mammoplasty, preoperative imaging to assess for occult malignancy is recommended for average-risk women 40 years of age and older, as well as women of any age who are at high-risk of developing breast cancer (14). Mammography is the most cost-effective and widely available screening method in eligible patients. Any suspicious lesions detected during preoperative imaging will require tissue diagnosis prior to surgery. Infrequently (0.8%), malignancy is discovered during reduction mammoplasty, posing a diagnostic dilemma if no preoperative imaging was

obtained (15). In the event of a postoperative diagnosis of breast cancer, the patient will need additional diagnostic evaluation; however, the sensitivity of breast magnetic resonance imaging for malignancy is reduced in the immediate post-reduction breast due to the expected postoperative enhancement of inflamed and healing tissue. In a large cohort of 4,804 women examined by Tang et al. (15), 48% of patients with an incidental diagnosis of malignancy at mammoplasty had postoperative breast magnetic resonance imaging to assess the extent of disease. The majority of the initial cancers discovered were low grade and small. In fact, 8% of invasive cancers and 72 % of DCIS were grade 1 or 2, and 94% of invasive cancers were stage T1. The authors found that postoperative magnetic resonance imaging had limited sensitivity for detecting any residual malignancy, hypothesizing that this was due to the small size of any

residual cancer and masking from postsurgical changes (15). At our institution, we have observed similar limitations in the immediate postoperative period and therefore recommend that the patient wait at least 6 weeks after surgery before undergoing magnetic resonance imaging to evaluate for residual disease in order to lessen these postoperative changes. After treatment for the primary malignancy, if mastectomy is not performed, repeat bilateral breast magnetic resonance imaging in 6 months could be considered for reevaluation after the postsurgical changes have resolved. Cancer detection and recall rates in breasts that have undergone reduction mammoplasty have been reported to be comparable to native breast (16). For average-risk women, routine annual or biennial mammographic screening following reduction mammoplasty is the appropriate recommendation. The postoperative baseline mammogram is usually the most difficult to interpret because significant changes in the configuration of the breast parenchyma have occurred in addition to the expected interval postoperative changes (7). Any interval changes, such as a developing asymmetry or mass, after this baseline mammogram should be viewed with caution, and an appropriate diagnostic evaluation should be recommended (Figure 9).

Differentiating fat necrosis from residual or new cancer can sometimes be difficult with any breast imaging modality, especially if

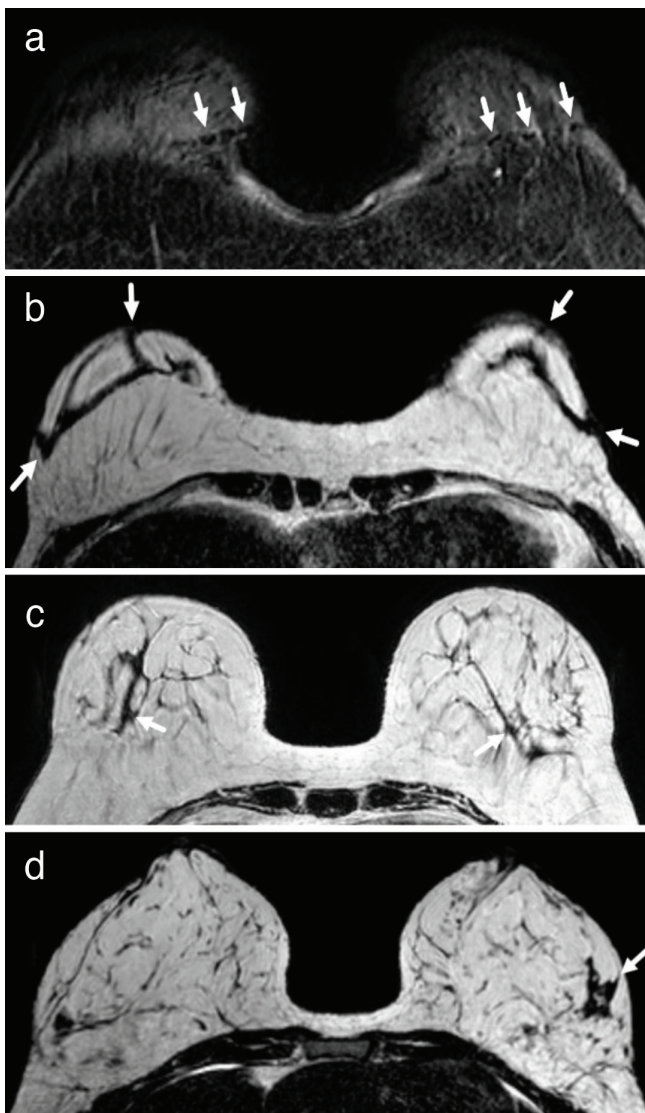


Figure 7. Post-surgical magnetic resonance appearance after reduction mammoplasty. **(a)** Signal void along the bilateral inframammary folds on a fat saturated T1-weighted axial image corresponds to surgical staples and/or sutures (arrows). **(b)** Scarring is represented by dark bands (arrows) on a T1-weighted axial image along the inframammary fold region bilaterally. **(c)** A T1-weighted axial image shows parenchymal bands (arrows) similar to those seen mammographically. **(d)** An axial post-contrast image shows an island of non-enhancing fibroglandular tissue (arrow) in the lateral left breast

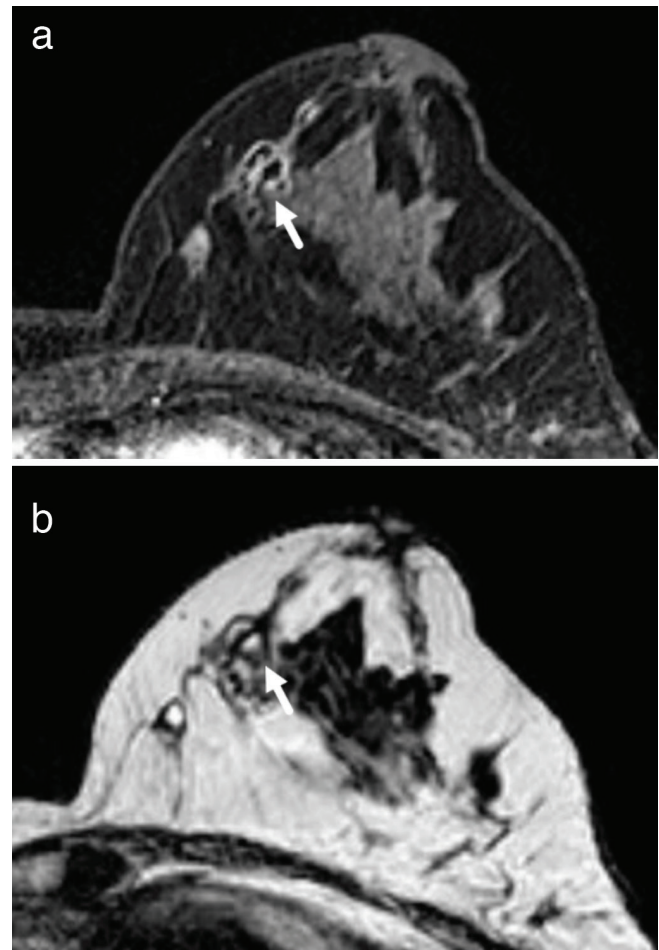


Figure 8. Fat necrosis seen with magnetic resonance imaging. **(a)** Rim enhancement (arrow) in the medial left breast on post-contrast T1-weighted image corresponds with **(b)** a fat-containing lesion (arrow) seen on T1-weighted pre-contrast image, both confirming fat necrosis

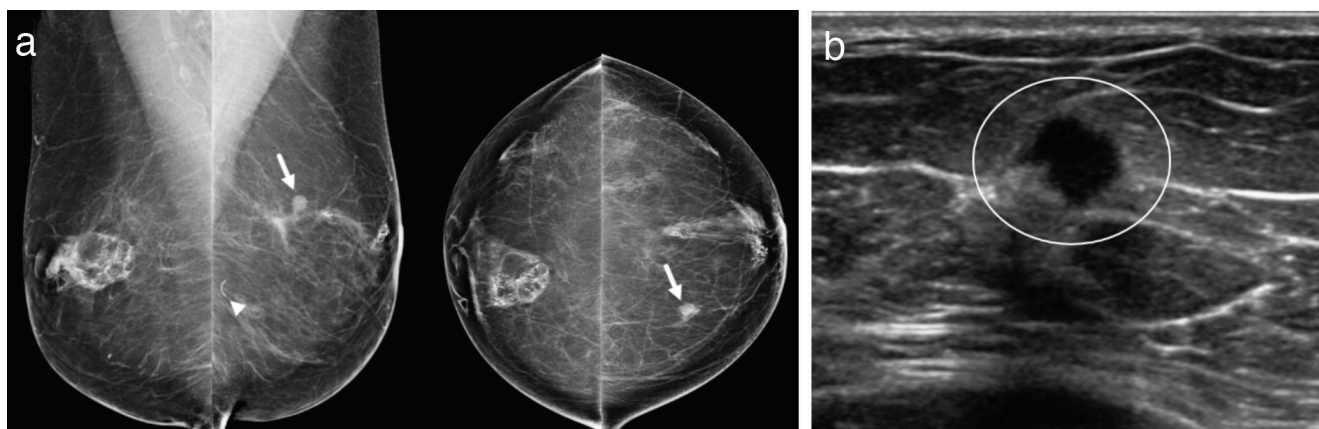


Figure 9. Interval cancer development following reduction mammoplasty. **(a)** This 58-year-old woman was found to have a new mass (arrows) in the 11 o'clock position of the left breast, middle depth, on routine screening mammography. Reduction changes, including areas of fat necrosis, are seen bilaterally. A suture needle (arrowhead) from the prior reduction surgery is noted posteriorly on the left mediolateral oblique projection. **(b)** Ultrasound imaging confirmed an irregularly shaped hypoechoic mass with indistinct margins (circle), with subsequent ultrasound-guided biopsy yielding triple-negative invasive ductal carcinoma

there is excessive degree of tissue fibrosis and no discernible internal fat. The enhancement kinetics for fat necrosis are highly variable, with a wide range of kinetic curves reported in the literature (13). Depending on the degree of diagnostic certainty, some lesions may be allowed short-term follow-up. However, if there is moderate to high clinical suspicion of malignancy, percutaneous sampling should be recommended.

Calcifications in the postoperative breast may also pose a diagnostic dilemma. Over time, benign calcifications caused by surgical changes tend to coarsen and become more dystrophic. As calcifications begin to form, they may appear amorphous and coarse heterogeneous within the BI-RADS 4b intermediate suspicion category (17). Moreover, calcifications with a high likelihood of benignity ($\leq 2\%$ risk of malignancy) may be classified as probably benign and followed as a precautionary measure. Any calcifications that remain suspicious after thorough mammographic work-up and/or follow-up should be subjected to stereotactic biopsy for histopathologic diagnosis (Figure 10).

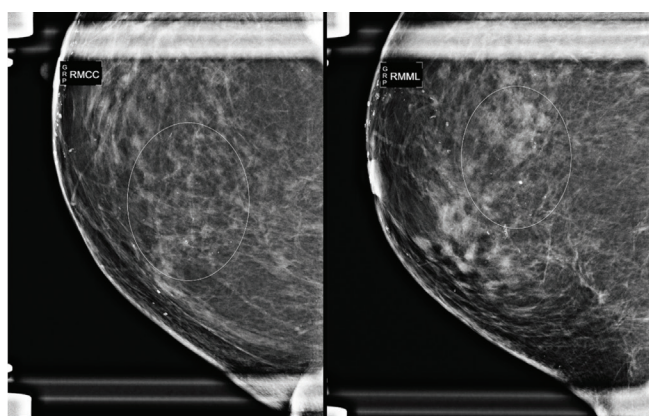


Figure 10. Developing malignant calcifications after reduction mammoplasty. This 66-year-old patient developed grouped, amorphous calcifications (circles) in the 3 o'clock position of the right breast 11 years after reduction mammoplasty, demonstrated on spot magnification diagnostic mammogram

Conclusion

All common breast imaging modalities reliably predict the imaging features of reduction mammoplasty. To avoid confusion with developing malignancy, radiologists interpreting these studies should be able to recognize the described patterns of distortion, scarring, and calcification. When there are indeterminate lesions, a biopsy or close short-term follow-up should be performed.

Peer-review: Externally and internally peer-reviewed.

Author Contributions

Surgical and Medical Practices: S.H.G., M.A.W., S.J.S.; Conception: S.H.G., M.A.W., S.J.S.; Design: S.H.G., M.A.W., S.J.S.; Analysis and/or Interpretation: S.H.G., M.A.W., S.J.S.; Literature Search: S.H.G., M.A.W., S.J.S.; Writing: S.H.G., M.A.W., S.J.S.

Conflict of Interest: The authors have no conflicts of interest to declare.

Financial Disclosure: The authors declared that this study has received no financial support.

References

1. American Society of Plastic Surgeons. 2018 Plastic Surgery Statistics Report 2019. Last Accessed Date: 21.04.2020. Available from: <https://www.plasticsurgery.org/documents/News/Statistics/2018/plastic-surgery-statistics-full-report-2018.pdf> [Crossref]
2. Davis GM, Ringle SL, Short K, Sherrick D, Bengtson BP. Reduction mammoplasty: long-term efficacy, morbidity, and patient satisfaction. *Plast Reconstr Surg* 1995; 96: 1106-1110. (PMID: 7568486). [Crossref]
3. Glatt BS, Sarwer DB, O'Hara DE, Hamori C, Bucky LP, LaRossa D. A retrospective study of changes in physical symptoms and body image after reduction mammoplasty. *Plast Reconstr Surg* 1999; 103: 76-82; discussion 3-5. (PMID: 9915166). [Crossref]
4. Azurin DJ, Fisher J, Maxwell GP. Mastopexy. In: Weinzweig J, editor. *Plastic Surgery Secrets Plus*. Chicago, IL: Mosby/Elsevier; 2010. p. 453-457.
5. Miller CL, Feig SA, Fox JWt. Mammographic changes after reduction mammoplasty. *AJR Am J Roentgenol* 1987; 149: 35-38. (PMID: 3495989). [Crossref]

6. Brown FE, Sargent SK, Cohen SR, Morain WD. Mammographic changes following reduction mammoplasty. *Plast Reconstr Surg* 1987; 80: 691-698. (PMID: 3671561). [\[Crossref\]](#)
7. Danikas D, Theodorou SJ, Kokkalis G, Vasiou K, Kyriakopoulou K. Mammographic findings following reduction mammoplasty. *Aesthetic Plast Surg* 2001; 25: 283-285. (PMID: 11568832). [\[Crossref\]](#)
8. Margolis NE, Morley C, Lotfi P, Shaylor SD, Palestrant S, Moy L, et al. Update on imaging of the postsurgical breast. *Radiographics* 2014; 34: 642-660. (PMID: 24819786). [\[Crossref\]](#)
9. Burk KS, Seiler SJ, Porembka JH. Diagnosis, management, and percutaneous sampling of nipple-areolar calcifications: how radiologists can help patients avoid the operating room. *AJR Am J Roentgenol* 2021; 216: 48-56. (PMID: 33170739). [\[Crossref\]](#)
10. Hogge JP, Robinson RE, Magnant CM, Zuurbier RA. The mammographic spectrum of fat necrosis of the breast. *RadioGraphics* 1995; 15: 1347-1356. (PMID: 8577961). [\[Crossref\]](#)
11. Shaheen R, Schimmelpenninck CA, Stoddart L, Raymond H, Slanetz PJ. Spectrum of diseases presenting as architectural distortion on mammography: multimodality radiologic imaging with pathologic correlation. *Semin Ultrasound CT MR* 2011; 32: 351-362. (PMID: 21782125). [\[Crossref\]](#)
12. Cakir M, Kucukkartallar T, Tekin A, Selimoglu N, Poyraz N, Belviranli MM, et al. Comparison of mammography sensitivity after reduction mammoplasty targeting the glandular and fat tissue. *Ulus Cerrahi Derg* 2015; 31: 68-71. (PMID: 26170752). [\[Crossref\]](#)
13. Daly CP, Jaeger B, Sill DS. Variable appearances of fat necrosis on breast MRI. *AJR Am J Roentgenol* 2008; 191: 1374-1380. (PMID: 18941072). [\[Crossref\]](#)
14. Kerrigan CL, Slezak SS. Evidence-based medicine: reduction mammoplasty. *Plast Reconstr Surg* 2013; 132: 1670-1683. (PMID: 24281593). [\[Crossref\]](#)
15. Tang R, Acevedo F, Lanahan C, Coopey SB, Yala A, Barzilay R, et al. Incidental breast carcinoma: incidence, management, and outcomes in 4804 bilateral reduction mammoplasties. *Breast Cancer Res Treat* 2019; 177: 741-748. (PMID: 31317348). [\[Crossref\]](#)
16. Muir TM, Tresham J, Fritschi L, Wylie E. Screening for breast cancer post reduction mammoplasty. *Clin Radiol* 2010; 65: 198-205. (PMID: 20152275). [\[Crossref\]](#)
17. Tan PH, Lai LM, Carrington EV, Opaluwa AS, Ravikumar KH, Chetty N, et al. Fat necrosis of the breast--a review. *Breast* 2006; 15: 313-318. (PMID: 16198567). [\[Crossref\]](#)



Treatment with Radiopharmaceuticals and Radionuclides in Breast Cancer: Current Options

Burcu Altıparmak Güleç¹, Fatma Yurt²

¹Department of Nuclear Applications, Institute of Nuclear Science, Ege University, İzmir, Turkey (Graduated)

²Department of Nuclear Applications, Institute of Nuclear Science, Ege University, İzmir, Turkey

ABSTRACT

Radiopharmaceutical therapy (RPT) is an effective and safe treatment for many types of cancer. RPT acts by binding radioactive atoms to tumor-associated antigens, monoclonal antibodies, nanoparticles, peptides, and small molecules. These treatments ensure that a concentrated dose is delivered to the targeted tumor tissue while preserving the normal tissues surrounding the tumor. Given these features, RPT is superior to traditional methods. This review article aimed to perform a comprehensive review and evaluation of the potential of radionuclides and radiopharmaceuticals used in breast cancer treatment in preclinical studies conducted in the last five years.

Keywords: Breast cancer, radioisotopes, radionuclide therapy, radiopharmaceuticals

Cite this article as: Altıparmak Güleç B, Yurt F. Treatment with Radiopharmaceuticals and Radionuclides in Breast Cancer: Current Options. Eur J Breast Health 2021; 17(3): 214-219

Key Points

- Radiopharmaceutical therapy is a safe and effective method for cancer treatment.
- Radiopharmaceutical therapies have minimal toxicity compared to other cancer treatments, making the option successful and useful.
- The design of radiopharmaceuticals requires various pharmacokinetic and biofunctional procedures, and the selection of the appropriate method increases specificity and provides a successful treatment method.
- For the *in vitro* and *in vivo* experiments to be performed comprehensively, conditions in the limited competition environment must be provided equally in terms of cost and quality.
- According to breast cancer types, increasing specific radiopharmaceutical designs in breast cancer treatment has increased the probability of success.

Introduction

The World Health Organization (WHO) reported that 18.1 million people were diagnosed with cancer in 2018 and 9.6 million people died in the same year. With the increase in diagnostic modalities, more people are being diagnosed with cancer, and the ensuing public health problem has led to the investigation of more treatment options in this field. Worldwide, the most common types of cancer in men are lung, prostate, stomach, and liver cancers, where as the most common types in women are breast, lung, cervical, and colon cancers. In a 2018 WHO report, it was stated that 2.09 million women were diagnosed with breast cancer that year. Attention is drawn to the importance of new treatment options considering this rate and the fact that breast cancer is the most common type of cancer in women (1, 2). The application of radioisotope and radiopharmaceutical therapies in many cancer treatments [thyroid (3), gastrointestinal system (4), prostate (5), gastroenteropancreatic, lung (6), non-Hodgkin's lymphoma (7), cancers such as prostate bone metastases (8), breast bone metastases (9)] and positive results obtained have directed researchers to preclinical studies about the applicability of these treatment methods to breast cancer.

These treatments aim to target cancerous cells directly and protect healthy tissues. Radionuclide therapy (RT) involves sending radioactive elements with different emission properties into cancerous tissue. RT has the advantage of delivering a highly concentrated dose to the targeted tumor tissue while protecting the normal tissues surrounding the tumor. The fact that these treatment practices are minimally invasive, and the duration of treatment is shorter than that of chemotherapy has made them one of the most preferred cancer treatment methods recently (10).

Corresponding Author:
Burcu Altıparmak Güleç; burcu@synapse.com.tr

Received: 03.03.2021
Accepted: 20.03.2021

Radiopharmaceutical therapy (RPT) is carried out by sending radionuclides conjugated to tumor-targeted pharmaceuticals or bioactive molecules (nanoparticles, antibodies, peptides, small molecules, and various structures of each) that predominantly accumulate in neoplastic cells within tumors into the tumor tissue (11). Recently, RT has attracted attention as a safe and effective method for cancer treatment, and research continues (12).

In this review article, the effectiveness of preclinical studies conducted in the last five years with radionuclides and radiopharmaceuticals in breast cancer will be discussed.

Therapeutic radionuclides used as radiopharmaceuticals

History of radiopharmaceuticals

To understand RPT, we first need to talk about radioactive atoms and their history. In 1930, Rutherford mentioned three important discoveries in the publications of Chadwick and Ellis named "Radiation from radioactive materials". These were the discovery of X-rays by Roentgen in 1895, the discovery of the radioactivity of uranium by Becquerel in 1896, and the discovery of the electron in 1897 by J.J.Thomson. Briefly, the discovery of atomic physics went through the following stages (13). Radiography was not discovered until 1895, when Wilhelm Conrad Roentgen was exposed to X-rays by chance while working in the laboratory with a cathode ray (X-ray) tube. Shortly after the discovery of X-rays, French scientist Henri Becquerel found that uranium mineral fluoresces when exposed to sunlight, and in 1903 Marie and Pierre Curie shared the Nobel Prize in Physics with this discovery. Subsequently, Henri Becquerel and Marie Curie worked together to discover radioactive elements other than uranium, including radium and polonium. Curie believed that radium could be used to relieve pain (14).

According to the history of radiation in medicine, in 1901, Becquerel noticed burning caused by radium he carried in his pocket, which made him realize diseases were caused by radioactive materials. Henri Alexander Danlos and Eugene Block placed radium in contact with a skin lesion and initiated the first use of RT. Alexander Graham Bell suggested placing radium sources in and near tumors in 1903 and published Frederick Proesher's first study with intravenous injection of radium in 1913 (10). Radium beams were used in certain diseases, including systemic lupus, cancer, and nerve diseases (14). The use of radiation for therapeutic purposes dates back this far.

In recent years, although radiopharmaceuticals containing particle-emitting radionuclides such as ^{90}Y -ibritumomab tiuxetan (Zevalin), strontium-89 chloride (Metatron), and iobenguane (^{131}I -Azedra) were once preferred in therapeutic radiopharmaceutical research, radionuclides that emit alpha particles have now become the focus of attention. In 1997, the US Food and Drug Administration (FDA) approved the ^{213}Bi radionuclide for use in clinical trials. The first radiopharmaceutical approved by the US-FDA in 2013 was $^{223}\text{RaCl}_2$ (15).

Physical and biological efficacy of therapeutic radionuclides

To understand RPT, it is first necessary to understand what type of ionizing radiation is emitted by the radioisotopes used in these compounds. There are three different types of ionizing radiation: photons, electrons, and alpha particles. Photons are made up of X-rays and γ -rays, and X-rays have lower energy than γ -rays. Photon emissions

are useful for monitoring responses to therapy after treatment but are not suitable for localizing cytotoxic radiation in tumor cells (16). Therefore, the preferred ionizing radiation types for the treatment of tumor tissue are electrons and alpha particles. Alpha particles have a high linear energy and a short range; beta particles have a low linear energy and a long range (17).

For RPT to be effective, the distance these particles reach, the amount of energy they accumulate in cells, and direct interaction with DNA are of great importance. Beta particles form free radicals by breaking the covalent bonds of water molecules in tissues, and these radicals cause DNA damage by causing double-strand breakage. When these two particles are compared to each other based on double-stranded DNA breakage, cell death requires one alpha particle or hundreds of beta particles. The high linear energy and short range of alpha particles in the tissue ensure that toxicity around the tumor tissue is low, and the cancer cells sustain a high level of damage. Therefore, it is considered that the cytotoxicity of alpha particles is much higher than that of beta particles (8). Radiopharmaceuticals have been used in diagnostics and therapeutics for more than half a century. Compared with other cancer treatment options, RPT has minimal toxicity. The features of an ideal RPT include aspects such as good radionuclide radiation type (alpha, beta, and auger electron) selection, radiation energy higher than 1MeV, effective half-life in hours or days, high target tissue ratio/non-target tissue ratio, low cost, and ease of procurement, and ease of preparation in the laboratory (18). The remarkable potential of RPT against primary and long-distance metastases has led to its acceptance as an appropriate treatment method because it is effective, safe, and economical (16).

Selection of radionuclides for therapeutic purposes

In nuclear medicine, 95% of radiopharmaceuticals are used for diagnosis and 5% for treatment. Radionuclides are divided into two types: diagnostic and treatment radionuclides. The most common and ideal radionuclide used for diagnosis is $^{99\text{m}}\text{Tc}$. The reason for the preference of this radionuclide in diagnosis is that it emits pure gamma radiation with an energy between 100 and 250 keV; is easily available and affordable; has an effective half-life; has a high target/non-target ratio; and is sterile, pyrogenic, isotonic, and isohydric. Imaging radionuclides used other than $^{99\text{m}}\text{Tc}$ include fluorine-18 (^{18}F), carbon-11 (^{11}C), nitrogen-13 (^{13}N), oxygen-15 (^{15}O), and gallium-68 (^{68}Ga). For nearly 50 years, ^{131}I was used for the treatment of thyroid cancer (19). Apart from this, some beta radionuclides used for therapeutic purposes include ^{153}Sm , ^{177}Lu , Y-90, and ^{131}I , along with the alpha radionuclides ^{211}As , ^{212}Bi , ^{212}Pb , ^{213}Bi , ^{225}Ac , ^{223}Ra , and ^{227}Th . The physical properties of some therapeutic radionuclides are given in Table 1 (16, 17, 20).

When choosing a therapeutic radionuclide, attention should be paid to its physical and biochemical properties. Physical properties include physical half-life, types of emission, the energy of radiation(s), by-product(s), method of production, and radionuclide purity. Biochemical properties include tissue targeting, retention of radioactivity in the tumor, *in vivo* stability, and toxicity (21). When choosing the treatment radionuclide, attention should be paid to its effective half-life. The effective half-life is calculated from the biological and physical half-life in the body or organs. The effective half-life (T_e) is calculated by $T_e = T_p \cdot T_b / (T_p + T_b)$. The physical half-life (T_p) is included in the literature for each radionuclide, but the biological half-life (T_b) requires the biodistribution of the radiopharmaceutical

Table 1. Therapeutic Radionuclides (16,17, 20)

Radionuclides	Mode of decay	Physical half-life (t _{1/2})	E _{max} (MeV)
⁹⁰ Y	β ⁻	64.10 hours	2.3
¹³¹ I	β ⁻	8.02 days	0.6
¹⁷⁷ Lu	β ⁻	6.73 days	0.5
¹⁵³ Sm	β ⁻	46.50 hours	0.8
¹⁸⁶ Re	β, EC	3.72 days	1.1
¹⁸⁸ Re	β ⁻	17.00 hours	2.1
²²⁵ Ac	α	10.00 days	5.8
²¹³ Bi	α, β ⁻	45.61 mins	5.9
²¹² Bi	α, β ⁻	60.55 mins	6.1
²¹¹ At	α, EC	7.21 hours	5.9
²¹² Pb	α, β ⁻	10.64 hours	0.6
²²³ Ra	α	11.44 days	5.8
²²⁴ Ra	α	3.63 days	5.7
²²⁷ Th	α	18.68 days	6.0

α: Alpha, β: Beta, EC: Electron capture, Y: Yttrium, I: Iodine, Lu: Lutetium, Sm: Samarium, Re: Rhenium, Ac: Actinium, Bi: Bismuth, At: Astatine, Pb: Lead, Ra: Radium, Th: Thorium

in the organs. The biodistribution of the radiopharmaceutical includes its transmission to organs, its uptake, metabolism, clearance, and excretion. The appropriate physical half-life for therapeutic radionuclides is between six hours and seven days. If we choose a radionuclide with a very short physical half-life, it will not be efficient and practical. If we choose a radionuclide with a long half-life, the exposure of the patient and the people around them will increase, since the dose absorbed in the patient's body is large. Having a very long physical half-life means that patients stay in the hospital for a long time, and the duration of isolation increases. This increases the cost of treatment. Information about the biological half-life depends on the pharmaceutical used. If the pharmaceutical remains in the patient's body too long, the physical half-life of the radionuclide should not be too long. Therefore, for effective radiopharmaceutical treatment, a radionuclide with a balanced biological and physical half-life should be selected (8, 10, 22).

Therapeutic radiopharmaceuticals used in breast cancer

Types of breast cancer

Breast cancer is the most common type of cancer among women in the world and is a heterogeneous disease with different molecular subtypes. It is considered to be a mixture of four diseases: hormone receptor (HR)-positive and human epidermal growth factor 2 (HER2)-negative cancer; HR-positive and HER2-positive cancer; HR-negative and HER2-positive cancer and triple-negative cancer (23). In HR (+) tumors, cancer cells carry the receptors for hormones such as estrogen and progesterone. These hormones trigger the growth of HR (+) tumors. In HER2 (+) tumors, cancer cells overproduce a protein responsible for cell growth and proliferation called HER2/neu. Knowing these subtypes of breast cancer forms the basis of diagnosis and treatment (24). Estrogen receptors (ERs) are overexpressed in

cancer cells and are highly effective in therapies targeting ER-positive (ER+) breast cancers. ER + breast cancer is the most common subtype of breast cancer (25). Therapeutic approaches designed according to these subtypes in breast cancer treatment have increased interest in the potential for the use of radionuclide and radiopharmaceuticals in breast cancer treatment. These studies are included in this compilation.

Therapeutic radiopharmaceuticals for breast cancer

The exploration of breast cancer treatment began in the 19th century. Radiation therapy was applied in addition to surgical intervention in 1937 to protect the breast. The FDA approved the drug tamoxifen in 1978 for use in breast cancer treatment. In 1996, the FDA approved anastrozole as a breast cancer treatment that inhibits estrogen production. Another drug approved by the FDA in 1998 was trastuzumab, which targets HER2, which is overproduced by cancer cells. In 2006, raloxifene, which showed lower toxicity than tamoxifen, was found to reduce the risk of breast cancer (26, 27). Targeted RT has been developed, and research continues to design new targeted radiopharmaceuticals using various FDA approved drugs.

New studies have gained momentum with the discovery of RT in addition to the known traditional methods used for breast cancer treatment. These new studies are based on radiopharmaceuticals formed by chelating a radioactive element (radionuclide) to a conjugate that targets tumor tissue (11). To give an example of one of these radiopharmaceuticals, in a preclinical breast cancer treatment study conducted by Luo et al. (28) in 2009, the breast cancer treatment drug trastuzumab (Herceptin) was conjugated with SOCTA and labeled with the radionuclide ¹⁸⁸Re. ¹⁸⁸Re-SOCTA-trastuzumab was administered intravenously to xenograft mice bearing BT-474 breast cancer overexpressing HER-2/neu. They suggested that ¹⁸⁸Re-SOCTA-trastuzumab was a potential candidate for radioimmunotherapy (28). To date, preclinical studies conducted

in the last five years on radiopharmaceuticals used in breast cancer treatment are listed below.

Various nanoparticles (organic nanoparticles such as polymeric matrices and liposomes, as well as inorganic nanoparticles such as gold, metal oxides, and insoluble metal salts) are used as radioisotope carriers in RPT. Yook et al. (29) designed a new radiopharmaceutical for the treatment of triple-negative breast cancer (TNBC), in which epidermal growth factor receptors (EGFR) are overexpressed. Gold nanoparticles (AuNP; 30 nm) were complexed with 1,4,7,10-tetraazacyclododecane-1,4,7,10-tetraacetic acid (DOTA) conjugate to form a complex with emitter ^{177}Lu with polyethylene glycol (PEG) chains (4 kDa). After this modification, they bound panitumumab (selectively binds to the epidermal growth factor receptor). EGFR-targeted AuNP (^{177}Lu -T-AuNP) and non-targeted ^{177}Lu -NT-AuNP were subcutaneously injected into CD-1 athymic mice bearing EGFR-positive MDA-MB-468 human breast cancer tumors and imaging studies were conducted. It was concluded that ^{177}Lu -T-AuNP is a potential and promising application for TNBC therapy (29, 30).

Radioimmunotherapy represents the use of isotopes conjugated to monoclonal antibodies (mAb) in therapy (31). Trastuzumab (Herceptin) is a monoclonal antibody that binds to HER2 receptors overexpressed on cancer cells and is covalently bound with 3-phosphonopropionic acid (CEPA) nanoparticles. This conjugate alpha emitter is marked with ^{225}Ac . Superparamagnetic iron oxide-based nanoparticles (cipions) were used as the targeting conjugate ($^{225}\text{Ac}^{\circ}\text{Fe}_3\text{O}_4$). $^{225}\text{Ac}^{\circ}\text{Fe}_3\text{O}_4$ -CEPA-trastuzumab radio bioconjugate was shown to have high receptor affinity in *in vivo* studies and exhibit properties suitable for breast cancer treatment (32).

Morgenroth et al. (33) in their study evaluated the potential of the prostate-specific membrane antigen PSMA to target small molecules for radioligand therapy of TNBC. For *in vivo* experiments, nude mice were xenografted with MDA-MB231 estrogen receptor-expressing TNBC cells or MCF-7 breast cancer cells. In their therapeutic study with ^{177}Lu -PSMA-617, they demonstrated the potential of PSMA as a unique and specific targeting agent for TNBC.

Hernandez et al. (34) conducted a promising study by labeling tumor-targeting alkyl phosphocholine (NM600) with ^{177}Lu radionuclide for targeted RT of TNBC. ^{177}Lu -NM600 was administered to BALB/C mice carrying 4T07 and 4T1 mammary tumor grafts. This study suggested that the radiopharmaceutical ^{177}Lu -NM600 is an appropriate therapy for targeted RT, and it was reported to show a favorable biodistribution (34).

Hagemann et al. (35) evaluated mesothelin (MSLN)-targeted ^{227}Th labeled conjugate (BAY2287411), which is an overexpressed membrane glycoprotein in breast cancer, in breast xenograft models produced from the patient. It was shown that this synthesized conjugate had *in vivo* and *in vitro* potential, and a dose-dependent regression in tumor growth was observed in treatment due to the increase in MSLN in breast cancer cells (35).

In their study, Yin et al. (25) created MCF-7 cell xenografts of ^{131}I -fulvestrant in nude mice by radioiodine labeling fulvestrant (an endocrine treatment drug for breast cancer) and monitored tumor growth and critical organ function. The ^{131}I -fulvestrant conjugate was determined to maintain its binding affinity to ER-positive (ER+) MCF-7 cells and exert a tumor suppressor effect on these cells. As a result, they noted that radioiodine labeling of fulvestrant was

successful and could therefore be used to develop new drugs for breast cancer (25).

Thorek et al. (36) applied androgen receptor pathway activation to targeted alpha particle immunotherapy in breast cancer. To specifically treat breast cancer xenografts expressing androgen receptors, the anti-hK2 (hu11B6 antibody) alpha particle emitting ^{225}Ac radionuclide was labeled. Very promising results were obtained in aggressive androgen receptor-positive breast cancer cell lines with a ^{225}Ac -hu11B6 radiopharmaceutical (36).

Gastrin-secreting peptide receptor (GRPr) is overexpressed in more than 75% of breast cancer cells. Gibbens-Bandala et al. (37) targeted ^{177}Lu -Bombesin (^{177}Lu -BN) to GRPr and labeled it with paclitaxel (PTX), one of the main drugs in cancer therapy. In this study, MDA-MB-231 breast cancer cells (GRPr-positive) were used. *In vitro* and *in vivo* studies of ^{177}Lu -BN-PLGA (PTX) showed high tumor uptake in MDA-MB-231 lesions. This makes it possible to monitor the progression of the disease with this conjugate.

Kasten et al. (38) investigated the potential of the ^{212}Pb -labeled antibody 225.28, which targets chondroitin sulfate proteoglycan 4 (CSPG4), in the treatment of TNBC in mouse models. ^{212}Pb -225.28 bound to CSPG4 with high affinity in TNBC cells and specifically inhibited its growth. These results support future therapeutic studies using ^{212}Pb -225.28 or other CSPG4-targeted radioimmunoconjugates, alone or in combinatorial approaches, against the TNBC model (38).

Costa et al. (39) investigated the effect of ^{223}Ra for the treatment of bone metastases in breast cancer patients. In light of this study, it was found that ^{223}Ra treatment can be used for the treatment of bone metastases in breast cancer patients. In a study conducted by Juzeniene et al. (40), the effects of alpha-emitting ^{224}Ra radionuclide treatment on osteolytic bone metastasis of MDA-MB-231 (SA)-GFP human breast cancer cells injected intracardially into mice were investigated. Treatment with ^{224}Ra solution was found to reduce the number of bone metastases. In light of these results, ^{224}Ra solution was proposed as a promising candidate for the treatment of breast cancer patients (40).

AuNP (30 nm) were labeled with ^{177}Lu radionuclide by binding to trastuzumab, PEG, or DOTA. ^{177}Lu -AuNP-trastuzumab binds specifically to HER2-positive breast cells and enables effective radiopharmaceutical therapy (41). Cai et al. (42) linked 30 nm AuNP to trastuzumab with trastuzumab targeting HER2-positive breast cancer cells and ^{111}In labeled with diethylenetriaminepentaacetic acid. The ^{111}In -AuNP-trastuzumab radiopharmaceutical was shown to inhibit tumor growth without normal tissue toxicity for treatment in CD1 athymic mice (42).

Conclusion

Recent studies about the therapeutic efficacy of radiopharmaceuticals prepared using alpha and beta-emitting radionuclides for the treatment of breast cancer have shown significant potential. In the treatment of advanced breast cancer, radiolabeling the beta particle emitter ^{177}Lu radionuclide with nanoparticles and radioimmunotherapy with low-molecular-weight protein ligands of the alpha emitters ^{225}Ac or ^{213}Bi appear promising due to the favorable pharmacokinetic properties of these radiopharmaceuticals. Radioiodine labeling of fulvestrant found that it can be used for breast cancer treatment. Other radioimmunoconjugates targeted to ^{212}Pb -225.28 or CSPG4 support therapy against the TNBC model. Local radiation therapy for HER2-positive breast cancer based

on AuNP modified with trastuzumab and labeled with an auger electron emitter ¹¹¹In was developed and was shown to arrest tumor growth without normal tissue toxicity. Enhancement of the radiopharmaceutical ¹⁷⁷Lu-BN-PLGA (PTX) proved it to be suitable as a targeted paclitaxel delivery system with a concurrent radiotherapeutic effect for the treatment of GRPr-positive breast cancer. Additionally, ²²³Ra and ²²⁴Ra radionuclides were shown to have potential utility in the treatment of bone metastases in breast cancer patients.

In light of preclinical studies, radionuclides and radiopharmaceuticals used for breast cancer treatment represent an area of huge potential.

Peer-review: Externally peer-reviewed.

Authorship Contributions

Conception: B.A.G., F.Y.; Design: B.A.G., F.Y.; Data Collection and/or Processing: B.A.G., F.Y.; Analysis and/or Interpretation: B.A.G., F.Y.; Literature Search: B.A.G., F.Y.; Writing: B.A.G., F.Y.

Conflict of Interest: The authors declare no conflict of interest.

Financial Disclosure: The authors declare that this study received no financial support.

References

1. World Health Organization. Cancer Report, September 2018. Available from: https://www.who.int/health-topics/cancer#tab=tab_1 [Crossref]
2. Mattiuzzi C, Lippi G. Current cancer epidemiology. *J Epidemiol Glob Health* 2019; 9: 217-222. (PMID: 31854162) [Crossref]
3. Kayano D, Kinuya S. Current consensus on ¹³¹I-MIBG therapy. *Nucl Med Mol Imaging* 2018; 52: 254-265. (PMID: 30100938) [Crossref]
4. Das S, Al-Toubah T, El-Haddad G, Strosberg J. ¹⁷⁷Lu-DOTATATE for the treatment of gastroenteropancreatic neuroendocrine tumors. *Expert Rev Gastroenterol Hepatol* 2019; 13: 1023-1031. (PMID: 31652074) [Crossref]
5. Fendler WP, Rahbar K, Herrmann K, Kratochwil C, Eiber M. ¹⁷⁷Lu-PSMA radioligand therapy for prostate cancer. *J Nucl Med* 2017; 58: 1196-1200. (PMID: 28663195) [Crossref]
6. Naraev BG, Ramirez RA, Kendi AT, Halfdanarson TR. Peptide receptor radionuclide therapy for patients with advanced lung carcinoids. *Clin Lung Cancer* 2019; 20: e376-e392. doi: 10.1016/j.clcc.2019.02.007 (PMID: 30910575) [Crossref]
7. Mukherjee S, Ayanambakkam A, Ibrahim S, Schmidt S, Charkrabarty JH, Khawandanah M. Ibritumomab tiuxetan (Zevalin) and elevated serum human anti-murine antibody (HAMA). *Hematol Oncol Stem Cell Ther* 2018; 11: 187-188. (PMID: 29406240) [Crossref]
8. Tafreshi NK, Doligalski ML, Tichacek CJ, Pandya DN, Budzevich MM, El-Haddad G, et al. Development of targeted alpha particle therapy for solid tumors. *Molecules* 2019; 24: 4314. (PMID: 31779154)
9. Langbein T, Weber WA, Eiber M. Future of theranostics: an outlook on precision oncology in nuclear medicine. *J Nucl Med* 2019; 60: 13S-19S. doi: 10.2967/jnumed.118.220566 (PMID: 31481583) [Crossref]
10. Yeong CH, Cheng MH, Ng KH. Therapeutic radionuclides in nuclear medicine: current and future prospects. *J Zhejiang Univ Sci B* 2014; 15: 845-863. (PMID: 25294374) [Crossref]
11. Sgouros G. Radiopharmaceutical therapy. *Health Phys* 2019; 116: 175-178. (PMID: 30585960) [Crossref]
12. Jadvar H. Targeted α -therapy in cancer management: synopsis of preclinical and clinical studies. *Cancer Biother Radiopharm* 2020; 35: 475-484. (PMID: 32202923) [Crossref]

13. Williams WSC, Nuclear and particle physics. 1st ed. Oxford: Oxford University; 1991. [Crossref]
14. Reed AB. The history of radiation use in medicine. *J Vasc Surg* 2011; 53(Suppl 1): 3S-5S. doi: 10.1016/j.jvs.2010.07.024 (PMID: 20869835) [Crossref]
15. Ferrier MG, Radchenko V, Wilbur S. Radiochemical aspects of alpha emitting radionuclides for medical application. *Radiochim Acta* 2019; 107: 1065-1085. [Crossref]
16. Sgouros G, Bodei L, McDevitt MR, Nedrow JR. Radiopharmaceutical therapy in cancer: clinical advances and challenges. *Nat Rev Drug Discov* 2020; 19: 589-608. (PMID: 32728208) [Crossref]
17. Ferrier MG, Radchenko V. An Appendix of radionuclides used in targeted alpha therapy. *J Med Imaging Radiat Sci* 2019; 50(4 Suppl 1): S58-S65. doi: 10.1016/j.jmir.2019.06.051 (PMID: 31427258) [Crossref]
18. Uenak, P. Nuclear applications in life sciences. National Nuclear Science and Technologies Congress Proceedings Full Texts. 2009; 1: 387. [Crossref]
19. Gündoğdu EA, Özgenç E, Ekinci M, Özdemir ID, Aşıkoğlu M. Nükleer Tıpta Görüntüleme ve Tedavide Kullanılan Radyofarmasötikler. *Türkiye Klinikleri J Pharm Sci* 2017. [Crossref]
20. Yong K, Brechbiel MW. Towards translation of ²¹²Pb as a clinical therapeutic; getting the lead in! *Dalton Trans* 2011; 40: 6068-6076. (PMID: 21380408) [Crossref]
21. Ertay T. New radiopharmaceuticals and preclinical Imaging. *Nuc Med Semin* 2019; 5: 1-9. doi:10.4274/nts.galenos.2019.0001 [Crossref]
22. Jadvar H. Targeted α -therapy in cancer management: synopsis of preclinical and clinical studies. *Cancer Biother Radiopharm* 2020; 35: 475-484. (PMID: 32202923) [Crossref]
23. Lakhtakia R, Burney I. A brief history of breast cancer: part III -tumour biology lays the foundation for medical oncology. *Sultan Qaboos Univ Med J* 2015; 15: 34-38. (PMID: 25685382) [Crossref]
24. Fisusi FA, Akala EO. Drug combinations in breast cancer therapy. *Pharm Nanotechnol* 2019; 7: 3-23. (PMID: 30666921) [Crossref]
25. Yin G, Zeng B, Peng Z, Liu Y, Sun L, Liu C. Synthesis and application of ¹³¹I-fulvestrant as a targeted radiation drug for endocrine therapy in human breast cancer. *Oncol Rep* 2018; 39: 1215-1226. (PMID: 29328488) [Crossref]
26. Akram M, Iqbal M, Daniyal M, Khan AU. Awareness and current knowledge of breast cancer. *Biol Res* 2017; 50: 33. (PMID: 28969709) [Crossref]
27. Healthline. History of Breast Cancer, April 2017, Available from: <https://www.healthline.com/health/history-of-breast-cancer> [Crossref]
28. Luo TY, Tang IC, Wu YL, Hsu KL, Liu SW, Kung HC. Evaluating the potential of ¹⁸⁸Re-SOCTA-trastuzumab as a new radioimmunoagent for breast cancer treatment. *Nucl Med Biol* 2009; 36: 81-88. (PMID: 19181272) [Crossref]
29. Yook S, Cai Z, Lu Y, Winnik MA, Pignol JP, Reilly RM. Radiation nanomedicine for egfr-positive breast cancer: panitumumab-modified gold nanoparticles complexed to the β -particle-emitter, (¹⁷⁷)Lu. *Mol Pharm* 2015; 12: 3963-3972. (PMID: 26402157) [Crossref]
30. Yook S, Cai Z, Lu Y, Winnik MA, Pignol JP, Reilly RM. Intratumorally injected ¹⁷⁷Lu-labeled gold nanoparticles: gold nanoseed brachytherapy with application for neoadjuvant treatment of locally advanced breast cancer. *J Nucl Med* 2016; 57: 936-942. (PMID: 26848176)
31. Goldenberg DM. Targeted therapy of cancer with radiolabeled antibodies. *J Nucl Med* 2002; 43: 693-713. (PMID: 11994535) [Crossref]
32. Cędrowska E, Pruszyński M, Gawęda W, Żuk M, Krysiński P, Bruchertseifer F, et al. Trastuzumab conjugated superparamagnetic iron oxide nanoparticles labeled with ²²⁵Ac as a perspective tool for combined α -radioimmunotherapy and magnetic hyperthermia of HER2-positive breast cancer. *Molecules* 2020; 25: 1025. (PMID: 32106568) [Crossref]

33. Morgenroth A, Tinkir E, Vogg ATJ, Sankaranarayanan RA, Baazaoui F, Mottaghy FM. Targeting of prostate-specific membrane antigen for radioligand therapy of triple-negative breast cancer. *Breast Cancer Res* 2019; 21: 116. (PMID: 31640747) [\[Crossref\]](#)
34. Hernandez R, Grudzinski JJ, Aluicio-Sarduy E, Massey CF, Pinchuk AN, Bitton AN, et al. ¹⁷⁷Lu-NM600 targeted radionuclide therapy extends survival in syngeneic murine models of triple-negative breast cancer. *J Nucl Med* 2020; 61: 1187-1194. (PMID: 31862799) [\[Crossref\]](#)
35. Hagemann UB, Ellingsen C, Schuhmacher J, Kristian A, Mobergslie A, Cruciani V, et al. Mesothelin-targeted thorium-227 conjugate (MSLN-TTC): preclinical evaluation of a new targeted alpha therapy for mesothelin-positive cancers. *Clin Cancer Res* 2019; 25: 4723-4734. (PMID: 31064781) [\[Crossref\]](#)
36. Thorek DLJ, Ku AT, Mitsiades N, Veach D, Watson PA, Metha D, et al. Harnessing androgen receptor pathway activation for targeted alpha particle radioimmunotherapy of breast cancer. *Clin Cancer Res* 2019; 25: 881-891. (PMID: 30254080) [\[Crossref\]](#)
37. Gibbens-Bandala B, Morales-Avila E, Ferro-Flores G, Santos-Cuevas C, Meléndez-Alafort L, Trujillo-Nolasco M, et al. ¹⁷⁷Lu-Bombesin-PLGA (paclitaxel): a targeted controlled-release nanomedicine for bimodal therapy of breast cancer. *Mater Sci Eng C Mater Biol Appl* 2019; 105: 110043. doi: 10.1016/j.msec.2019.110043 (PMID: 31546458) [\[Crossref\]](#)
38. Kasten BB, Oliver PG, Kim H, Fan J, Ferrone S, Zinn KR, et al. ²¹²Pb-labeled antibody 225.28 targeted to chondroitin sulfate proteoglycan 4 for triple-negative breast cancer therapy in mouse models. *Int J Mol Sci* 2018; 19: 925. (PMID: 29561763) [\[Crossref\]](#)
39. Costa RP, Tripoli V, Princiotta A, Murabito A, Licari M, Piazza D, et al. Therapeutic effect of ²²³Ra in the management of breast cancer bone metastases. *Clin Ter* 2019; 170: e1-e3. doi: 10.7417/CT.2019.2100 (PMID: 30789190) [\[Crossref\]](#)
40. Juzeniene A, Bernoulli J, Suominen M, Halleen J, Larsen RH. Antitumor activity of novel bone-seeking, α -emitting ²²⁴Ra-solution in a breast cancer skeletal metastases model. *Anticancer Res* 2018; 38: 1947-1955. (PMID: 29599310) [\[Crossref\]](#)
41. Cai Z, Yook S, Lu Y, Bergstrom D, Winnik MA, Pignol JP, et al. Local radiation treatment of HER2-positive breast cancer using trastuzumab-modified gold nanoparticles labeled with ¹⁷⁷Lu. *Pharm Res* 2017; 34: 579-590. (PMID: 27987070) [\[Crossref\]](#)
42. Cai Z, Chattopadhyay N, Yang K, Kwon YL, Yook S, Pignol JP, et al. ¹¹¹In-labeled trastuzumab-modified gold nanoparticles are cytotoxic *in vitro* to HER2-positive breast cancer cells and arrest tumor growth *in vivo* in athymic mice after intratumoral injection. *Nucl Med Biol* 2016; 43: 818-826. (PMID: 27788375) [\[Crossref\]](#)



Oncoplastic Breast-Conserving Surgery According to Tumor Location

Nuh Zafer Cantürk¹, Turgay Şimşek¹, Sibel Özkan Gürdal²

¹Department of General Surgery, Kocaeli University School of Medicine, Kocaeli, Turkey

²Department of General Surgery, Tekirdağ University School of Medicine, Tekirdağ, Turkey

ABSTRACT

The use of oncoplastic breast surgery is an essential cornerstone for breast cancer management. The main aim of breast cancer surgery is to obtain an adequate oncological safety margin. Still, the cosmetic outcome also seems important for social and psychological wellbeing and quality of life. After breast-conserving surgery, the remaining breast may be reconstructed with volume displacement or volume replacement techniques. A better cosmetic outcome can be achieved by selecting appropriate surgical techniques according to tumor location. In this review, we show each technique step-by-step based on the tumor's location for each quadrant. The most important thing is to select the technique first for oncological safety and then for better cosmesis.

Keywords: Breast-conserving surgery, breast neoplasms, oncoplastic surgery

Cite this article as: Cantürk NZ, Şimşek T, Özkan Gürdal S. Oncoplastic Breast-Conserving Surgery According to Tumor Location. Eur J Breast Health 2021; 17(3): 220-233

Key Points

- Oncoplastic breast surgery aims to perform breast cancer treatment without deviating from the oncological principles
- The oncoplastic surgical methods selected vary by the location of the tumor.
- Level II oncoplastic breast surgery may be performed for the necessity of 20%–50% of breast tissue excision during the partial mastectomy in moderate- to large-sized breasts with moderate to severe ptosis.
- Techniques of Oncoplastic Breast-Conserving Surgery for the Upper or Central Breast Tumors are Crescent mastopexy, batwing or hemi batwing mastopexy, donot mastopexy, Grisotti or Racket mastopexy.
- Techniques of Oncoplastic Breast-Conserving Surgery for the Lower Quadrant Breast Tumors are triangular resection, inframammary resection, J, V or S mastopexy and reduction mammoplasty.
- In literature, there is no difference in surgical complications when compared OPS and breast-conserving surgery.

Introduction

Following oncoplastic breast-conserving surgery, the postoperative success rate is mainly related to appropriate patient selection, proper planning, a systematic examination, and preoperative drawing. Patients must be informed about the operative processes, postoperative outcomes, and possible complications.

The basics of oncoplastic surgery (OPS) stand on “primum nil nocere,” which is also essential to general medicine. At every step, the patient's demands must be considered and noted in her file. Also, the following questions must be answered.

- Is the patient appropriate for breast-conserving surgery?
- Does the patient have diabetes mellitus or any other comorbidity that would delay wound healing?
- Is there any addictive habit, including smoking, alcohol consumption, or other?
- Does the patient have any previous wound healing problems, such as keloid formation?
- Is there any previous breast surgery history or scar in the operation field?
- Is there any neoadjuvant chemotherapy history or malnutrition signs and symptoms? (1-3).

Corresponding Author:
Nuh Zafer Cantürk; canturkz@yahoo.com

Received: 19.01.2021
Accepted: 28.03.2021

Oncoplastic breast surgery aims to perform breast cancer treatment without deviating from the oncological principles and making the patient feel better by providing a better appearance. The indication of treatment is identified by the following:

- patients request,
- tumor characteristics,
- size and shape of the ipsilateral and contralateral breast,
- experience of the surgeon (4).

Understanding the patient's perspectives and sharing decision-making with her is critical.

First, surgeons must foster a comfortable setting. They should introduce themselves and their teams which helps them while providing the details on their skills. Surgeons must explain why they need to learn not only conditions related to the patient's disease but other personal issues. Also, surgeons need to take some measurements of her breast and take images of her breast and body naked. In addition, the surgeon has to provide her a chance to ask questions about the operative techniques, unexpected results, and complications. Surgeons should discuss with the patient a warranty for taking care of her, paying extreme attention to her individual preferences, allowing her to think about what to do and what she prefers before proceeding.

Next, surgeons need to determine what she knows about breast cancer and then offer options according to OPS standards.

During this step, if needed, surgeons can recommend neoadjuvant treatment. They must pay attention to making scars as small as possible with minimal asymmetry during one-stage breast reconstruction preferred or delayed reconstruction if post-mastectomy radiotherapy is required. So, surgeons will give the patient the chance to understand their aim to maximize reshaping. Surgeons must assist the patient with decision-making by providing the patient with a description of options and then summarizing everything.

In the last step, surgeons must analyze the patient's values and preferences. It is essential to remember that patients typically want fewer scars, the shortest hospitalization, less foreign materials, the lowest complication risk, a suitable and natural-looking appearance when naked, and the fewest number of surgeries. Surgeons must inform the patient that she can defer her decision, or if decided, she can change her mind before the operation without hesitation. This flexibility will build confidence and trust between the patient and surgeon. On the other hand, there are still some challenges about sharing decision-making. These are patient's reticents about deciding, difficulties understanding options, socioeconomic barriers, and request against evidence (1, 4-6).

The oncoplastic surgical methods selected vary by the tumor's location. Although radial ellipse segmentectomy and circumareolar segmental resection methods may be used for a tumor located in any breast region, more appropriate surgeries may be preferred by the tumor's location (1). Technique selection based on location is shown in Table 1. Surgeons should select the round block and batwing techniques for superior-medial quadrant lesion; lateral mastopexy for superior-lateral quadrant lesions, V mammoplasty for inferior medial and J-mammoplasty for inferolateral quadrant lesions, round block and inferior pedunculated mastectomy for lesions between the upper medial and lateral quadrant, and superior pedunculated mastectomy between the inferior medial and lateral quadrant lesions. Oncoplastic techniques, proposed by the French surgeon Krishna Clough, can include level I and level II OPS. Level I oncoplastic breast surgery is defined as the excision of less than 20% of the breast volume during breast-conserving surgery in small- to moderate-sized breasts with minimal ptosis (7).

In contrast, Level II oncoplastic breast surgery is defined as the necessary excision of 20% to 50% of the breast tissue during partial mastectomy in moderate- to large-sized breasts with moderate-to-severe ptosis. If the breasts' maximum excision volume is less than 20%

Table 1. Quadrant per quadrant techniques preferred

Location	Size of breast		
	Small	Medium	Large
Upper			
• Outer quadrant	Round block	Round block, inferior pedicle reduction	Round block, inferior pedicle reduction
• Middle quadrant	Round block Batwing	Round block, inferior pedicle reduction Batwing	Round block, inferior pedicle reduction
• Inner quadrant	Round block	Round block, inferior pedicle reduction	Round block, inferior pedicle reduction
Lower			
• Outer quadrant	Grisotti	Superior pedicle reduction, Grisotti, J mammoplasty	Superior pedicle reduction, inferior pedicle reduction
• Middle quadrant	Superior pedicle reduction, Grisotti	Superior pedicle reduction, Grisotti, triangular resection	Superior pedicle reduction, Grisotti, triangular resection
• Inner quadrant	Grisotti, triangular resection, inframammarian resection	Superior pedicle reduction, Grisotti, V mammoplasty	Superior pedicle reduction, inferior pedicle reduction, inframammarian resection
Central	Batwing, central, quadraneotomy	Grisotti, Batwing, inferior pedicle reduction	Inferior pedicle reduction, inverted T resection, Grisotti

and skin excision for reshaping and mammoplasty is not a necessity, it is called Level I. In contrast, Level II oncoplastic breast surgery excises more than 20% of breast tissue with skin and mammoplasty for moderate- to large-sized breasts with moderate-to-severe ptosis for breast cancer treatment (4, 8).

Level I OPS

One of the crucial points for Level I OPS techniques is having a sufficient amount of subcutaneous undermining. For undermining, the mastectomy plane must be followed and extended from one-fourth to two-thirds of the breast's surface area. It helps to both resect and redistribute the glandular tissue after the tumor excision. The recommended approach is to perform a full-thickness excision from the subcutaneous fat to the pectoralis fascia to ensure free anterior and posterior margins. The excision is made in a fusiform pattern for a better orientation toward the nipple-areolar complex (NAC) and easy re-approximation. Extensive tissue resection leads to NAC deviation. For both levels I and II OPS, a complete transection of the terminal ducts and separation of the NAC from the underlying tissue with 0.5–1 cm width to ensure vascularization. The tissue must be mobilized from the remaining breast's lateral positions or recruited from the breast's central portion (Figure 1) (9-12).

Level II OPS

Oncoplastic Breast-Conserving Surgery for Upper or Central Breast Tumors

Crescent Mastopexy Resection

Location and indication

It is suitable for a superior central tumor that does not involve the nipple or areola. The ideal lesion for this method is a lesion located between the periareolar ten to one o'clock position. Using this procedure in more medial or lateral lesions is not recommended because it may change the NAC's position.

Technique

An incision parallel to the areola is made to resect the skin and glandular tissue surrounding the mass with wide macroscopic margins on the breast. The incision is resected up to the pectoralis muscle in the presence of a small breast and large lesion. However, the procedure may be performed with a more superficial incision on a large breast because the two margins' approximation is more straightforward. The wound closure may be accomplished by approximating the superior and inferior dermoglandular edges in the retro-areolar fatty region to enable closure of the glandular tissue and skin (Figure 2) (13).

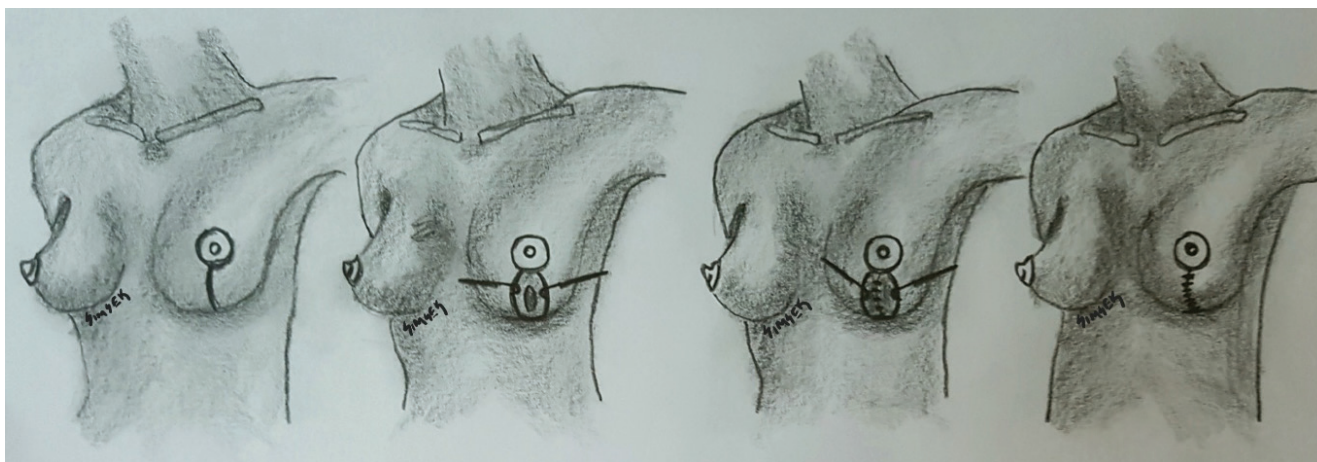


Figure 1. Step by step Level I Oncoplastic Breast Surgery (Drew by Turgay Şimşek)

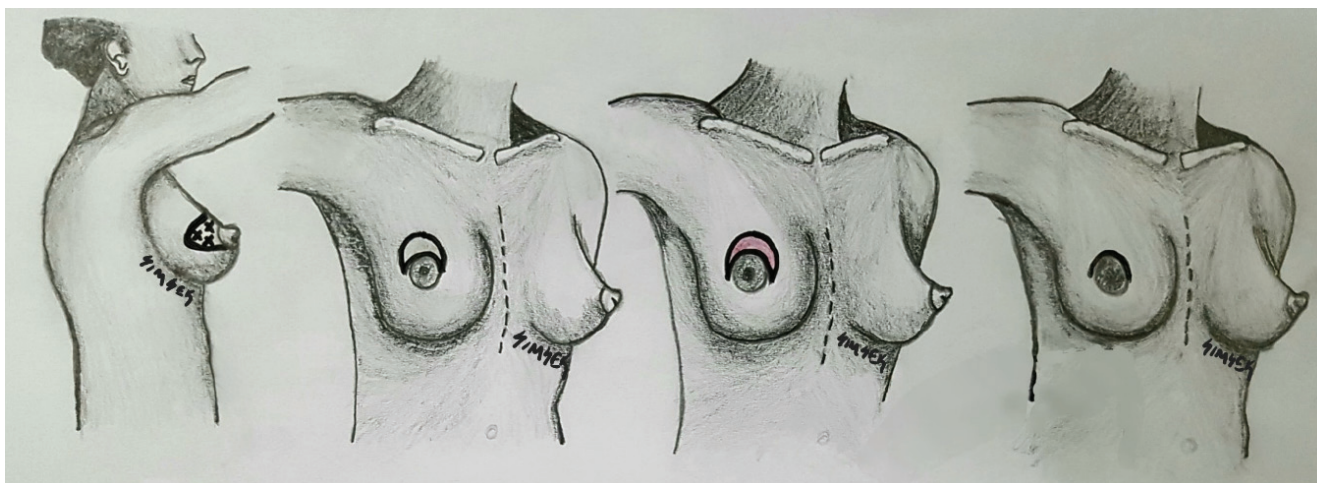


Figure 2. Crescent Mastopexy (Drew by Turgay Şimşek)

Batwing Resection

Location and indication

Batwing resection is used for wider excisions of the upper central regions within a few centimeters of the nipple but does not involve the nipple. Unlike crescent mastopexy, breast surgeons usually prefer to use this technique or hemibatwing resection when the areola is smaller and the tumor is more extensive.

Technique

Arches and wings parallel to the areola are drawn to provide triangular sections on both edges in addition to two rings as in the crescent incision, and then the incision is performed. Next, a full-thickness fibroglandular resection is extended to the chest wall to include the mass. It is essential to avoid performing a suture on the chest wall. However, bilateral closure of the released deep tissues is performed using absorbable sutures. The superficial tissues are closed as in the lumpectomy. The main problem with this technique is the unilateral nipple elevation and asymmetry. The correction procedures may be performed on the non-cancer breast to avoid this problem (Figures 3, 4) (13, 14).

Hemibatwing Resection

Location and indication

This method's optimal condition is the wide excision of superior outer periareolar lesions similar to 9–10 (on the right) or 2–3 (on the left)

o'clock. This method is not the preferred method for medial lesions because of possible visible scars.

Technique

A triangular excision is performed only on a single side. This is the difference between the hemibatwing resection and the batwing resection (Figure 5) (13).

Donut Mastopexy Resection (Round Block Technique)

Location and indication

Surgeons prefer this technique to treat tumors located in the upper and lateral quadrants. It is a beneficial technique for long and narrow segment resections of the breast. Its disadvantage is that the areolar complex and the nipple-areolar region will be denervated when the full-thickness skin excision is performed.

Technique

A second circular incision is performed in the areola's surrounding area and opening, and the ring-shaped skin in between is excised in full or partial thickness. Thus, access to approximately every section of the breast is enabled by subcutaneous releasing. The breast portions are closed using a 2-0 absorbable suture after the required resection is completed. Subcutaneous purse-string continuous sutures are used on the outer skin incision and are narrowed, and a new areolar margin is generated by suturing the two-incision sections (Figure 6) (15-17).

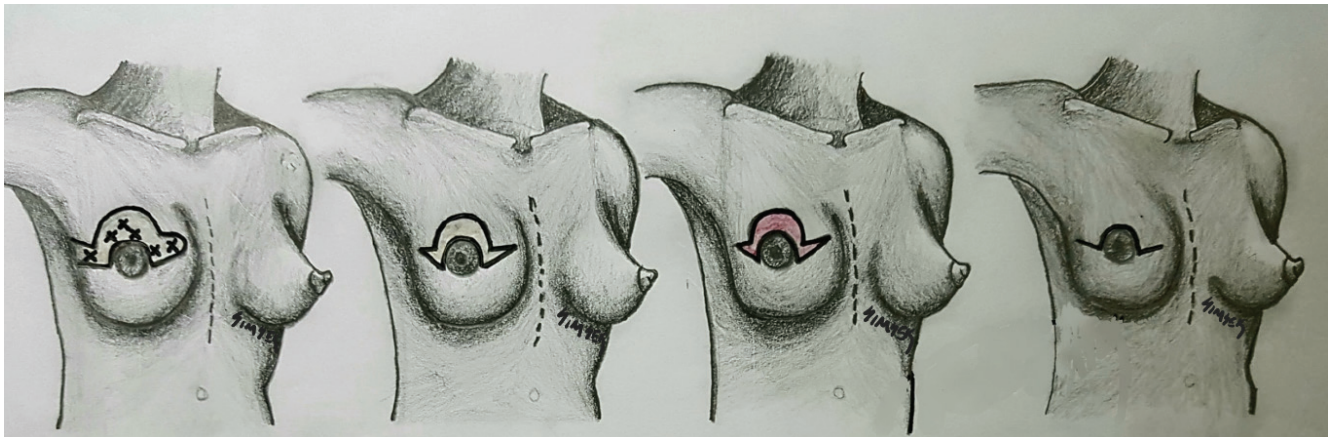


Figure 3. Batwing mammoplasty (Drew by Turgay Şimşek)

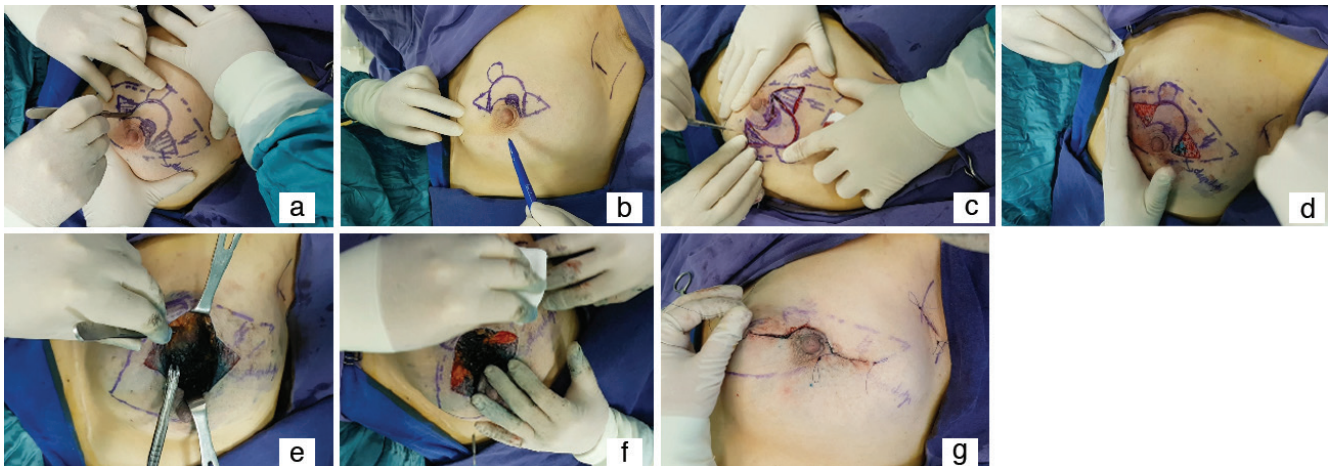


Figure 4a-g. Batwing procedure a-b) drawing c-f) excision, de-epithelization and preparation new nipple localization g) closing of incision

B-Flap Resection (Grisotti Mastopexy Technique)

Location and indication

This method is ideal for reconstructing the central breast when NAC resection is required because of the tumor's proximity in women with sufficient breast volume and moderate breast ptosis.

Technique

The NAC is resected until reaching the pectoral fascia. The breast tissue and the skin section in the shape of the areolar region from the lower quadrant are repositioned to the areola (new areola) as the inferior pedicle in this method, referred to as the B-flap resection. Also, the nipple formation and areola tattoo may be performed later (Figures 7, 8) (18-21).

Central Quadrantectomy

Location and indication

Apart from other techniques for centrally located lesions explained above, this technique is preferred for centrally located lesions in patients with widely ranging breast sizes.

Technique

The circumareolar incision includes 50% of the areola in this method and may be used mainly in women with larger breasts. The nipple-areola is preserved relatively thick for adequate vascular supply and nutrition in this method. The entire region behind it, which might have been marked using localizing wires, is resected in a cylinder shape from the subareolar plane to the pectoral muscle. Dissection of the subareolar plane can be extended in all directions to separate the areolar skin from the central gland. The tissue and skin layers are then closed by the tissues' approximation using 2–3 layers of several purse-string sutures (18, 19).

Racquet Mammoplasty

Location and indication

Breast-conserving surgery can easily excise large tumors in the upper outer quadrant without any deformity. More than a 20% excision of the breast may cause a deformity in small- or medium-sized breasts.

Technique

First, the NAC's circular line, another circular line situated 1–2 cm away from the NAC line, and a wedge-shaped line extending from

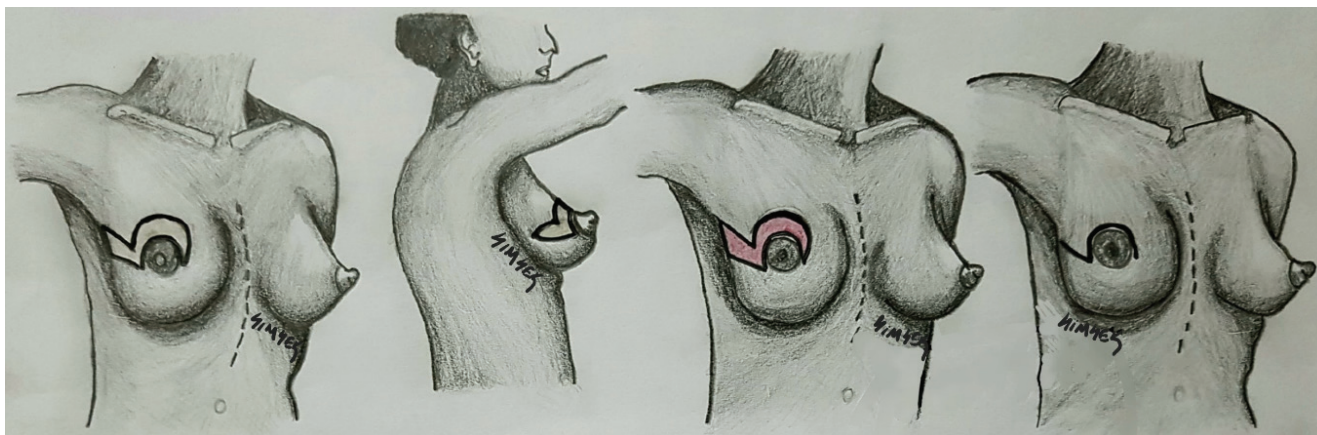


Figure 5. Hami- Batwing mammoplasty (Drew by Turgay Şimşek)

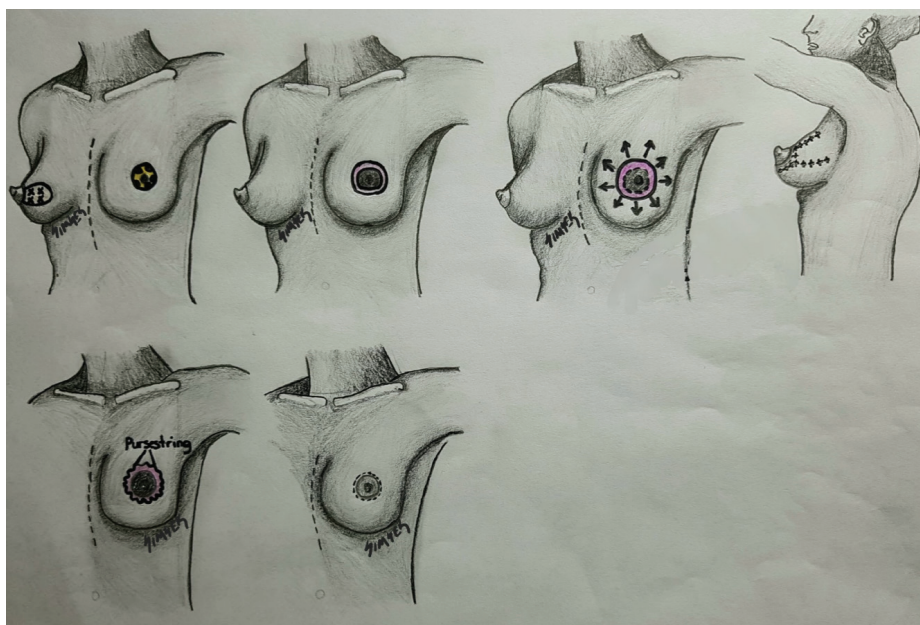


Figure 6. Donut mastopexy (Drew by Turgay Şimşek)

the areola to the axilla, are drawn and then incised. The next step is excision of the tumor, surrounding glandular tissue, and the pectoralis fascia with a wedge-shaped incision and de-epithelization between two circular lines around the NAC. Undermining the skin flap from the glandular tissue is the initial procedure. After that, the medial and lateral glandular tissue is mobilized from the pectoralis muscle. Following these procedures, four to six marking clips should be placed at the cavity's base. Both epithelial tissues are reapproximated with interrupted absorbable sutures to close the hole. If needed, the central gland could be undermined by the NAC. The subcutaneous tissue and the skin over the cavity are closed with absorbable sutures (Figure 9) (22, 23).

Oncoplastic Breast-Conserving Surgery for Lower Quadrant Breast Tumors

Triangular Resection

Location and indication

Cosmetic problems, such as a “bird beak” deformity, may develop after the tumors' excision is located in the breast's lower quadrants. However, the breast's lower pole may be reformed with the surrounding tissues' dislocating to the lumpectomy cavity. Relatively larger lesions located in that region may also be resected with this technique in which the total thickness wedge-shaped skin specimen and glandular tissue are resected.

Technique

- A triangular or wedge incision is made on the skin of the lesion in the breast.
 - The base of the triangle corresponds to the inframammary fold, and the apex points upward; however, it should not exceed the inferior areolar margin.
- The underlying glandular tissue is resected toward the chest wall after the skin is passed through.
 - The dissection plane during the resection is widened. It is completed on the surface of the serratus anterior muscle or through the incision of the rectus fascia toward the inframammary fold.
 - The rectus fascia and serratus anterior may be resected to ensure a negative deep surgical border posterior to the specimen if required.
 - Surgeons must generate a perpendicular glandular dissection plane compared with the skin to allow for the surgical margin. Surgeons must pay attention to avoid the specimen's excessive traction during dissection, resulting in the unintended dissection of tissue below the nipple and normal glandular tissue.
- The surrounding lower outer and lower inner quadrant glandular tissues are approximated in full-thickness on wound closure.
 - This is accomplished by extending the inframammary fold incision toward the breast's medial and lateral edges.

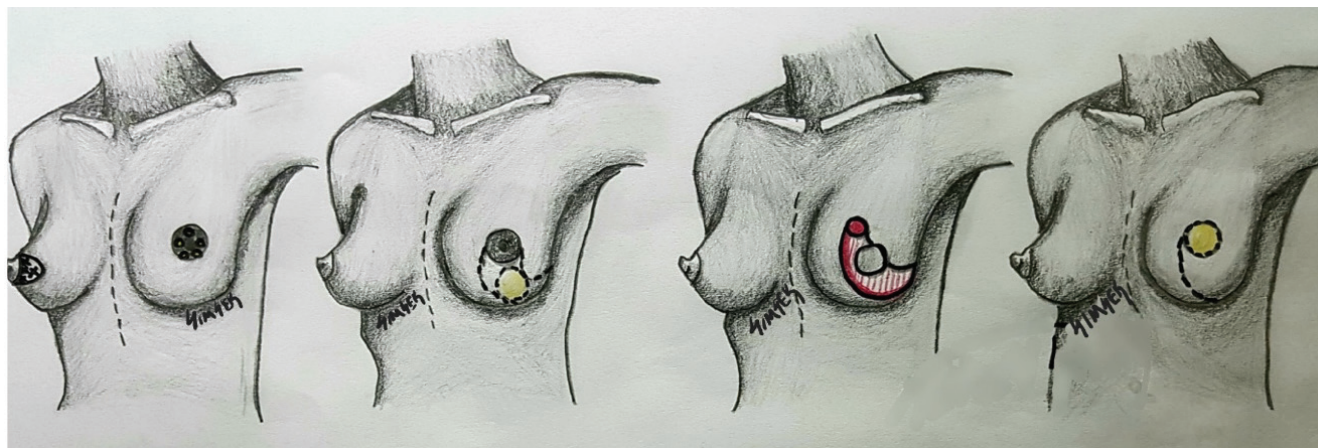


Figure 7. Step by step Grisotti Flap (Drew by Turgay Şimşek)

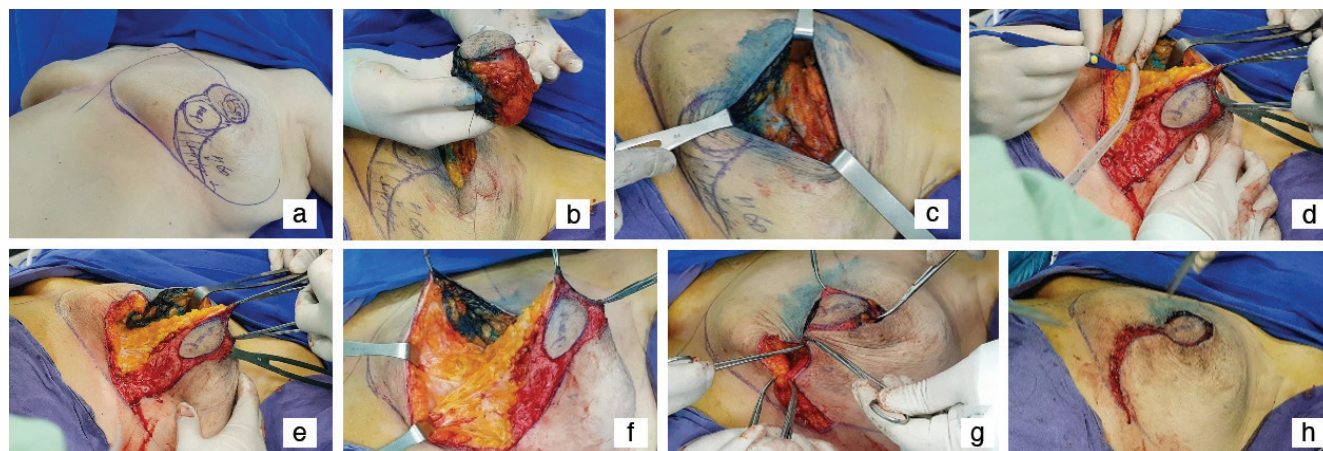


Figure 8a-h. Grisotti Flap preparation and operation processes a) drawing b-f) excision, de-epithelization and preparation new nipple localization g-h) closing of incision

- o The generated dermoglandular flaps are approximated layer-by-layer using 2-0 or 3-0 absorbable sutures.
- o The length discrepancy between the breast and inframammary fold edges may be overcome using a skin stapler with the redistribution of the short edge along the long edge.
- o The incision to be performed on the inframammary fold may be extended laterally and medially to enable more mobilization to the dermoglandular flap and avoid excessive tension on the breast skin's edges.
- The inframammary fold is closed using multiple layers by approximating the breast's fibrous and glandular tissues with the inframammary fold fibrous tissue.
- Then, the skin closure is completed using a smaller suture material (Figure 10) (4, 13).

Inframammary Resection

Location and indication

This technique is a suitable incision to resection tumors located in the lower and posterior breast regions. The resection is performed from an incision applied to the inframammary fold hidden below the breast. The inframammary approach is not recommended for removing the superficially located breast cancers to decrease the positive surgical border risk because the skin corresponding to the lesion is preserved. The surgeon must have the opportunity to perform marking using multiple wires or intraoperative ultrasonography to ensure that the malignancy is resected with an adequate surgical border while performing the resection using the indirect or "back door" approach.

Technique

- The incision is performed on the inframammary fold in the inframammary approach and maintains through the subcutaneous and fibrous layers toward the thoracic wall.

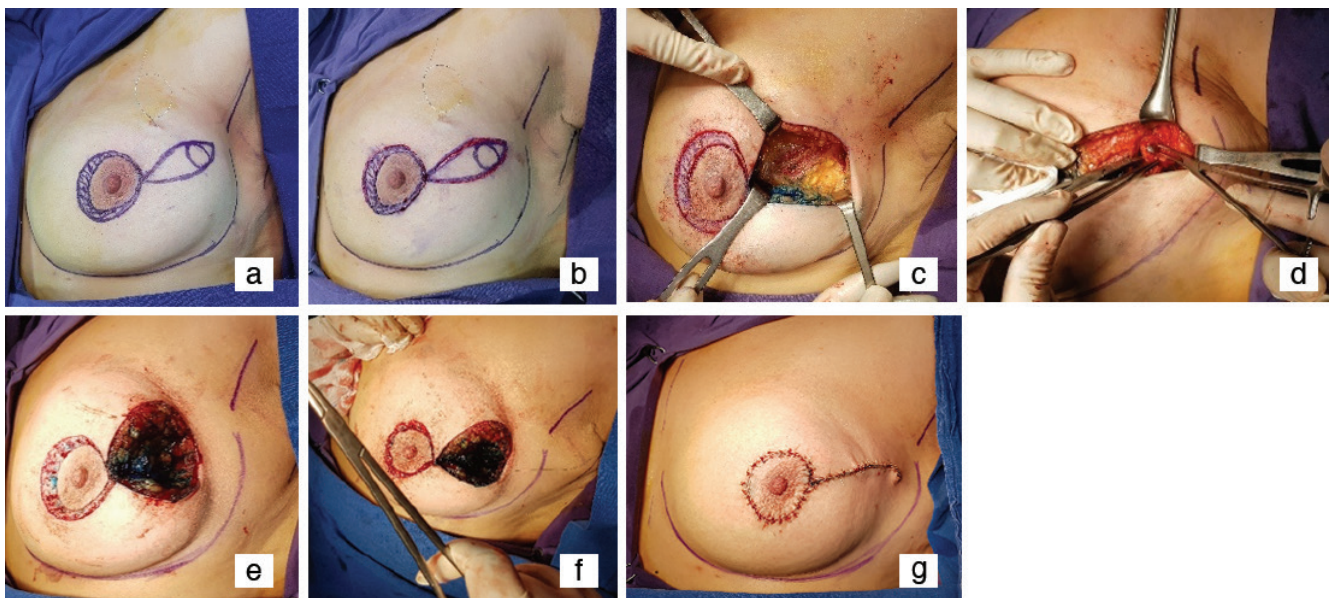
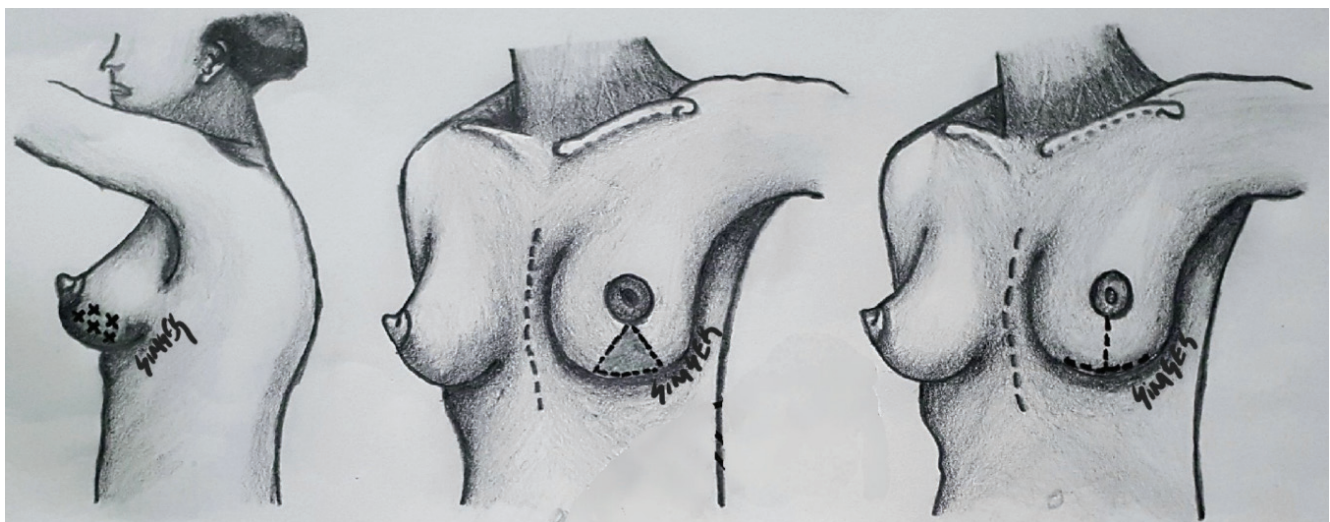


Figure 9a-g. Rocket Mammoplasty a, b) drawing c-f) excision and de-epithelization g) closing of incision



o The incision length depends partially on the lesion size, location, the mobilization required to access the lesion and close the surgical cavity.

♣ The larger lesions located in the upper parts will require a longer incision to access the breast's upper sides.

♣ The smaller and more distally located lesions may be accessed using a shorter incision on the medial, central, and lateral inframammary folds.

♣ The incision is made on the breast's posterior on the lesion perimetry and is extended toward the anterior for a broader resection of the tumor with possible superficial borders.

• The dissection is performed toward the retro-mammary fatty plane at least 3 cm above the tumor. The bimanual examination identifies the position, skin markings, wire markings, ultrasound, or the combination of all methods.

o The anterior of the lesion is more easily cleaned with the wires placed just above the lesion.

o The wire must be placed inside the gland when wire marking is used.

o The end of the wire must show the breast's posterior surface in the surgical cavity.

• The muscle fascia must also be resected with the surrounding tissues for deeper lesions.

• The wound closure is initiated with the approximation of the surgical borders to the cavity for decreasing or preventing skin retraction. This step is performed relatively more easily on breasts which are mobilized significantly wider from the chest wall. However, if additional mobilization is required, the dissection of the retro-mammary fatty plane or subcutaneous tissue plane may be performed to accomplish cavity closure.

• Finally, wound closure is completed with the approximation of the inframammary tissues using 2-0 or 3-0 absorbable sutures following the layered closure with smaller absorbable sutures (Figure 11) (13).

J-Mammoplasty

Location and indications

When the tumor is located in the lower inner or outer breast quadrants, the inverted T mammoplasty is not always appropriate.

Filling of the excision cavity with glandular flap in these locations is not comfortable with this technique. A tumor at the 4–5 o'clock position for the left breast is optimally managed with J-mammoplasty. A J-mammoplasty provides a chance to avoid lateral breast retraction and NAC deviation due to classical breast-conserving surgery. This technique is recommended for large, lower, outer quadrant tumors and tumors with extensive ductal carcinoma *in situ* and/or multifocality.

Technique

Two circular lines around NAC are prepared. The first line is located at the border of NAC, and the other is situated 1–2 cm away from it. The skin in between the two lines must be de-epithelized so that the tumor with its surrounding glandular tissue is excised with the skin, subcutaneous tissue, and pectoralis fascia. The incision patterns should be J-shaped for the left breast and reverse J-shaped for the right breast. After excision, the medial and lateral glandular tissue from the pectoralis muscle without skin undermining is necessary for closing the defect. It is necessary to monitor the tension during these procedures. After placing four to six marking clips, the skin is reapproximated with interrupted absorbable sutures. Rarely seen complications include hematomas, infections, skin necrosis, and wound dehiscence (Figure 12) (24, 25).

V-Mammoplasty

Location and indications

Breast conservation in the lower inner quadrant is a challenge and usually requires level II OPS to prevent deformities and poor outcomes. A V mammoplasty can be recommended as a solution for a lower inner quadrant tumor instead of the Wise pattern reduction mammoplasty or, else, a mastectomy. This technique is suitable for medium- or large-sized breasts with a broad base.

Technique

Breast mobilization and extensive posterior undermining of the lower gland can be performed through an inframammary incision. The tumor and surrounding breast tissue are removed en bloc with the overlying skin down to the pectoralis fascia. It is pyramidally excised with the apex located at the areola and its base in the inframammary fold's medial portion. Surgical clips are placed to

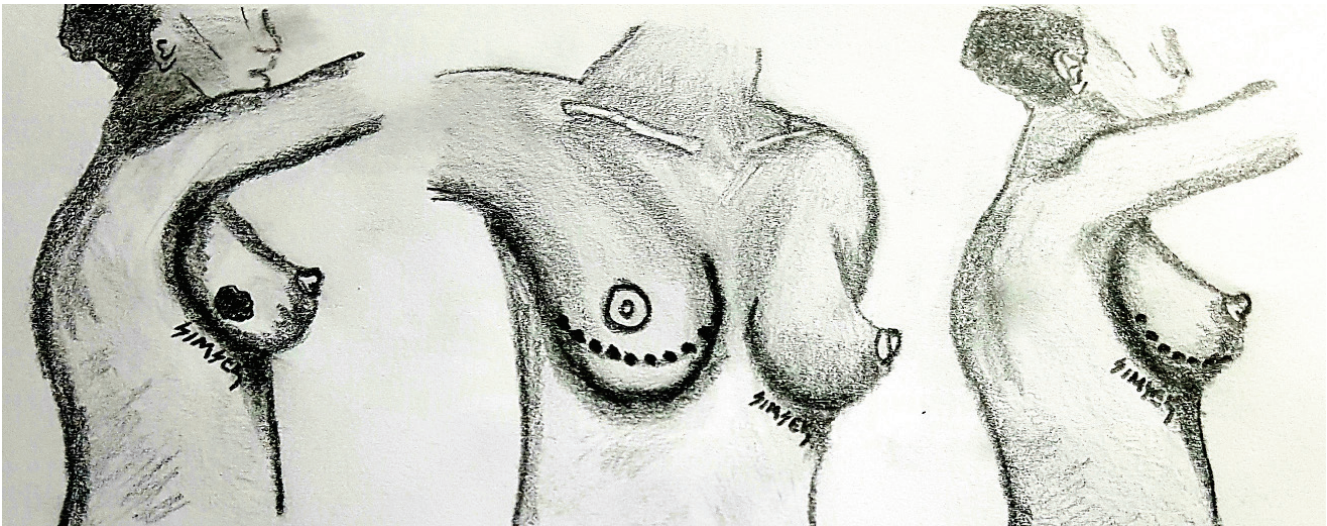


Figure 11. Inframammary resection (Drew by Turgay Şimşek)

mark the tumor as usual. The inframammary fold incision's lateral limit should be extended to at least 4 o'clock for the left breast. For selected cases, it can be extended to 3 or 2 o'clock in the lateral fold. So, you can mobilize more breast tissue medially and prevent tension on the incision without doing any additional skin undermining. Then, the NAC can be repositioned with the patient placed in the sitting position for an accurate comparative evaluation of the breast and the NAC symmetry. The NAC is recentralized directly opposite the initial tumor position by de-epithelizing the upper outer periareolar skin (26) (Figure 13).

S-Mammoplasty

Location and indications

This technique is recommended to young patients with plump breasts with mild to moderate ptosis and hypertrophy and lesions located in the lower quadrant. It is contraindicated for older patients with flaccid skin, Breast Imaging-Reporting and Data System I glandular tissue density, severe ptosis, large breasts, and tumors located in the NAC or upper quadrant.

Technique

After obtaining written informed consent and performing preoperative imaging, the midclavicular, midsternal, and inframammary lines are marked and drawn in the standing and sitting positions.

- Mark the midsternal and then the midclavicular point and draw the lines from top to bottom.

- Prepare a new site for the NAC at 18–22 cm on the breast meridian from the midclavicular point and 9–11 cm away from the midsternal line.

- Delineate the original NAC by marking A, B, C, and D at 12, 3, 9, and 6 o'clock around it.

- Draw the upper part of the new NAC parallel to the original one through points A1, B1, and C1.

- Mark, each of the new NAC points D1 and D2 with a 7–8 cm distance to point D, making the new NAC 4 cm above the inframammary fold and 18–21 cm lateral to the sternal notch along the nipple line. Mark point E on the inframammary line.

- The distance between A1-B1, A1-C1, and D2-E should be equal to those of B1-D2, C1-D1, and D1-E, respectively.

- De-epithelize the area between A, B, C, and A1, B1, and C1.

- A tumor located under the old NAC can be resected with the surrounding normal breast tissue. The wedge resection of the expected volume of lower breast tissue is made, and removal of more than the whole hemisphere is achieved.

- First, approximate the bilateral glandular tissues and suspend them to the fifth rib periosteum transversely above the inframammary fold with three large nonabsorbable sutures through the pectoralis muscle.

- Then, the new NAC can be approximated with a purse-string suture. The excess skin flap is minimal and well-tailored (Figure 14).



Figure 12a-d. J Mammoplasty a) drawing b) excision and c-d) closing of incision

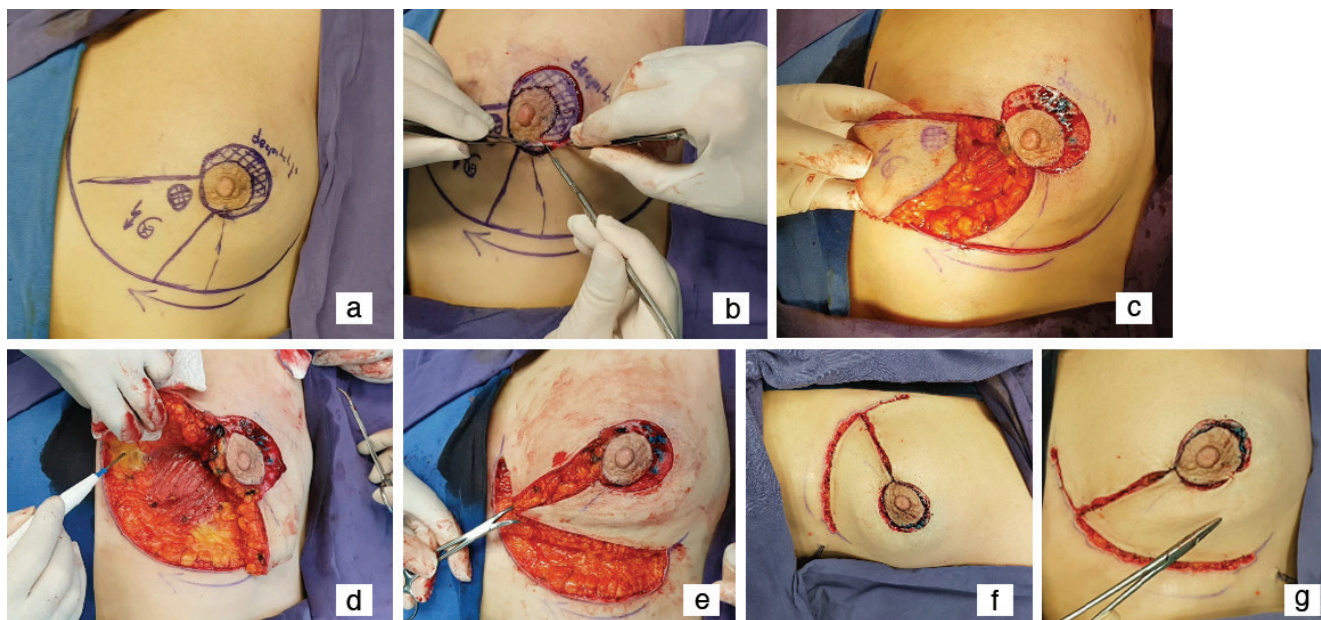


Figure 13a-g. V mammoplasty a) drawing b) de-epithelization, c, d) excision and e-g) closing of incision

A mild comprehensive dressing is recommended for about three days, and a post-mammoplasty garment and gentle massage are warranted for at least six months (27, 28).

Reduction Mammoplasty (RM)

Resection with reduction mammoplasty (RM) is a procedure that combines performing reduction mammoplasty and wide local tumor excision in a patient who requires breast reduction. RM resection, one of the more complex oncoplastic breast preserving procedures, should not be performed by surgeons who have inadequate plastic or OPS training. The reason for mentioning this issue is to provide an overview of the wide range of possibilities for surgeons who received or who will receive their training in OPS. Resection with RM may be accomplished by preserving or not preserving the nipple by the tumor region. When the NAC is maintained, the new nipple location is completed with the dislocation of the NAC to a more anterior and superior region.

The advantages of RM include:

1. Enabling the resection of larger masses with a wider local excision compared with the standard lumpectomy,
2. Enabling breast reconstruction, hiding more comprehensive segmental defects and providing aesthetic breast concavity. This approach also enables the resection of lesions, particularly at 4–8 o'clock level, in addition to retro-areolar or supra-areolar lesions.

The main goal of reduction techniques is to preserve the NAC's vascular nutrition and the residual breast.

1. The first technical issue in RM is incision planning. Although the conventional approach is a "Wise pattern" incision, the vertical reduction has become increasingly popular.

- "Wise pattern" is closed in the shape of the classic inverted T and generates the inferior dermoglandular pedicle base.

- The central skin incision forms the shape of the inverted V after the resection of the NAC. The apex reaches the NAC. Generally, the apex of the V is formed in the intersection of the two lines, one of which is the intersection line of inner and medial one-third of the clavicle with the nipple, and the second transverse line drawn in the level of inframammary fold suitable with the superior breast skin in sitting position. The apex of V is at an 18–20 cm distance to the suprasternal notch. The intersection point is the superior of the areola. V's legs from the superior areolar point extend from both sides of the NAC with approximately 10 cm length with 3–5 cm plus 5 cm or more length. The lines extend horizontally in the medial and lateral directions from this point to reach both sides of the inframammary fold. Skin marking is performed in a sitting or standing position.

- The mass preserves the NAC. As described above, the first marking is performed with the reversed U on the apex, and the reversed U incision is replaced instead of a V-shaped incision. After the wound closure on the breast, the vertical lines extend to the inframammary fold from the inferior areolar point. The horizontal lines form the superior skin borders of the new inframammary fold. The modifications of the standard inferior, medial, or lateral incisions were developed for utilizing breast preserving surgery and included correcting the incision suitable for the resection region.

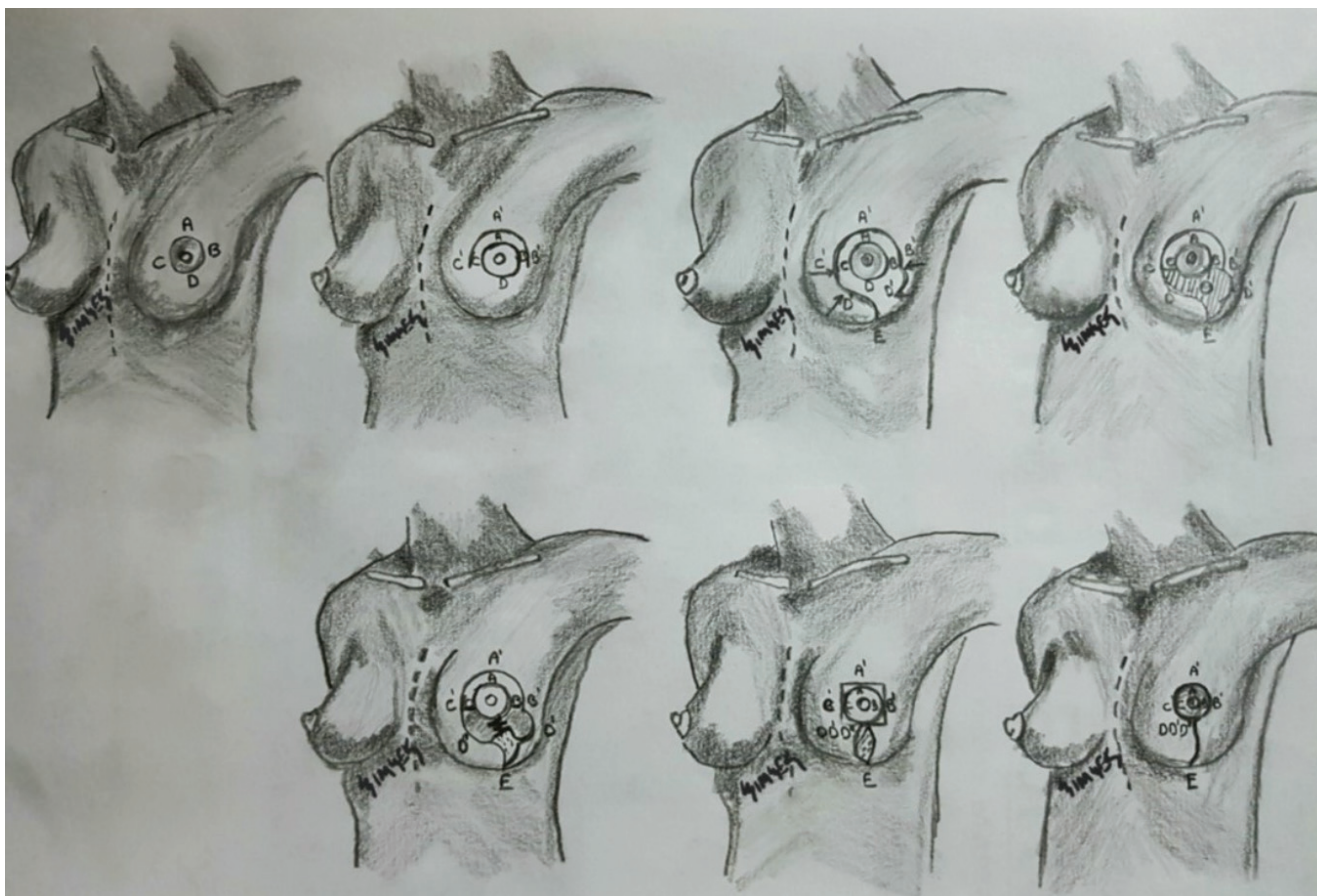


Figure 14. S Mammoplasty from drawing to closing of incision (Drew by Turgay Şimşek)

2. After planning the incision on the skin, the breast tumor resection, incision of the inframammary fold, the glandular parts on the affected skin toward the chest wall, and the dissection plane to the skin surface toward the right side are maintained. In cases where preserving the nipple and areola are planned, surgeons must try their best to provide the NAC's vascularity by avoiding the NAC's ignorance of the parenchyma's pedicle and preserving the residual dermis at least through two-thirds of the areolar circle. Besides, the region's epithelization between the residual areolar border and new superior skin border may increase the perfusion and enable the NAC's innervation. The surgeon may resect a larger portion medially or laterally in the glandular resection to obtain sufficiently healthy tissues in the neighboring region of the tumor in eccentrically located lesions (3–4 clock, or 7–8 clock positions). The dermoglandular flap where the residual breast tissue is used may be utilized to fill the defect after the tumor's complete removal.

3. The wound closure is initiated with the approximation with several staples, mainly performed in the inferior, medial, and lateral incisions.

- The nipple may be placed in between with the placing of the de-epithelized tissue below the incision if the drawn line on the apex of the Wise pattern (U shaped) is symmetrical. A cookie-cutter is used to generate a new superior incision after the reversed T incision is closed to obtain a better NAC. The removal of the additional skin tissue is accomplished with de-epithelization.
- A transverse or vertical closure may be used in accordance with the skin reduction type after the removal of the NAC.

4. The layered closure of the parenchyma, dermis, and skin enables forming the breast's final shape (Figures 15, 16).

Skin and fat necrosis are the most frequently detected complications, particularly in smokers and obese patients. Nipple-areola necrosis is detected in approximately 3% of patients (4).

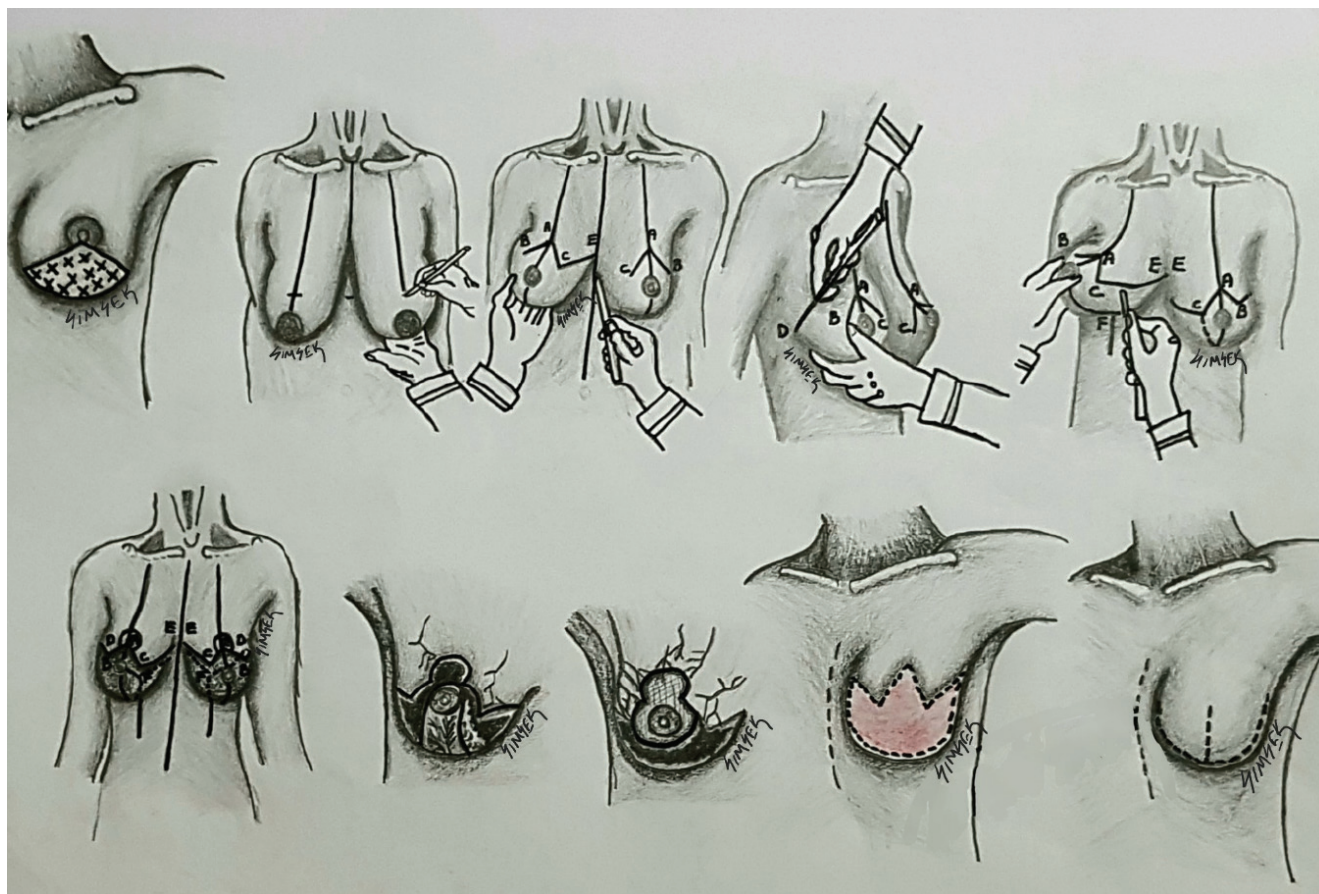
Inferior Pedicle Reduction

Location and indication

It is performed depending on one or more factors: the physical, psychological, medical, and social factors. This technique is particularly suitable for lesions located just above the nipple or lower inner or outer quadrants. This technique may be used in patients with various breast dimensions from smaller to larger breasts, including macromastia and breasts with significant ptosis.

Technique

The inferior pedicle's blood supply is enabled toward the axial region by the external branch of the internal mammarian artery and the fifth intercostal and lateral thoracic artery. The branches of the third, fourth, and fifth intercostal regions that extend to the skin are preserved in this technique and patients with macromastia. The pedicle consists of breast tissue with the dermis or only breast tissue without the dermis. The preservation of the dermis decreases the possibility of nipple necrosis because it preserves the subdermal vascular plexus. However, the de-epithelized dermis located in the pedicle is not necessarily required for the pedicle's or nipple's viability. The pedicle attaches to the muscle with an 8–10 cm thickness structure. Maintaining such



230 **Figure 15.** Step by step reduction mammoplasty with wise pattern (Drew by Turgay Şimşek)

a connection is required for adequate vascularization to preserve the required vessels and intact nerves, generate a better contour and enable sensation.

- Draw a line from the midclavicular point to pass through the nipple and inframammary fold.
- The point on the line will be the ideal point for the new nipple when you put your hand on the inframammary fold and hold the breast with your thumb.
- The new nipple corresponds to the intersection of a line of 19–21 cm extending from the midclavicular line and sternal notch, or to the junction of the line drawn from the intersection point of 2/3 below of humerus.
- Two lines of 7–8 cm length are drawn from this point with degrees of 90° and 140°. These points are named A and B.
- A new line is drawn from the points A and B to correspond to the inframammary fold with 90° and 110° degrees.
- The diameter of the new areola will be 3.5–4 cm.
- The Figure shown here is called the “Wise pattern” (Figure 15).
- An incision is made on the lower half of the areola, and the lower inframammary fold on the pedicle only on the epidermis level. A small triangular region is reserved in the middle point to facilitate the closure.
- The skin on the pedicle is de-epithelized to preserve the intradermal vascular pedicle.
- The parenchyma is dissected toward the chest wall. This dermoglandular pedicle supports the nipple with approximately a

10 cm base and 3 cm deepness. The length should not exceed 15–20 cm. Otherwise, it cannot provide enough vascular supply, and the reduction specimen is disunited from the breast.

- A temporary approximation of the incisions is performed using staples on the breast.
- The nipple is first embedded in the subcutaneous region and is removed at a later stage. The NAC's standard distance to the inframammary fold is approximately 5 cm; however, space is longer in more considerable reductions.
- A tangential dissection must be performed for prominent breast concavity to avoid skin thinning. The pedicle's excessive mobilization and traction must be avoided to protect the perforating vessels from damage (Figure 16).
- The NAC should not be elevated too high. In the suspicion of an incident, lifting down the NAC may be preferred by distancing from the part described as the “no man's land.”
- Enabling a triangular connection on the mammarian fold will prevent potential tension at the T's intersection point.

The limitations of this technique

- Though infrequent, the length of the horizontal scar may cause a problem.
- Pseudoptosis is the extension of the majority of the breast below the inframammary fold. However, the nipple is located at this level or slightly below this location. This is mainly a problem in obese patients with pendulous breasts. This is due to the shrinkage of the vertical portion of the inframammary scar, which is associated with the reconstruction of the nipple redundantly above (29–34).

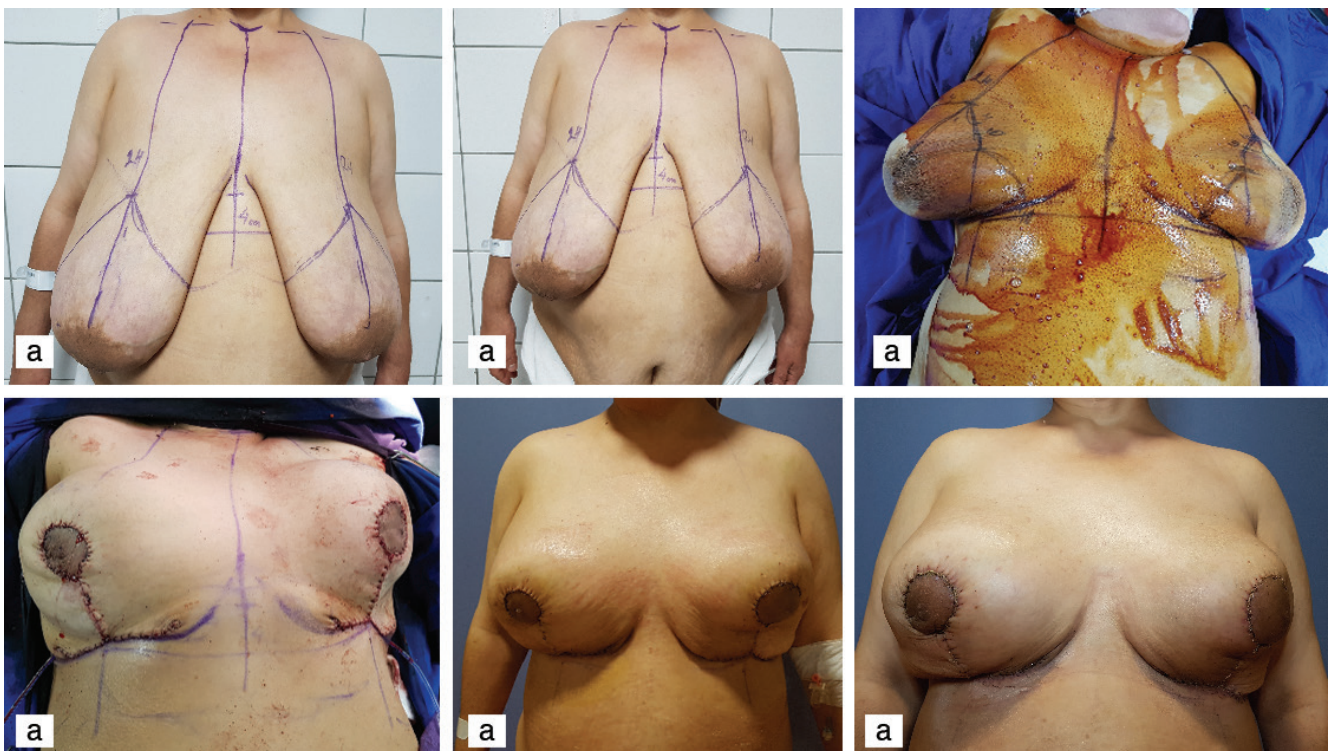


Figure 16a-f. Reduction Mastopexy **a-c)** Drawing (wise pattern), **d)** peroperative result and **e, f)** early postoperative pictures

Superior Pedicle Reduction

Location and indication

This technique is particularly suitable for the situations where the wide resection of the lesions on 5, 6, and 7 o'clock level. "Comma-shaped mammoplasty" is particularly recommended for the small or medium-size breasts for the lesions at the 6 o'clock position. This technique and inferior pedicle RM may also be used to maintain symmetry with the contralateral breast.

Technique

Mastopexy and RM may be accomplished with these techniques with the small part of the parenchyma's excision.

1. Median sternal and the inframammary line is drawn for the Wise pattern mammoplasty. The line is extended from the midclavicular point to the inframammary line of the nipple. Two legs of the Wise pattern region are drawn to provide a mean diameter of 5 cm.

2. The vertical line is drawn to the inframammary line with the "comma-shaped mammoplasty." The broader breast tissue will be resected by the distance in this type of mammoplasty. The line is drawn to intersect the inframammary line from the end of the oblique/vertical line. The diameter of the areola must be approximately 3.5–4.5 cm. The possibility of a deformity such as an inferior nipple retraction may develop due to a conventional wide resection may be decreased using this type of mammoplasty (4, 34).

Outcome and Safety of Level I and Level II OPS

Resection margin and re-excision rates

OPS for breast cancer allows broader tissue resection. Oncoplastic surgeons still argue that the reduction positive margin rate and the re-excision rate with wider resections are lower than standard breast-conserving surgery. However, wider negative margins are not associated with lower recurrence rates. In addition, eight of 13 comparative studies showed better positive margins, re-excisions, and mastectomy conversion rates following oncoplastic breast cancer surgery (35-38).

Local recurrence and oncological outcome

The studies highlight the importance of local control following breast cancer surgery regarding patient survival. Most studies demonstrated no significant difference between OPS and control arms, including breast-conserving surgery and mastectomy. Still, Carter et al. (36) showed that the OPS arm in their most extensive comparative study had a better recurrence rate than the mastectomy arm. Mansell et al. (39), in 2017, also confirmed the same result when radiation treatment was added to mastectomy (35, 36, 39, 40).

Complications and Cosmetic Outcome

Complications following OPS include liponecrosis, skin necrosis, hematoma, seroma, delayed wound healing, nipple necrosis, and/or infection. Most studies that compared OPS and breast-conserving surgery showed no difference in surgical complications (35, 36).

Conclusion

OPS is a fundamental tool for breast cancer treatment. A large amount of breast tissue can be safely excised without poor cosmetic outcomes while ensuring oncological safety and potentially reducing the number

of re-excisions and mastectomy. Although patient satisfaction rates seem high with breast-conserving surgery, it is recommended to select the appropriate OPS technique based on each patient's characteristics and tumor location.

Peer-review: Externally peer-reviewed.

Author Contributions

Conception: N.Z.C., T.Ş., S.Ö.G.; Design: N.Z.C., T.Ş., S.Ö.G.; Literature Search: N.Z.C., T.Ş., S.Ö.G.; Writing: N.Z.C., T.Ş., S.Ö.G. Drawings: T.Ş.

Conflict of Interest: No conflict of interest was declared by the authors.

Financial Disclosure: The authors declared that this study has received no financial support.

References

1. Bildham A, Bisjop H, Boland G, Dalglish M, Davies L, Fatah F, et al. Oncoplastic breast surgery- a guide to good practice. *Eur J Surg Oncol* 2007; 33(Suppl 1): S1-23. doi: 10.1016/j.ejso.2007.04.014 (PMID: 17604938) [[Crossref](#)]
2. Association of Breast Surgery at BASO. Surgical guidelines for the management of breast cancer. *Eur J Surg Oncol* 2009; 35(Suppl 1): 1-22. (PMID: 19299100) [[Crossref](#)]
3. Emiroğlu M, Kuru B, Soybir G. *Onkoplastik meme cerrahisi atlası*. İzmir: Birleşik Matbaacılık; 2015. [[Crossref](#)]
4. Holmes DR, Schooler W, Smith R. Oncoplastic approach to breast conservation. *Int J Breast Cancer* 2011;303879:1-16. [[Crossref](#)]
5. Shiffman MA. Preoperative consultation. Shiffman MA (ed.) *Mastopexy and breast reduction: Principles and practice*. Berlin: Heidelberg Springer-Verlag; 2019. p. 11-12.
6. Macmillan RD, McCulley SJ. Variations of classical reduction patterns for oncoplastic purposes. Rovere GQ, Benson JR, Nava M (eds.) *Oncoplastic and re constructive surgery of the breast*. London: Informa; 2011. p.155-160.
7. Clough KB, Benyahi D, Nos C, Charles C, Sarfati I. Oncoplastic surgery: pushing the limits of breast-conserving surgery. *Breast J* 2015; 21: 140-146. (PMID: 25676776) [[Crossref](#)]
8. Clough KB, Kaufman GJ, Nos C, Buccimazza I, Sarfati IM. Improving breast cancer surgery: a classification and quadrant per quadrant atlas for oncoplastic surgery. *Ann Surg Oncol* 2010; 17: 1375-1390. (PMID: 20140531) [[Crossref](#)]
9. Kraissl CJ. The selection appropriate lines for elective surgical incisions. *Plast Reconstr Surg* 1951; 8: 1-28. (PMID: 14864071) [[Crossref](#)]
10. Schlenz I, Rigel S, Schemper M, Kuzbari R. Alteration of nipple and areola sensitivity by reduction mammoplasty: a prospective comparison of five techniques. *Plast Reconstr Surg* 2005; 115: 743-751. (PMID: 15731673) [[Crossref](#)]
11. Petit JY, De Lorenzi F, Rietjens M, Intra M, Martella S, Garusi C, et al. Technical tricks to improve the cosmetic results of breast conserving treatment. *Breast* 2007; 16: 13-16. (PMID: 17070051) [[Crossref](#)]
12. O'Dey D, Prescher A, Pallua N. Vascular reability of nipple areola complex-bearing pedicles. An anatomical microdissection study. *Plast Reconstr Surg* 2007; 119: 1167-1177. (PMID: 17496587) [[Crossref](#)]
13. Nahabedian MY. *Oncoplastic surgery of the breast*. 2nd ed. China: Elsevier; 2009.
14. Anderson BO, Masetti R, Silverstein MJ. Oncoplastic approaches to partial mastectomy: an overview of volume displacement techniques. *Lancet Oncol* 2005; 6: 145-157. (PMID: 15737831) [[Crossref](#)]

15. Masetti R, Pirulli PG, Magno S, Franceschini G, Chiesa F, Antinori A. Oncoplastic techniques in the conservative surgical treatment of breast cancer. *Breast Cancer* 2000; 7: 276-280. (PMID: 11114849) [\[Crossref\]](#)
16. Amanti C, Moscaroli A, Lo Russo M, Papaspyropoulos V, Luzzatto L, Catracchia V, et al. Periareolar subcutaneous quadrenectomy: a new approach in breast cancer surgery. *G Chir* 2002; 23: 445-449. (PMID: 12652922) [\[Crossref\]](#)
17. Amanti C, Regolo L, Moscaroli A, Lo Russo M, Catracchia V. [Total periareolar approach in breast conserving surgery.] *Tumori* 2003; 89(Suppl 4): 169-172. (PMID: 12903581) [\[Crossref\]](#)
18. Wagner E, Schrenk P, Huemer GM, Sir A, Schreiner M, Wayand W. Central quadrenectomy with resection of the nipple-areola complex compared with mastectomy in patients retroareolar breast cancer. *The Breast J* 2007; 13: 557-563. (PMID: 17983395) [\[Crossref\]](#)
19. Naguib SE. Oncoplastic resection of retroareolar breast cancer: central quadrenectomy and reconstruction by local skin-glandular flap. *J Egypt Natl Canc Inst* 2006; 18: 334-347. (PMID: 18301457) [\[Crossref\]](#)
20. Regnault P. Reduction mammoplasty by the "B" technique. *Plast Reconstr Surg* 1974; 53: 19-24. (PMID: 4588595) [\[Crossref\]](#)
21. Grisotti A. Immediate reconstruction after partial mastectomy. *Op Technique Plast Reconstr Surg* 1994; 1: 1-12. [\[Crossref\]](#)
22. Clough KB, Ihrai T, Oden S, Kaufman G, Massey E, Nos C. Oncoplastic surgery for breast cancer based on tumor location and a quadrant-per-quadrant atlas. *Br J Surg* 2012; 99: 1389-1395. (PMID: 22961518) [\[Crossref\]](#)
23. Yang JD, Lee JW, Cho YK, Kim WW, Hwang SO, Jung JH, et al. Surgical techniques for personalized oncoplastic surgery in breast cancer patients with small- to moderate-sized breasts (part 1): volume displacement. *J Breast Cancer* 2012; 15: 7-14. (PMID: 22493623) [\[Crossref\]](#)
24. Gesperoni C, Salgarello M, Gasperoni P. A personal technique: mammoplasty with J scar. *Ann Plast Surg* 2002; 48: 124-130. (PMID: 11910216) [\[Crossref\]](#)
25. Elbaz JS. [Technic of mammoplasty by a J cicatrix.] *Ann Chir Plast* 1975; 20: 101-111. (PMID: 1103701) [\[Crossref\]](#)
26. Clough KB, Oden S, Ihrai T, Massey E, Nos C, Serfati I. Level 2 oncoplastic surgery for lower inner quadrant breast cancers: the LIQ-V-Mammoplasty. *Ann Surg Oncol* 2013; 20: 3847-3854. (PMID: 23838910) [\[Crossref\]](#)
27. Sanidas EE. S-mammoplasty no man's land. Fitzal F, Schrenk P (eds). *Oncoplastic breast surgery*. 2nd ed. New York: Springer; 2015. p.45-48. [\[Crossref\]](#)
28. Chen TH, Wei FC. Evolution of the vertical reduction mammoplasty: the S Approach. *Aesth Plast Surg* 1997; 21: 97-104. (PMID: 9143424) [\[Crossref\]](#)
29. Georgiade NG, Serafin D, Morris R, Georgiade G. Reduction mammoplasty utilizing an inferior pedicle nipple areolar flap. *Ann of Plast Surg* 1979; 3: 211-218. (PMID: 543656) [\[Crossref\]](#)
30. Wise RJ. A preliminary report on a method of planning mammoplasty. *Plast Reconstr Surg* (1946) 1956; 17: 367-375. (PMID: 13335513) [\[Crossref\]](#)
31. Lejour M, Abboud M, Declety A, Kertesz P. Reduction des cicatrices de plastimammaire de L'ancre courte a la verticale. *Annales de Chirurgie Plastique Esthétique* 1990; 35: 369-379. [\[Crossref\]](#)
32. Mathes S. *Plastic Surgery*, St. Louis, US: Quality Medical Publishing; 2006.
33. Hudson DA. A modified excision for combined reduction mammoplasty and breast conservation therapy in the treatment of breast cancer. *Aesthetic Plastic Surg* 2007; 31: 71-75. (PMID: 17235466) [\[Crossref\]](#)
34. Munhoz AM, Montag E, Arruda EG, Claudia Aldrighi, Rolf Gemperli, José Mendes Aldrighi JM, et al. Critical analysis of reduction mammoplasty techniques in combination with conservative breast surgery for early breast cancer treatment. *Plast Reconstr Surg* 2006; 117: 1091-1111. (PMID: 16582770) [\[Crossref\]](#)
35. Campbell EJ, Romics L. Oncological safety and cosmetic outcomes in oncoplastic breast conservation surgery, a review of the best level of evidence literature. *Breast Cancer (Dove Med Press)* 2017; 9: 521-530. (PMID: 28831273) [\[Crossref\]](#)
36. Carter SA, Lyons GR, Kuerer HM, Bassett Jr RL, Oates S, Thompson A, et al. Operative and oncological outcomes in 9861 patients with operable breast cancer single-institution analysis of breast conservation with oncoplastic reconstruction. *Ann Surg Oncol* 2016; 23: 3190-3198. (PMID: 27406093) [\[Crossref\]](#)
37. Haloua MH, Krekel Nm, Winters HA, Rietveld DHE, Meijer S, Bloemers FW, et al. A systemic review of oncoplastic breast conserving surgery: current weakness and future prospects. *Ann Surg* 2013; 257:609-620. (PMID: 23470508) [\[Crossref\]](#)
38. Jeevan R, Cromwell DA, Trivella M, Lawrence G, Kearins O, Pereira J, et al. Reoperation rates after breast conserving surgery for breast cancer among women in England: retrospective study of hospital episode statistics. *BMJ* 2012; 345: e4505. doi: 10.1136/bmj.e4505 (PMID: 22791786) [\[Crossref\]](#)
39. Mansell J, Weiler-Mithoff E, Martin J, Khan A, Stallard S, Doughty JC, et al. How to compare the oncological safety oncoplastic breast conservation surgery-to wide local excision or mastectomy? *Breast* 2015; 24: 497-501. (PMID: 26009307) [\[Crossref\]](#)
40. Mansell J, Weiler-Mithoff E, Stallard S, Doughty JC, Mallon E, Romics L. Oncoplastic breast conservation surgery is oncologically safe when compared to wide local excision and mastectomy. *Breast*. 2017; 32: 179-185. (PMID: 28214785) [\[Crossref\]](#)



American Joint Committee on Cancer's Staging System for Breast Cancer, Eighth Edition: Summary for Clinicians

Haoling Zhu, Başak E. Doğan

Department of Radiology UT Southwestern Medical Center, Dallas, Texas

ABSTRACT

Breast cancer is commonly staged using the American Joint Committee on Cancer (AJCC) staging system. The 7th edition of the AJCC Staging Manual, was a purely anatomic staging method, which uses primary tumor size (T), nodal involvement (N), and metastasis (M) based on clinical and pathological evaluations. Advancements in tumor biology and prognostic biological markers, such as estrogen receptor (ER)/progesterone receptor (PR), HER2/neu, and Ki-67, have allowed clinicians to understand why similarly staged patients had significantly different outcomes. The most recent update to the staging system integrates molecular markers with disease extent for more optimal estimation of prognosis. This change improves the prognosis of breast cancer patients and better informs physicians in the planning of treatments. This review summarizes the changes in the AJCC Staging Manual, 8th edition and their impact on practicing radiologists in breast cancer management.

Keywords: AJCC, biomarkers, Breast cancer, Breast imaging, cancer staging

Cite this article as: Zhu H, Doğan BE. American Joint Committee on Cancer's Staging System for Breast Cancer, Eighth Edition: Summary for Clinicians. Eur J Breast Health 2021; 17(3): 234-238

Key Points

- Until the implementation of the 8th edition of the AJCC Staging Manual, a purely anatomic staging method, which uses primary tumor (T) size, nodal (N) involvement, and metastasis (M) based on clinical and pathological evaluations, was employed.
- Advancements in tumor biology and prognostic biological markers, such as estrogen receptor (ER)/progesterone receptor (PR), HER2/neu, and Ki-67, have allowed clinicians to understand why similarly staged patients had significantly different outcomes.
- The most recent update to the staging system integrates molecular markers with disease extent for more optimal estimation of prognosis.

Introduction

Breast cancer is the most diagnosed cancer among women in the United States (US). It is also the leading cause of cancer-related deaths following lung cancer. In 2020, 276,480 new cases of breast cancer were projected to be diagnosed among American women along with 48,530 new cases of non-invasive breast cancer. One out of eight American women is projected to develop invasive breast cancer at some point in her life (1). In 1959, the American Joint Committee for Cancer Staging and End-Results Reporting, now the American Joint Committee on Cancer (AJCC), standardized the tumor, node, and metastasis (TNM) cancer staging system. The first edition of the AJCC Staging Manual, published in 1977, allowed clinicians to standardize treatment and evaluate treatment results between different institutions (2, 3). Since then, the manual has been periodically updated to reflect clinical and technological advancements in the field.

Until the implementation of the 8th edition of the AJCC Staging Manual in 2018, a purely anatomic staging method, which uses primary tumor (T) size, nodal (N) involvement, and metastasis (M) based on clinical and pathological evaluations, was employed. Advancements in tumor biology and prognostic biological markers [estrogen receptor (ER) and progesterone receptor (PR), HER2/neu, and Ki-67] have allowed clinicians to understand why similarly staged patients had significantly different outcomes. The most recent update to the staging system integrates anatomic staging with prognostic staging, which uses tumor grade, hormone receptors and oncogene expression, and multigene testing (4). Incorporating the prognostic stage into the breast cancer staging system has allowed physicians to individualize the patient prognosis, leading to a more optimal estimation of prognosis.

Corresponding Author:

Başak E. Doğan; basak.dogan@utsouthwestern.edu

Received: 06.04.2021

Accepted: 06.06.2021

This article highlights key changes from the 7th edition to the 8th edition of the AJCC breast cancer staging system, with multimodality imaging demonstration of its application. We will review the anatomic TNM staging categories: clinical staging, pathologic staging, post-therapy or post-neoadjuvant therapy staging, and restaging. Furthermore, we will summarize the prognostic staging (both clinical and pathological), the implementation of gene assays, and how they are integrated in different scenarios. Other changes in the AJCC Staging Manual, 8th Edition, will also be discussed, including re-categorization of lobular carcinoma *in situ* (LCIS) and the clinical N stage based on physical examination and imaging studies (4).

Anatomic staging

Anatomic TNM staging is further categorized into: clinical staging, which relies on physical examination, imaging, and biopsy of the affected areas; pathologic staging, which is determined after a patient has had surgery to remove the primary tumor and regional lymph nodes; post-neoadjuvant therapy staging, which determines how much cancer remains after a patient completes preoperative systemic or radiation therapy, and may incorporate both clinical and pathologic staging; and restaging, which is performed if a cancer recurs after treatment and determines the extent of disease recurrence. Since this review is primarily for radiologists, we will spend most of this section discussing clinical anatomic staging. Importantly, imaging findings are considered relevant to staging if obtained within 4 months of diagnosis or completion of surgery, whichever confers a longer time period, provided the disease has not worsened.

Clinical anatomic staging

Clinical staging of the primary T begins with the measurement of the tumor size based on physical examination and imaging (4). The staging categories range from Tis to T4 and are the same for both clinical and pathological staging of the primary tumor, where the prefixes “c” and “p” indicate clinical stage and pathologic stage, respectively. Tis refers to ductal carcinoma in situ with no invasive cancer. T1–T4 refers to the tumor size, ranging from 2 cm to >5 cm, and the involvement of chest wall and/or skin (ulceration or macroscopic nodules), respectively. The T4 category is further subdivided into T4a–T4d, where T4a indicates chest wall involvement; T4b skin indicates involvement through ulceration, ipsilateral macroscopic satellite nodules, and/or skin edema (e.g., peau d’orange), which does not meet the criteria for inflammatory carcinoma; T4c is indicated when both T4a and T4b are present; and T4d inflammatory carcinoma. Lastly, LCIS is no longer staged via TNM in the Tis category, as it is now viewed as benign; however, it carries a risk of future malignancy.

Similar to primary tumor staging, clinical staging of regional axillary lymph nodes (N) should begin with the prefix “c.” The staging categories range from N0 to N3, where N0 indicates no regional lymph node metastases as revealed by imaging or clinical examination; N1 indicates metastases to movable ipsilateral level I-II [where level I nodes are lateral to the lateral border of the pectoralis minor muscle and level II nodes are between the medial and lateral borders of the pectoralis minor and also include the interpectoral (Rotter’s) lymph nodes] axillary lymph nodes; N2 indicates metastases to ipsilateral level I-II axillary nodes that are clinically fixed or matted, or metastases to ipsilateral internal mammary nodes without axillary lymph node involvement (N2a and N2b, respectively); N3 indicates metastases to level III (ipsilateral infraclavicular) lymph nodes, ipsilateral internal

mammary lymph nodes with level I-II axillary node metastases, or metastases to ipsilateral supraclavicular lymph nodes (N3a, N3b, and N3c, respectively). Moreover, for most patients, category cNX (suggesting regional lymph nodes cannot be assessed) is considered invalid and should be listed as cN0, unless the patient has been previously subjected to axillary dissection.

Assessment of the metastases (M) stage involves categorizing patients into M0 or M1 using clinical examination. The M0 category indicates no clinical or radiographic evidence of distant metastases; however, this stage is designated cM0 since category pM0 is invalid (4). The designation pM1 may be used for patients with histologically proven metastases with at least 1 tumor deposit >0.2 mm. We also have cM0 (+), which indicates no clinical or radiographic evidence of distant metastases in the presence of histologically detected tumor deposits that are <2 mm in circulating blood, bone marrow, or other non-regional nodal tissues, without symptoms of metastases. The designation M1 indicates distant metastases, where cM1 is detected clinically or radiographically and pM1 is histologically detected with at least 1 tumor deposit >0.2 mm. Finally, if a patient is assigned the M1 category, he/she is categorized as stage IV of the disease. The patient remains in stage IV regardless of response to any preoperative systemic therapy; however, if the patient has not received preoperative therapy, the stage should be updated if postoperative imaging within 4 months of diagnosis reveals distant metastases.

Prognostic staging

Reflected in the 8th edition of the AJCC staging system, prognostic staging incorporates tumor grade, hormone receptors and oncogene status [estrogen receptors (ER), progesterone receptors (PR), and human epidermal growth factor receptor 2 (HER2)], and multigene panel results, in addition to the anatomic staging system discussed above.

Tumor grade

The AJCC 8th edition manual highlights that, along with other factors, such as proliferative index, hormone receptor expression, and gene expression profiles, grade is a key assessment of tumor differentiation, which in turn is an important tool for prognosis. Tumor grade used by the manual for staging is defined by the histologic grading system of Scarff, Bloom, and Richardson and standardized by the Nottingham group (4). Regardless of hormonal therapy or chemotherapy, high-grade or poorly differentiated tumors have a worse prognosis than low-grade or well-differentiated tumors. Furthermore, the Survey, Epidemiology, and End Results Program of the National Cancer Institute revealed that histologic grade is a valuable prognostic factor, regardless of tumor size or number of positive lymph nodes (5).

Hormone receptors and HER2

According to the AJCC 8th edition manual, hormone receptor and HER2 status need to be determined for all invasive breast cancers. Previous studies have demonstrated that ER- and PR- positive tumors can be effectively treated with selective ER modulators (SERMs), such as tamoxifen, to slow or stop tumor progression. Moreover, the higher the hormone receptor expression, the more effective the treatment becomes (6, 7). While ER- and PR-positive tumors are most likely to respond to SERMs, the response rate is lower for ER-positive and PR-negative, ER-negative and PR-positive, and ER-negative and PR-negative tumors, in descending order (6–8).

Gene amplification or protein overexpression of the oncogene HER2 in untreated patients, whether node-positive or node-negative, has been associated with a worse prognosis (9, 10). Since HER2 positivity is associated with poor differentiation, it is more likely to be observed in high-grade invasive ductal carcinoma than invasive lobular carcinoma (11). Moreover, it is also associated with higher cell proliferation rates and hormone receptor negativity (12–14). The emergence of anti-HER2 targeted therapies has drastically improved the prognosis of patients with HER2-positive breast cancer. Particularly, the use of the monoclonal antibody trastuzumab in combination with a chemotherapeutic regimen significantly improves the disease-free and overall survival of these women (15).

Biological subtypes

In addition to tumor grade, hormone receptor, and oncogene expression, breast cancers vary widely on a genetic basis and this variation plays a significant role in prognosis. Four subtypes of breast cancer have been identified by genomic analysis: Luminal A, Luminal B, HER2-like, and Basal-like (16, 17). Categorizing cancers in such manner guides clinicians in both prognosis and treatment (18).

Particularly, luminal A-type tumors are deemed to have a favorable prognosis since they are typically low-grade invasive ductal carcinomas (not otherwise specified type) or special types, including tubular, cribriform, or mucinous carcinomas. This subtype is responsive to endocrine therapy but has a poor response to traditional chemotherapy. In contrast, luminal B-type tumors are typically poorly differentiated and respond better to traditional chemotherapy than endocrine therapy. Although HER2-like tumors previously had the worst prognosis among all subtypes, the introduction of anti-HER2 therapy has drastically improved prognosis of patients with these cancers. Finally, basal-like tumors, which usually have a triple-negative (ER-negative, PR-negative, and HER2-negative) phenotype, have the worst

prognosis and are the most challenging to treat with adjuvant therapy (4, 16, 17).

Multigene panels

Multigene panels can be used to obtain expression levels of multiple genes in breast cancer tissue. Many of these panels are useful prognostic tools; particularly, the Oncotype DX Breast Recurrence Score (Genomic Health, Redwood City, Calif), which measures 21 genes to predict likelihood of recurrence, has been incorporated into the updated staging system (19, 20). Despite this, one disadvantage of multigene panels is the substantial cost currently associated with their use. Thus, the AJCC 8th edition manual states that hormone receptor and HER2 expression should be tested before obtaining a multigene panel and that the panel should be used only for certain subsets of cancers. Specifically, smaller (T1-T2) node-negative, hormone receptor-positive, HER2-negative tumors, and multigene panels may be incorporated into prognostic staging. When these tumors have an Oncotype DX score of <11, they can be considered stage IA, which can result in a downstage (4).

Implementing the new staging system and challenges

Upon the implementation of the AJCC 8th edition staging system, many patients are restaged to better reflect their prognosis (Figures 1-3). A previous analysis was conducted to compare the 7th edition to the revised 8th edition staging system using the data obtained from 501,451 women in the National Cancer Database diagnosed from 2004 to 2014, excluding patients who underwent neoadjuvant chemotherapy. It was found that 23% of patients in stages I–III were downstaged and 19% of patients in stages I–III were upstaged (3).

Several studies involving large cohorts have revealed that these changes to patients' stages reflect more refined stratification and prediction of

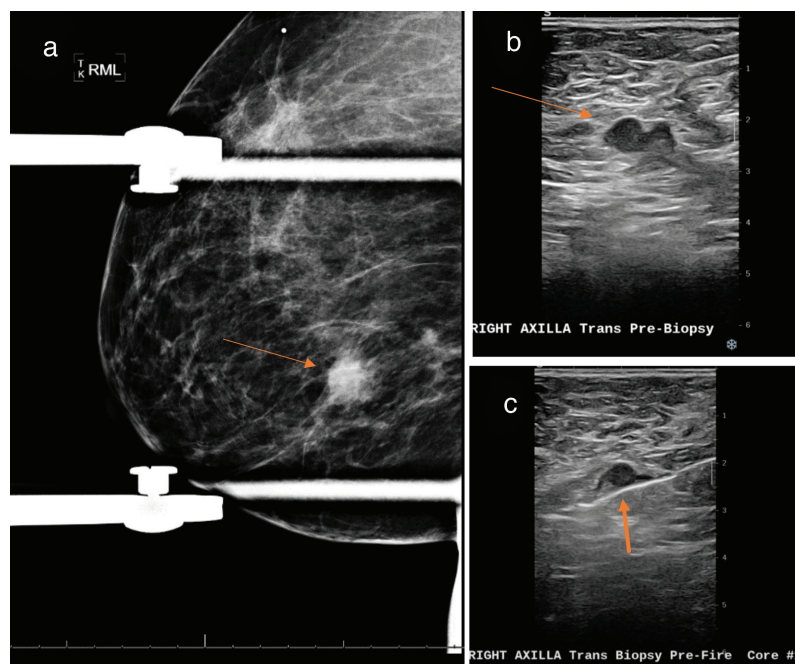


Figure 1. A 34-year-old woman with right breast cancer (a), 2.5 cm, with a single metastatic axillary adenopathy identified with axillary ultrasound (b), and needle biopsy (c). Anatomic T2N1M0, Stage IIA (AJCC 7th edition).

Patient's pathologic prognostic factors: Grade 2, ER, PR, and HER2-negative, which places her at stage IIIB (AJCC 8th edition)

disease outcome. One study including 3327 patients who underwent surgery as an initial intervention at the University of Texas MD Anderson Cancer Center database revealed that the incorporation of grade, ER, and HER2 status into AJCC prognostic staging provided a more refined stratification in terms of patients' disease-specific survival (21). Furthermore, an analysis of 54,727 patients in the California Cancer Registry revealed that the AJCC 8th edition prognostic stage provided more accurate prognostic information than the anatomic stage alone (22).

Despite the benefits associated with incorporating prognostic markers into breast cancer staging, there are challenges to the implementation of this new staging system. In many parts of the world, biological markers and multigene panels are not routinely available (23). Also,

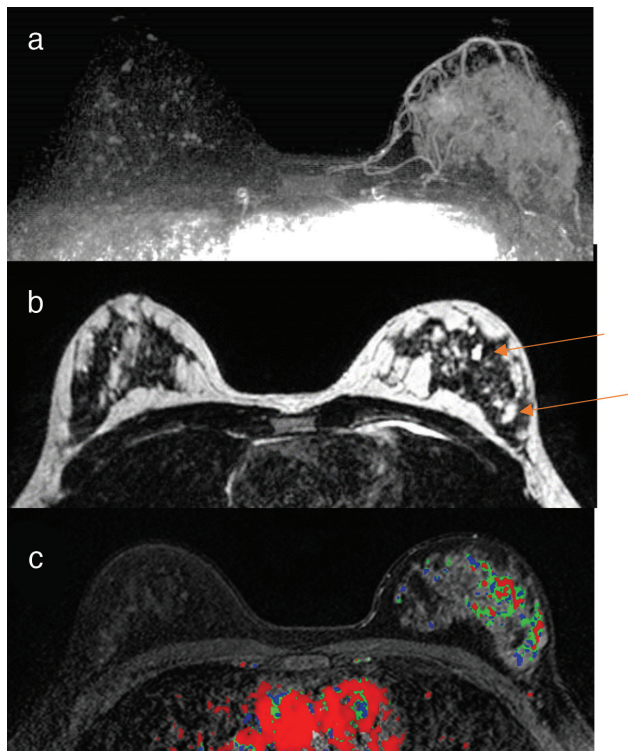


Figure 2. A 47-year-old pre-menopausal woman with a strong family history of breast cancer undergoing annual MRI screening. Figure reveals axial dynamic contrast-enhanced (DCE) MRI findings. (a) Maximum intensity projection (MIP) reveals cancer occupying a substantial portion of her left breast, (b) T2-weighted imaging reveals associated cysts (arrows) consistent with the micropapillary component, and (c) dynamic early subtraction image with overlying time intensity map. There is diffuse, non-mass-like enhancement involving all four quadrants of the left breast with no evidence of nipple involvement or axillary lymphadenopathy identified in the remainder of the MRI study.

Mastectomy pathology revealed multifocal invasive ductal carcinoma, grade 1, largest tumor measuring 56.0 × 25.0 mm. Additional foci of invasive carcinomas ranged in size from 1.0 mm to 7.0 mm. Extensive ductal carcinoma *in situ*, Nuclear Grade 1, micropapillary and papillary types, measuring 95.0 × 75.0 mm. No axillary nodes were involved in pathology.

Anatomic T3N0M0, Stage IIB (AJCC 7th edition).

Patient's pathologic prognostic factors: Grade 1, ER, PR, and HER2-positive, which places her at stage IB (AJCC 8th edition).

AJCC: American Joint Committee on Cancer; MRI: Magnetic resonance imaging; ER: Estrogen receptors; PR: Progesterone receptors; HER2: Human epidermal growth factor receptor 2

even in other parts of the world where biomarkers are more accessible, such as Europe, barriers in policy, reimbursement, and regulation have also delayed the widespread adoption of prognostic testing compared to the US (24). Therefore, the continued use of anatomic TNM staging in these regions emphasizes both its relevance and consistent usage.

Conclusion

The 8th edition of the AJCC Cancer Staging Manual incorporates validated prognostic molecular biomarkers with standard tumor (T), node (N), and metastasis (M) anatomic categories. Given the large number of possible combinations of T, N, and M categories combined with grade, ER, PR, and HER2 status, integrating prognostic staging into multidisciplinary breast cancer care will be more complicated than with anatomic staging. Despite these challenges, prognostic staging facilitates more refined and accurate stratification of patients regarding

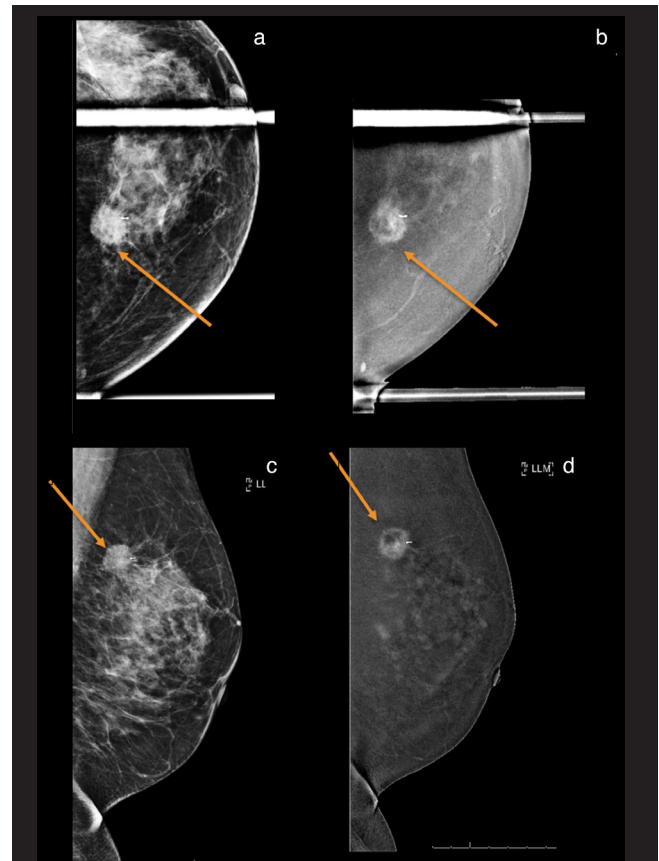


Figure 3. A 49-year-old woman with left breast invasive ductal cancer, grade 3.

Dual energy contrast-enhanced mammogram was performed to assess disease extent using iodinated low osmolar contrast injected at 3 ml/sec. Spot compression craniocaudal low energy (a), high energy (b), left lateromedial low (c), and high energy (d) images reveal a 1.7 cm round mass with speculated margins. There was no palpable or imaging-detected lymphadenopathy in the axillary or internal mammary chains. Immunohistochemistry revealed ER/PR-negative cancer, HER2-negative cancer, and 90% Ki-67.

Anatomic T1N0M0, Stage IA (AJCC 7th edition)

Patient's pathologic prognostic factors: Grade 3, ER-, PR-, and HER2-negative, which places her at Stage IIA (AJCC 8th edition). The patient went on to receive neoadjuvant chemotherapy as first-line treatment.

AJCC: American Joint Committee on Cancer; ER: Estrogen receptors; PR: Progesterone receptors; HER2: Human epidermal growth factor receptor 2

survival outcomes than anatomic staging alone, thereby ultimately allowing clinicians to better serve their patients. Although prognostic staging is preferred for patient care, anatomic staging is retained as a key component of cancer care in regions of the world where biomarker tests are not routinely available (4).

Peer-review: Externally peer-reviewed.

Authorship Contributions

Conception: H.Z., B.E.D.; Design: H.Z., B.E.D.; Supervision: H.Z., B.E.D.; Data Collection and/or Processing: H.Z., B.E.D.; Analysis and/or Interpretation: H.Z., B.E.D.; Literature Search: H.Z., B.E.D.; Writing: H.Z., B.E.D.; Critical Review: H.Z., B.E.D.

Conflict of Interest: No conflict of interest was declared by the authors.

Financial Disclosure: The authors declared that this study received no financial support.

References

1. Breastcancer.org. U.S. Breast Cancer Statistics. 2021. Last Accessed Date: 28.02.2021. Available from: https://www.breastcancer.org/symptoms/understand_bc/statistics [Crossref]
2. Amin MB, Greene FL, Edge SB, Compton CC, Gershenwald JE, Brookland RK, et al. The Eighth Edition AJCC Cancer Staging Manual: continuing to build a bridge from a population-based to a more “personalized” approach to cancer staging. *CA Cancer J Clin* 2017; 67: 93-99. (PMID: 28094848) [Crossref]
3. Plichta JK, Campbell BM, Mittendorf EA, Hwang ES. Anatomy and breast cancer staging: is it still relevant? *Surg Oncol Clin N Am* 2018; 27: 51-67. (PMID: 29132565) [Crossref]
4. Hortobagyi GN, Connolly JL, D’Orsi CJ, Edge SB, Mittendorf EA, et al. Breast. In: Amin MB, Edge S, Greene F, et al, eds; American Joint Committee on Cancer. *AJCC cancer staging manual*. 8th ed. New York, NY: Springer, 2017.
5. Schwartz AM, Henson DE, Chen D, Rajamarthandan S. Histologic grade remains a prognostic factor for breast cancer regardless of the number of positive lymph nodes and tumor size: a study of 161 708 cases of breast cancer from the SEER Program. *Arch Pathol Lab Med* 2014; 138: 1048-1052. (PMID: 25076293) [Crossref]
6. Davies C, Godwin J, Gray R, Clarke M, Cutter D, Darby S, et al. Early Breast Cancer Trialists’ Collaborative Group (EBCTCG). Relevance of breast cancer hormone receptors and other factors to the efficacy of adjuvant tamoxifen: patient-level meta-analysis of randomised trials. *Lancet* 2011; 378: 771-784. (PMID: 21802721) [Crossref]
7. Barnes DM, Harris WH, Smith P, Millis RR, Rubens RD. Immunohistochemical determination of oestrogen receptor: comparison of different methods of assessment of staining and correlation with clinical outcome of breast cancer patients. *Br J Cancer* 1996; 74: 1445-1451. (PMID: 8912543) [Crossref]
8. Hammond ME, Hayes DF, Dowsett M, Allred DC, Hagerty KL, Badve S; American Society of Clinical Oncology; College of American Pathologists. American Society of Clinical Oncology/College of American Pathologists guideline recommendations for immunohistochemical testing of estrogen and progesterone receptors in breast cancer (unabridged version). *Arch Pathol Lab Med* 2010; 134: e48-e72. doi: 10.5858/134.7.e48. (PMID: 20586616) [Crossref]
9. Slamon DJ, Clark GM, Wong SG, Levin WJ, Ullrich A, McGuire WL. Human breast cancer: correlation of relapse and survival with amplification of the HER-2/neu oncogene. *Science* 1987; 235: 177-182. (PMID: 3798106) [Crossref]

10. Ross JS, Slodkowska EA, Symmans WF, Pusztai L, Ravdin PM, Hortobagyi GN. The HER-2 receptor and breast cancer: ten years of targeted anti-HER-2 therapy and personalized medicine. *Oncologist* 2009; 14: 320-368. (PMID: 19346299) [Crossref]
11. Rosenthal SI, Depowski PL, Sheehan CE, Ross JS. Comparison of HER-2/neu oncogene amplification detected by fluorescence in situ hybridization in lobular and ductal breast cancer. *Appl Immunohistochem Mol Morphol* 2002; 10: 40-46. (PMID: 11893034) [Crossref]
12. Eccles SA. The role of c-erbB-2/HER2/neu in breast cancer progression and metastasis. *J Mammary Gland Biol Neoplasia* 2001; 6: 393-406. doi: (PMID: 12013529) [Crossref]
13. Piccart M, Lohrisch C, Di Leo A, Larsimont D. The predictive value of HER2 in breast cancer. *Oncology* 2001;61(Suppl 2):73-82. (PMID: 11694791) [Crossref]
14. Yarden Y. Biology of HER2 and its importance in breast cancer. *Oncology* 2001;61(Suppl 2):1-13. (PMID: 11694782) [Crossref]
15. Slamon D, Eiermann W, Robert N, Pienkowski T, Martin M, Press M, et al; Breast Cancer International Research Group. Adjuvant trastuzumab in HER2-positive breast cancer. *N Engl J Med* 2011; 365: 1273-1283. (PMID: 21991949) [Crossref]
16. Konecny G, Pauletti G, Pegram M, Untch M, Dandekar S, Aguilar Z, et al. Quantitative association between HER-2/neu and steroid hormone receptors in hormone receptor-positive primary breast cancer. *J Natl Cancer Inst* 2003; 95: 142-153. (PMID: 12529347) [Crossref]
17. Eiermann W, Rezai M, Kümmel S, Kühn T, Warm M, Friedrichs K, et al. The 21-gene recurrence score assay impacts adjuvant therapy recommendations for ER-positive, node-negative and node-positive early breast cancer resulting in a risk-adapted change in chemotherapy use. *Ann Oncol* 2013; 24: 618-624. (PMID: 23136233) [Crossref]
18. Coates AS, Winer EP, Goldhirsch A, Gelber RD, Gnant M, Piccart-Gebhart M, et al; Panel Members. Tailoring therapies--improving the management of early breast cancer: St Gallen International Expert Consensus on the Primary Therapy of Early Breast Cancer 2015. *Ann Oncol* 2015; 26: 1533-1546. (PMID: 25939896) [Crossref]
19. Xin L, Liu YH, Martin TA, Jiang WG. The era of multigene panels comes? The clinical utility of oncotype dx and mammaPrint. *World J Oncol* 2017; 8: 34-40. (PMID: 29147432) [Crossref]
20. Goncalves R, Bose R. Using multigene tests to select treatment for early-stage breast cancer. *J Natl Compr Canc Netw* 2013; 11: 174-182; quiz 182. (PMID: 23411384) [Crossref]
21. Mittendorf EA, Chavez-MacGregor M, Vila J, Yi M, Lichtensztajn DY, Clarke CA, et al. Bioscore: a staging system for breast cancer patients that reflects the prognostic significance of underlying tumor biology. *Ann Surg Oncol* 2017; 24: 3502-3509. (PMID: 28726077) [Crossref]
22. Weiss A, Chavez-MacGregor M, Lichtensztajn DY, Yi M, Tadros A, Hortobagyi GN, et al. Validation study of the American Joint Committee on cancer eighth edition prognostic stage compared with the anatomic stage in breast cancer. *JAMA Oncol* 2018; 4: 203-209. (PMID: 29222540) [Crossref]
23. Giuliano AE, Connolly JL, Edge SB, Mittendorf EA, Rugo HS, Solin LJ, et al. Breast cancer-major changes in the American Joint Committee on Cancer eighth edition cancer staging manual. *CA Cancer J Clin* 2017; 67: 290-303. Erratum in: *CA Cancer J Clin* 2017; 67: 345. (PMID: 28294295) [Crossref]
24. Horgan D, Ciliberto G, Conte P, Baldwin D, Seijo L, Montuenga LM, et al. Bringing greater accuracy to europe’s healthcare systems: the unexploited potential of biomarker testing in oncology. *Biomed Hub* 2020; 5: 182-223. (PMID: 33564664) [Crossref]



Treatment of Granulomatous Mastitis: Is There a Role for Antibiotics?

Meagan S. Williams¹, Adelaide H. McClintock¹, Lori Bourassa², Mary B. Laya³

¹Department of Medicine, Division of General Internal Medicine, University of Washington, Washington, USA

²Department of Laboratory Medicine and Pathology, Division of Clinical Microbiology, University of Washington, Washington, USA

³Department of Medicine, Division of General Internal Medicine, Breast Care Program, University of Washington, Washington, USA

ABSTRACT

Objective: To perform a retrospective review of the clinical characteristics, microbiological data, and clinical outcomes in patients with granulomatous mastitis (GM) who were treated at our institution with a unique strategy of prolonged antibiotic therapy as the primary treatment modality.

Materials and Methods: A retrospective case series was performed on patients (n = 42) with GM seen at the breast specialty clinic of our institution between the years 2004 and 2014. Patients were primarily treated with lipophilic antibiotics, and steroids and surgery were reserved for refractory cases.

Results: Bacteria were identified in 34 samples from 22/42 patients (52.3%). Diphtheroids (presumptive *Corynebacterium* spp.) were most commonly identified, followed by *Corynebacterium* spp. and *Propionibacterium acnes* (now *Cutibacterium acnes*). Antibiotics were our preferred first-line medical therapy and were used in 33/36 (91.7%) patients. The mean duration of antibiotic therapy was 7.0±4.5 months. Clarithromycin was our antibiotic of choice and was the initial antibiotic used in 15 of the 33 patients (45.5%) treated with antibiotics. Eleven patients required adjunctive therapy with prednisone. The mean duration of steroid therapy was 4.3±2.5 months. Surgery for therapeutic purposes included incision and drainage in seven patients, fine needle aspiration in eight patients, and excision of the fistulous tract in one patient. No patients had large-volume excisions. The average time from the first breast clinic visit to clinical resolution was 8.0±4.6 months.

Conclusion: GM may be the result of a bacterial process that induces a unique form of inflammatory response. Clinicians should consider special requests to microbiology laboratories to attempt to isolate *Corynebacterium* spp. in the evaluation of samples sent to the laboratory for analysis. An extended course of a lipophilic antibiotic is a largely unexplored but potentially effective treatment option with low associated morbidity. More research is needed in this area.

Keywords: Granulomatous mastitis, idiopathic granulomatous mastitis, breast disease, benign breast disease

Cite this article as: Williams MS, McClintock AH, Bourassa L, Laya MB. Treatment of Granulomatous Mastitis: Is There a Role for Antibiotics?. Eur J Breast Health 2021; 17(3): 239-246

Key Points

- A retrospective case series was performed on patients with GM seen at the breast specialty clinic of our institution.
- Diphtheroids (presumptive *Corynebacterium* spp.) were the most commonly identified bacteria in breast tissue samples, followed by *Corynebacterium* spp. and *Propionibacterium acnes* (now *Cutibacterium acnes*)
- Patients were primarily treated with lipophilic antibiotics; steroids and surgery were reserved for refractory cases.
- The mean duration of antibiotic therapy was 7.0±4.5 months, and the mean duration of steroid therapy was 4.3±2.5 months. The average time from the first breast clinic visit to clinical resolution was 8.0±4.6 months.
- Clinicians should consider requesting inclusion of *Corynebacterium* spp. in the evaluation of samples sent for laboratory analysis by asking for species-level identification of any corynebacteria recovered in culture, adding Tween 80 (a lipid source) and esculin to growth media, and incubating cultures for a sufficient duration to recover slow-growing organisms such as *C. kroppenstedtii*.
- An extended course of a lipophilic antibiotic, such as clarithromycin, that has adequate tissue penetrance within lipid-filled spaces may be an option for treating GM.

Introduction

Granulomatous mastitis (GM) is a challenging clinical condition first described in 1972 by Kessler and Wolloch (1). There remains a lack of consensus around both a unifying pathophysiologic model of this disease and a standard treatment protocol. Patients often present to a women's health or primary care provider and are frequently initially managed as typical non-lactation mastitis or malignancy (2). After failure of a standard short course of antibiotics, chronic inflammation develops, often with the formation of a fistula and an abscess (2-4).

Multiple theories have been proposed about the etiology of GM, including autoimmune disease, elevated hormonal states such as hyperprolactinemia, and infection (3). However, none of these theories have been widely accepted, hence the continued reference to this disease as "idiopathic" GM in the literature. There exists wide variability in treatment approaches, including observation only (5, 6), short courses of antibiotics, long courses of immunosuppressants (2, 7-9), and surgical interventions (10).

Common immunosuppressant therapies include methotrexate and corticosteroids (2, 8, 11). There is a pathophysiologic basis for corticosteroid use, since steroids inhibit granuloma formation through inhibition of the production of inflammatory cytokines (TNF alpha and IFN-gamma) and are used in other noninfectious granulomatous diseases such as sarcoidosis (12). Surgical approaches vary depending on clinical presentation and can include incision and drainage, wide local excision, or even mastectomy (10, 13, 14). Differing degrees of success have been reported in the literature with regard to surgery, with some studies concluding that surgery is the ideal treatment strategy (15-17) and others either advising against it or reserving it for refractory cases only due to surgical site complications, recurrence after excision, and morbidity associated with large-volume excisions (14, 18, 19).

In 2003, Taylor et al. (20) were the first to observe the presence of Gram-positive bacilli within granulomas of women with GM and also noted that *Corynebacterium kroppenstedii* was isolated in 44% of their case series. This led to the assertion that corynebacteria, though often considered to be contaminants, are likely truly pathogenic when isolated from breast tissue. Subsequently, several other studies have demonstrated an association of GM with *Corynebacterium* spp. (21-24). However, consistent isolation remains a challenge as some *Corynebacterium* spp. require prolonged incubation or specialized growth media. *C. kroppenstedii* in particular requires lipid supplementation to grow consistently on synthetic media (25). This lipid requirement may explain its propensity for growth in lipid-rich environments, such as that found in mammary glands. Even if *Corynebacterium* spp. do grow on conventional media, they may be dismissed as non-pathogenic "diphtheroid" skin contaminants. Dobinson also noted that isolation of the bacteria declines on subsequent cultures (23).

Prior studies with short courses of beta lactams have demonstrated low rates of resolution. However, this may be attributable to the high minimum inhibitory concentrations of these antibiotics in *Corynebacterium* spp. (23, 24, 26). Additionally, the bacteria are not accessible to these antibiotics within macrophages.

Granulomas are highly complex immune system structures formed in response to a variety of infectious and noninfectious agents. In the quintessential granulomatous infection, infection with *Mycobacterium tuberculosis*, granulomas appear to be an only partially effective host defense which, though containing the bacilli, may also provide safe shelter from the immune system (27, 28). This may in part explain the necessity of prolonged courses of antibiotics, with treatment needed for many months to years before clinical resolution.

More recently, longer courses of lipophilic antibiotics have been proposed, to allow for better penetration and tissue concentration of antibiotics (23, 29), as *Corynebacterium* spp. are typically found within lipid-filled vacuoles within the granuloma rather than in the surrounding inflamed tissue.

Given the growing body of literature suggesting an infectious etiology for GM, particularly by corynebacteria, we developed an approach to evaluation and treatment that was targeted toward an infectious process with these organisms in particular. This strategy involve 1) requesting species-level identification of *Corynebacterium* spp. isolated in culture or identified by polymerase chain reaction (PCR), 2) the use of lipophilic antibiotics or higher doses of non-lipophilic antibiotics for tissue penetrance, 3) prolonged medical treatment, since the structure and function of granulomas inhibit antibiotic effectiveness, 4) adjuvant glucocorticoid treatment for refractory cases, and 5) surgery when drainable lesions were present or for symptomatic treatment if desired. The purpose of this study was to review the clinical characteristics, microbiological data, and clinical outcomes of patients managed with this approach.

Materials and Methods

A retrospective chart review was performed on patients with GM seen at the breast specialty clinic of our urban, tertiary care academic medical center between the years 2004–2014. The University of Washington Institutional Review Board reviewed and approved the study (human subjects application with no: #49769). Clinical, radiological, microbiological, and histological data, as well as management and treatment outcomes were extracted from patient charts. Diagnoses of GM were histopathologically confirmed from deep-tissue samples from either core or excisional biopsies. If obtained at our institution, deep-tissue samples were examined with special stains for bacterial, acid-fast, and fungal organisms, and PCR was performed for tuberculous and non-tuberculous mycobacteria. As our diagnostic algorithm evolved, species-level identification of *Corynebacterium* spp. isolated in culture or identified by PCR were requested from deep-tissue samples and from fluid obtained from incision & drainage (I&D) and fine needle aspiration (FNA).

Clinical resolution of GM was defined as a) absence of subjective symptoms such as pain or tenderness and b) lack of evidence of active disease by either clinical breast exam or breast ultrasound. Redevelopment of either symptoms or clinical abnormalities within two months of cessation of therapy was considered an incompletely treated primary episode of GM. Recurrence was defined as redevelopment of symptoms or clinical abnormalities greater than two months after cessation of therapy.

Data from a chart review was entered and stored in Research Electronic Data Capture (REDCap), a secure web-based software platform (30). Ten percent of the data was spot checked by an independent party. Descriptive statistics were used to describe the demographic and clinical characteristics of the sample. Time to resolution was analyzed using methods for survival time analysis for censored data. Kaplan-Meier curves were used to describe the distribution, and the log rank test was used to test whether time to resolution differed according to patient characteristics.

Forty-two patients with GM were identified by chart review. Six patients had active GM at the time of their last clinic visit and were subsequently lost to follow-up. Their clinical outcome is unknown. The remaining 36 patients were followed up at our clinic to clinical resolution. Patients lost to follow-up were not included in the survival time analysis, Kaplan-Meier curves, or log rank test.

Results

Demographics

All patients were women with an average age at disease onset of 32 (range: 18–64) (Table 1). Fifty percent identified as Hispanic, with nearly 1/3 originating from Mexico. The majority of patients

Table 1. Demographics (n = 42)

Table 1. Demographics (n = 42)	
Gender	
Female	100%
Male	0%
Mean age at onset (years)	32 (18–64)
Race/ethnicity	
Hispanic	50%
Non-Hispanic white	21%
Asian	17%
Black	7%
Mixed	5%
Country of birth	
USA	40%
Mexico	29%
Korea	7%
Vietnam	2%
Honduras	2%
El Salvador	2%
Guatemala	2%
Moldova	2%
Unstated	12%
Parous	93%
Nulliparous	7%
Pregnant at onset	19%
Breastfeeding at onset	0%

USA: United States of America; n: Number

(93%) were parous. Eight patients were pregnant at symptom onset.

The most common initial breast symptoms were presence of a mass/lump, pain/tenderness, and erythema (Table 2). Close to one-quarter of patients had a fever, and 19% reported erythema nodosum. Patients most commonly presented first to primary care, obstetrics/gynecology, and emergency medicine.

The average duration of symptoms before presentation to our institution's breast clinic was 7.2 months (range: 0.2–32 months). Eighty-one percent of patients received antibiotics prior to their first breast clinic visit and 33% had been treated with immunosuppressive therapy. Most patients were unable to recall the details regarding those treatments, such as medication names, dosages, and duration.

Radiographic and histologic findings

Breast ultrasound was performed on 40 (95.2%) patients, with common findings being a lobulated or irregular hypoechoic mass, sinus tract, and complex fluid collection. A mammogram was obtained in 25 (59.5%) patients and most commonly demonstrated focal

Table 2. Clinical characteristics and presentation (n = 42)

Breast symptoms at disease onset	n (%)
Mass/lump	37 (88.1)
Pain/tenderness	34 (81.0)
Erythema	26 (61.9)
Abscess	7 (16.7)
Induration	6 (14.3)
Itching	3 (7.1)
Fistula	3 (7.1)
Associated symptoms at disease onset	
Fever	10 (23.8)
Erythema nodosum	8 (19.0)
Chills	7 (16.7)
Breast trauma prior to disease onset	2 (4.4)
Initial presenting specialty	
Primary care	17 (40.4)
Ob/gyn	8 (19.0)
Emergency medicine/urgent care	7 (16.7)
Not stated	10 (23.8)
Mean time from symptom onset to breast clinic provider (months)	7.2
Mean size of lesion by exam at first breast clinic visit (cm)	7.4 × 6.6
Patients who had been treated with antibiotics prior to first breast clinic visit	34 (81.0)
Patients who had been treated with immunosuppressive therapy prior to first breast clinic visit	14 (33.3)
Average number of procedures per patient prior to first breast clinic visit	1.8

asymmetric density, a lobulated irregular mass, and skin thickening. Three patients had a breast magnetic resonance imaging.

Tissue for histopathology was obtained by core needle biopsy in 38 (90.5%) patients and excisional biopsy in seven (16.7%) patients. Histology was characterized by lobular-centric active granulomatous inflammation with or without concomitant chronic inflammation and no evidence of malignancy. Associated abscess formation, fat necrosis, and stromal fibrosis were also seen.

Microbiology

Bacteria were identified in 34 samples from 22/42 patients (52.3%) (Table 3). Diphtheroids (presumptive *Corynebacterium* spp.) were

most commonly identified, followed by *Corynebacterium* spp. and *Propionibacterium acnes* (now *Cutibacterium acnes*).

Twenty-eight patients (66.7%) presented to their first breast clinic visit with microbiological data obtained from an outside institution. A total of 51 samples were collected from these patients. Twelve patients overall had samples that grew one or more organisms, and nine of these patients had samples that grew presumed *Corynebacterium* speciated and non-speciated organisms. Fourteen patients either did not have microbiological data prior to their first visit or did have microbiology studies but the results were unclear or unknown. Details regarding antibiotic status when samples were collected was also unknown.

Table 3. Organisms identified from samples both outside and within our institution

Presumed <i>Corynebacterium</i> speciated and non-speciated				
	Organism	No of samples*	Sampling technique	Microbiology test
Obtained outside institution	Diphtheroids	11	FNA (4) I&D (5) Biopsy (1) Superficial sample†(1)	Bacterial culture
	<i>C. kroppenstedtii</i>		FNA (2) I&D (1)	Bacterial culture (2) DNA sequencing (1)
	<i>Corynebacterium</i> spp. (species not determined)		I&D	Bacterial culture
Obtained within institution	<i>C. kroppenstedtii</i>	2	Superficial sample† (1) FNA (1)	Bacterial culture
	<i>Corynebacterium tuberculostearicum</i> or <i>Corynebacterium</i> group G2	1	Biopsy	Bacterial PCR
Other organisms	Organism	No of samples*	Sampling technique	Microbiology test
Obtained outside institution	<i>P. acnes</i>	3	Biopsy (1) I&D (1) Superficial sample† (1)	Culture
	<i>Stenotrophomonas maltophilia</i>		Biopsy (1)	Culture
	<i>Actinomyces odontolyticus</i>	1	Superficial sample† (1)	Culture
	Coagulase negative staphylococcus	3	FNA (1) Superficial sample† (2)	Culture
Micrococcus	I&D (1) FNA (1)		Culture	
Obtained within institution	<i>P. acnes</i>	1	Biopsy (1)	Culture
	<i>Citrobacter freundii</i>	1	I&D	Culture
	Enterococcus	1	I&D (1)	Culture
	<i>Klebsiella pneumoniae</i>	1	Superficial sample† (1)	Culture
	<i>Mycobacterium chelonae</i>	1	Biopsy	AFB PCR
	<i>Serratia marcescens</i>	1	Superficial sample† (1)	Culture

*Of 90 samples obtained within and outside our institution, 34 samples from 22/42 patients (52.3%) grew one or more organisms; †Superficial samples were obtained from either nipple discharge or fluid from draining sinus tracts
I&D: Incision & drainage; FNA: Fine needle aspiration; PCR: Polymerase chain reaction; AFB: Acid-fast bacillus

Within our institution, a total of 39 microbiology samples were obtained from 24 patients (57.1%). 21/39 (53.8%) samples were collected while the patient was currently on antibiotics or had finished a course of antibiotics within the last week. Ten patients overall had samples that grew one or more organisms.

Management

Six patients (14%) had active GM at the time of their last visit and were subsequently lost to follow-up. The remaining 36 were followed to clinical resolution. Their management is outlined in Table 4.

Antibiotics were our preferred first-line medical therapy and were used in 33/36 (91.7%) patients. The mean duration of antibiotic therapy was 7.0±4.5 months. Clarithromycin was our antibiotic of choice given its lipophilic properties and its ability to concentrate within macrophage-derived elements of granulomas. It was the initial agent used in 15 of the 33 patients (45.5%) treated with antibiotics. Patients were treated with typical doses of clarithromycin at 500 mg twice daily. The remaining 18 patients received an alternate antibiotic because they either a) were already on an alternate antibiotic at the time of their first breast clinic visit and were showing clinical improvement on this agent or b) had a contraindication to clarithromycin, such as pregnancy or allergy. Twelve of these patients were eventually switched to clarithromycin due to lack of continued clinical improvement on an alternate antibiotic. There were no major adverse effects of clarithromycin therapy. Two patients experienced gastrointestinal side effects, and one patient had QTC prolongation and was therefore transitioned to high-dose amoxicillin.

Eleven patients required adjunctive therapy with prednisone due to worsening or plateau of symptoms on antibiotic therapy. Steroid doses varied, but we generally avoided high-dose steroid therapy and typically started at 20–30 mg/day followed by taper based on clinical improvement. The mean duration of steroid therapy was 4.3±2.5 months. No patients required discontinuation of steroid therapy due to adverse effects, although two patients declined initiating treatment with steroids due to concerns about weight gain.

Surgery for therapeutic, not diagnostic, purposes included incision and drainage in seven patients, FNA in eight patients, and excision of fistulous tract in one patient. No patients had large-volume excisions.

Table 4. Management of patients followed to clinical resolution (n = 36)

Therapy	n (%)
Antibiotics only*	18 (50.0)
Antibiotics + steroids*	3 (8.3)
Antibiotics + surgery*	4 (11.1)
Antibiotics + steroids + surgery*	8 (22.2)
Steroids only	1 (2.7)
Observation only	2 (5.6)

*81.8% of patients treated with antibiotics received a course of macrolides

Outcomes

The average time from the first breast clinic visit to clinical resolution was 8.0±4.6 months. The estimated probability of resolution was 41% within 6 months, 37% between 6 and 12 months, and 22% in more than 12 months. Time to resolution was not significantly associated with baseline lesion size ($p = 0.135$), identification of a pathogenic organism ($p = 0.738$), or time since symptom onset ($p = 0.127$).

Recurrence was defined as redevelopment of symptoms or clinical abnormalities greater than two months after cessation of therapy. In all, 17/36 (47%) patients were followed by either a breast clinic provider or another provider within our system after clinical resolution. Five of these patients (29%) developed recurrence of GM. The average number of months from clinical resolution to recurrence was 30.2.

Discussion and Conclusion

The results of our study lend support to the theory that an infectious process, particularly one initiated by corynebacteria, may play a role in the pathogenicity of GM. Historically, corynebacteria have been overlooked due to a lack of association of these bacteria with infection. However, the hypothesis that these organisms can be pathogenic in the breast is gaining momentum (20-23), and is consistent with what is understood about granuloma formation in other settings. *Mycobacterium tuberculosis*, for example, is also found in lipid-laden macrophages and produces a chronic inflammatory response, requiring long courses of antibiotics for effective treatment.

It is worth noting that 12/28 patients who presented to our breast clinic with microbiology data obtained from an outside institution had a microorganism identified in one or more samples. Though this may seem like a high yield compared with the low rates of positive cultures seen in prior studies, the majority of organisms identified in these patients were diphtheroids. For a number of reasons, diphtheroids may have been under-reported or under-detected in prior studies, including a paucity of organisms present in clinical specimens, fastidious growth requirements of *C. kroppenstedii*, and dismissal of diphtheroids isolated in culture as contaminants. Additionally, details about how tissue samples were obtained and cultured are not included in many studies. If samples were of superficial rather than deep-tissue, this may also explain the lower yield observed in other papers. Furthermore, antibiotic status at time of sampling can also affect the culture results. This could explain the relatively lower yield from cultures obtained at our institution, as a high percentage of patients were on antibiotics when samples were obtained for culture.

Despite the increasing literature suggesting a pathogenic role of *Corynebacterium* spp. in inflammatory breast disease and GM, it is not commonplace to request that laboratory staff consider isolation and identification of corynebacteria in specimens sent for analysis. We therefore suggest that when sending samples to the laboratory, clinicians alert laboratory staff to possible bacterial etiology and request that they provide a species-level identification of any corynebacteria recovered in culture. To evaluate for other secondary infectious etiologies of GM and improve overall yield, we suggest that samples (tissue, fluid, or purulent material) be submitted for Gram staining, bacterial culture, fungal staining and culture, and acid-fast bacilli staining and culture. To improve recovery of *C. kroppenstedii* in particular, laboratories

should consider adding Tween 80 (a lipid source) and esculin to growth media. Cultures should be incubated for a sufficient duration to recover slow-growing organisms such as *C. kroppenstedtii*. As the culture can be negative, the addition of a broad range bacterial, fungal, or acid-fast bacillus PCR can be considered to improve detection of infectious etiologies.

Based on the supposition that GM is the result of a bacterial infection, we prioritized treatment with prolonged courses of lipophilic antibiotics for adequate tissue penetrance within lipid-filled spaces. It is difficult to compare the results presented here to other studies in terms of time to resolution, as many existing studies do not include information about when a case was considered to have started (1st presentation vs 1st clinical encounter with subspecialist or date of diagnosis). One recent systematic review of cases from around the world demonstrated an average delay in diagnosis of four to five months (31). Still, accounting for heterogeneity in reporting of “start” and “completion” of therapy, our treatment strategy appears to be similar to those of other studies in terms of time to resolution, with a mean antibiotic therapy duration of seven months, and a mean total time from “first visit” to “resolution” of eight months.

While additional studies are needed to further evaluate the emerging theory regarding the role of corynebacteria in GM, given the growing evidence and the low morbidity associated with antibiotic treatment, it is reasonable for clinicians to consider treating GM with empiric antibiotic therapy in cases where an organism is not identified. Should a clinician choose this strategy, we suggest treatment with either clarithromycin 500 mg twice daily or doxycycline 100 mg twice daily. Clarithromycin is preferred in the absence of contraindications to its use. Like other macrolides, it concentrates in macrophages, which are integral to the formation and structure of granulomas (32). Possible side effects of clarithromycin include gastrointestinal side effects, elevated liver function tests, and QT prolongation. Water soluble agents used at the higher end of dosing (e.g., Amoxicillin 1000 mg every 8 hours) are another option if the above are contraindicated or not tolerated.

The response to antibiotic treatment can be slow, and careful measurement of the area of induration from visit to visit is essential. Based on our experience, signs of improvement—reduction in size, reduction in pain and erythema, organization of the phlegmon-like involvement into a drainable abscess—should be evident within 2–4 weeks. Clinic visits should be scheduled every 1–3 months to allow close monitoring for the above signs. Worsening or the absence of improvement should prompt a change to a second antibiotic. Antibiotic therapy should be continued until clinical resolution. If disease fails to improve with antibiotic therapy, addition of prednisone at 20–30 mg a day for 10–14 days with tapering based on the clinical response can be added to the antibiotic. Clinicians should be aware of the multitude of possible side effects of steroid therapy, including weight gain, mood disorders, hyperglycemia, hypertension, immunosuppression, and osteoporosis. The risk of these side effects can be mitigated by limiting the dose and duration of steroids to the minimum necessary for clinical effectiveness.

In our patients, we opted to avoid treatment with surgical excision, aside from excision of the fistulous tract in one patient. Multiple studies suggest that, although medical therapy or observation may be

a longer course to recovery than surgical excision, patients may in fact achieve resolution with non-surgical treatments and thus potentially be spared disfiguring surgeries or surgical complications (5, 7, 11, 33). Conservative needle drainage of well-formed abscesses and surgical drainage of larger ones did play a role in our treatment strategy but was reserved for refractory cases or for patients who desired more rapid symptom relief.

Confirmation of the superiority of an antibiotic-centered approach versus surgery, immunosuppressive treatment, or observation only requires a randomized trial. The roles of multi-drug therapy and intralesional injections are largely unexplored.

This study had a predominance of non-White patients, the majority being Hispanic. This pattern has been echoed in other studies (6, 8, 34) in the United States and is of unclear significance. Additionally, the Mediterranean region, specifically Turkey, has made a large contribution to the body of literature about GM, which raises the question of whether this disease has an epidemiologic clustering in certain ethnicities (35–37). One hypothesis to explain this may be due to differing natal microbiomes or environmental exposures in different ethnic groups. More research is needed to understand the epidemiology of this disease.

This study is limited in its scope to one academic center, which may limit its generalizability. However, our institution is typically a referral center for this disease, seeing perhaps a much larger volume than would be predicted based on the prevalence of the disease in the general population. Additional limitations include the retrospective nature of the data collection and limitations on access to patients’ microbiological and medication details from outside institutions.

In summary, this study suggests that GM may be the result of a primarily infectious process and highlights the need for further research. Until there is more definitive data in this area, we suggest that clinicians request inclusion of *Corynebacterium* spp. in the evaluation of samples sent for laboratory analysis. Extended courses of lipophilic antibiotics such as clarithromycin may be a viable treatment option; this approach has the potential to reduce the application of more harmful interventions such as prolonged steroid use (mean duration of steroid use only four months) or surgery, including mastectomy.

Acknowledgements

We would like to thank Nina Tan, MD for help with early literature review.

Ethics Committee Approval: The University of Washington Institutional Review Board reviewed and approved the study on 6/2/2015 (human subjects application with no: #49769).

Informed Consent: Granted waivers of consent by the University of Washington Institutional Review Board in Subcommittee EB.

Peer-review: Externally peer-reviewed.

Conflict of Interest: No conflict of interest was declared by the authors.

Financial Disclosure: The authors declared that this study received no financial support.

Authorship Contributions

Conception: A.H.M., M.B.L.; Design: A.H.M., M.B.L.; Supervision: M.B.L.; Editing: A.H.M.; Data Collection and/or Processing: M.S.W., M.B.L.; Analysis and/or Interpretation: M.S.W., M.B.L.; Literature Review: M.S.W., M.B.L., L.B.; Writing: M.S.W., M.B.L., L.B.; Critical Review: M.B.L.

References

- Kessler E, Wolloch Y. Granulomatous mastitis: a lesion clinically simulating carcinoma. *Am J Clin Pathol* 1972; 58: 642-646. (PMID: 4674439) [\[Crossref\]](#)
- Sheybani F, Sarvghad M, Naderi HR, Gharib M. Treatment for and clinical characteristics of granulomatous mastitis. *Obstet Gynecol* 2015; 125: 801-807. (PMID: 25751209) [\[Crossref\]](#)
- Pereira FA, Mudgil AV, Macias ES, Karsif K. Idiopathic granulomatous lobular mastitis. *Int J Dermatol* 2012; 51: 142-151. (PMID: 22250621) [\[Crossref\]](#)
- Patel RA, Strickland P, Sankara IR, Pinkston G, Many W Jr, Rodriguez M. Idiopathic granulomatous mastitis: case reports and review of literature. *J Gen Intern Med* 2010; 25: 270-273. (PMID: 20013067) [\[Crossref\]](#)
- Bouton ME, Jayaram L, O'Neill PJ, Hsu CH, Komenaka IK. Management of idiopathic granulomatous mastitis with observation. *Am J Surg* 2015; 210: 258-262. (PMID: 25746911) [\[Crossref\]](#)
- Davis J, Cocco D, Matz S, Hsu CH, Brown MJ, Lee J, et al. Re-evaluating if observation continues to be the best management of idiopathic granulomatous mastitis. *Surgery* 2019; 166: 1176-1180. (PMID: 31400951) [\[Crossref\]](#)
- Joseph KA, Luu X, Mor A. Granulomatous mastitis: a New York public hospital experience. *Ann Surg Oncol* 2014; 21: 4159-4163. (PMID: 25008030) [\[Crossref\]](#)
- Pandey TS, Mackinnon JC, Bressler L, Millar A, Marcus EE, Ganschow PS. Idiopathic granulomatous mastitis--a prospective study of 49 women and treatment outcomes with steroid therapy. *Breast J* 2014; 20: 258-266. (PMID: 24673796) [\[Crossref\]](#)
- Sakurai K, Fujisaki S, Enomoto K, Amano S, Sugitani M. Evaluation of follow-up strategies for corticosteroid therapy of idiopathic granulomatous mastitis. *Surg Today* 2011; 41: 333-337. (PMID: 21365412) [\[Crossref\]](#)
- Freeman CM, Xia BT, Wilson GC, Lewis JD, Khan S, Lee SJ, et al. Idiopathic granulomatous mastitis: a diagnostic and therapeutic challenge. *Am J Surg* 2017; 214: 701-706. (PMID: 28739122) [\[Crossref\]](#)
- Akbulut S, Arikanoğlu Z, Senol A, Sogutcu N, Basbug M, Yeniaras E, et al. Is methotrexate an acceptable treatment in the management of idiopathic granulomatous mastitis? *Arch Gynecol Obstet* 2011; 284: 1189-1195. (PMID: 21207047) [\[Crossref\]](#)
- Valeyre D, Prasse A, Nunes H, Uzunhan Y, Brilllet PY, Müller-Quernheim J. Sarcoidosis. *Lancet* 2014; 383: 1155-1167. (PMID: 24090799) [\[Crossref\]](#)
- Li J. Diagnosis and treatment of 75 patients with idiopathic lobular granulomatous mastitis. *J Invest Surg* 2019; 32: 414-420. (PMID: 29381437) [\[Crossref\]](#)
- Prasad S, Jaiprakash P, Dave A, Pai D. Idiopathic granulomatous mastitis: an institutional experience. *Turk J Surg* 2017; 33: 100-103. (PMID: 28740959) [\[Crossref\]](#)
- Akcan A, Oz AB, Dogan S, Akgun H, Akyuz M, Ok E, et al. Idiopathic granulomatous mastitis: comparison of wide local excision with or without corticosteroid therapy. *Breast Care (Basel)* 2014; 9: 111-115. (PMID: 24944554) [\[Crossref\]](#)
- Asoglu O, Ozmen V, Karanlik H, Tunaci M, Cabioglu N, Igci A, et al. Feasibility of surgical management in patients with granulomatous mastitis. *Breast J* 2005; 11: 108-114. (PMID: 15730456) [\[Crossref\]](#)
- Bani-Hani KE, Yaghan RJ, Matalka I, Shatnawi NJ. Idiopathic granulomatous mastitis: time to avoid unnecessary mastectomies. *Breast J* 2004; 10: 318-322. (PMID: 15239790) [\[Crossref\]](#)
- Chirappapha P, Thaweepworadej P, Supsamutchai C, Biadul N, Lertsithichai P. Idiopathic granulomatous mastitis: a retrospective cohort study between 44 patients with different treatment modalities. *Ann Med Surg (Lond)* 2018; 36: 162-167. (PMID: 30479764) [\[Crossref\]](#)
- Wilson JP, Massoll N, Marshall J, Foss RM, Copeland EM, Grobmyer SR. Idiopathic granulomatous mastitis: in search of a therapeutic paradigm. *Am Surg* 2007; 73: 798-802. (PMID: 17879688) [\[Crossref\]](#)
- Taylor GB, Paviour SD, MUSAAD S, Jones WO, Holland DJ. A clinicopathological review of 34 cases of inflammatory breast disease showing an association between corynebacteria infection and granulomatous mastitis. *Pathology* 2003; 35: 109-119. (PMID: 12745457) [\[Crossref\]](#)
- Paviour S, MUSAAD S, Roberts S, Taylor G, Taylor S, Shore K, et al. Corynebacterium species isolated from patients with mastitis. *Clin Infect Dis* 2002; 35: 1434-1440. (PMID: 12439810) [\[Crossref\]](#)
- Wong SCY, Poon RWS, Chen JHK, Tse H, Lo JYC, Ng TK, et al. Corynebacterium kroppenstedtii Is an emerging cause of mastitis especially in patients with psychiatric illness on antipsychotic medication. *Open Forum Infect Dis* 2017; 4: ofx096. doi: 10.1093/ofid/ofx096 (PMID: 28852671) [\[Crossref\]](#)
- Dobinson HC, Anderson TP, Chambers ST, Doogue MP, Seaward L, Werno AM. Antimicrobial treatment options for granulomatous mastitis caused by corynebacterium species. *J Clin Microbiol* 2015; 53: 2895-2899. (PMID: 26135858) [\[Crossref\]](#)
- Kutsuna S, Mezaki K, Nagamatsu M, Kunimatsu J, Yamamoto K, Fujijya Y, et al. Two cases of granulomatous mastitis caused by corynebacterium kroppenstedtii infection in nulliparous young women with hyperprolactinemia. *Intern Med* 2015; 54: 1815-1818. (PMID: 26179543) [\[Crossref\]](#)
- Tauch A, Schneider J, Szczepanowski R, Tilker A, Viehoveer P, Gartemann KH, et al. Ultrafast pyrosequencing of corynebacterium kroppenstedtii DSM44385 revealed insights into the physiology of a lipophilic corynebacterium that lacks mycolic acids. *J Biotechnol* 2008; 136: 22-30. (PMID: 18430482) [\[Crossref\]](#)
- Goh Z, Tan AL, Madhukumar P, Yong WS. Recurrent corynebacterium kroppenstedtii breast abscess in a young asian female. *Breast J* 2015; 21: 431-432. (PMID: 26136183) [\[Crossref\]](#)
- Gibson SER, Harrison J, Cox JAG. Modelling a silent epidemic: a review of the in vitro models of latent tuberculosis. *Pathogens* 2018; 7: 88. (PMID: 30445695) [\[Crossref\]](#)
- Silva LC, Geluk A, Arnone M, Romiti R, Franken KC, Duarte AJ, et al. Infliximab partially impairs the anti-Mycobacterium tuberculosis immune responses of severe psoriasis patients with positive tuberculin skin-test. *J Eur Acad Dermatol Venereol* 2012; 26: 319-324. (PMID: 21623925) [\[Crossref\]](#)
- Johnson MG, Leal S, Plongla R, Leone PA, Gilligan PH. The brief case: recurrent granulomatous mastitis due to corynebacterium kroppenstedtii. *J Clin Microbiol* 2016; 54: 1938-1941. (PMID: 27458268) [\[Crossref\]](#)
- Harris PA, Taylor R, Thielke R, Payne J, Gonzalez N, Conde JG. Research electronic data capture (REDCap)--a metadata-driven methodology and workflow process for providing translational research informatics support. *J Biomed Inform* 2009; 42: 377-381. (PMID: 18929686) [\[Crossref\]](#)
- Martinez-Ramos D, Simon-Monterde L, Suelves-Piqueres C, Queralt-Martin R, Granel-Villach L, Laguna-Sastre JM, et al. Idiopathic granulomatous mastitis: A systematic review of 3060 patients. *Breast J* 2019; 25: 1245-1250. (PMID: 31273861) [\[Crossref\]](#)
- Jain R, Danziger LH. The macrolide antibiotics: a pharmacokinetic and pharmacodynamic overview. *Curr Pharm Des* 2004; 10: 3045-3053. (PMID: 31273861) [\[Crossref\]](#)

33. Lai EC, Chan WC, Ma TK, Tang AP, Poon CS, Leong HT. The role of conservative treatment in idiopathic granulomatous mastitis. *Breast J* 2005; 11: 454-456. (PMID: 16297091) [[Crossref](#)]
34. Idiopathic Granulomatous Mastitis in Hispanic Women --- Indiana, 2006--2008. Last Accessed Date : 12.02.2009 Available from: <https://www.cdc.gov/mmwr/preview/mmwrhtml/mm5847a1.htm>. [[Crossref](#)]
35. Karanlik H, Ozgur I, Simsek S, Fathalizadeh A, Tukenmez M, Sahin D, et al. Can steroids plus surgery become a first-line treatment of idiopathic granulomatous mastitis? *Breast Care (Basel)* 2014; 9: 338-342. (PMID: 25759614) [[Crossref](#)]
36. Korkut E, Akcay MN, Karadeniz E, Subasi ID, Gursan N. Granulomatous mastitis: a ten-year experience at a University Hospital. *Eurasian J Med* 2015; 47: 165-173. (PMID: 26644764) [[Crossref](#)]
37. Oran ES, Gurdal SO, Yankol Y, Oznur M, Calay Z, Tunaci M, et al. Management of idiopathic granulomatous mastitis diagnosed by core biopsy: a retrospective multicenter study. *Breast J* 2013; 19: 411-418. (PMID: 23663101) [[Crossref](#)]



Evaluation of Three-Dimensional Conformal Radiotherapy and Intensity Modulated Radiotherapy Techniques for Left Breast Post-Mastectomy Patients: Our Experience in Nigerian Sovereign Investment Authority-Lagos University Teaching Hospital Cancer Center, South-West Nigeria

Samuel Adeneye¹, Michael Akpochafor¹, Bolanle Adegboyega², Adewumi Alabi¹, Nusirat Adedewe¹, Adedayo Joseph³, Omolara Fatiregun⁴, Akintayo Omojola⁵, Abe Adebayo², Esther Oluwadara¹

¹Department of Radiation Biology, Division of Radiotherapy and Radiodiagnosis, College of Medicine, University of Lagos/NSIA-LUTH Cancer Centre, Lagos, Nigeria

²Department of Radiotherapy, Lagos University Teaching Hospital, Lagos, Nigeria

³Department of Radiotherapy, Nigeria Sovereign Investment Authority-Lagos University Teaching Hospital, Lagos, Nigeria

⁴Medical Physics Unit, Federal Medical Centre Asaba, Asaba, Nigeria

⁵Department of Radiology, Lagos State University College of Medicine, Lagos, Nigeria

ABSTRACT

Objective: This study aimed to evaluate the dosimetric properties of treatment plans obtained from three-dimensional conformal radiotherapy (3D-CRT) and intensity-modulated radiotherapy techniques (IMRT) plans for left chest wall breast cancer patients.

Materials and Methods: A total of 20 patients with left-sided chest wall radiotherapy were randomly selected with the dose prescriptions: 42 Gy and 45 Gy in 15 and 18 fractions, respectively. Treatment plans were obtained using 3D-CRT and IMRT for each patient. Five to seven beams were used for IMRT, while tangential beams were used for 3D-CRT. Planning target volume, $D_{near-max}$ (D_2), $D_{near-min}$ (D_{99}), D_{mean} , Homogeneity and Conformity Indices (HI and CI) were obtained. Similarly, mean doses to organs at risk (OAR), V_5 , V_{10} , V_{20} , V_{25} were generated from the dose-volume histogram and compared.

Results: IMRT showed a significant improvement in HI compared to 3D-CRT ($p < 0.0001$). Although there was no significant difference in sparing of the left lung between both plans for high-dose volumes (V_{20} : 18.2 vs 30.55, $p < 0.0001$), (V_{25} : 11.17 vs 28.12, $p < 0.0001$). IMRT however showed supremacy to 3D-CRT with high-dose volumes for the heart, including V_{20} (4.44 vs 10.29, $p = 0.02$), V_{25} (2.08 vs 8.94, $p = 0.002$). 3D-CRT was better than IMRT in low-dose volumes for left lung (V_5 : 92.23 vs 56.60, $p < 0.001$; V_{10} : 60.98 vs 47.20, $p = 0.04$) and heart (V_5 : 57.45 vs 30.39, $p = 0.004$).

Conclusion: IMRT showed better homogeneity and sparing of high-dose volumes to OAR than 3D-CRT. On the other hand, 3D-CRT showed a reduction of low-dose volumes to OARs than IMRT.

Keywords: IMRT, 3D-CRT, PMRT, organs at risk, radiotherapy

Cite this article as: Adeneye S, Akpochafor M, Adegboyega B, Alabi A, Adedewe N, Joseph A, Fatiregun O, Omojola A, Adebayo A, Oluwadara E. Evaluation of Three-Dimensional Conformal Radiotherapy and Intensity Modulated Radiotherapy Techniques for Left Breast Post-Mastectomy Patients: Our Experience in Nigerian Sovereign Investment Authority-Lagos University Teaching Hospital Cancer Center, South-West Nigeria. Eur J Breast Health 2021; 17(3): 247-252

Key Points

- The dosimetric properties of 3D-CRT and IMRT for left-chestwall in breast cancer patients were evaluated on 20 patients.
- Dosimetric parameters of PTV and OARs were obtained and analyzed from the DVH.
- HI and CI were also calculated and compared.
- Although, HI was better in IMRT than 3D-CRT, showed better sparing of low-dose volumes to OARs.

Introduction

Breast cancer is the most frequently diagnosed life-threatening malignancy that affects women, and the leading cause of cancer death in women globally (1). It accounts for 15.3% of cancer diagnosed globally and 7% of cancer-related deaths (2). Unlike in developing countries, the survival rate of breast cancer has increased in developed countries over the past 20 years, and more women are now being treated successfully than in previous years. The majority of patients in developing countries present an advanced stage of the disease, owing to several factors that include late presentations, delay in making an appropriate diagnosis, lack of access to cancer treatment, unavailability of advanced technology and infrastructure, poor health practices, ignorance, poverty, and several others (3). Breast cancer treatment is multifactorial-dependent, involving surgery, chemotherapy, radiotherapy, hormonal therapy, and targeted therapy. Over the years, advances in technology have helped to improve the survival rate.

Moreover, newer technologies and treatment methods are currently being developed. Radiotherapy plays a significant role in preventing local and regional recurrence in breast cancer care. It is an important aspect of breast cancer treatment, which minimizes the risk of regional recurrence and enhances the overall life of early-stage breast cancer and the locally advanced disease following mastectomy (4, 5). However, chest wall and regional lymph node irradiation is one of the most complex challenging strategies of radiation. Radiotherapy has a significant impact in the management of breast cancer. Radiating the chest wall and regional lymph nodes, such as supraclavicular, axillary, and internal mammary nodes, requires special care for lung, cardiac, and contralateral breast doses. The main aim of radiotherapy is to treat the target volume and protect the surrounding healthy tissues. Three-dimensional conformal radiotherapy (3D-CRT) and intensity-modulated radiotherapy (IMRT) are most often used in the treatment of breast cancer. IMRT is a form of 3D-CRT that further modifies the radiation beam, varying the intensity of radiation to allow optimal treatment precision and dose delivery. It directs radiation at the post-mastectomy tumor bed and modulates the intensity of the radiation beams with laser accuracy, thus ensuring the sparing of surrounding healthy tissues (6). This study was conducted at our cancer center to compare the dosimetric properties in 3D-CRT and IMRT on patients with left post-mastectomy breast cancer who received chest wall radiation.

Materials and Methods

Patients

Between June 2019 and September 2020, a total of 20 women (aged over 18 years) with invasive ductal carcinoma (T0–T3, N0–N1), left-sided breast cancer treated with modified radical mastectomy, followed by radiotherapy to the chest wall, axillary lymph nodes levels I-III, and supraclavicular fields were randomly selected at the NSIA-LUTH Cancer center, Lagos, Nigeria. All patients were treated with IMRT. Chest walls, including supraclavicular and axillary lymph nodes, were re-planned using 3D-CRT on the Varian's eclipse treatment planning system (TPS) version 15.6 (7).

Computed tomography simulation

Patients were scanned with 16-slice General electric computed tomography (CT) scanner with 2.5 mm thickness. With the aid of a

breast board, CT Simulation was performed in a supine position, with arms raised and head in a fixed position. Images were obtained in digital imaging and communication in medicine format and transferred to the Eclipse TPS version 15.6 (VARIAN medical systems) (7).

Target definition

Under the protocol of the International Commission on Radiation Units and Measurements (ICRU report 83, 2010), all volumes, gross tumor volume, clinical target volume (CTV), planning target volume (PTV), heart, ipsilateral and contralateral lung, contralateral breast, and whole body were delineated. The PTV was restricted to the chest wall, nodes, and supraclavicular, which encloses the CTV with a 1 mm margin. All patients were treated with the Varian Linear accelerator (Varian Medical System, Palo Alto, CA, USA), which utilizes the Eclipse TPS with 6 MV and 10 MV photon beam. Dose and fractionation for all targets were between 42 Gy and 45 Gy for 15 and 18 fractions, respectively. The goal of each plan was to deliver 95% of the prescribed dose to 100% of the target volume. The PTV was in the range of 99.5–937.2 cm³.

Treatment plan

For treatment planning, 6 MV and 10 MV beams from Vital-beam linear accelerator (Varian Medical Systems, Palo Alto, California, USA) integrated with 120 millennium multi-leaf collimator (MLC) was used. Two tangential fields were applied in 3D-CRT plan with the use of more fields (where necessary) to improve the dose distribution. Field-in-fields technique with MLCs were used to reduce hot spots and the maximum dose. Tools, such as field weightings, plan normalization, and normalization at isocenter, were utilized at appropriate situations to achieve a better dose coverage. All MLCs were positioned to block a part of the lung, while the heart was considered using the beams eye view, keeping both organs at the lowest dose achievable.

The IMRT treatment plan was created with an inverse plan optimization, and the algorithm used was dose-volume optimizer. The number of fields used for plans ranged between five and seven beams with 6 MV photon beam. The beam selection or arrangement was based on the discretion of the physicist on the best possible plan achievable. Digital reconstructed radiograph was obtained for all fields in each plan to verify the patients' position. The plans were optimized to cover the whole PTV, while sparing the organs at risk. In some cases, a 0.5 mm thickness of bolus was used for the optimal dose. Priority was given to the PTV and Organ at risk (OAR), which were gradually increased as deemed fit until a balance was reached between achieving good coverage and sparing OARs. The optimization process was done with the Eclipse TPS using the anisotropic analytical algorithm for calculation. The overall goal was to cover 95% of the PTV with the prescription and maximum dose below 107%. The dose constraints for OAR used in this study was recommended by QUANTEC (2010) (8). For the ipsilateral lung, 10% of the total volume should not receive more than 20 Gy ($V_{25} < 10\%$), while $\leq 5\%$ of the volume of the heart should not receive more than 25 Gy (contralateral breast mean dose ≤ 3 Gy).

Plan evaluation

For dosimetric analysis, the data collated from the dose volume histograms (DVHs) includes: $D_{near-max}$ (D_2), defined as the dose delivered to 2% of the PTV; $D_{near-min}$ (D_{98}), which is the dose delivered to 98% of the volume of PTV; mean dose to the PTV, D_{mean} , and

D_p , defined as the prescribed dose. Homogeneity index (HI) and conformity index (CI) were calculated according to the definition proposed by International Commission on Radiation Units and Measurements (ICRU Report 83) (9). HI and CI are estimated as:

$$HI = \frac{D_{2\%} - D_{98\%}}{D_p} \text{ and } CI = \frac{V(RI)}{TV}$$

Where $V(RI)$ is defined as volume of reference isodose (95% of the prescribed dose), while TV is the Target Volume. A more homogenous dose distribution is described by a HI value closer to zero and the closer the CI is to 1, the higher the conformity of the dose conforms to the PTV. In other words, 0 is the ideal value for HI and 1 is the ideal value for CI.

The percentage volume of the left lung receiving V_5 (5 Gy), V_{10} (10 Gy), V_{20} (20 Gy), V_{25} (25 Gy), and D_{mean} , as well as the percentage volume receiving $V_5, V_{10}, V_{20}, V_{25}$, and D_{mean} to the heart were all obtained from the DVH.

Statistical analysis

All data were recorded on Microsoft Excel 2010. Statistical Package for Social Sciences for Windows, Version 18.0 (IBM Corp. Armonk, NY, USA) was used to analyze the data obtained from the DVHs. Student t-test for two independent means was used to analyze the dosimetric differences between parameters. P-value <0.05 was considered statistically significant.

Results

All patients IMRT plans were reviewed and approved by a radiation oncologist before treatment. A total of 20 plans for 3D-CRT and IMRT plans were created for this study, obtaining a comparison of the dosimetric parameters between both techniques. Table 1 summarizes the results of PTV in terms of $D_{near-max}, D_{near-min}, D_{mean}, V_{95}, HI$, and CI.

There was a non-significant difference with IMRT compared to 3D-CRT in terms of conformity (CI) (0.994 vs 1.1586, $p = 0.5786$). Similar results were seen for D_{mean} (43.20 vs 43.13, $p = 0.893$) and V_{95} (567.43 vs 518.42, $p = 0.390$). A huge significant difference was seen among these parameters in both techniques. However, there was significant difference between the two planning techniques in terms of $D_{near-max}$ (44.55 vs 46.25, $p = 0.002$), $D_{near-min}$ (D_{98}) at (41.73 vs 37.71,

$p = 0.001$), and HI (0.065 vs 0.1984, $p = 0.0001$). Figure 1a shows the 95% dose coverage and beam arrangement of 3D-CRT plans. Figure 1b shows the DVH of 3D-CRT plans. Figure 2a shows the 95% dose coverage and beam arrangement of IMRT plans. Figure 2b shows the DVH of IMRT plans. Regarding dose constraint to OAR, particularly the left lung and heart, immense consideration was given in all plans. All IMRT plans were clinically acceptable and fit for treatment. The left lung and heart were both within recommended constraints (QUANTEC 2010) used by the center for the IMRT plans.

Table 2 analyzes the dosimetric parameters of the OARs between the 3D-CRT plans and IMRT plans. The mean dose to the left lung was within tolerance and considered not significant between both plans (13.66 vs 18.25, $p = 0.05$), while that of the Heart showed a significant difference at (7.55 vs 8.21, $p = 0.7$). There was no significant difference

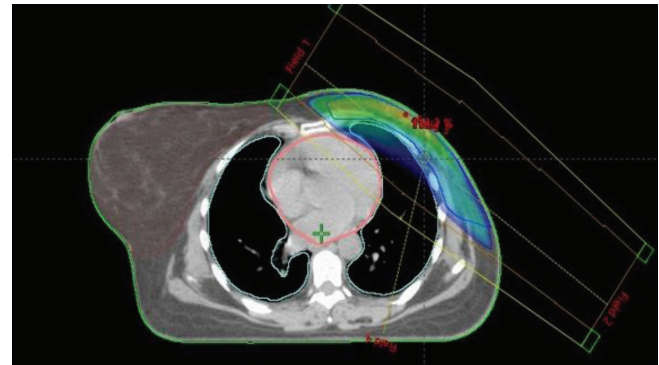


Figure 1a. PTV beam arrangement for 3D-CRT

PTV: Planning target volume; 3D-CRT: Three-dimensional conformal radiotherapy

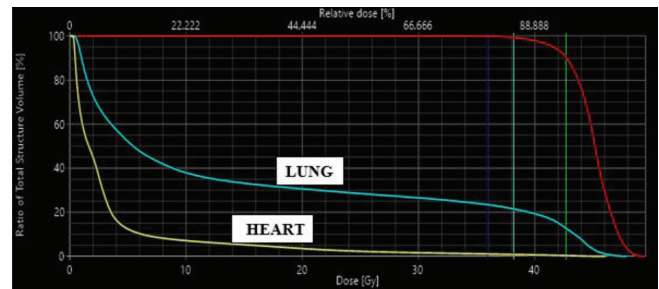


Figure 1b. PTV dose volume histogram for 3D-CRT

PTV: Planning target volume; 3D-CRT: Three-dimensional conformal radiotherapy

Table 1. Dosimetric comparison of PTV using 3D-CRT and IMRT

Parameters	3D-CRT	IMRT	p-value
PTV volume (cm ³)	569.57±227.95	571±187.84	0.983
$D_{near-max}$ (D_2), (Gy)	46.25±1.63	44.55±1.52	0.002
$D_{near-min}$ (D_{98}), (Gy)	37.71±2.28	41.73±1.30	<0.001
Prescribed dose (D_p), (Gy)	43.05±1.49	43.05±1.49	1.000
D_{mean} , (Gy)	43.13±1.95	43.20±1.77	0.893
V_{95} , (%)	518.42±169.30	567.43±186.48	0.390
HI	0.1984±0.065	0.065±0.009	<0.0001
CI	1.1586±1.314	0.994±0.005	0.579

PTV; D_2 and D_{98} -Dose delivered to 2% and 98% of PTV, respectively; D_p -Prescribed dose; D_{mean} -Mean dose; HI: homogeneity; CI: Conformity index; 3D-CRT: Three-dimensional conformal radiotherapy; IMRT: Intensity modulated radiotherapy techniques

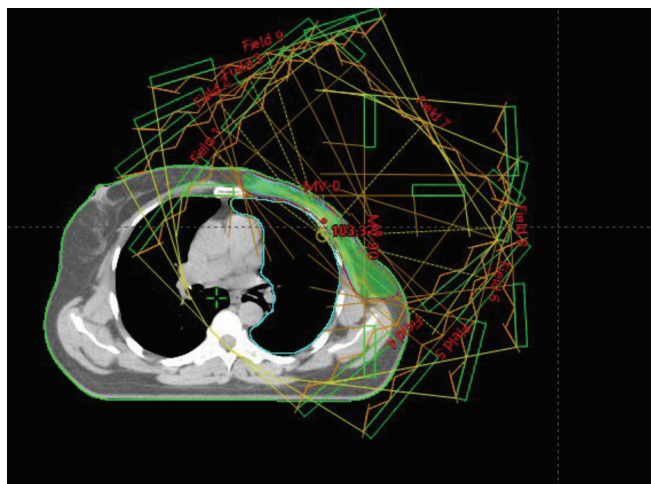


Figure 2a. PTV beam arrangement for IMRT

PTV: Planning target volume; IMRT: Intensity modulated radiotherapy techniques

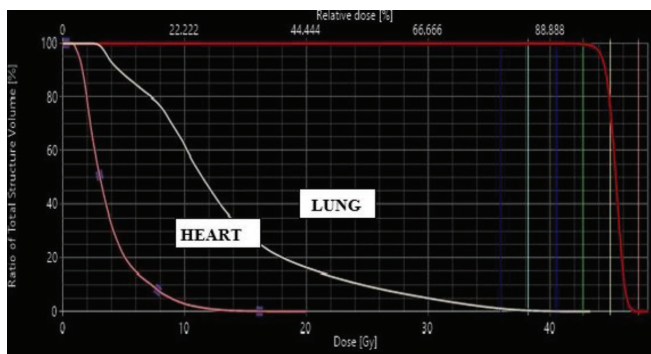


Figure 2b. PTV dose volume histogram for IMRT

PTV: Planning target volume; IMRT: Intensity modulated radiotherapy techniques

in sparing of the left lung between both plans for high-dose volumes, including V_{20} and V_{25} . IMRT significantly reduced the dose to the volumes V_{20} and V_{25} when compared to 3D-CRT (V_{20} : 18.2 vs 30.55, $p < 0.0001$; V_{25} : 11.17 vs 28.12, $p < 0.0001$). For the heart, there was no significant variation, since IMRT showed supremacy to 3D-CRT at high-dose volumes (V_{20} : 4.44 vs 10.29, $p = 0.02$; V_{25} : 2.08 vs 8.94, $p = 0.002$). On the other hand, 3D-CRT showed a significant exceptionality to IMRT in terms of low-dose volumes for left lung (V_5 : 92.23 vs 56.60, $p < 0.001$, V_{10} : 60.98 vs 47.20, $p = 0.04$) and heart (V_5 : 57.45 vs 30.39, $p = 0.004$). A significant difference was seen for V_{10} in heart (24.48 vs 24.23, $p = 0.974$) for 3D-CRT.

However, there was no significant difference between the two planning techniques in terms of $D_{near-max}$ (D_2) at (44.55 vs 46.25, $p = 0.002$), $D_{near-min}$ (D_{98}) at (41.73 vs 37.71, $p = 0.001$) and the Homogeneity index (HI) at (0.065 vs 0.1984, $p = 0.0001$). In comparing the dose to the contralateral breast, the mean dose and V_5 were statistically significant (2.35 vs 1.235, $p = 0.0016$; 12.01 vs 4.76, $p = 0.008$, respectively). On the other hand, the mean dose and V_5 to the contralateral lung showed no significant variation (4.036 vs 2.457, $p = 0.153$; 30.105 vs 16.885, $p = 0.127$, respectively).

Discussion and Conclusion

This study provides an optimal plan to every patient whose chest wall were radiated by IMRT, thereby protecting the OARs. Many studies have been conducted to demonstrate the superiority of one technique over another. In several trials, the advantages of IMRT over 3D-CRT with lower dose to OARs and improved dosage compliance to PTV were found in whole breast cancers. There are few accounts of radiotherapy after mastectomy (PMRT). In this study, the dose conformity, homogeneities, and sparing of OAR were analyzed for PMRT in our center. A dosimetric comparison of 3D-CRT and IMRT with left-sided mastectomy patients was done by Fiorentino et al. (10) and it was found that there was no significant difference between the two treatment planning techniques in terms of maximum dose (5.579

Table 2. Dosimetric comparison of OARs using 3D-CRT and IMRT

Organ at risk	Parameters	3D-CRT	IMRT	p-value
Ipsilateral lung	V_5	56.60%±25.06%	92.23%±5.64%	<0.001
	V_{10}	47.20%±26.60%	60.98%±12.89%	0.04
	V_{20}	30.55%±9.95%	18.2%±2.51%	<0.0001
	V_{25}	28.12%±9.21%	11.17%±1.96%	<0.0001
	D_{mean} (Gy)	18.25±10.2	13.66±1.29	0.05
Heart	V_5	30.39%±33.23%	57.45%±20.77%	0.004
	V_{10}	24.23%±31.61%	24.48%±13.58%	0.9741
	V_{20}	10.29% ±10.47%	4.44%±3.12%	0.02
Contralateral breast	V_{25}	8.94%±8.98%	2.08%±1.56%	0.002
	D_{mean} (Gy)	8.21±7.66	7.55±2.25	0.7
	d_{mean} (Gy)	1.234±1.069	2.35±1.004	0.0016
Contralateral lung	V_5	4.76±4.98	12.01±10.63	0.008
	d_{mean} (Gy)	2.457±4.614	4.036±1.479	0.153
Contralateral lung	V_5	16.885± 33.766	30.105±17.4	0.127

D_{mean} : Mean dose; V_x : Volume of tissue receiving X Gy; 3D-CRT: Three-dimensional conformal radiotherapy; IMRT: Intensity modulated radiotherapy techniques; OAR: Organ at risk

vs 5.529, $p = 0.51$), minimum dose (3.900 vs 3.887, $p = 0.85$), mean dose (4.698 vs 5.137, $p = 0.33$), and homogeneity index (1.17 vs 1.16, $p = 0.47$). Recently, Shanei et al. (11) conducted a radiobiological comparison of 3D-CRT and IMRT in left-sided radiotherapy breast cancer. Their results showed a significant increase in mean dose of the target ($p < 0.001$) and a significant difference in CI and HI for six to nine fields IMRT plans than 3D-CRT at $p < 0.001$. In the current study, there was a non-significant difference in mean dose to the target ($p = 0.983$) and CI ($p = 0.5786$), with HI significant at ($p < 0.001$). In 2013, Moorthy et al. (12) compared the dosimetric properties of SIB-IMRT and SIB-3D-CRT for breast cancer using breath-holding gated technique. Although no significant difference was seen in HI ($p = 0.45$) for both techniques, an improvement in CI from 3D-CRT (0.18) to IMRT (0.14) at ($p = 0.01$) was observed. Also, it was stated that IMRT reduced the dose to the OAR better than 3D-CRT. In a research study regarding PMRT in 3D-CRT and IMRT, Rastogi et al. (13) concluded that IMRT significantly improves CI at $p < 0.001$ and that no significant difference was seen in both techniques for mean dose, although IMRT, in comparison with 3D-CRT, significantly reduced the high-dose volumes of ipsilateral lung and heart, 3D-CRT is superior in low-dose volume. Li et al. (14) also investigated IMRT and 3D-CRT in post-mastectomy irradiation of chest wall and regional nodes and found that low-dose volumes to the ipsilateral lung were better spared in 3D-CRT, while high-dose volumes to the lungs were better spared in IMRT; and homogeneity and conformity were also better in IMRT than in 3D-CRT. Findings from these studies are similar to those of our study for HI, which showed a significant variation, the current CI is considered non-significant. It is worthy to state that the heterogenous dose distribution, hot/cold spots due to irregular breast contour, difficulty in establishing dose consistency, and homogeneity are few of the challenges found in 3D-CRT technique. Normal tissues are exposed to radiation during treatment of primary cancer. The dose to the contralateral breast and lung has been proven to cause secondary cancer. The IMRT treatment plans adhered to the QUANTEC constraint of less than 3 Gy for contralateral breast. A significant difference was seen in mean dose and V_5 for contralateral breast ($p = 0.0016$). This was in line with the results reported in Serhat et al. (15).

Radiation pneumonitis and cardiac morbidity are major concerns in patients who have received radiotherapy after a mastectomy. Many factors, including radiation fractionation, volume of lung radiated, intake of chemotherapy drugs, and increasing use of CT, have been implicated in the increasing rate of this complication (16, 17). Although there is no threshold or safe dose to which they do not occur, dose to the lungs and heart should be kept as low as achievable and this is seen in the present study. IMRT showed better sparing in V_{20} and V_{25} to the left lung and heart. The geometric difference between whole breast cancers and PMRT (chest wall radiation) may have an impact on the dose distribution; in other words, the anatomical structure of the whole breast and chest wall are much different. This may be a reason for the differences in dose distribution to OAR found in other studies. We encountered a few limitations during the research, one of which was the less number of patients. Another was a short follow-up on radiation toxicity and local control in IMRT plans, which was not addressed in this work. In the future, further studies are encouraged to address these limitations.

In conclusion, this work showed better homogeneity and conformity of dose to target volume in IMRT than in 3D-CRT. However, the 3D-CRT was found to be exceptional in low-dose volumes for left

lung and heart (V_5 and V_{10}) than IMRT. IMRT showed superiority in high-dose volumes (V_{20} and V_{25}) to the organ at risk. IMRT was proven to be a better technique than 3D-CRT in terms of dose homogeneity and sparing of OAR, however, no substantial difference was seen in CI.

Acknowledgements

We want to appreciate Abdallah E Kotkat, Ibrahim EL Hamamsi, Mr Lawal Rasak, Dr. Tolu Adewole, Prof. Fasanmade, Prof. Durosinmi-Etti and Prof. Aweda for their great contribution towards the success of this work.

Ethics Committee Approval: ADM/DCST/HREC/APP/3783, 13/08/2020, Lagos University Teaching Hospital Health Research Ethics Committee.

Informed Consent: It was taken.

Peer-review: Externally peer-reviewed.

Authorship Contributions

Conception: S.A., B.A.; Design: S.A., M.A., B.A.; Supervision: M.A., B.A.; Materials: A.A., N.A.; Data Collection and/or Processing: A.A., E.O.; Analysis and/or Interpretation: N.A., O.F.; Literature Review: A.J., A.O.; Writing: S.A., N.A. Ad.A.; Critical Review: A.A., O.F.

Conflict of Interest: No conflict of interest was declared by the authors.

Financial Disclosure: The authors declared that this study received no financial support.

References

1. Youlden D, Cramb S, Yip CH, Baade P. Incidence and mortality of female breast cancer in the Asia-Pacific region. *Cancer Biol Med* 2014; 11: 101-115. (PMID: 25009752) [Crossref]
2. National Cancer Institute. SEER-Medicare: Brief description of the SEER-Medicare database. Last Accessed Date: 10.06.2020. Available from: <http://healthservices.cancer.gov/seermedicare/overview/brief.html> [Crossref]
3. Awofeso O, Roberts AA, Salako O, Balogun L and Okediji P. Prevalence and pattern of late-stage presentation in women with breast and cervical cancers in Lagos University Teaching Hospital, Nigeria. *Niger Med J* 2018; 59: 74-79. (PMID: 31423046) [Crossref]
4. Darby S, McGale P, Correa C, Taylor C, Arriagada R, Clarke M, et al. Effect of radiotherapy after breast-conserving surgery on 10-year recurrence and 15-year breast cancer death; meta-analysis of individual patient data for 10,801 women in 17 randomized trials. *Lancet* 2011; 378: 771-784. (PMID: 22019144) [Crossref]
5. Clarke M, Collins R, Darby S, Davies C, Elphinstone P, Evans V, et al. Effect of radiotherapy and of differences in the extent of surgery for early breast cancer on local recurrence and 15-year survival: an overview of the randomized trials. *Lancet* 2005; 366: 2087-2106. (PMID: 16360786) [Crossref]
6. Rastogi K, Sharma S, Gupta S, Agarwal N, Bhaskar S, Jain S. Dosimetric comparison of IMRT versus 3DCRT for post-mastectomy chest wall irradiation. *Radiat Oncol J* 2018; 36: 71-78. (PMID: 29621872) [Crossref]
7. 2018 Varian Eclipse Plan Challenge Aims to Improve Lung SBRT Plan Quality, 2018. Last Accessed Date: 11.12.2020. Available from: <https://www.varian.com/resources-support/blogs/clinical-oncology-news/2018-varian-eclipse-plan-challenge-aims-improve-lung> [Crossref]
8. Bentzen SM, Constine LS, Deasy JO, Eisbruch A, Jackson A, Marks LB, et al. Quantitative Analyses of Normal Tissue Effects in the Clinic

- (QUANTEC): an introduction to the scientific issues. *Int J Radiat Oncol Biol Phys* 2010; 76(Suppl 3): S3-S9. doi: 10.1016/j.ijrobp.2009.09.040 (PMID: 20171515) [[Crossref](#)]
9. Menzel HG. International Commission of Radiological Units (ICRU) Report 83. *J ICRU*. 2010; 10: Report 83 Oxford University.
 10. Fiorentino A, Ruggieri R, Giaj-Levra N, Sicignano G, Di Paola G, Naccarato S, et al. Three-dimensional conformal versus intensity modulated radiotherapy in breast cancer treatment: Is necessary a medical reversal? *Radiol Med* 2017; 122: 146-153. (PMID: 27778239). [[Crossref](#)]
 11. Shanei A, Amouheidari A, Abedi I, Kazemzadeh A, Jaafari A. Radiobiological comparison of 3D conformal and intensity modulated radiation therapy in the treatment of left-sided breast cancer. *Int J Radiat Res* 2020; 18: 315-322. [[Crossref](#)]
 12. Moorthy S, Sakr H, Hasan S, Samuel J, Al-Janahi S, Murthy N. Dosimetric study of SIB-IMRT versus SIB-3DCRT for breast cancer with breath-hold gated technique. *Int J Cancer Ther Oncol* 2013; 1: 010110. doi:10.14319/ijcto.0101.10 [[Crossref](#)]
 13. Rastogi K, Sharma S, Gupta S, Agarwal N, Bhaskar S, Jain S. Dosimetric comparison of IMRT versus 3DCRT for post-mastectomy chest wall irradiation. *Radiat Oncol J* 2018; 36: 71-78. (PMID: 29621872) [[Crossref](#)]
 14. Li W, Ma J, Chen J, Zhang Z. IMRT versus 3D-CRT for postmastectomy irradiation of chest wall and regional nodes: a population-based comparison of normal lung dose. *Int J Radiat Oncol Biol Phys* 2014; 1: S246-S247. [[Crossref](#)]
 15. Serhat A, Turkan I, Meryem A. Dosimetric comparison of Three-Dimensional Conformal Radiotherapy (3D-CRT) and Intensity Modulated Radiotherapy Techniques (IMRT) with radiotherapy dose simulations for left-sided mastectomy patients. *Eur J Breast Health* 2019; 15: 85-89. (PMID: 31001609) [[Crossref](#)]
 16. Lingos T, Recht A, Vicini F, Abner A, Silver B, Harris JR. Radiation pneumonitis in breast cancer patients treated with conservative surgery and radiation therapy. *Int J Radiat Oncol Biol Phys* 1991; 21: 355-360. (PMID: 2061112) [[Crossref](#)]
 17. Travis E. Lung morbidity of radiotherapy. In: Plowman P, McElwain TJ, Meadows AT, editors. *Complications of cancer management*. Oxford (UK): Butterworth-Heinemann; 1991. p. 232-249. [[Crossref](#)]



How Do Breast Cancer Patients Present Following COVID-19 Early Peak in a Breast Cancer Center in Turkey?

Aysun Dauti Işıklar¹, Cem Deniz², Aykut Soyder¹, Nilgün Güldoğan¹, Ebru Yılmaz¹, Gül Başaran^{1,2}

¹Breast Health Center, Acibadem Altunizade Hospital, İstanbul, Turkey

²Acibadem University School of Medicine, İstanbul, Turkey

ABSTRACT

Objective: Coronavirus disease 2019 (COVID-19) has placed an unprecedented burden on healthcare systems and restricted resources for non-COVID patients worldwide. Treatment approaches and follow-up plans have been modified to prevent the risk of infection for patients and healthcare workers. Patients prefer to delay or cancel their treatments during the peak period of infection.

Materials and Methods: We retrospectively reviewed the characteristics of patients with breast cancer who were consulted at our outpatient clinic right after early COVID-19 peak in May and June 2020 and compared them with the same period in 2017 to 2019.

Results: The number of patients who consulted at our outpatient medical oncology clinic declined in May and June 2020. This decline was regardless of stage and was larger in May than in June 2020. In general, the distribution of tumor subtypes [luminal, human epidermal growth factor receptor 2 (HER-2) positive, and triple negative] was not different from 2017 to 2020. Less than half of the patients received adjuvant chemotherapy following early COVID-19 peak in May and June 2020. Few patients received chemotherapy for metastatic disease, whereas many metastatic patients received endocrine therapy. None of the consulted new patients had a non-invasive disease. More patients received endocrine therapy than chemotherapy.

Conclusion: The presentation patterns of patients with breast cancer after early COVID-19 peak differed from those during the same period in the last 3 years. The pandemic affected the number of new patients consulted and the way medical oncologists treat their patients.

Keywords: Breast cancer, COVID-19, early peak

Cite this article as: Dauti Işıklar A, Deniz C, Soyder A, Güldoğan N, Yılmaz E, Başaran G. How Do Breast Cancer Patients Present Following COVID-19 Early Peak in a Breast Cancer Center in Turkey?. Eur J Breast Health 2021; 17(3): 253-257

Key Points

- COVID-19 pandemic led to important changes in the breast units of hospitals.
- The number of consulted patients decreased because of early curfew and right after the early peak of pandemic.
- Medical oncologists preferred less toxic treatment modalities more in May and June 2020 than in the last 3 years.

Introduction

The coronavirus disease 2019 (COVID-19) pandemic has led to practical changes in the management of patients with breast cancer worldwide (1). Multidisciplinary oncology teams modified their treatment decisions with respect to surgical approach, radiotherapy, and optimal systemic therapy to ensure maximal protection from infection based on their regional dynamics (2).

The first documented COVID-19 case in Turkey was reported on March 11th 2020. The peak for active cases was reached in the last week of April 2020 (3). Acibadem Altunizade Hospital is one of the largest hospitals of the Acibadem Healthcare Health Group in Turkey with a capacity of 350 beds. It has a specific unit for the diagnostic and therapeutic management of breast cancer. At the outset of the COVID-19 pandemic, in line with the precautions of Acibadem Hospital, our breast center has adapted to the management of patients with breast cancer and delayed elective operations of elderly and follow-up patients until the end of April. New diagnoses and suspicious relapses were handled as usual. Ongoing chemotherapies continued throughout the pandemic, unless the performance and comorbidities of the patients were not restrictive/compromising. Endocrine therapy is opted for patients with hormone receptor-positive metastatic breast cancer, whereas oral chemotherapeutic agents are preferred for patients with newly diagnosed metastatic breast cancer or progressed metastatic breast cancer. Breast surgery was delayed

Corresponding Author:
Aysun Dauti Işıklar; aysun.isiklar@acibadem.com

Received: 22.10.2020
Accepted: 10.01.2021

253

for patients with early breast cancer if they were endocrine sensitive and can be managed by endocrine therapy until optimal settings are available. Following the peak, curfew restrictions for people over 65 years old, those with chronic illnesses, and young people under 20 years old were eased by government at the beginning of May 2020. Therefore, a number of patients who need oncological care and those who were referred for oncological therapy started to come to the medical centers. Surgery for early breast cancer started safely with precautions, and outpatient follow-ups commenced for patients with high risk of recurrence at oncology clinics in Istanbul. Patients with undiagnosed breast lumps during the peak or patients with biopsy-proven breast cancer right after the early peak sought radiological imaging and surgical attention in May and June 2020.

The present study aimed to characterize new patients who were evaluated at our center right after the early peak of COVID-19 infection in May and June 2020. Past patient records were analyzed to characterize new patients who were admitted in May and June 2017–2019. This study focused on the presentation of new cases in terms of stage, tumor subtype, age, and preferred therapy.

Materials and Methods

We retrospectively reviewed the records of patients who were consulted at our outpatient clinic and noted their stage at presentation, tumor subtype, and recommended therapy right after early peak of COVID-19 in May and June 2020. We also reviewed the same parameters for the patients who presented at the same period in 2017–2019. This cross-sectional retrospective study was approved by the institutional review board at Altunizade Acibadem Hospital Hospital (no: 755, date: 01.09.2020).

Results

The number of patients consulted at our outpatient medical oncology clinic declined. Figure 1 shows our patient profile based on the disease stage in 2017–2020. Fewer patients with early disease and metastatic disease were consulted in May and June 2020 than in the same months of 2017–2019. The number of patients who needed neoadjuvant therapy was similar between 2019 and 2020, greater than that in 2017 and less than that in 2018.

We have consulted 428, 702, 610, and 521 patients (patients on chemotherapy, new patients, and follow-up patients were all included) in May and June of 2017, 2018, 2019, and 2020, respectively, at our center (Table 1). Among 521 patients consulted in May and June 2020, 36 were new cases. Median age was 50 and similar to that of the last 3 years. Eighteen out of 36 patients have been recently operated for early breast cancer during the peak months of COVID-19

infection. One patient who underwent breast-conserving surgery 3 years ago presented with ipsilateral local relapse, and mastectomy was recommended. Thus, these patients were recorded as having early-stage disease. Of the 18 patients who underwent breast surgery, 11 received breast-conserving surgery, one mastectomy, two bilateral subcutaneous mastectomy, and four subcutaneous mastectomy. Among early-stage patients, 14 had node-negative and three had node-positive disease.

Neoadjuvant therapy was recommended for 11 patients, and five patients had metastatic disease at the time of admission. Among metastatic presentations, one patient had de novo disease, one patient relapsed while on adjuvant endocrine therapy, one patient had progressive disease while on therapy for metastatic breast cancer, and 2 patients were consulted for a second opinion. Three of the metastatic patients had visceral metastases. Table 2 shows patient and treatment characteristics in May and June 2017–2020.

In general, the distribution of tumor subtypes by immunohistochemistry as luminal, HER-2 positive, and triple negative showed no significant difference from 2017 to 2020 (Figure 2). Table 3 shows the distribution of tumor subtypes for patients who received adjuvant and neoadjuvant therapy and for metastatic patients.

The recommended adjuvant therapy for patients who had breast surgery in May and June 2017, 2018, 2019, and 2020 is shown in Figure 3. Two thirds of the patients received adjuvant chemotherapy in May and June 2017–2019. Less than half of the patients received adjuvant chemotherapy following early COVID-19 peak in May and June 2020. Few patients received chemotherapy for metastatic disease, and many metastatic patients received endocrine therapy (Figure 4). Two patients received neoadjuvant endocrine therapy in 2019

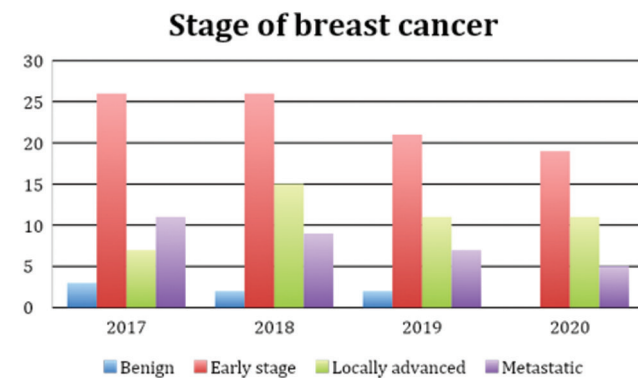


Figure 1. Patient profile based on the disease stage in May and June 2017–2020

Table 1. Patient consulted in May–June between 2017–2020

Patient consulted (n)	2017		2018		2019		2020	
	May	June	May	June	May	June	May	June
New patients	24	23	35	18	32	11	9	27
Follow-up	105	76	197	119	144	136	59	180
On IV therapy	102	98	177	156	168	119	124	120

IV: Intravenous therapy; n: Number

and 2020, and none of the patients received neoadjuvant endocrine therapy in 2017 and 2018 (Figure 5). Two patients who received neoadjuvant therapy in 2020 were elderly patients aged 87 and 72 years old. Similarly, the two other patients who received neoadjuvant endocrine therapy in 2019 were elderly patients aged 95 and 72 years old.

Tumor subtypes by IHC between 2017-2020

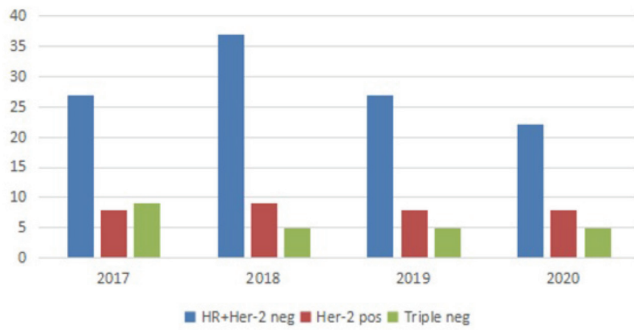


Figure 2. Tumor subtype in May–June 2017–2020

IHC: Immunohistochemistry; HR: Hormon receptor; HER2: Human epidermal growth factor receptor 2

Patients who received adjuvant therapy

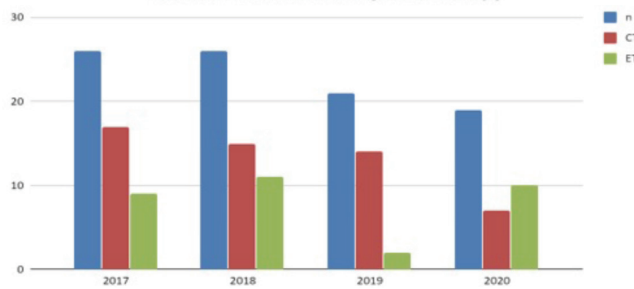


Figure 3. Recommended adjuvant therapy

CT: Chemotherapy; ET: Endocrinotherapy; n: Number

Discussion and Conclusion

The COVID-19 pandemic has dramatically changed inpatient and outpatient care in oncology clinics as in other healthcare workers. All preventive and follow outpatient visits are postponed to decrease the risk of transmitting the virus to either patients or healthcare workers. Oncological emergencies and new diagnoses requiring urgent therapy were continued. Telemedicine visits were organized for elderly patients or patients with comorbidities. Patients with cancer are susceptible to infection because of their systemic immunosuppressive state caused by malignancy and anticancer treatments, such as

Metastatic breast cancer patients



Figure 4. Patients with metastatic breast cancer

CT: Chemotherapy; ET: Endocrinotherapy; n: Number

Patients who received neoadjuvant therapy

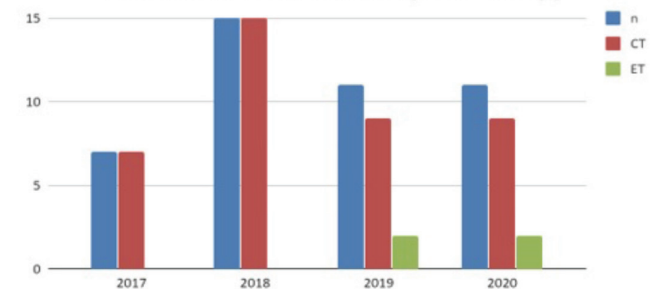


Figure 5. Patients who received neoadjuvant therapy

CT: Chemotherapy; ET: Endocrinotherapy; n: Number

Table 2. Patient characteristics in May and June 2017–2020

Period	May–June 2017	May–June 2018	May–June 2019	May–June 2020
Number	47	53	42	36
Median age	48 (26–83)	45 (26–85)	49 (33–95)	50 (27–82)
DCIS or LCIS	3	2	2	0
Received adjuvant therapy following breast surgery	26	26	21	19
Received neoadjuvant therapy	7	15	11	11
Metastatic (total)	11	9	7	5
De novo	6	2	2	1
Relapsed	2	1	1	1
Second opinion	1	6	2	2
PD on therapy for MBC	2	0	2	1
Metastatic site				
Visceral	7	7	3	3
Non-visceral	4	2	0	3

DCIS: Ductal carcinoma *in situ*; LCIS: Lobular carcinoma *in situ*; PD: Progression disease; MBC: Metastatic breast cancer

Table 3. Tumor subtype for patients who received adjuvant, neoadjuvant therapy, and for metastatic patients

Period	Tumor subtype	May–June 2017	May–June 2018	May–June 2019	May–June 2020
Operated and received adjuvant therapy	HR-positive HER-2 negative	16	20	15	12
	HER-2 positive	6	4	4	4
	Triple-negative	4	3	3	3
	HR-positive HER-2 negative	4	10	8	6
Received neoadjuvant therapy	HER-2 positive	2	3	3	3
	Triple-negative	1	2	1	2
	HR-positive HER-2 negative	7	7	4	5
Metastatic	HER-2 positive	2	2	1	1
	Triple-negative	2	0	1	0

HR: Hormon receptor; HER-2: Human epidermal growth factor receptor 2

chemotherapy or surgery (4-7). A study from China has shown that rate of SARS-CoV-2 infection in patients with cancer is 0.79% at their institution (8). Another Chinese study reported a mortality rate of 7.6% in all cancer patients (9). The need for intensive care, invasive ventilation, and mortality rates are slightly higher in patients with cancer than in individuals without cancer (hazard ratio: 2.29–3.50) (10). At our breast center, only six patients had COVID-19 infection in March and April 2020, and all were follow-up patients with early breast cancer. Two of them were living in another city. None of them required intensive care, and no deaths were due to COVID-19 infection.

Many patients avoid hospital visits to decrease their risk of exposure. In addition, many patients could not attend necessary medical visits because of local restrictions by government (such as curfew for people >65 years old). Chemotherapies were delayed or substituted by oral regimens for some patients during the early pandemic. All these changes decreased the number of hospital outpatient visits.

This study found that the presentation patterns of new breast cancer cases right after the early COVID-19 peak differed from those during the same period in the last 3 years. Data covering only two months of 2017–2020 were analyzed. Therefore, the number of new patients was low and did not allow us to make statistical comparisons between years. Despite the low number of new patients, our findings have shown that follow-up patients with breast cancer or women with undiagnosed breast tumors were terrified and did not visit hospitals right after the peak. A small proportion of new consultations (three, two, and two patients in 2017, 2018, and 2019, respectively) were ductal carcinoma *in situ* or lobular carcinoma *in situ* in the last 3 years, and no patients were consulted with a non-invasive histology in May and June 2020. Non-invasive disease was considered low priority during the pandemic. Therefore, all diagnostic and therapeutic procedures were postponed for these cases. Our findings revealed that oncologists preferred endocrine therapy more than chemotherapy in May/June 2020 irrespective of the disease stage.

Its retrospective nature and the small number of patients are the main limitations of our study. The number of new COVID-19 cases are

still increasing following the early peak in April in Turkey and globally (1). Analyzing the patient presentation patterns of patients until the pandemic could be more informative because many patients avoid hospital visits with the fear of COVID-19 infection. Hence, the number of patients with local relapse and metastatic presentations may increase in the upcoming months.

Acknowledgements

We thank Aslınur Moral and Beren Büyükçolak for their valuable contributions in preparing the database for this retrospective study.

Ethics Committee Approval: This cross-sectional retrospective study was approved by the institutional review board at Altunizade Acibadem Hospital (no: 755, date: 01.09.2020).

Consent to participate: It is a retrospective study.

Peer-review: Externally peer-reviewed.

Author Contributions

Conception: A.D.I., C.D., A.S., N.G., E.Y., G.B.; Design: A.D.I., C.D., A.S., N.G., E.Y., G.B.; Data Collection and/or Processing: C.D.; Analysis and/or Interpretation: A.D.I.; Literature Review: C.D.; Writing: G.B.; Critical Review: A.S., N.G., E.Y.

Conflict of Interest: There is no conflict of interest.

Financial Disclosure: The authors declared that this study received no financial support.

References

1. Available from: <https://www.cdc.gov/coronavirus/2019-ncov/healthcare-facilities/guidance-hcf.html> [Crossref]
2. Ontario Health, Cancer Care Ontario, "Pandemic Planning Clinical Guideline for Patients with Cancer". Last Accessed Date: 23.03.2020. Available from: <https://www.acc-cancer.org/docs/document/cancer-program-fundamentals/oh-ccopan-demicplanning-clinical-guidelines> [Crossref]

3. Worldometer. COVID-19 Coronavirus Pandemic. Last Accessed Date: 12.09.2020. Available from: <https://www.worldometers.info/coronavirus> [Crossref]
4. Kamboj M, Sepkowitz KA. Nosocomial infections in patients with cancer. *Lancet Oncol* 2009; 10: 589-597. (PMID: 19482247) [Crossref]
5. Li JY, Duan XF, Wang LP, Xu YJ, Huang L, Zhang TF, et al. Selective depletion of regulatory T cell subsets by docetaxel treatment in patients with non-small cell lung cancer. *J Immunol Res* 2014; 2014: 286170. doi: 10.1155/2014/286170 (PMID: 24868562) [Crossref]
6. Longbottom ER, Torrance HD, Owen HC, Fragkou PC, Hinds CJ, Pearse RM, et al. Features of postoperative immune suppression are reversible with interferon gamma and independent of interleukin-6 pathways. *Ann Surg* 2016; 264: 370-377. (PMID: 26445474) [Crossref]
7. Sica A, Massarotti M. Myeloid suppressor cells in cancer and autoimmunity. *J Autoimmun* 2017; 85: 117-125. (PMID: 28728794) [Crossref]
8. Yu J, Ouyang W, Chua MLK, Xie C. SARS-CoV-2 Transmission in patients with cancer at a tertiary care hospital in Wuhan, China. *JAMA Oncol* 2020; 6: 1108-1110. (PMID: 32211820) [Crossref]
9. Report of the WHO-China Joint Mission on Coronavirus Disease 2019 (COVID-19) Available from: <https://www.who.int/docs/default-source/coronaviruse/who-china-joint-mission-on-covid-19-final-report.pdf> [Crossref]
10. Guan W-J, Liang W-H, Zhao Y, Liang H-R, Chen Z-S, Li Y-M, et al. Comorbidity and its impact on 1590 patients with covid-19 in China: a nationwide analysis. *Eur Respir J* 2020; 55: 2000547. doi: 10.1183/13993003.00547-2020 (PMID: 32217650) [Crossref]



Results of Excision of Unknown Papillary Neoplasms Detected on Core Biopsy

İD Ayşe Nur Uğur Kılınç¹, İD Zeynep Bayramoğlu¹, İD Yaşar Ünlü¹, İD Nahide Baran², İD Ayşegül Altunkeser², İD Nergis Aksoy³, İD Mehmet Ali Eryılmaz³, İD Elif Nur Öztürk Yıldırım⁴

¹Department of Pathology, Konya Training and Research Hospital, Konya, Turkey

²Department of Radiology, Konya Training and Research Hospital, Konya, Turkey

³Department of General Surgery, Konya Training and Research Hospital, Konya, Turkey

⁴Department of Public Health, Konya Akşehir Health Management, Konya, Turkey

ABSTRACT

Objective: This study aimed to find out valuable parameters that predict the nature of breast papillary lesions before excision, and we compared our results with those in the literature.

Materials and Methods: We reviewed the medical records and pathology slides of patients diagnosed with papillary neoplasm after undergoing a core-needle biopsy between 2010 and 2020, who, subsequently, underwent surgical excision in a single tertiary care institution. The core biopsy results and pathology results of excision materials were compared with the radiological, pathological, and demographic findings.

Results: A total of 51 patients were included in the study. According to the excision results, the patients were divided into two groups: the atypical group, which included 20 patients (39.3%), and the benign group, which included 31 patients (61.7%). The results of the core biopsy showed that the loss of myoepithelial cell layer was identified in 18 patients in the atypical group, while it was present in all patients in the benign group. Tumor sizes were larger and patient ages were older in the atypical group compared with the benign group. No significant difference was found between atypical and benign groups in terms of breast imaging-reporting and data system (BI-RADS) classification and location (right vs left; central vs peripheral). The upgrade rate was between 0% and 16% in literature, while it was 4% in our study.

Conclusion: There is no consensus on whether patients diagnosed with papillary neoplasia as a result of core biopsy will undergo excision. According to our results, patients with following criteria should have their lesions excised: those who are advanced in age, those who are diagnosed with a papillary lesion as a result of core biopsies with loss of myoepithelial cell layer, and those who are diagnosed with large-sized lesions without loss of myoepithelial cell layer. Patients diagnosed with small-sized lesions without loss of myoepithelial cell layer and who are young in age are to be followed up without the need for lesion excision. The lesions should be adequately sampled.

Keywords: Breast neoplasm, core biopsy, papillary neoplasm

Cite this article as: Uğur Kılınç AN, Bayramoğlu Z, Ünlü Y, Baran N, Altunkeser A, Aksoy N, Eryılmaz MA, Öztürk Yıldırım EN. Results of Excision of Unknown Papillary Neoplasms Detected on Core Biopsy. Eur J Breast Health 2021; 17(3): 258-264

Key Points

- In particular, there is no consensus on whether patients with a diagnosis of papillary neoplasia resulting from core biopsy will undergo excision.
- According to the results of our study, patients with advanced age, a diagnosis of papillary lesions as a result of core biopsy with loss of myoepithelial layer, and large-sized lesions should have their lesions excised.
- In patients who did not experience loss of myoepithelium, it should be ensured that it is adequately sampled if the lesion will not be excised.

Introduction

Papillary breast neoplasms are lesions with a fibrovascular core surrounded by an epithelial cell layer. Most of the papillary lesions are restricted to cystically dilated ducts and have thick fibrous walls. Intraductal papillary neoplasms of the breast are intraductal papilloma with atypical ductal hyperplasia/ductal carcinoma in situ (DCIS), papillary DCIS, and solid and encapsulated papillary carcinomas *in situ*. Papillary lesions of the breast span the spectrum of benign, atypical, and malignant. While the myoepithelial cell layer reveals continuity in all benign intraductal

papillary neoplasms, the type of the lesion in atypical papillary lesions varies according to the presence of the myoepithelial cell layer inside and around the papilla (1).

In all breast lesions, core biopsies can efficiently predict the nature of the lesion. In papillary lesions, histopathological assessment of core biopsies is very effective when deciding on excision or follow-up of the lesion. However, in some papillary lesions, the nonhomogeneity of the lesion decreases the reliability of core biopsy (1).

In our study, we included patients who were diagnosed with papillary neoplasm as a result of core biopsies done at our hospital and whose excision materials were present in our hospital, but the type of their lesions could not be specified. The demographic, radiological, and histopathological characteristics of the patients were analyzed. We aimed to find out valuable parameters for predicting the nature of breast papillary lesions before excision and compared our results with those in the literature.

Materials and Methods

The pathological data of patients who were diagnosed with papillary neoplasia as a result of core-needle biopsies done at our hospital between 2010 and 2020 and whose excision materials were present in our hospital were assessed. The radiological images and pathological slides of all patients were reassessed.

The excision results of patients were classified according to the International Classification of Diseases for Oncology, Third Edition, Second Revision (ICD-O-3.2) determined by WHO. Papillary lesions are classified as benign, malignant, or uncertain behavior lesions according to ICD-O-3.2 (1). We divided them into two groups: the atypical group, which included the malignant and uncertain behavior lesions, and benign group, which included the benign lesions (1).

Radiological parameters such as ductal ectasia, microcalcification, mean size of the lesion, peripheral or central location of the lesion, and BI-RADS category, pathological parameters, such as immunohistochemical markers, and demographic data were analyzed in selected patients. At least two myoepithelial markers, one cytoplasmic and the other nuclear [high molecular weighted cytokeratin (HMWCK), SMA, CK5/6, CK14, and p63], were routinely used in all core biopsy specimens and excision materials. In addition to these, the estrogen receptor was investigated in patients when necessary.

There were less than six months between durations of excision materials and core biopsy of patients included in the study.

Patients whose excision was not performed at our hospital and patients whose final diagnosis and classification were identified using core biopsy materials were excluded from our study.

We compared between the atypical papillary lesion and benign papillary lesion groups. We used the Statistical Package for Social Sciences version 21 (IBM SPSS Corp; Armonk, NY, USA) for statistical analysis. The results of categorical variables are shown in tables and charts where appropriate. Differences between groups were determined using the Mann–Whitney U test for numerical variables. Categorical variables were determined using the chi-square test. $p < 0.05$ was considered statistically significant.

Results

Fifty-one patients were included in the study: 31 in the benign group and 20 in the atypical group (Table 1). Excision diagnoses of the 51 patients with papillary neoplasm are shown in Table 2.

The median age of the patients included in the study was 44 (24–79). 90% of the patients were older than 40 years. The mean age was 59.4 (40–79) in the atypical group and 48 (23–70) in the benign group (Table 1).

The mean size of the largest tumor detected on ultrasound was 14.2 ± 0.9 mm in the benign group and 31.15 ± 1.2 mm in the atypical group (Table 1).

Papillary lesions were observed more on the left (61%) than on the right (39%). However, no significant difference was found between the atypical and benign groups in terms of lesion laterality ($p > 0.01$).

Five of the patients underwent only ultrasonography (USG), four underwent USG and magnetic resonance imaging (MRI), 21 underwent USG and mammography (MMG), and 20 patients underwent all three imaging methods.

According to ultrasonographic locations, lesions of only three patients (10%) in the benign group were located in the peripheral ducts and the rest of the patients (28; 90%) had centrally located lesions. In the atypical group, 11 patients (55%) had centrally located lesions and nine patients (45%) had peripherally located lesions (Table 1).

According to the results of the USG BI-RADS classification, 24 patients were reported as BI-RADS 4A, three patients as BI-RADS 4C, two patients as BI-RADS 3, one patient as BI-RADS 4B, and one patient as BI-RADS 5 in the benign group. In the atypical group, 12 patients were reported as BI-RADS 4A, four patients as BI-RADS 4B, three patients as BI-RADS 5, and one patient as BI-RADS 4C (Table 1; Figures 1 and 2).

Forty-one patients underwent MMG. Microcalcification was monitored at a rate of 6% (2/31) in the benign group. This rate was higher (25%; 5/20) in the atypical group (Table 1).

While the rate of ductal ectasia was 54% (17/31) in the benign group, it was 6% (3/20) in the atypical group. All three ductal ectasias monitored in the atypical group were centrally located, and their excision diagnoses were intraductal papilloma with DCIS (Table 1).

Eighteen out of 20 patients, who were diagnosed with papillary neoplasia and in whom loss of myoepithelial cell layer was detected as a result of core biopsy, were diagnosed with atypical papillary lesions based on the excision materials. The loss of myoepithelial cell layer was not detected in the biopsy material of the other two patients in the atypical group, and they were diagnosed with intraductal papilloma with DCIS based on the excision materials (upgrade rate was 4%). Myoepithelial cell layers were continuous in the core biopsies and excision materials of all patients in the benign group.

In only four patients in the benign group, intraductal papilloma was accompanied by atypical ductal hyperplasia in the excision materials. Their mean age was 48 (35–67). In three of the four patients, the lesions were centrally located, while it was peripherally located in one patient. The mean size of the lesions was 13.75 mm.

In our series, the mean age of patients with papillomas with DCIS (5/51) was 50.5±11.4 years. The mean size of large lesions was 28.5 mm. Four of the aforementioned five patients had centrally located lesions and one had peripherally located lesions. Four of them were diagnosed as BI-RADS 4A and one was diagnosed as BI-RADS 4C. Ductal ectasia was detected in three patients, and microcalcification was detected in two patients. Histopathological images of one of the patients with papilloma with DCIS are shown in Figures 3 and 4.

Core biopsies and ultrasound were performed in 50 patients, while only one patient underwent excisional biopsy. All biopsies were sampled with 16-gage (G) (16 G; 38 patients) or 18-gage (G) (18 G;

13 patients) needles. In our study, the mean size of core-needle biopsy tissue samples was 26 mm (Table 1).

Discussion and Conclusion

To date, several studies have been conducted to predict preoperative atypia in papillary breast lesions (2-6). Our study also contributes to the literature as it contains detailed radiological, pathological, and demographic data.

According to studies in literature, lesions located on the left breast and peripherally, advanced age, large-sized lesions, and high BI-RADS category may help predict atypia (6-10).

Table 1. Demographic, pathological, and radiological descriptive findings and statistical value of the groups

	All papillary neoplasms (n = 51)	Benign papillary neoplasms (n = 31)	Atypical papillary neoplasms (n = 20)	p-value
Number	51	31	20	-
Age				
Mean ± SD	44	49.09±12.31	57.65±12.82	0.05
<40	7	6	1	
≥40	44	25	19	
BI-RADS category				
3	2	2	0	*
4a	36	24	12	
4b	5	1	4	
4c	4	3	1	
5	4	1	3	
Mass size (mm)				
Mean ± SD	23.2±19 mm	14.2±0.9 mm	31.15±1.2 mm	<0.01
<1 cm	10	10	0	
>1 cm	41	21	20	
Loss of myoepithelial cell layer	18	0	18	p<0.001
Location				
Peripheral	12	3	9	*
Central	39	28	11	
Lesion laterality				
Right	15	10	5	>0.05
Left	36	21	15	
Microcalcification	7	2	5	*
Ductal ectasia	23	17	6	<0.01
Needle gage size	37	22	15	*
16 G				
Needle gage size	14	9	5	*
18 G				
Core biopsy sample (mean)	18 mm	17 mm	17.5 mm	>0.05

*: Statistical test result is not available due to limited data.

BI-RADS: Breast Imaging Reporting and Database System score; SD: Standard deviation; n: Number

In our study, the mean age of the atypical group was 59.4 years (40–79), which is higher than that of the benign group, 48 years (23–70). This is consistent with literature data (1).

The mean size of the largest tumor detected on ultrasound was higher in the atypical group (31.15±1.2 mm) compared with the benign

group (14.2±0.9 mm), which is consistent with literature data. No lesion smaller than 1 cm was detected in the atypical group (0%/0/20), while 35% (11/31) of the lesions in the benign group were 1 cm and smaller. In some studies in the literature, lesions larger than 1 cm were associated with atypia, which agrees with our results (1, 7, 8).

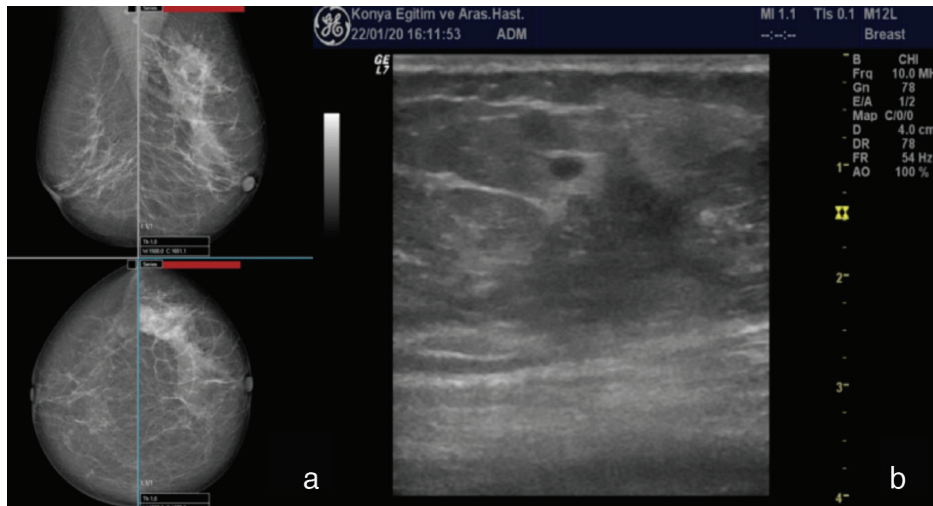


Figure 1. A 64-year-old woman presenting with pain in the left breast. **(a)** On the mammogram (MMG), there was a global asymmetric density increase in the upper left quadrant of the left breast. **(b)** On breast ultrasonography (USG), an irregular spiculated contoured mass lesion with a size of 22 x 16 mm was detected at a distance of 7 cm nipple, at 2 o'clock of the left breast. Imaging findings (MMG + USG) were reported as BI-RADS 5. The pathological result of the core biopsy taken from the defined lesion and USG was reported as a papillary neoplasm. The final pathological result of the excision was reported as encapsulated papillary carcinoma

BI-RADS: Breast Imaging Reporting and Database System score

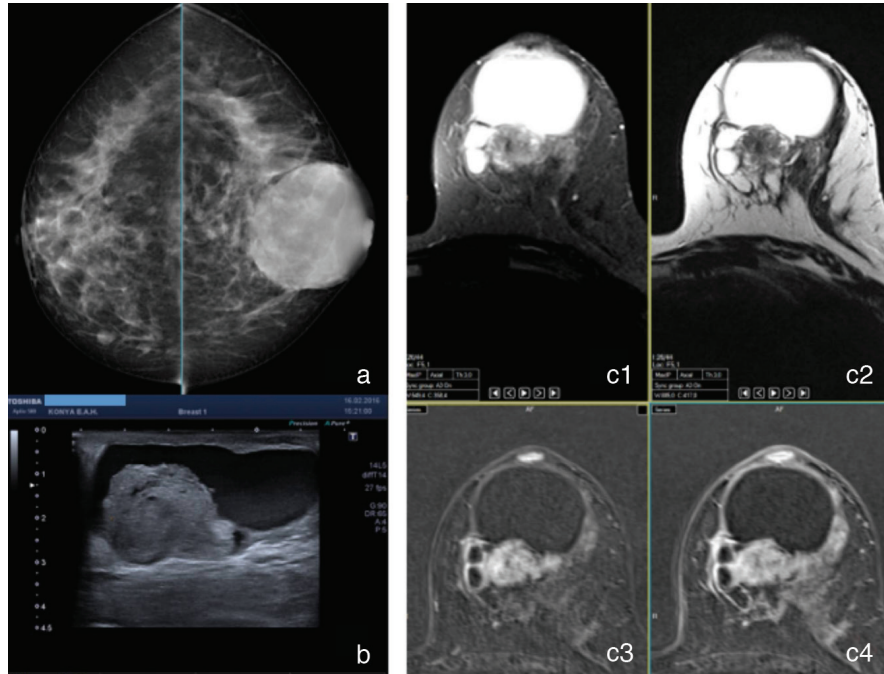


Figure 2. A 45-year-old female patient presenting due to stiffness in the left breast. **(a)** Increased nodular density increase in left breast retro areolar area on MMG, **(b)** on the USG, a solid component with dimensions of 24 x 28 mm was detected in the posterior wall of the cyst of 65 x 60 mm in the left breast retroareolar area. In the breast MRI examination, **(c1)**, in the posterior wall of the cyst in the retroareolar area. Isointense with fibroglandular tissue on T1A images. **(c2)** Mild hyperintense from fibroglandular tissue in T2A images. **(c3 and c4)** On the contrast dynamic series, a mass lesion showing pathological contrast enhancement in the early phase and drawing a plateau of the contrast curve in the late phase was observed. Imaging findings (MMG + USG + MRI) were reported as BI-RADS 4b. The pathological result of a Tru-Cut biopsy taken from the defined lesion with USG was reported as papillary lesion. As a result of the excision, the final pathological result was reported as intraductal /intracystic papilloma.

USG: Ultrasonography; MMG: Mammogram; MRI: Magnetic resonance imaging; BI-RADS: Breast Imaging Reporting and Database System score

Although studies assert that the BI-RADS category can predict atypical papillary lesions, there was no difference between the two groups in terms of the BI-RADS category according to our study results (4).

When tumor locations were evaluated, it was found in a study in the literature that the rate of peripheral location in the atypical group was 57%, while the rate of central location was 42% (3). Similarly, these rates were 55% (11/20) and 45% (9/20), respectively, in our study. Lesions of only three patients (10%) in the benign group were located peripherally, and the rest of the patients (28; 90%) had centrally located lesions. In such a case, although the peripheral location is relatively higher in atypical lesions, the location of the lesion will not help give a certain result.

Table 2. Results of excision of 51 patients diagnosed with papillary neoplasm as a result of core biopsy

Atypical papillary lesions	
Encapsulated papillary carcinoma	4
Invasive encapsulated papillary carcinoma	1
Invasive papillary carcinoma	5
Solid papillary carcinoma	2
Papillary DCIS	3
Intraductal papilloma with DCIS	5
Total	20
Benign papillary lesions	
Intraductal papilloma	27
Intraductal papilloma with atypical ductal hyperplasia	4
Total	31

DCIS: Ductal carcinoma *in situ*

Microcalcification was detected in two patients (6%) in the benign group and five patients (20%) in the atypical group. Although the rate of microcalcification was relatively higher in the atypical group in our study, studies in the literature did not find MMG results reliable for papillary lesions (10).

In our study, the mean size of lesions was 21 mm, the mean size of core biopsy samples was 17.2 mm, and mean sample length per cm calculated as 8 mm, which resulted in a low upgrade rate (4%). We recommend collecting at least a 1 cm sample per lesion size in papillary lesions since this increases diagnostic sensitivity and decreases the upgrade rate. Therefore, the clinician must check if the lesion is adequately sampled before the decision of excision or follow-up is made.

In core biopsies, the myoepithelial cell layer was regular in all benign lesions. There was a partial or complete loss of myoepithelial cell layer in all atypical lesions except for two patients whose lesions were associated with an upgrade (Figures 3 and 4). Our findings were consistent with literature data (1, 7, 11, 12).

Although heterogeneity in papillary lesions is still a source of concern, comprehensive studies generally show low upgrade rates. A large number of studies were conducted on the increase in the histopathological degree of the lesion in excision material after core biopsy, which is defined as an upgrade. In recent literature, intraductal papilloma has an incidence of upgrade ranging from 0% to 16% (5, 12, 13). According to our results, the upgrade rate was 4% (2/51), which is consistent with literature data. The excision diagnosis of two papillary lesions that were upgraded was intraductal papilloma with DCIS. In core biopsy material of papillary neoplasia, where the myoepithelial cell layer is regular and cytological atypia is not observed, papilloma with DCIS can be missed due to the heterogeneity of the lesion.

In our series, the loss of the myoepithelial cell layer was the most significant parameter in predicting atypical papillary lesions. Apocrine cells are more common in benign papillomas that were associated with the loss of myoepithelial cell, which may be misleading in that case. In

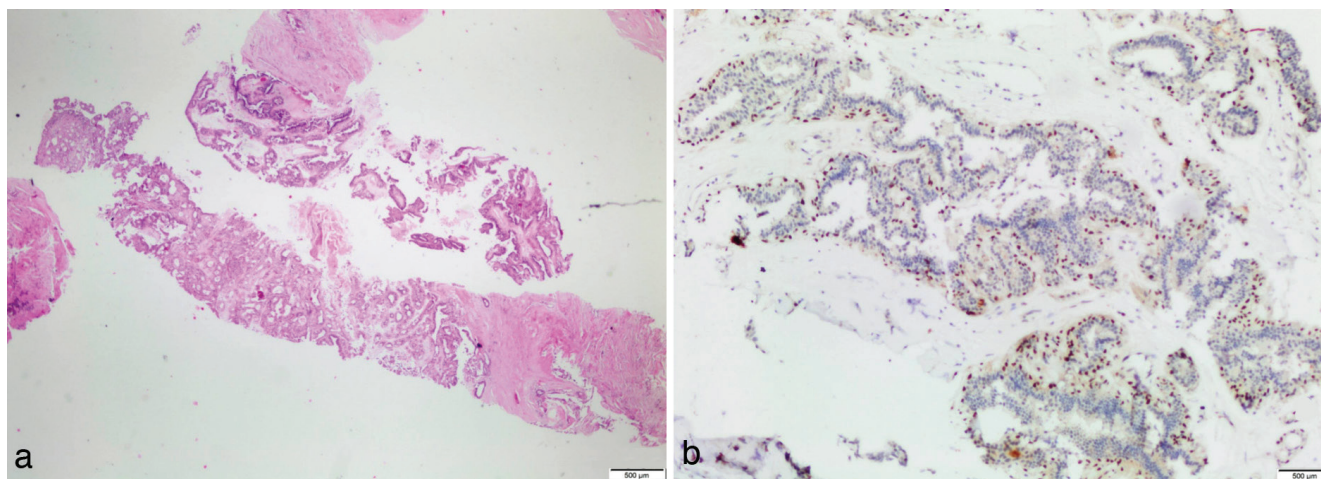


Figure 3. A 40-year-old female patient with a 3.5 cm diameter mass presented with pain in the left breast. Imaging findings (MMG + USG + MRI) were reported as BI-RADS 4a. The pathological result of a Tru-Cut biopsy taken from the defined lesion with USG was reported as papillary neoplasm. **(a)** In the core biopsy sample, the papillary neoplasm was diagnosed (H&E; 20x). **(b)** The myoepithelial layers are shown regularly with p 63. As a result of the excision, the final pathological result was reported as intraductal papilloma with DCIS (one of our patients whose lesion was associated with an upgrade)

USG: Ultrasonography; MMG: Mammogram; MRI: Magnetic resonance imaging; BI-RADS: Breast Imaging Reporting and Database System score; H&E: Hematoxylin and eosin; DCIS: Ductal carcinoma *in situ*

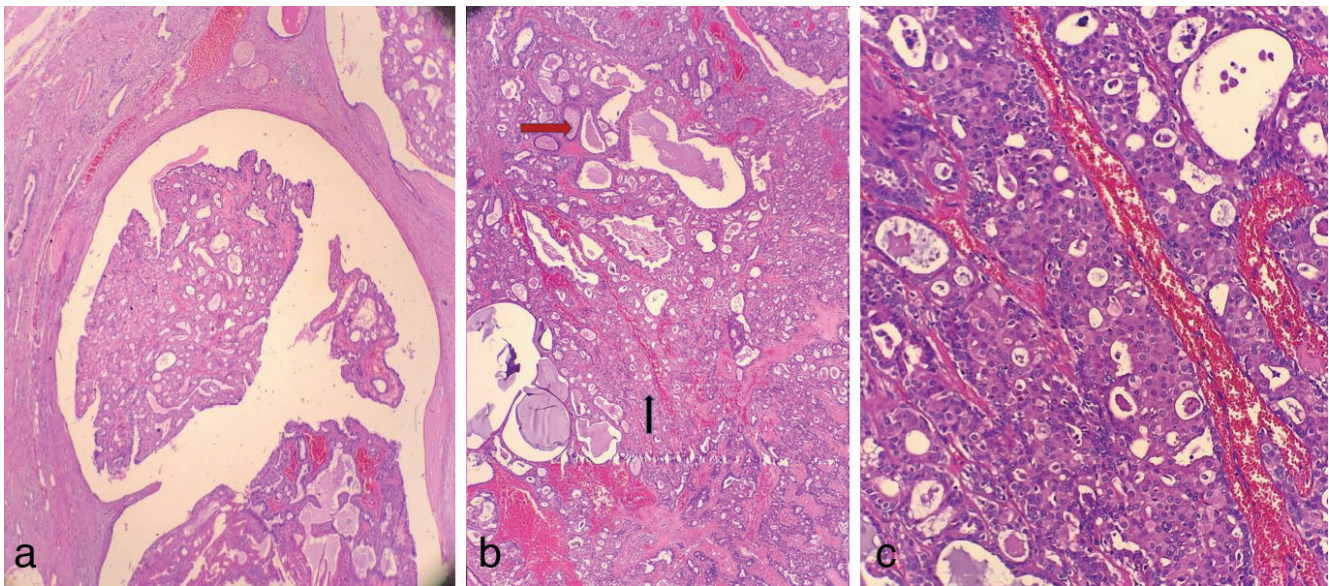


Figure 4. Histopathological images of the excision material of patient with intraductal papilloma with DCIS. The core biopsy sample of this patient is shown in Figure 3. **(a)** Benign areas of lesion (H&E; 40x). **(b)** Benign/intraductal papilloma and atypical/ductal carcinoma in situ areas of the lesion (H&E; 40x). **(c)** Higher magnification of DCIS areas of the intraductal papilloma (H&E; 400x)

H&E: Hematoxylin and eosin; DCIS: Ductal carcinoma in situ

such cases, the absence or extremely rare presence of mitosis in benign papillomas will be a clue for us (1).

According to our findings, papillary lesions must be excised if loss of myoepithelial cell layer was detected as a result of core biopsy, which is consistent with literature data (1). If the myoepithelial cell layer is the regular size of the lesion and the size of the sample should be assessed and the lesion's other parts that cannot be represented on core biopsy should be considered in that case. If the size of the lesion is larger than 1 cm (lesion size was larger than 3 cm in two patients whose lesions were associated with an upgrade) and patient is older than 40 years, new samples or excision may be recommended. If the lesion size is smaller than 1 cm and the patient is young and does not want an operation, a close follow-up is recommended.

According to our results, although lesion size, advanced patient's age, and loss of myoepithelial cell layer can guide us, taking a 1 cm sample per cm of tumor size will decrease the possibility of histopathological upgrade. In radiological studies, defining suspected areas of papillomas with DCIS and focusing on sampling from these areas may help decrease the upgrade rates.

We recommend that when encountering a core biopsy sample of a papillary lesion without significant cytological atypia and malignancy, it should be reported as papillary neoplasia with regular myoepithelial cell layer or focal/complete loss of the myoepithelial cell layer.

As our study included many radiological and histopathological data, it can guide breast surgeons, radiologists, and pathologists in clinical practice in terms of papillary neoplasms.

Ethics Committee Approval: The Local Ethics Committee of Konya Training and Research Hospital (decision no: 48929119/774, date: 02.07.2020) approved this study.

Informed Consent: Written informed consent was obtained from patients who participated in this study.

Peer-review: Externally peer-reviewed.

Authorship Contributions

Conception: A.N.U.K., Z.B.; Design: A.N.U.K., Z.B., A.A.; Supervision: Y.Ü., M.A.E.; Resources: A.N.U.K., N.B.; Materials: A.N.U.K., Z.B.; Data Collection and/or Processing: A.N.U.K., N.B., A.A.; Analysis and Interpretation: A.N.U.K., Z.B.; Literature Search: Y.Ü., N.B.; Writing: A.N.U.K., Z.B., N.A., E.N.Ö.Y.; Critical Review: N.A., M.A.E.

Conflict of Interest: The authors have no conflicts of interest to declare.

Financial Disclosure: The authors declare that this study received no financial support.

References

1. Brogi E, Horii R, Mac Grogan G, Rakha EA, Troxelli ML, Tse G, et al. Papillary neoplasms: breast tumours, WHO classification of tumours. 5th ed. WHO Classification Editorial Board, 2019: 49. [\[Crossref\]](#)
2. Cheng TY, Chen CM, Lee MY, Lin KJ, Hung CF, Yang PS, et al. Risk factors associated with conversion from nonmalignant to malignant diagnosis after surgical excision of breast papillary lesions. *Ann Surg Oncol.* 2009; 16: 3375-3379. (PMID: 19641969) [\[Crossref\]](#)
3. Rizzo M, Linebarger J, Lowe MC, Pan L, Gabram SG, Vasquez L, et al. Management of papillary breast lesions diagnosed on core-needle biopsy: clinical pathologic and radiologic analysis of 276 cases with surgical follow-up. *Jx Am Coll Surg* 2012; 214: 280-287. (PMID: 22244207) [\[Crossref\]](#)
4. Youk JH, Kim EK, Kwak JY, Son EJ, Park BW, Kim SI. Benign papilloma without atypia diagnosed at US-guided 14-gauge core-needle biopsy: clinical and US features predictive of upgrade to malignancy. *Radiology* 2011; 258: 81-88. (PMID: 20971773) [\[Crossref\]](#)
5. Wen X, Cheng W. Nonmalignant breast papillary lesions at core-needle biopsy: a meta-analysis of underestimation and influencing factors. *Ann Surg Oncol* 2013; 20: 94-101. (PMID: 22878621) [\[Crossref\]](#)

6. Nayak A, Carkaci S, Gilcrease MZ, Liu P, Middleton LP, Bassett Jr RL, et al. Benign papillomas without atypia diagnosed on core needle biopsy: experience from a single institution and proposed criteria for excision. *Clin Breast Cancer* 2013; 13: 439-449. (PMID: 24119786) [\[Crossref\]](#)
7. Hong YR, Song BJ, Jung SS, Kang BJ, Kim SH, Chae BJ. Predictive factors for upgrading patients with benign breast papillary lesions using a core needle biopsy. *J Breast Cancer* 2016; 19: 410-416. (PMID: 28053629) [\[Crossref\]](#)
8. Wiratkapun C, Keeratitragoon T, Lertsithichai P, Chanplakorn N. Upgrading rate of papillary breast lesions diagnosed by core-needle biopsy. *Diagn Interv Radiol* 2013; 19: 371-376. (PMID: 23748032) [\[Crossref\]](#)
9. Agoff SN, Lawton TJ. Papillary lesions of the breast with and without atypical ductal hyperplasia: can we accurately predict benign behavior from core needle biopsy? *Am J Clin Pathol* 2004; 122: 440-443. (PMID: 15362376) [\[Crossref\]](#)
10. Pathmanathan N, Albertini AF, Provan PJ, Milliken JS, Salisbury EL, Bilous AM, et al. Diagnostic evaluation of papillary lesions of the breast on core biopsy. *Mod Pathol* 2010; 23: 1021-1028. (PMID: 20473278) [\[Crossref\]](#)
11. Yang Y, Suzuki K, Abe E, Li C, Uno M, Akiyama F, et al. The significance of combined CK5/6 and p63 immunohistochemistry in predicting the risks of subsequent carcinoma development in intraductal papilloma of the breast. *Pathol Int* 2015; 65: 81-88. (PMID: 25572436) [\[Crossref\]](#)
12. Grimm LJ, Bookhout CE, Bentley RC, Jordan SG, Lawton TJ. Concordant, non-atypical breast papillomas do not require surgical excision: a 10-year multi-institution study and review of the literature. *Clin Imaging* 2018; 51: 180-185. (PMID: 29859481) [\[Crossref\]](#)
13. Pareja F, Corben AD, Brennan SB, Murray MP, Bowser ZL, Jakate K, et al. Breast intraductal papillomas without atypia in radiologic-pathologic concordant core-needle biopsies: Rate of the upgrade to carcinoma at excision. *Cancer* 2016; 122: 2819-2827. (PMID: 27315013) [\[Crossref\]](#)



Comparison of the Magnetic Resonance Imaging Findings of Paget's Disease of the Breast and Malignant Tumor Invasion of the Nipple-Areola Complex

Almila Coşkun Bilge, Hale Aydın, Işıl Esen Bostancı, Özge Tanışman, Diba Saygılı Öz

Department of Radiology, Dr Abdurrahman Yurtaslan Ankara Oncology Training and Research Hospital, Ankara, Turkey

ABSTRACT

Objective: We aimed to investigate the distinction between Paget's disease of the breast (PDB) and malignant tumor invasion of nipple-areolar complex (MTION) with Magnetic resonance imaging (MRI) findings without the need for skin punch biopsy.

Materials and Methods: MRI findings of 16 patients with pathologically proven PDB and 11 patients with pathologically proven MTION were reviewed retrospectively. MRI images were assessed for nipple morphological changes; areolar-periareolar skin changes; thickness, classification, and kinetic characteristics of the nipple-areolar complex (NAC) enhancement; morphological pattern, size, and pathological diagnosis of concomitant malignant lesions; kinetic characteristics of the concomitant malignant lesions enhancement; continuity of enhancement between the nipple and closest concomitant malignant lesion; similarity of enhancement kinetics of the NAC and concomitant malignant lesions; and nipple-to-malignant lesion distance in both patient groups.

Results: Areolar-periareolar skin thickening was statistically different between the patient groups. Enhancement kinetic pattern was classified as persistent in four patients with MTION and plateau in seven patients with PDB. Moreover, NAC enhancement kinetic characteristics were statistically different between the groups. Invasive ductal carcinoma was detected in three patients with PDB and five patients with MTION. A statistically significant difference in malignant lesion pathological types was detected between the patient groups.

Conclusion: The significant MRI findings in patients with MTION diagnosed as invasive ductal carcinoma were areolar-periareolar skin thickening and asymmetric NAC enhancement with persistent kinetics pattern. In patients diagnosed with ductal carcinoma in situ, a plateau pattern of asymmetric NAC enhancement without any areolar-periareolar skin changes on MRI may indicate PDB.

Keywords: MRI, breast imaging, nipple-areola complex, breast cancer

Cite this article as: Coşkun Bilge A, Aydın H, Esen Bostancı I, Tanışman Ö, Saygılı Öz D. Comparison of the Magnetic Resonance Imaging Findings of Paget's Disease of the Breast and Malignant Tumor Invasion of the Nipple-Areola Complex. Eur J Breast Health 2021; 17(3): 265-273

Key Points

- The nipple-areola complex may be affected by malignancies.
- Dynamic breast MRI findings help us to diagnose Paget's disease of the breast and malignant tumor invasion of the nipple-areolar complex without skin punch biopsy.
- Areolar-periareolar skin changes and the kinetic pattern of nipple-areola complex enhancement and pathologic diagnosis of the concomitant malignant lesion are critical MRI findings in the differentiation of Paget's disease of the breast and malignant tumor invasion of the nipple-areolar complex.
- 3.0-T MRI is superior to 1.5-T MRI in obtaining areolar-periareolar skin thickness.

Introduction

The nipple-areola complex (NAC) is a specialized breast structure for breastfeeding that involves the pigmented squamous epithelium, a layer of circumferential smooth muscle, and sebaceous glands (1). The skin of the nipple is continuous with the epithelium of the ducts (2). Cancer of the ducts may spread to the NAC (3).

The NAC may be affected by malignancies such as invasive cancer, ductal carcinoma *in situ* (DCIS), or Paget's disease of the breast (PDB) (4). NAC involvement in breast cancers has an incidence rate of 5.6%–24.6% (5). The different pathological mechanisms of NAC involvement include a direct tumor invasion and dissemination of the tumor within ducts or lymphatics (6). Tumor size and distance between the tumor

and nipple are significant factors for NAC involvement. Tumors that are small and far from the nipple pose lower risk of NAC involvement (5, 7). PDB is a rare malignant entity that accounts for 0.7%–4.9% of all breast carcinomas. PDB is usually accompanied by underlying invasive cancer or DCIS (8). Two hypotheses regarding the etiopathology of PDB were noted. The epidermotropic theory suggests that ductal cancer cells migrate through the basement membrane, whereas another theory implicates malignant neoplastic transformation of the intraepidermal clear cells of the NAC (9, 10), which may explain the absence of an underlying malignancy in 1%–6% of PDB cases (8). Definitive diagnosis of diseases of the NAC is made by histopathological examination of wedge biopsy and mastectomy or lumpectomy samples (9). The NAC is examined using imaging methods before skin punch biopsy. Magnetic resonance imaging (MRI) has a higher sensitivity than mammography and ultrasonography in evaluating diseases of the NAC and underlying malignancy (5, 11).

There are no previous studies in the literature comparing the MRI findings of PDB and malignant tumor invasion of the NAC (MTION). Therefore, this study aimed to differentiate between PDB and MTION by dynamic breast MRI findings without the need for skin punch biopsy.

Materials and Methods

This study was approved by the Medical Ethics Committee of Dr Abdurrahman Yurtaslan Ankara Oncology Training and Research Hospital and was in accordance with the principles of the Declaration of Helsinki (approval number: 2020-10/834; approval date: October 21st, 2020).

Study population

We reviewed the pathology results of patients who underwent preoperative dynamic breast MRI between June 2016 and September 2019. Patients who had preoperative breast MRI examination images in our archive and were diagnosed as having PDB or MTION as a result of pathology examination of operative material were included in this study. Patients who received neoadjuvant chemotherapy or did not have postoperative pathology report of PDB or MTION were excluded.

Of 620 patients who underwent preoperative breast MRI examination, 35 patients were diagnosed by pathologic examination as having nipple malignancy such as PDB or MTION. Eight patients received neoadjuvant chemotherapy before surgery and were excluded. Finally, the study group included 27 patients with a mean age of 51.4 years (age range: 31–76 years). All patients were women and underwent mastectomy within 1 month of breast MRI. Pathology reports indicated PDB in 16 patients and MTION in 11 patients.

MRI technique

Among the patients, 17 were examined with a 1.5-Tesla (T) magnetic resonance (MR) scanner (Signa HDx; GE Healthcare, Wisconsin, USA) and 10 with a 3.0-T MR scanner (Skyra; Siemens Healthineers, Erlangen, Germany) before surgery. All patients were examined in the prone position using a breast array coil. Imaging parameters on the 1.5-T MR scanner were as follows: TR/TE, 6500/45; TI, 150 ms; field of view (FOV), 320 mm; matrix, 416 × 224; and number of excitations (NEX), 1 and slice thickness (ST) of 5 mm for axial STIR sequences; TR/TE, 400/8.8; FOV, 320

mm; matrix, 448 × 224; and NEX, 1 and ST of 5 mm for axial T1-weighted (T1W) images; TR/TE, 4/1.5; FA, 10°; FOV, 320 mm; matrix, 350 × 350; and NEX, 1 and ST of 2.8 mm for dynamic axial fat-suppressed T1W images (before and after contrast injection); and TR/TE, 1000/83; FOV, 320 mm; matrix, 192 × 192; and NEX, 4 and ST of 5 mm for echo-planar imaging (EPI)-based diffusion weighted imaging (DWI). In contrast, the imaging parameters on 3.0-T MR scanner were as follows: TR/TE, 5000/88; FOV, 350 mm; matrix, 576 × 768; NEX, 2; and ST, 4 mm for axial fat-saturated T2-weighted (T2W) sequences; TR/TE, 800/11; FOV, 350 mm; matrix, 448 × 640; NEX, 1; and ST, 4 mm for axial T1W images; TR/TE, 4.3/1.6; FA, 10°; FOV, 350 mm; matrix, 352 × 352; NEX, 1; and ST, 1 mm for dynamic axial gradient fat-suppressed T1W images (before and after contrast injection); and TR/TE, 6000/85; FOV, 361 × 401 mm; matrix, 180 × 200; NEX, 1; and ST, 5 mm for EPI-based DWI. Gadobutrol/gadopentetate dimeglumine at of 0.1 mmol/kg was used as the contrast agent for dynamic contrast-enhanced sequences. Images were taken once before contrast and five times after contrast injection. Standard subtraction images were generated by subtracting precontrast images from postcontrast images. Maximum-intensity projection (MIP) and multiplanar reconstruction images were reconstructed. Conventional kinetic analysis was done using a time-intensity curve for the NAC, mass lesions, and nonmass enhancing lesions.

Analysis of magnetic resonance images

MR images were evaluated retrospectively on two workstations by two radiologists who had at least 5 years of experience in breast imaging. The radiologists were blinded to the pathology reports. Each case was evaluated through a consensus between the two radiologists.

We evaluated nipple changes such as nipple inversion or retraction and skin thickness of the NAC on T1W and fat-suppressed T2W images. Complete and partial pulling inward of normal nipple was accepted as inversion and retraction of the nipple, respectively (12, 13). The thickness of the areolar-periareolar skin is normally between 0.5 and 2 mm (2). Asymmetric thickening of the areolar-periareolar skin relative to the contralateral breast was evaluated. The characteristic enhancement of the NAC is symmetric, with superficial linear enhancement thickness of 1–2 mm (1, 13). We evaluated thickness and classification of NAC enhancement on postcontrast T1W MR images. Symmetric absent, mild, and intense nipple enhancement patterns were considered normal (1). Asymmetric NAC enhancement was considered pathologic enhancement. Pathologic NAC enhancement was classified as nodular, discoid, linear, and irregular (11). We evaluated NAC enhancement on postcontrast T1W subtraction and MIP images. Concomitant malignant lesions were classified as single mass, multiple masses, nonmass enhancement (NME), or mass with NME. The largest dimension of the malignant lesions was recorded. Enhancement kinetics of the NAC and concomitant malignant lesions were evaluated as washout, plateau, or persistent enhancement. The enhancement patterns of the NAC and concomitant malignant lesions were compared. The continuity of contrast enhancement in the area between the nipple and subareolar mass or NME was evaluated and classified as discontinuous if a non-enhancing area was observed between the NAC and mass or NME. The distance between the nipple and malignant lesion was measured. If a gap between the mass or NME and NAC was not noted, it was classified as a continuous enhancement (12). The nipple-to-malignant lesion distance was accepted as 0 mm in these cases.

Statistical analysis

SPSS 15.0 for Windows program was used for statistical analysis. As descriptive statistics, numbers and percentages are presented for categorical variables and mean, standard deviation, minimum, and maximum values for numerical variables. Student's *t*-test was used for between-group comparisons of normally distributed variables and Mann-Whitney U test for non-normally distributed variables. Categorical variables were compared using chi-square test. Statistical significance was accepted at $p < 0.05$.

Results

Pathological evaluation determined 16 patients with PDB and 11 patients with MTION. MRI showed nipple inversion or retraction in 19 cases: nine patients (56.3%) in the PDB group and 10 patients (90.9%) in the MTION group. Nipple inversion was more common in patients with MTION (63.6%) than in those with PDB (25%); however, the difference was not significant ($p = 0.093$) (Figure 1).

Areolar-periareolar skin thickening was detected in a total of 12 patients: two (12.5%) in the PDB group and 10 (90.9%) in the MTION group ($p < 0.001$) (Figure 1).

NAC enhancement was observed in 26 patients. In seven of these patients, enhancement was symmetrical, superficial, and linear, which

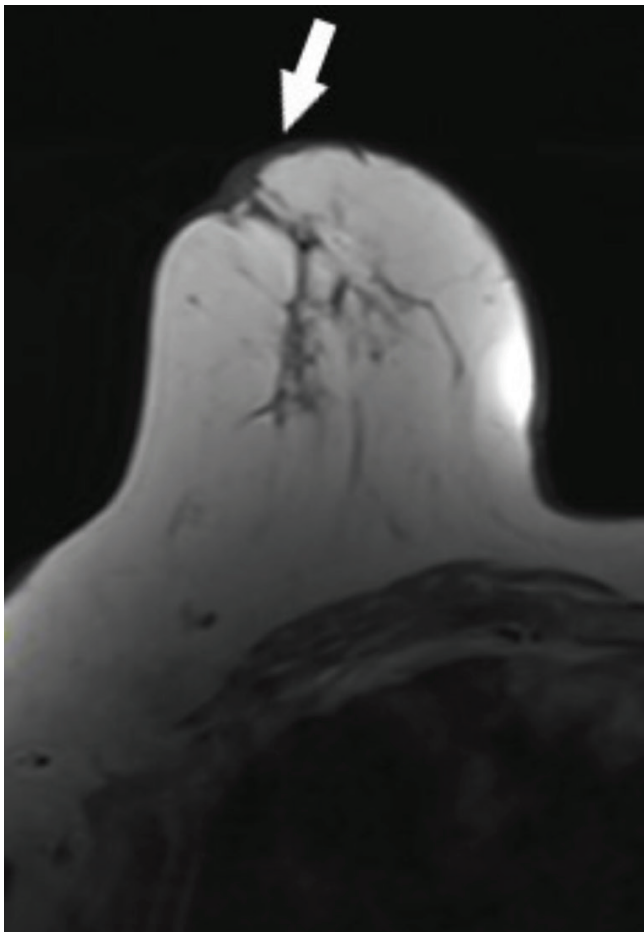


Figure 1. Axial T1-weighted MRI of a 66-year-old woman with ductal carcinoma *in situ* and malignant tumor invasion of the nipple-areola complex shows areolar-periareolar skin thickening (white arrow)

MRI: Magnetic resonance imaging

was considered normal (Figure 2). Only one patient with PDB showed no NAC enhancement. Pathological NAC enhancement was detected in 12 (75.1%) of the patients with PDB and seven (63.7%) of the patients with MTION. Pathological NAC enhancement was evaluated as nodular in four, discoid in three, linear in two, and irregular in 10 patients. Irregular NAC enhancement was more common in both patient groups (Figure 3a). Enhancement patterns were not statistically different between the groups ($p = 0.086$).

Median thickness of the NAC enhancement was 0.47 ± 0.29 cm in the PDB group and 0.32 ± 0.15 cm in the MTION group ($p = 0.141$).

NAC enhancement kinetics are summarized in Table 1. Persistent enhancement pattern was more common in MTION and plateau enhancement pattern in PDB. The distribution of NAC enhancement kinetics differed significantly between the groups ($p = 0.026$).

Morphological pattern of the concomitant malignant lesion was classified as mass in three, NME in 17, and mass with NME in seven patients. NME was the most common in both patient groups. The distribution of morphological patterns did not differ significantly between the groups ($p = 0.078$). The median size of the concomitant malignant lesions was 2.99 ± 2.12 cm in patients with PDB and 2.9 ± 1.63 cm in patients with MTION ($p = 0.863$).

Concomitant malignant lesion enhancement kinetics were evaluated as washout, plateau, and persistent enhancement pattern in six (37.5%), seven (43.8%), and three (18.8%) patients in the PDB group and four (36.4%), three (27.3%), and four (36.4%) patients in the MTION group, respectively ($p = 0.551$).

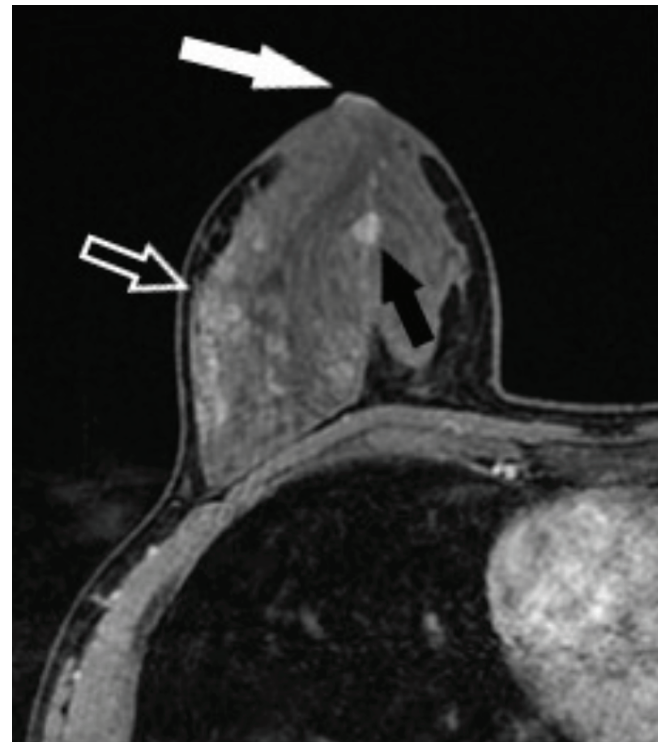


Figure 2. Axial dynamic postcontrast T1-weighted MRI of the right breast of a 45-year-old woman with invasive ductal carcinoma and Paget's disease of the breast shows a normal thin, superficial enhancement (white arrow) of the skin of the nipple-areola complex, concomitant mass (black arrow), and concomitant nonmass enhancement (empty white arrow)

MRI: Magnetic resonance imaging

On comparison of the enhancement kinetic curves of the NAC and concomitant malignant lesions, different patterns were observed in nine patients (56.3%) in the PDB group and eight patients (72.7%) in the MTION group (Table 2; Figures 3b and 3c). There was no statistically significant difference between the groups ($p = 0.448$).

The mean nipple-to-malignant lesion distances in the PDB and MTION groups were 0.29 ± 0.64 cm and 0.06 ± 0.16 cm, respectively. The average distance was longer in patients with PDB; however, the difference was not statistically significant ($p = 0.799$).

Table 1. MRI findings compared by pathologic diagnosis of nipple-areola complex involvement

MRI findings (n)	Pathologic diagnosis of NAC involvement		p-value
	PDB (n = 16) (%)	MTION (n = 11) (%)	
Nipple change			
None (n = 8)	7 (43.7%)	1 (9.1%)	0.093
Inversion (n = 11)	4 (25.0%)	7 (63.6%)	
Retraction (n = 8)	5 (31.3%)	3 (27.3%)	
Areolar/periareolar skin thickening			
Absent (n = 15)	14 (87.5%)	1 (9.1%)	<0.001
Present (n = 12)	2 (12.5%)	10 (90.9%)	
NAC enhancement			
Classification			
None (n = 1)	1 (6.3%)	0 (0.0%)	0.086
Normal (n = 7)	3 (18.7%)	4 (36.4%)	
Nodular (n = 4)	4 (25.0%)	0 (0.0%)	
Discoïd (n = 3)	3 (18.7%)	0 (0.0%)	
Linear (n = 2)	0 (0.0%)	2 (18.2%)	
Irregular (n = 10)	5 (31.3%)	5 (45.4%)	
Thickness (mm), mean \pm SD	4.71 \pm 2.97	3.22 \pm 1.55	0.141
Kinetic pattern			
Persistent (n = 13)	4 (26.7%)	9 (81.8%)	0.026
Plateau (n = 8)	7 (46.6%)	1 (9.1%)	
Washout (n = 5)	4 (26.7%)	1 (9.1%)	
Concomitant malignant lesion			
Morphological pattern			
Single mass (n = 3)	0 (0.0%)	3 (27.3%)	0.078
NME (n = 17)	12 (75.0%)	5 (45.4%)	
NME + mass (n = 7)	4 (25.0%)	3 (27.3%)	
Maximum size (mm), mean \pm SD	29.9 \pm 21.2	29.0 \pm 16.3	0.863
Enhancement kinetic pattern			
Persistent (n = 7)	3 (18.7%)	4 (36.4%)	0.551
Plateau (n = 10)	7 (43.8%)	3 (27.2%)	
Washout (n = 10)	6 (37.5%)	4 (36.4%)	
Pathological diagnosis			
Inflammatory carcinoma (n = 2)	2 (12.5%)	0 (0.0%)	0.025
Invasive ductal carcinoma (n = 8)	3 (18.7%)	5 (45.5%)	
DCIS (n = 10)	9 (56.3%)	1 (9.1%)	
Invasive breast carcinoma (n = 6)	2 (12.5%)	4 (36.3%)	
Invasive lobular carcinoma (n = 1)	0 (0.0%)	1 (9.1%)	

NAC: Nipple-areola complex; MRI: Magnetic resonance imaging; PDB: Paget's disease of the breast; MTION: Malignant tumor invasion of the nipple-areola complex; SD: Standard deviation; NME: Nonmass enhancement; DCIS: Ductal carcinoma *in situ*; n: Number

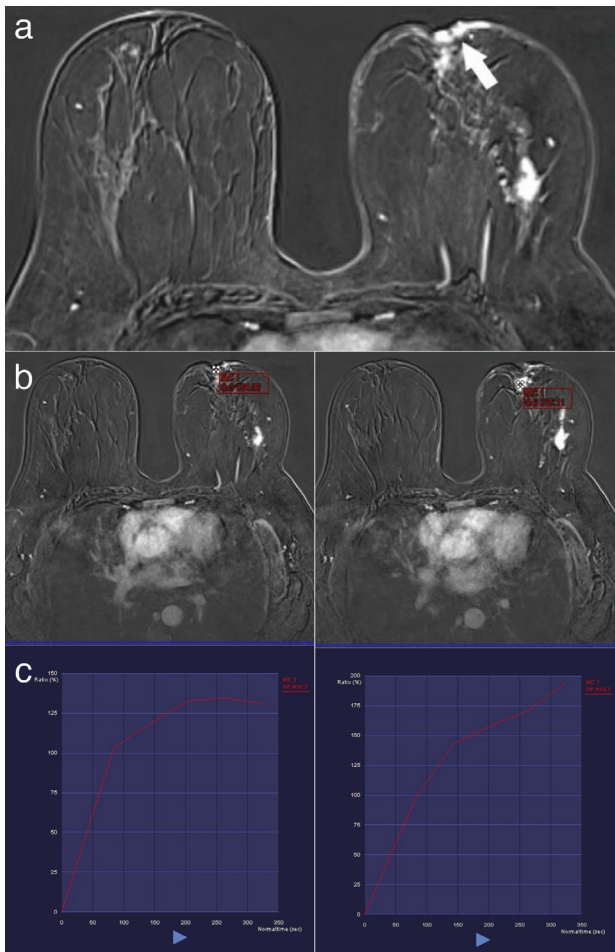


Figure 3. MRI of a 50-year-old woman with invasive breast carcinoma and malignant invasion of the nipple-areola complex. **(a)** Axial dynamic postcontrast T1-weighted subtraction MRI of the left breast shows pathologic irregular enhancement (white arrow) in the nipple-areola complex. Conventional kinetic analysis by time-intensity curve shows **(b)** plateau pattern of pathologic NAC enhancement and **(c)** persistent enhancement pattern for the closest concomitant mass lesion

MRI: Magnetic resonance imaging; NAC: Nipple-areola complex

Continuous enhancement between the NAC to the concomitant malignant lesion was seen in 22 patients: 13 (81.3%) in the PDB group and nine (81.8%) in the MTION group ($p = 1.00$).

The distribution of pathological types of concomitant malignant lesions is shown in Table 1. DCIS was diagnosed in nine (56.3%) patients with PDB and one (9.1%) of the patients with MTION. Invasive ductal carcinoma (IDC) was detected in three patients with PDB (18.8%) and five patients with MTION (45.5%). The distribution of pathological types of concomitant malignancy differed significantly between the groups ($p = 0.025$).

Preoperative breast MRI examinations were conducted with a 1.5-T MR scanner in 17 patients and a 3.0-T MR scanner in 10 patients. Furthermore, 13 of 17 patients examined with 1.5-T MRI were patients with PDB (76.4%), seven of 10 patients examined with 3.0-T MRI were patients with MTION (70%) ($p = 0.04$). Areolar-periareolar skin thickening was detected in four (23.5%) and eight (80%) of the patients imaged with 1.5-T and 3.0-T MRI, respectively ($p = 0.007$). No pathological NAC enhancement was detected in five patients (29.4%) consisting of four patients with PDB and one patient with MTION imaged with 1.5 T MRI and three patients with MTION (30%) imaged with 3.0 T MRI ($p = 1.00$) (Table 3). There were no statistically significant differences in nipple change; the classification, thickness, and kinetic pattern of NAC enhancement; the morphological pattern, size, enhancement kinetic pattern, and pathological diagnosis of concomitant malignant lesion; the similarity of enhancement kinetics pattern of the NAC and concomitant malignant lesions; nipple-to-malignant lesion distance; and the relationship between enhancement of the NAC and concomitant malignant lesions between the patients imaged with 1.5-T and 3.0-T MR (Table 4).

Discussion and Conclusion

Nipple inversion and retraction are terms used to describe changes in the nipple. Retraction is defined as partial pulling in of the nipple, whereas inversion is complete pulling in. Nipple inversion and retraction may occur secondary to malignant lesions, as well

Table 2. Comparison of concomitant malignant lesions and nipple-areola complex MRI findings according to pathologic diagnosis of nipple-areola complex involvement

MRI findings (n)	Pathologic diagnosis of NAC involvement		p-value
	PDB (n = 16) (%)	MTION (n = 11) (%)	
Nipple-to-malignant lesion distance (cm), mean ± SD	2.88±6.40	0.69±1.63	0.799
Relationship between enhancement of the NAC and concomitant malignant lesions			
Continuous (n = 22)	13 (81.3%)	9 (81.8%)	1.000
Discontinuous (n = 5)	3 (18.8%)	2 (18.2%)	
Enhancement kinetic pattern of the NAC and concomitant malignant lesions			
Same (n = 10)	7 (43.8%)	3 (27.3%)	0.448
Different (n = 17)	9 (56.3%)	8 (72.7%)	

NAC: Nipple-areola complex; MRI: Magnetic resonance imaging; PDB: Paget’s disease of the breast; MTION: Malignant tumor invasion of the nipple-areola complex; SD: Standard deviation; n: Number

Table 3. Comparison of presence of pathological nipple-areola complex enhancement according to magnetic field strength of MRI scanner

Pathological NAC enhancement (n)	1.5-T (n = 17)		3.0-T (n = 10)		p-value
	PDB (n = 13) (%)	MTION (n = 4) (%)	PDB (n = 3) (%)	MTION (n = 7) (%)	
Absent	4 (23.5%)	1 (5.8%)	0 (0.0%)	3 (30%)	1.000
Present	9 (52.9%)	3 (17.6%)	3 (30%)	4 (40%)	

NAC: Nipple-areola complex; PDB: Paget's disease of the breast; MTION: Malignant tumor invasion of the nipple-areola complex; MRI: Magnetic resonance imaging; n: Number

Table 4. MRI findings compared by magnetic field strength of MRI scanner

MRI findings (n)	Magnetic field strength of MRI scanner		p-value
	1.5-T (n = 17) (%)	3.0-T (n = 10) (%)	
Nipple change			
None (n = 8)	6 (35.3%)	2 (20%)	0.877
Inversion (n = 11)	6 (35.3%)	5 (50%)	
Retraction (n = 8)	5 (29.4%)	3 (30%)	
Areolar/periareolar skin thickening			
Absent (n = 15)	13 (76.5%)	2 (20%)	0.007
Present (n = 12)	4 (23.5%)	8 (80%)	
NAC enhancement			
Classification			
None (n = 1)	1 (5.9%)	0 (0%)	0.299
Normal (n = 7)	4 (23.5%)	3 (30%)	
Nodular (n = 4)	4 (23.5%)	0 (0%)	
Discoid (n = 3)	2 (11.8%)	1 (10%)	
Linear (n = 2)	2 (11.8%)	0 (0%)	
Irregular (n = 10)	4 (23.5%)	6 (60%)	
Thickness (mm), mean ± SD	3.80±2.52	4.61±2.67	
Kinetic pattern			
Persistent (n = 13)	7 (43.7%)	6 (60%)	0.770
Plateau (n = 8)	6 (37.5%)	2 (20%)	
Washout (n = 5)	3 (18.8%)	2 (20%)	
Concomitant malignant lesion			
Morphological pattern			
Single mass (n = 3)	1 (5.9%)	2 (20%)	0.528
NME (n = 17)	12 (70.6%)	5 (50%)	
NME + mass (n = 7)	4 (23.5%)	3 (30%)	
Maximum size (mm), mean ± SD	26.3 ± 14.4	35.0 ± 24.8	
Enhancement kinetic pattern			
Persistent (n = 7)	5 (29.4%)	2 (30%)	0.211
Plateau (n = 10)	8 (47.1%)	2 (20%)	
Washout (n = 10)	4 (23.5%)	6 (60%)	

Table 4. Continued

MRI findings (n)	Magnetic field strength of MRI scanner		
	1.5-T (n = 17) (%)	3.0-T (n = 10) (%)	p-value
Pathological diagnosis			
Inflammatory carcinoma (n = 2)	2 (11.8%)	0 (0%)	
Invasive ductal carcinoma (n = 8)	3 (17.6%)	5 (50%)	
DCIS (n = 10)	8 (47.1%)	2 (20%)	0.258
Invasive breast carcinoma (n = 6)	3 (17.6%)	3 (30%)	
Invasive lobular carcinoma (n = 1)	1 (5.9%)	0 (0%)	
Nipple-to-malignant lesion distance (cm), mean ± SD	2.85±6.19	0.50±1.58	0.354
Relationship between enhancement of the NAC and concomitant malignant lesions			
Continuous (n = 22)	13 (76.5%)	9 (90%)	0.621
Discontinuous (n = 5)	4 (23.5%)	1 (10%)	
Enhancement kinetic pattern of the NAC and concomitant malignant lesions			
Same (n = 10)	7 (41.2%)	3 (30%)	0.692
Different (n = 17)	10 (58.8%)	7 (70%)	
Pathologic diagnosis of NAC involvement			
PDB (n = 16)	13 (76.5%)	3 (30%)	0.040
MTION (n = 11)	4 (23.5%)	7 (70%)	

NAC: Nipple-areola complex; MRI: Magnetic resonance imaging; PDB: Paget's disease of the breast; MTION: Malignant tumor invasion of the nipple-areola complex; SD: Standard deviation; NME: Nonmass enhancement; DCIS, Ductal carcinoma *in situ*; n: Number

as congenital or benign causes, and a detailed history and physical examination are crucial to distinguish them (3). In the literature, central, symmetric, slit-like, long-term retraction is generally associated with benign processes, whereas rapid inversion with distortion of the areola usually indicates malignancy (1, 3). Although the difference was not statistically significant, nipple inversion on MRI was more frequent among patients with pathologically proven MTION than those with pathologically proven PDB in our study. In a study by Moon et al. (12), nipple change was detected in all six patients with pathologically proven MTION and six of 10 patients with pathologically proven PDB. Contrary to our study, they did not subdivide nipple changes as inversion and retraction. However, the rates of nipple changes in the two patient groups were similar to those in our study.

Areolar-periareolar skin thickening on MRI was significantly detected more frequently in patients with MTION than in patients with PDB. These findings are consistent with those of Moon et al. (12), although the difference between the two groups in their study was smaller compared to that in our study. Patients with MTION may exhibit more edema and areolar-periareolar skin thickening because MTION involves all layers of the skin or areolar lymphatics, whereas PDB is located within the epidermis of the NAC (2, 14, 15).

Asymmetric NAC enhancement has been emphasized in the literature as a significant indicator of NAC invasion (5, 7, 16). Symmetric NAC enhancement, which is accepted as normal, was more common in patients with PDB and MTION in our study compared to that in the literature. This may be related to the stage or extent of the disease in the patients analyzed. However, these were not investigated in our study. We compared the presence and types of NAC enhancement

in pathologically proven PDB and MTION cases. Irregular NAC enhancement was more common than the other patterns in both groups, and no significant difference in distribution was found between the groups.

Due to the small size of the NAC area and motion artifacts, kinetic curve assessment may not be reliable for NAC enhancement. Therefore, NAC enhancement kinetics have not been adequately studied and we were not able to find adequate literature data to compare with our findings. In our study, we observed a significant difference between the groups, with persistent enhancement being more common in MTION and plateau pattern more common in PDB. Contrary to our results, Echevarria et al. (17) detected persistent nipple enhancement in two of three patients with PDB, whereas plateau enhancement was detected in only one patient with PDB.

In terms of concomitant malignancies, DCIS was more frequently detected in patients with PDB than those with MTION in our study. DCIS was reported as the concomitant malignancy in 50% of PDB cases in the study by Moon et al. (12), in two of three patients with PDB in the study by Echevarria et al. (17), and in 88% of PDB cases in a study by Frei et al. (18) (2, 17). These results are compatible with our study.

DCIS usually appears as NME on breast MRI (19, 20). High prevalence of DCIS in patients with PDB was observed in our study; further, the prevalence of NME was higher in the PDB group than in the MTION group. Moon et al. (12) reported that multiple masses were most common in PDB cases. This difference may explain the lower prevalence of DCIS among patients with pathologically proven PDB in their study than in ours.

In MTION, the malignant tumor either invades the NAC directly or through ducts or lymphatics (6). In contrast, MRI findings of NAC involvement in PDB are mostly associated with eczematous and inflammatory changes of the nipple (13). Therefore, we expected that tumor and NAC contrast enhancement kinetics would be more similar in MTION than PDB; however, we found the opposite. This result may be related to the technically difficult nature of nipple enhancement kinetics analysis due to the small size of the NAC and motion degradation artifacts.

In the literature, it has been reported that a distance of more than 2 cm between the tumor and NAC and tumor size greater than 2 cm may increase the risk of malignant NAC invasion (5, 12). In our study, we compared these parameters in pathologically proven PDB and pathologically proven MTION cases and found no statistically significant difference. However, we noted smaller distances between the tumor and NAC in MTION cases.

In the present study, enhancement of the NAC and the concomitant malignant lesion was predominantly continuous in both patient groups. In most studies in the literature, continuous enhancement was found to be correlated with NAC invasion (5, 7, 16, 21). However, pathologically proven cases of MTION and PDB were not compared. Moon et al. (12) reported that discontinuous enhancement was more prevalent in pathologically proven MTION, whereas continuous and discontinuous enhancement patterns were equally represented in pathologically proven PDB cases.

3.0-T MRI has higher spatial and temporal resolution than 1.5-T MRI (22, 23). The evaluation of the morphology of the breast lesions improved with 3.0-T MRI (22, 23). The spectral separation of fat and water is better in 3.0-T MRI. Therefore, fat suppression is superior in 3.0-T MRI images and lesion enhancements are more clearly visualized (23). In our study, the number of patients with increased areolar-periareolar skin thickness was statistically significantly higher in patients imaged with 3.0-T MRI than those imaged with 1.5-T MRI. This may be because of the higher resolution of 3.0-T MRI or that 70% of patients imaged with 3.0-T MRI were patients with MTION, in whom we found a more frequent increase in areolar-periareolar skin thickness. To clarify this, patients should have been examined with both 1.5-T and 3.0-T MRI and the obtained findings compared. This was not possible because our study was retrospective. In our study, no significant difference was found between 1.5-T and 3.0-T MRI in detecting pathological NAC enhancement in nipple malignancy. When we examined the pathology reports, we found that all cases in which pathological findings in the NAC could not be detected with 1.5-T and 3.0-T MRI were in the early phase of the disease.

Our study had several limitations. First, the sample was selected retrospectively from patients with pathologically proven MTION and PDB who underwent preoperative breast MRI. Although the radiologists were blinded to patient groups while reevaluating the breast MRI images, they knew that all patients had a diagnosis of NAC malignancy. This may have caused bias in the evaluation. Second, since our study was retrospective, we could not evaluate the possible contribution of the results to treatment management and planning for these patient groups. Third, the study population was small. Since PDB is a rare NAC disease and preoperative MRI of every patient in both patient groups is required, the study population was small. A prospective study with a larger sample size is warranted to overcome these limitations.

In conclusion, areolar-periareolar skin thickening and asymmetric NAC enhancement with persistent kinetics curve were significant MRI findings for MTION in patients diagnosed with IDC. In contrast, the plateau kinetic pattern of asymmetric NAC enhancement without areolar-periareolar skin changes may support PDB in patients diagnosed with DCIS. 3.0-T MRI was superior to 1.5-T MRI in detecting the presence of areolar-periareolar skin thickness.

Ethics Committee Approval: Approval was received for this study from the Medical Specialty Education Board of Dr. Abdurrahman Yurtaslan Ankara Oncology Training and Research Hospital (2020-10/834).

Informed Consent: Retrospective study.

Peer-review: Externally peer-reviewed.

Authorship Contributions

Conception: A.C.B.; Design: A.C.B., H.A.; Supervision: A.C.B., H.A.; Materials: I.E.B.; Data Collection and/or Processing: A.C.B., I.E.B., Ö.T., D.S.Ö.; Analysis and/or Interpretation: A.C.B.; Literature Review: A.C.B.; Writing: A.C.B.; Critical Review: H.A.

Conflict of Interest: The authors declare that they have no conflict of interest.

Financial Disclosure: The authors declared that this study received no financial support.

References

1. Da Costa D, Taddese A, Cure ML, Gerson D, Poppiti R, Esserman LE. Common and unusual diseases of the nipple-areolar complex. *Radiographics* 2007; 27(Suppl 1): S65-S77. doi: 10.1148/rg.27si07512 (PMID: 18080236) [[Crossref](#)]
2. Stone K, Wheeler A. A review of anatomy, physiology, and benign pathology of the nipple. *Ann Surg Oncol* 2015; 22: 3236-3240. (PMID: 26242366) [[Crossref](#)]
3. Nicholson BT, Harvey JA, Cohen MA. Nipple-areolar complex: normal anatomy and benign and malignant processes. *Radiographics* 2009; 29: 509-523. (PMID: 19325062) [[Crossref](#)]
4. Friedman EP, Hall-Craggs MA, Mumtaz H, Schneidau A. Breast MR and the appearance of the normal and abnormal nipple. *Clin Radiol* 1997; 52: 854-861. (PMID: 9392464) [[Crossref](#)]
5. Cho J, Chung J, Cha ES, Lee JE, Kim JH. Can preoperative 3-T MRI predict nipple-areolar complex involvement in patients with breast cancer? *Clin Imaging* 2016; 40: 119-124. (PMID: 26423158) [[Crossref](#)]
6. Santini D, Taffurelli M, Gelli MC, Grassigli A, Giosa F, Marrano D, et al. Neoplastic involvement of nipple-areolar complex in invasive breast cancer. *Am J Surg* 1989; 158: 399-403. (PMID: 2817219) [[Crossref](#)]
7. Machida Y, Shimauchi A, Igarashi T, Hoshi K, Fukuma E. Preoperative breast MRI: reproducibility and significance of findings relevant to nipple-areolar complex involvement. *Breast Cancer* 2018; 25: 456-463. (PMID: 29464515) [[Crossref](#)]
8. Seetharam S, Fentiman IS. Paget's disease of the nipple. *Womens Health (Lond)* 2009; 5: 397-402. (PMID: 19586431) [[Crossref](#)]
9. Challa VR, Deshmane V. Challenges in diagnosis and management of Paget's disease of the breast: A retrospective study. *Indian J Surg* 2015; 77: 1083-1087. (PMID: 27011515) [[Crossref](#)]
10. Morandi L, Pession A, Marucci GL, Foschini MP, Pruneri G, Viale G, et al. Intraepidermal cells of Paget's carcinoma of the breast can be genetically different from those of the underlying carcinoma. *Hum Pathol* 2003; 34: 1321-1330. (PMID: 14691919) [[Crossref](#)]

11. Lim HS, Jeong SJ, Lee JS, Park MH, Kim JW, Shin SS, et al. Paget disease of the breast: mammographic, US, and MR imaging findings with pathologic correlation. *Radiographics* 2011; 31: 1973-1987. (PMID: 22084182) [[Crossref](#)]
12. Moon JY, Chang YW, Lee EH, Seo DY. Malignant invasion of the nipple-areolar complex of the breast: usefulness of breast MRI. *AJR Am J Roentgenol* 2013; 201: 448-455. (PMID: 23883228) [[Crossref](#)]
13. Gao Y, Brachtel EF, Hernandez O, Heller SL. An analysis of nipple enhancement at breast MRI with radiologic-pathologic correlation. *Radiographics* 2019; 39: 1-18. (PMID: 30547729) [[Crossref](#)]
14. Rakha EA, Miligy IM, Gorringer KL, Toss MS, Green AR, Fox SB, et al. Invasion in breast lesions: the role of the epithelial-stroma barrier. *Histopathology* 2017; 72: 1075-1083. (PMID: 29177112) [[Crossref](#)]
15. Sanders MA, Brock JE, Harrison BT, Wiczorek TJ, Hong X, Guidi AJ, et al. Nipple-invasive primary carcinomas: Clinical, imaging, and pathologic features of breast carcinomas originating in the nipple. *Arch Pathol Lab Med* 2018; 142: 598-605. (PMID: 29431468) [[Crossref](#)]
16. Lim S, Park G, Choi HJ, WJ Kwon, Kang BS, Bang M. Use of preoperative mammography, ultrasonography, and MRI to predict nipple areolar complex involvement in breast cancer. *Br J Radiol* 2019; 92: 20190074. doi: 10.1259/bjr.20190074 (PMID: 31317763) [[Crossref](#)]
17. Echevarria JJ, Lopez-Ruiz JA, Martin D, Imaz I, Martin M. Usefulness of MRI in detecting occult breast cancer associated with Paget's disease of the nipple-areolar complex. *Br J Radiol* 2004; 77: 1036-1039. (PMID: 15569646) [[Crossref](#)]
18. Frei KA, Bonel HM, Pelte MF, Hylton NM, Kinkel K. Paget disease of the breast: findings at magnetic resonance imaging and histopathologic correlation. *Invest Radiol* 2005; 40: 363-367. (PMID: 15905723) [[Crossref](#)]
19. Amornsiripanitch N, Lam DL, Rahbar H. Advances in breast MRI in the setting of ductal carcinoma in situ. *Semin Roentgenol* 2018; 53: 261-269. (PMID: 30449344) [[Crossref](#)]
20. Rahbar H, Parsian S, Lam DL, Dontchos BN, Andeen NK, Rendi MH, et al. Can MRI biomarkers at 3 Tesla identify low risk ductal carcinoma in situ? *Clin Imaging* 2016; 40: 125-129. (PMID: 26365872) [[Crossref](#)]
21. Sakamoto N, Tozaki M, Hoshi K, Fukuma E. Is MRI useful for the prediction of nipple involvement? *Breast Cancer* 2013; 20: 316-322. (PMID: 22311582) [[Crossref](#)]
22. Pinker K, Grabner G, Bogner W, Gruber S, Szomolanyi P, Trattng S, et al. A combined high temporal and high spatial resolution 3 Tesla MR imaging protocol for the assessment of breast lesions: initial results. *Invest Radiol* 2009; 44: 553-558. (PMID: 19652611) [[Crossref](#)]
23. Butler RS, Chen C, Vashi R, Hooley RJ, Philpotts LE. 3.0 Tesla vs 1.5 Tesla breast magnetic resonance imaging in newly diagnosed breast cancer patients. *World J Radiol* 2013; 5: 285-294. (PMID: 24003354) [[Crossref](#)]



Evaluation of Liposomal and Microbubbles Mediated Delivery of Doxorubicin in Two-Dimensional (2D) and Three-Dimensional (3D) Models for Breast Cancer

Melek Aydın¹, Ekrem Özdemir², Zekiye Altun¹, Sevgi Kılıç², Safiye Aktaş¹

¹Department of Basic Oncology, Institute of Oncology, Dokuz Eylül University, İzmir, Turkey

²Department of Chemical Engineering, İzmir Institute of Technology, İzmir, Turkey

ABSTRACT

Objective: Liposomal cancer treatment strategies are useful in removing the side effects that were the main concern in recent years. In this study, we prepared microbubble (MBs) conjugated with DOX-loaded liposomes (DOX-loaded MBs) and investigated their effectiveness in *in vitro* breast cancer cells in two dimensions (2D) and three dimensions (3D).

Materials and Methods: With this aim, breast cancer cells with different features (4T1, MDA-MB231, MCF-7) were grown in 2D and 3D dimensions. The cytotoxic and cell death effects under different conditions, durations and doses were evaluated with WST-1, trypan-blue, colony counts. Apoptotic effects were investigated with flow cytometric Annexin-V-PI and immunohistochemical (Ki-67, caspase 3, 8, 9) methods.

Results: After free DOX and LipoDOX were applied, the proliferation index of three cell lines reduced. Intrinsic and extrinsic apoptotic pathways were activated in both 2D and 3D models. However, this effect was observed at lower levels in the 3D model due to the difficulty of diffusion of DOX into the spheroids. Additionally, the suitability of the 3D model for breast cancer cells was supported by formation of ductus-like structures and spheroids. Cell deaths were not observed significantly with the DOX-loaded microbubbles due to rising of MBs to the surface and not reaching spheroids held in matrigel of 3D model.

Conclusion: DOX and LipoDOX showed anti-proliferative and apoptosis-inducing effects in breast cancer cells. However, these effects indicated variability depending on the cell lines and 2D or 3D model types.

Keywords: 3D cell culture, breast cancer, doxorubicin, liposome, microbubble

Cite this article as: Aydın M, Özdemir E, Altun Z, Kılıç S, Aktaş S. Evaluation of Liposomal and Microbubbles Mediated Delivery of Doxorubicin in Two-Dimensional (2D) and Three-Dimensional (3D) Models for Breast Cancer. Eur J Breast Health 2021; 17(3): 274-282

Key Points

- Doxorubicin can be delivered with liposome and microbubbles.
- 3D spheroid model is suitable for *in vitro* breast cancer studies.
- 3D *in vitro* models are difficult to test microbubble loaded drugs.

Introduction

Cancer is one of the leading causes of deaths worldwide. In women, breast cancer is the most commonly diagnosed cancer. In fact, it is the second most common cause of cancer death among women (1, 2). In 2020, breast cancer accounted for ~ 684,000 deaths worldwide according to GLOBACON (<https://doi.org/10.3322/caac.21660>). Several studies are being conducted to devise new strategies to overcome or reduce the common side effects associated with the administration of chemotherapeutics (3, 4). One of the strategies that is being widely explored involves the use liposomes to deliver entrapped cancer drugs. Commercially approved liposomal formulations include lipoplatin (cisplatin encapsulated in liposome) and LipoDOX [doxorubicin (DOX) entrapped in liposome] (5-7). Currently, the therapeutic safety and efficacy of LipoDOX for the treatment of triple-negative breast cancer is being evaluated in clinical trials and experimental studies in different combinations (8, 9). Most of the current research is focused using of poly (ADP-ribose) polymerase (PARP) inhibitors (10), in modified tandem peptide form (11), with liposomal immunotherapy (12), and in local gel form (13).

Microbubbles (MB), small gas-filled bubbles with size 0.5–10 µm, find wide applications in industry, medicine, and life sciences. Generally, microbubble shell structure is characterized by the presence of phospholipid with polyethylene glycol (PEG) as emulsifying agent. When

ultrasound is applied to MBs, the high pressure induces a compression movement resulting in the reduction in the size of MBs. Further, the reduction in pressure is accompanied by an increase in the size of MBs (14). Thus, the ultrasound images generated from the signals obtained from oscillations of microbubbles provide high quality and clearly comprehensible information. All these features make MBs a promising contrast agent for ultrasound imaging. During ultrasound imaging, the oscillation of MBs results in the development of transient pores in the cell walls. As the intensity of ultrasound increases, MBs form a jet flow. This results in the opening of holes in cell walls, allowing the flow of chemotherapeutic drug into the cells (15). Thus, MBs act as excellent drug delivery agents.

In the present study, the suitability of MBs as delivery agents for DOX was explored. Doxorubicin-loaded MBs were developed by attachment of DOX-loaded liposomes to ultrasound contrast agent microbubbles via avidin-biotin bridge. The study aimed to evaluate and compare the therapeutic efficacy of DOX-loaded MBs and DOX-loaded liposomes with free DOX in *in vitro* two-dimensional (2D) and three-dimensional (3D) models for breast cancer.

Material and Methods

Chemicals

Clinical grade liposomal doxorubicin (Caelyx LipoDOX) was purchased from Janssen Pharmaceutica NV, Belgium. Doxorubicin HCl (Adriamycin) India, was procured from West-Ward, Franco Indian Pharmaceuticals. Distearoyl glycerophosphocholine (DSPC, 99%), 1,2 distearoyl glycerol 3 phosphoethanolamine N [methoxy(polyethylene glycol)2000] (DSPE-PEG2000), and biotinylated DSPE-PEG2000 were obtained from Avanti Polar Lipids (Alabaster AL). Cholesterol and polyoxyethylene-40-stearate (PEG40St) were purchased from Sigma Aldrich (St. Louis, MO).

Preparation and characterization of microbubbles, DOX-loaded liposomes (LipoDOX), and DOX-loaded MBs

Microbubbles were prepared using DSPC as lipid, (PEG40St) as emulsifier, and biotinylated DSPE-PEG2000. MBs were prepared using the process described previously by Onercan (16). Since Caelyx LipoDOX is not suitable for conjugation with MBs, LipoDOX was prepared in-house using a mixture of DSPC, cholesterol, DSPE-PEG, and biotinylated DSPE-PEG as described before (16). In order to prepare DOX-loaded MBs, preformed LipoDOX and MBs in same %50 weights were mixed and incubated for 15 min on a rotary mixer at room temperature. Unbound LipoDOX was removed from the solution by flotation technique. Unbound Lipodox was at bottom and MB loaded Lipodox was floating. The amount of DOX bound to the MBs was determined using a fluorescence spectrophotometer (SHIMADZU) with emission signal at 595 nm upon excitation

with a 470 nm laser. Characteristics for the various formulations used in the study are summarized in Table 1.

Formation of three-dimensional (3D) cell cultures and spherule diameter measurement

MCF-7 (HTB-22, ATCC) (hormone receptor positive human cell line), MDA-MB-231 (HTB-26, ATCC) (triple negative human cell line expressing human epidermal growth factor receptor 2 (HER2), non-amplified), and 4T1 (CRL-2539, ATCC) (triple negative mouse cell line) breast cancer cell lines were used in the study. The cells were cultivated using Dulbecco's Modified Eagle Medium, DMEM (Corning, 10-017 CV) for MDA-MB-231 and RPMI-1640 medium (Corning, 15-040 CV) for 4T1 and MCF7 supplemented with 1% L-glutamine (Corning, 25-005 CI), penicillin/streptomycin (Corning, 30-002-CI), and 10% fetal bovine serum (Corning, 35-010-CV). The cell lines were maintained at 37 °C in a humidified incubator under 5% CO₂. All the experiments were repeated thrice, at minimum three different time points.

For 3D cell culture, a Matrigel basement membrane matrix (Corning) was first brought to liquid state by incubation at 4 °C. The material was swirled to ensure proper dispersion of the material. In a 96 well plate, 1000 cells per well were seeded with Matrigel in 96 well plate, 6 wells per condition (17-19). The cells were incubated at 37 °C in a humidified incubator at 5% CO₂ for 24 hours. After 24 hours, the cells were treated with optimized doses of DOX, LipoDOX, and DOX-loaded MBs. For each treatment six wells were used. Samples were further incubated at 37 °C in a humidified incubator at 5% CO₂ for 48 hours. Post 48 hours, an inverted light microscope (LEICA DMIL) was used to image and count the number and diameter of spherules formed in each well. The cells were further stained with trypan blue to evaluate the number of live and dead cells. For trypan blue staining, 10 mL of the dye was added per 96 wells, media was removed, and number of blue and transparent cells were counted using a microscope. In addition to this, the cells seeded in 25 cm² flasks were treated with effective dose of DOX, LipoDOX, and DOX-loaded MBs for appropriate time and exposed to ultrasound. The cells without any treatment were used as controls for comparison. For immunohistochemical analysis, colonies were collected using a cell scraper and paraffin blocks were prepared. Immunohistochemical analysis was performed on the sections in 3D to evaluate the expression of Ki-67, caspase-3, caspase-8, and caspase-9.

This study was approved by Dokuz Eylül University, Noninvasive Ethics Committee (date: 09.11.2020, no: 2017/26-22).

Flow pattern

Breast cancer cells were grown on the surface of sterile slides inserted in a flask (4-well Multidish, Nunc). For 2D model, cells were directly seeded onto the slides at a cell density of 10,000 cell/ml. For *in vitro*

Table 1. Characterization results for various formulations used in the study

Sample	DOX concentration (mg/ml)	Sample	Concentration (MB/ml)	Mean size (mm)
LipoDOX	493.8	MB before conjugation	2.66×10^9	3.11
DOX-loaded MBs	15.4	MB after conjugation	7.90×10^8	2.99

LipoDOX: Doxorubicin (DOX) entrapped in liposome; MB: Microbubbles

3D studies, 21.8 cm²/well area was seeded with 10⁶ cells mixed in 1 mL of cold liquid Matrigel per unit surface. The cells were incubated at 37 °C to allow hardening of the Matrigel for 30 minutes. Further, complete medium was added and plate was incubated for 48 hours for spherule formation. After 48 hours, the cells were used for flow experiments. A special flow chamber was designed to perform the experiments in 2D and 3D. The cells were placed in the flow chamber and the flow experiments were performed. The MB loaded DOX were fluxed through the flowing apparatus over cells.

Measurement of cell proliferation using WST-1 assay

In a 96 well plate, the cells were seeded at a density of 10⁴ cells/well and treated with different doses of DOX and LipoDOX (0.5, 1.5, 2.5, 5, 10, and 20 µM). For each treatment six wells were used. Cell proliferation assay was performed after 24 and 48 hours of incubation using WST-1 solution (Roche, 11644807001). To evaluate the effect of dose and time on cell viability, the cells were treated with WST-1 at a concentration 10 µL/well and incubated at 37 °C for 1 hour. Cell proliferation was measured in terms of absorbance at 450 nm using an ELISA reader (Thermo). LD50 (50% Lethal dose) for DOX and LipoDOX on these breast cancer cell lines was calculated as [(absorbance of test sample - absorbance of control)/control].

Flow cytometry-based measurement of apoptosis and necroptosis using Annexin-V-FITC/PI staining

Post the treatment of cells with different formulations, treated and control cells were collected and centrifuged at 1,200 rpm for 5 min. The supernatant was carefully removed without disturbing the cell pellet. The resulting cell pellet was resuspended in 100 µL of PBS buffer. For FACS analysis, one tube for each sample without staining was used for gating. The remaining tubes were stained with propidium iodide (PI) alone, FITC-Annexin-V alone or combination of PI and Annexin-V (Sigma-Aldrich A9210). All the tubes were incubated for 15 minutes at 4 centigrade degree. After 15 minutes of incubation, binding buffer was added to each tube and flow cytometry analysis (BD-Accuri, C6 Flow Cytometer) was performed (FITC with FL 1 dedector at 530/30 nm filter and PI with FL2 dedector at 585/42 nm). After appropriate gating, early apoptotic and late apoptotic/necrotic cells were identified using Annexin-V staining alone and a combination of Annexin-V and PI, respectively. The data for flow cytometry analysis was expressed as percentage calculated in comparison to the initial cell counts.

TUNEL and immunohistochemistry

For each cell line, cells were seeded in a 25 cc flask and treated with LC50 doses (obtained in the previous assay) for 24 or 48 hours (time and dose for each treatment are given in results section). The cells were collected in 15 mL tubes and centrifuged at rpm. The supernatant was carefully removed and the cells were fixed by the addition of methanol. After 24 hours, the cells were blocked for tissue monitoring and paraffin blocking was performed. Sections of 5 µm thickness were placed on positive-loaded slides.

The sections were incubated in an oven at 60 °C overnight. Further, the sections were deparaffinized with water and TdT labeling was performed using Biotin d-UTP kit (Genscript L00290) according to the manufacturer's protocol. The resulting sections were further stained with diaminobenzidine, while background staining was performed using hematoxylin. In order to calculate % apoptosis, the number of brown positive cells were counted per 5,000 cells and normalized for total cell count. The identification of apoptotic cells was performed on the basis of the presence of double chain fractures.

For immunohistochemistry analysis, the samples were treated with primary antibody for Ki-67 (Elabscience, e-pp-24636), caspase-3 (Bioss, Bs-0081R), caspase-8 (Bioss, Bs-0052R), and caspase-9 (Bioss, Bs-0049R) for 30 minutes. This was followed by treatment with anti-rabbit haptoglobin related protein secondary antibody at 1:200 dilution in automatic immunohistochemistry staining device (Ventana Discovery). The treatment with diaminobenzidine resulted in dark brown color. During analysis, positivity was used as the sole criteria, while sample intensity was not considered. Number of positive and negative cells were counted and percentage was calculated. For background staining hematoxylin dye was used. All sections showed positive cell counts, and cells and colonies were imaged using a light microscope (Olympus, Germany).

Statistical analysis

Data are represented as mean ± standard deviation. Statistical analysis was performed using SPSS 22.0 program. Nonparametric tests were used for analysis and the results of the study were considered statistically significant for p<0.05.

Results

Cell proliferation assay using WST-1

The effect of DOX dose and duration of treatment on cell viability was evaluated in three breast cancer cell lines using WST-1. Each cell line was treated with six different concentrations of DOX (0.5, 1.5, 2.5, 5, 10, and 20 µg/mL) for 24 and 48 hours. As shown in Figure 1, the effective near LC50 dose for 4T1, MCF-7, and MDA-MB-231 cells was found to be 1.5, 1.5, and 3 µg/ml, respectively. Both 4T1 and MDA-MB-231 cell lines showed LC50 time of 48 hours, while MCF-7 was characterized by LC50 time of 24 hours (Figure 1).

To evaluate the effect of LipoDOX on cell viability, all three cell lines were treated with seven different doses of LipoDOX (0.1, 0.25, 0.5, 0.75, 1, 1.5, and 2 µg/ml) and LC50 time and dose were calculated. The effective near LC50 time and dose for 4T1 cells was 48 hours and 1.5 µg/ml, respectively. In comparison to this, MCF-7 and MDA-MB-231 showed lower LC50 doses of 0.75 µg/ml and 0.25 µg/ml, respectively, which were observed at LC50 time of 24 and 48 hours, respectively (Figure 2).

Assessment of spherule number and diameter in 3D matrigel model

To assess the number and diameter of spherules formed, the cells were grown in 3D Matrigel and treated with optimized doses of DOX, LipoDOX, and DOX-loaded MBs. After 48 hours of treatment, spherule formation was evaluated using light microscopy. Spheroids displayed significant variability in terms of size, diameter, and numbers. In the control group, large size spheroids with ductus structures were observed. Interestingly, spheroids formed in case of MDA-MB-231 cell were smaller in size as compared to the spheroids for MCF-7. In comparison to these, most successful and dense spheroid formation was observed in 4T1 cells, where large of number of spheroids were formed. The treatment of all the cell lines with DOX resulted in significant decrease in spheroid diameters as compared to the control cells. These DOX treated spheroids showed significant necrosis and apoptosis. In case of DOX treated MCF-7 cells, spheroids were preserved, however, they were smaller size. A lower apoptosis rate was observed in MCF-7 cells as compared to other cell lines, which was in agreement with the aforementioned observation. In comparison to this, DOX treatment in MDA-MB-231 cells resulted in fewer number

of spheroids that showed apoptotic morphology. For all three cell lines included in the study, spherule counts and diameter were significantly reduced post administration of DOX and LipoDOX. Mean values for number and diameter of spherules observed for different treatment groups are summarized in Table 2. Figure 3 shows microscopic images of the 3D spherules formed for three breast cancer cell lines.

Technical Issues associated with 3D model studies

After successful development of 3D culture models for three cell lines, paraffin blocks were prepared and spheroid morphologies were assessed using hematoxylin-eosin staining. In Matrigel matrix (Corning, 354234), the cells formed a specific structure around the spheroids which was similar to connective tissue. The occasional occurrence of

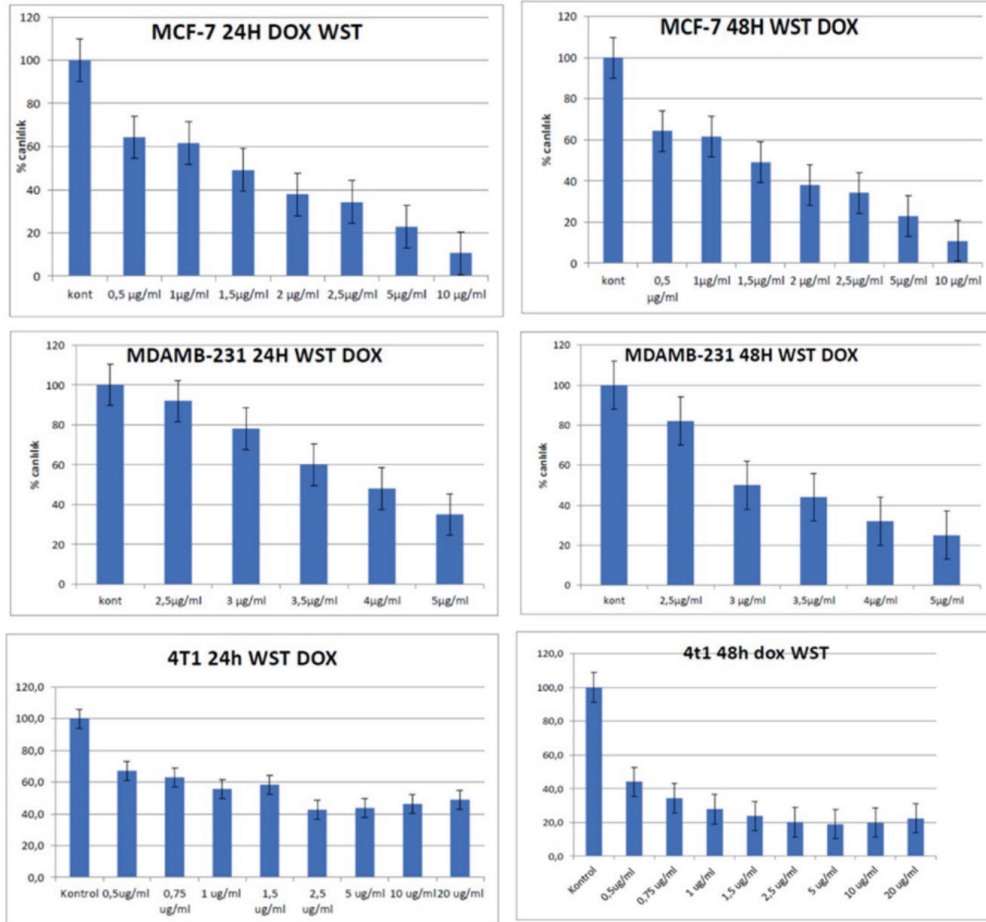


Figure 1. Doxorubicin WST-1 viability percentages compared with control in breast cancer cell lines. The effective near LD50 time and dose for 4T1 cells was 48 hours and 1.5 µg/ml, 24 hours and 1.5 µg/ml for MCF7 cells, 48 hours and 3 µg/ml for MDAMB-231 cells (p<0.05).

Table 2. Mean spherule number and diameters obtained in 3D cell culture model for three cancer cell lines. Mean spherule number and diameter were found to be reduced in DOX and LipoDOX treated groups as compared to control group, for all three cell lines (p<0.05)

3D Matrigel model	Mean spherule number	Standard derivation	Mean spherule diameter (µm)	Standard derivation
4T1 control	302	±18	306.2	±80.4
4T1 DOX	43	±8	104.4	±95.5
4T1 LipoDOX	82	±13	152.2	±46.2
MCF-7 control	338	±21	336.3	±90.1
MCF-7 DOX	182	±36	184.01	±50.8
MCF-7 LipoDOX	118	±42	227.04	±67.1
MDA-MB-231 control	286	±28	280.06	±120.8
MDA-MB-231 DOX	27	±7	76.21	±20.7
MDA-MB-231 LipoDOX	46	±15	117.01	±71.2

LipoDOX: Doxorubicin (DOX) entrapped in liposome; MB: Microbubbles

apoptotic objects in the center of the spheroids and ductus structures was quite significant, particularly in MCF-7. These observations provided evidence for the suitability of the structures formed in 3D cultures for breast cancer studies. The ductus structures were found to be located in the center of the spheroids.

In 4T1 cells, the number of spheroids were higher as compared to other two cell lines. The treatment of cells with DOX resulted in a reduction in spheroid diameters and cell counts per spheroid. However, the cell viability was found to be higher in 4T1 cells as compared to other cells in 3D model. Post DOX treatment, 4T1 cells in 3D model were characterized by disrupted and reduced ductus structures. All three cell lines exhibited high proliferation index in 3D cell cultures. However, the identification of 3D model proliferation index was difficult as compared to 2D cultures.

The treatment of cells with DOX-loaded MBs failed to produce any results. This was mainly attributed by rising of MBs to the surface that remained under the Matrigel and did not diffuse owing to their large size. DOX dissolved in the medium could easily diffuse through the pores of the Matrigel and bound to the cells; however, the spheroids formed above the Matrigel did not allow the transition of liposomes

and MBs into the pores. As a result, DOX-loaded MBs did not pass through the pores and failed to reach the cells. Therefore, DOX-loaded MBs were not included in the following proliferation and apoptosis experiments.

For all three cell lines, the decrease in mean spherule number and diameter upon treatment with DOX and LipoDOX was found to be statistically significant as studied using Mann-Whitney U test ($p < 0.05$).

Flow pattern findings

The flow experiments were successfully performed in 2D model; however, 3D model could not be used for flow pattern studies owing to the inability of the drug to enter the spherules. DOX and LipoDOX were successfully applied to the cells in 2D model. A model to perform shear stress formulation was adapted. Results for the same will be provided in our future studies. One of the aims of the flow experiments was to utilize ultrasound to burst the MBs near the cells. This would have allowed the release of DOX from the liposomes, while the formation of transient pores in the cells by sonoporation would have assisted in the passage of the drug molecules. However, the experiment could not be performed as the MBs added to the

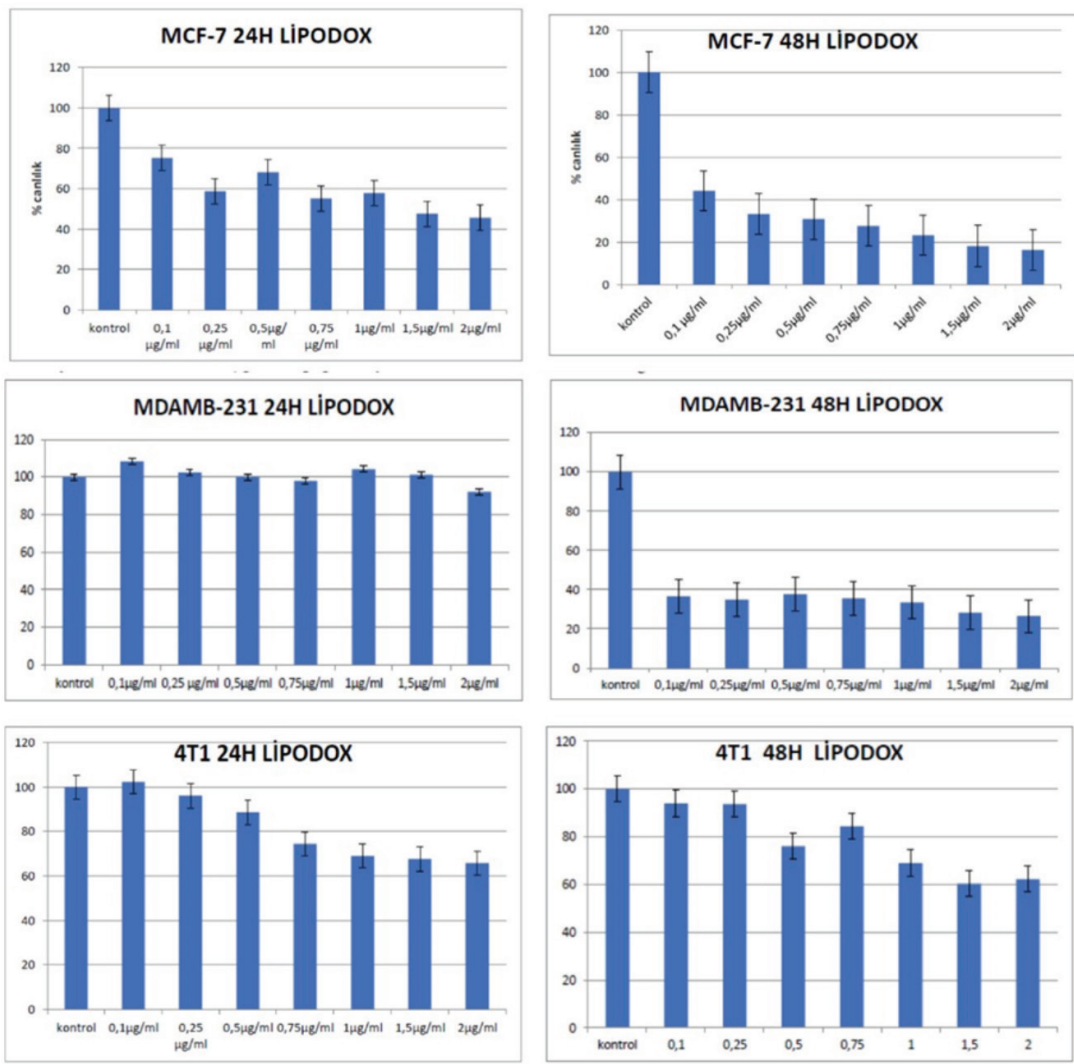


Figure 2. Liposomal-Doxorubicin WST-1 viability percentage compared with control in breast cancer cell lines. The effective near LD50 time and dose as 48 hours and 1.5 µg/ml for 4T1 cells, 24 hours and 0.75 µg/ml for MCF7 cells, 48 hours and 0.25 µg/ml for MDAMB-231 cells ($p < 0.05$).

medium for ultrasound destruction floated. As a result, these MBs did not contact the cells on the surface and failed to show any significant binding.

Apoptosis and necroptosis findings with flow cytometric Annexin-V-FITC/PI staining

The cells were treated with DOX and LipoDOX using the effective LC50 dose and time optimized in the previous experiments. Post treatment, the cells were collected, stained with Annexin-V-FITC/PI, and assessed using flow cytometry. The treatment of the three breast cancer cells with DOX and LipoDOX using optimized dose and incubation time resulted in the induction of cell death via necrosis (Table 3). For DOX treatment, the necrosis rate was found to be 95.5%–99.1%, while LipoDOX showed necrosis rate of 75.8%–87.4%. Mann-Whitney U analysis displayed statistically significant difference among control, DOX, and LipoDOX groups for all the cell lines ($p < 0.05$).

TUNEL and immunohistochemistry findings

In 3D model studies, terminal deoxynucleotidyl transferase dUTP nick end labeling (TUNEL) staining was used for the identification

of apoptosis in the cells. For 3D model of 4T1 cells, 3% and 35% apoptosis was observed in the control and DOX treated groups, respectively (Table 4). Similar increase in apoptosis was observed for MCF-7 cells with DOX treatment, where apoptosis of 5% and 25% was observed in the control and DOX treated cells, respectively. In case of MDA-MB-231 cells, DOX treatment resulted in an increase in apoptosis to 24%. The treatment of the cells with LipoDOX was also accompanied by an increase in apoptosis, however, the rate of apoptosis was low as compared to free DOX. The involvement of both extrinsic and intrinsic pathways in this DOX induced apoptotic effect could be deciphered by the evaluation of caspase expression. In addition to this, significant morphological changes along with necrosis were also observed in DOX treated cells. When the results of 3D and 2D models were compared, significant differences were observed in proliferation indices and caspase levels.

In 4T1 cells, mouse-derived progressive triple-negative breast cancer cells, Ki-67 analysis showed high proliferative activity of 80% which reduced to 27.2% after treatment with DOX. In case of 3D cultures for 4T1 cells, the expression of caspase-3, 8, and 9 increased by 20%, 40%, and 20%, respectively, as compared to the control cells. 2D cultures for MDA-MB-231 cells showed a reduction in

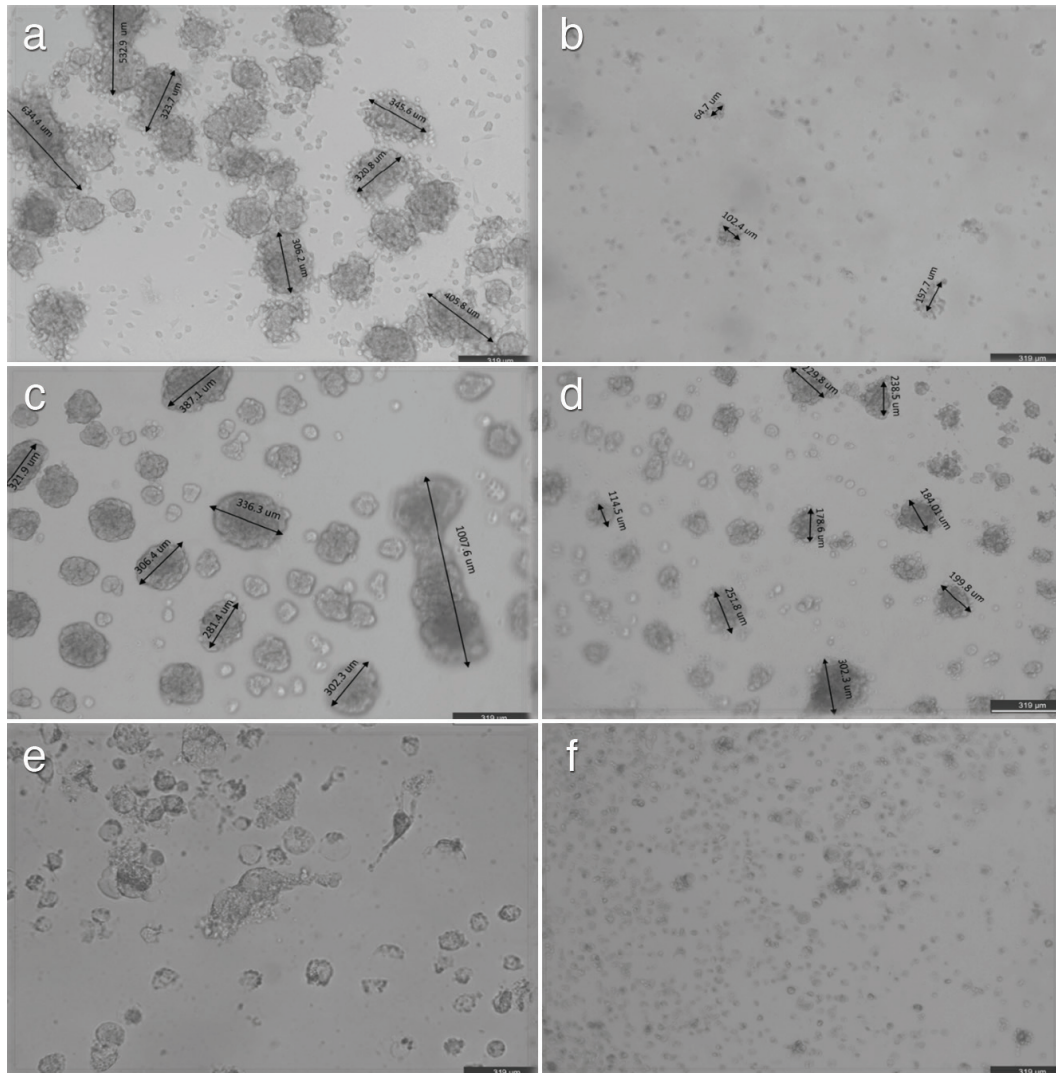


Figure 3. 3D Spherules in cell culture of **a)** Control 4T1 cells, **b)** DOX 4T1 cells; **c)** Control MCF7 cells, **d)** DOX MCF7 cells; **e)** control MDAMB231 cells and **f)** DOX MDAMB231 cells. Spherule number and diameters are prominently decreased in three cell lines after DOX incubation

3D: Three-dimensional; DOX: Doxorubicin

Ki-67 proliferation index from 98% to 13% upon treatment with DOX, while a significant increase was observed in the expression of caspase-3, 8, and 9. A comparative analysis for the three caspases showed maximum increase in case of caspase-8, indicating induction of both extrinsic and intrinsic pathways of apoptosis upon DOX treatment, but the activation of extrinsic pathway was comparatively higher.

In MDA-MB-231 cells, the activation of expression of caspase-3, 8, and 9 and reduction of proliferation index on DOX treatment was more significant as compared to 4T1 cells. These two cell lines are characterized by the presence of triple-negative breast cancer features. However, they differ in terms of their origin, one belongs to humans while the other is derived from mice. In human-derived MDA-MB-231 cells, DOX was found to be more effective in 2D cultures and its apoptosis-inducing effect was mediated via both extrinsic and intrinsic pathways. For MCF-7 cells, the increase in the expression

of caspase-3, 8, and 9 expressions was lower as compared to 4T1 and MDA-MB-231 cells.

In 3D spheroid model for 4T1 cell line, DOX treatment reduced Ki-67 proliferation index by 40%; however, the expression of caspase-3, 8, and 9 was higher in the control group. Higher expression of caspases in the control group of 3D models might be attributed to lower support provided by the Matrigel, which could have induced cell death in spheroids after certain duration owing to the absence of suitable vascularization. Additionally, identification of negative cells in terms of caspase expression within the spheroids indicated absence of any issue in immunohistochemical staining. In order to identify the apoptosis mechanism induced by DOX treatment, expression of caspase-3, 8, and 9 was evaluated, which are indicative of involvement of common apoptotic, extrinsic, and intrinsic pathways, respectively. Similar to 2D model studies, caspase-3, 8, and 9 were activated in 3D model for all three cells. However, in case of 3D model studies, the control groups

Table 3. Flow Cytometry results for the effect of DOX and LipoDOX treatment for three cancer cell lines used in the study. Both DOX and LipoDOX induced cell death majorly via necrosis for all three cell lines (p<0.05)

%	Viability AnnexinV-PI-	Early apoptosis AnnexinV +	Late apoptosis AnnexinV + PI +	Necrosis PI +
4T1 control	61.6	0.2	14.9	23.3
4T1 DOX	0.2	0.0	0.6	99.1
4T1 LipoDOX	21	2	1.2	75.8
MCF-7 control	46.8	0.3	1.3	51.6
MCF-7 DOX	2.0	0.0	2.7	95.3
MCF-7 LipoDOX	17.2	1	0.6	81.2
MDA-MB-231 control	78	0.0	5.6	16.4
MDA-MB-231DOX	1.5	0.3	8.4	89.8
MDA-MB-231 LipoDOX	4.6	2.8	5.2	87.4

Annexin-V (-) and PI (-) cells are indicative of viability, Annexin-V (+) PI (-) cells represent early apoptotic cells, Annexin-V (+) and PI (+) cells indicate late apoptotic cells, and only PI (+) cells are necrotic
LipoDOX: Doxorubicin (DOX) entrapped in liposome; MB: Microbubbles

Table 4. TUNEL and Immunohistochemistry results for 3D cell culture of breast cancer cell lines. Proliferation index was measured in terms of Ki-67, which decreased upon treatment of the cells with DOX and LipoDOX (p<0.05) as compared to the control, for all three cell lines used in the study. Activation of both intrinsic and extrinsic pathways was involved in the induction of apoptosis

%	TUNEL	Ki-67	Caspase-3	Caspase-8	Caspase-9
4T1 control	3	80	60	50	30
4T1 DOX	35	27	80	90	50
4T1 LipoDOX	23	50	100	100	85
MCF-7 control	5	80	30	49	20
MCF-7 DOX	25	19	60	82	81
MCF-7 LipoDOX	18	80	95	95	95
MDA-MB-231 control	6	98	36	21	21
MDA-MB-231 DOX	24	13	95	96	90
MDA-MB-231 LipoDOX	15	50	100	73	70

TUNEL: Terminal deoxynucleotidyl transferase dUTP nick end labeling; LipoDOX: Doxorubicin (DOX) entrapped in liposome; MB: Microbubbles

showed higher levels of expression for caspase-3, 8, and 9 as compared to 2D cultures. The treatment of MCF-7 cells with DOX resulted in 15% higher activation of caspase-3, 8, and 9 as compared to the control cells in 3D model. In addition to this, a 20% reduction in proliferation index was observed post DOX treatment. For MDA-MB-231 cells, DOX treatment in 3D cell cultures resulted in a lower reduction in the proliferative index as compared to 2D model. In 3D model studies, the proliferation index for all three cell lines was observed to reduce after DOX treatment. This reduction in proliferation for 3D models was low as compared to the reduction observed in 2D cell culture models. Thus, all these results are indicative of the reduction in intracellular diffusion of DOX in 3D cell culture model, which further highlights the suitability of 3D cell cultures for drug efficacy studies.

Discussion and Conclusion

2D cell culture models generally fail to mimic true *in vivo* tumor conditions (17, 18). In addition to this, 2D models generate very limited knowledge regarding the therapeutic efficacy of chemotherapeutic drugs. These limitations can be overcome by the use of 3D cell culture models. In comparison to 2D cultures, 3D cell culture models mimic *in vivo* tumor microenvironment in a much better way (17, 19). Several previous studies have reported significant differences in the results obtained for 2D and 3D cell culture models, particularly for the expression of various proteins and effects of chemotherapeutic drugs (19, 20). Similar results were obtained in the present study, where the expression of Ki-67, caspase-3, caspase-8, and caspase-9 in 2D cell cultures was comparatively low as compared to their 3D counterparts, irrespective of the cell line used for the evaluation.

In the present study, DOX and LipoDOX showed better 2D and 3D efficacy with increase in dose, for all the three cell lines studied. The observed change in efficacy was induced by the activation of apoptosis, particularly via induction of caspase-8. This was accompanied by a decrease in proliferative activity and viability in the 3D model, where significant reduction was observed in three-dimensional growth of the tumor cells. Moreover, the effective doses of LipoDOX required for the induction of cell proliferation inhibition and cell death were comparatively low as compared to free DOX, for all breast cancer cell lines used in the study. Thus, all these results suggest that lower doses of DOX would be safe for healthy cells, while ensuring effective inhibition of growth in breast cancer cells.

In the present study, the results obtained from the imaging studies highlighted the suitability of 3D cultures for breast cancer studies. In Matrigel matrix, the cells formed a structure similar to connective tissue around the spheroids. The occasional occurrence of apoptotic objects in the center of the spheroids and ductus structures was quite significant, especially in MCF-7 cells. These results were in agreement with a previous study, where establishment of spheroid like 3D model of breast cancer cell lines was associated with lower sensitivity toward chemotherapeutic drugs (18). These structures provided evidence for the suitability of the structures formed in 3D cultures for breast cancer studies.

In the present study, when spheroid structures were formed in 3D Matrigel model, DOX showed very limited diffusion into the cells, which was similar to *in vivo* conditions. Such a situation might be one of the responsible for the requirement of repeated administration of DOX at certain intervals under *in vivo* conditions. DOX showed antiproliferative and apoptosis-inducing effect in both 2D and 3D

models for all three cell lines used in the study; however, this effect was quite variable among the three cell lines. These findings might preclinically reflect the difference in treatment responses observed in different individuals diagnosed with same cancer type. This further highlights the importance of personalized therapy for cancer treatment.

The present study was associated with certain limitations. In 3D models, great difficulty was witnessed while evaluating proliferation of spheroids using absorbance-based WST-1. Thus, trypan blue staining might be more effective and reliable for testing viability of spheroids in 3D cell culture models. Since DOX is characterized by absorbance maxima of 480 nm, it might interfere with the absorbance-based measurements performed using WST-1.

In the present study, the effects of DOX and LipoDOX treatment on three different breast cancer cell lines were investigated in 2D and 3D cell culture models. Both drug formulations were found to be effective in all three breast cancer cells tested. The currently used strategies mainly focus on utilizing tumor targeting drug delivery vehicles to ensure local delivery of the drugs to the tissue of interest. Such targeted delivery minimizes the side effects and improves the antitumoral effect of the drug. In the present study, DOX-loaded MBs were targeted to the tumor cells by Epidermal growth factor receptor (EGFR); however, *in vitro* flow experiments could not be performed owing to the buoyancy of the MBs. The results for the antitumoral effects of DOX and LipoDOX obtained in the present study have laid down the foundation of a future study that will focus on the development of liposomal DOX-MB complex targeted specifically to breast cancer using EGFR. This study will also evaluate the local delivery of DOX in mouse model both in the presence and absence of ultrasound. Thus, the present study provided a suitable method for the evaluation of anti-proliferative and anti-apoptotic effects of liposomal doxorubicin in 3D cell culture models with different types of breast cancer cells.

Acknowledgements

This study was supported by Dokuz Eylül University Scientific Research Commission with project number 2018.KB.SAG.033. The flow experiments and MB production stages of the project were completed within the scope of the Scientific and Technological Research Council of Turkey: TÜBİTAK (project no: 213M668).

Ethics Committee Approval: This study was approved by Dokuz Eylül University, Noninvasive Ethics Committee (date: 09.11.2020, no: 2017/26-22).

Informed Consent: This study is done on cell lines so that it does not require consent form

Peer-review: Externally peer-reviewed.

Author Contributions

Conception: M.A., S.A.; Design: S.A., S.K.; Supervision: S.A., E.O., S.K.; Resources: M.A., S.A., E.O., Z.A., S.K.; Data Collection and/or Processing: M.A., S.A., S.K.; Analysis and/or Interpretation: M.A., S.A., S.K.; Literature Search: M.A., S.A., Z.A., S.K.; Writing Manuscript: M.A., S.A., Z.A., S.K.; Critical Review: S.A., S.K.O, E.O.

Conflict of Interest: The authors have no conflicts of interest to declare.

Financial Disclosure: This study was supported by Dokuz Eylül University Scientific Research Commission with project number: 2018.KB.SAG.033. The flow experiments and MB production stages of the project were completed within the scope of TÜBİTAK (project no: 213M668).

References

1. Mahvi DA, Liu R, Grinstaff MW, Colson YL, Raut CP. Local cancer recurrence: the realities, challenges, and opportunities for new therapies. *CA Cancer J Clin* 2018; 68: 488-505. (PMID: 30328620) [\[Crossref\]](#)
2. Narod SA. Personalised medicine and population health: breast and ovarian cancer. *Hum Genet* 2018; 137: 769-778. (PMID: 30328515) [\[Crossref\]](#)
3. Maffini MV, Soto AM, Calabro JM, Ucci AA, Sonnenschein C. The stroma as a crucial target in rat mammary gland carcinogenesis. *J Cell Sci* 2004; 117: 1495-1502. (PMID: 14996910) [\[Crossref\]](#)
4. Smalley M, Piggott L, Clarkson R. Breast cancer stem cells: obstacles to therapy. *Cancer Lett* 2013; 338: 57-62. (PMID: 22554712) [\[Crossref\]](#)
5. Cochran MC, Eisenbrey J, Ouma RO, Soulen M, Wheatley MA. Doxorubicin and paclitaxel loaded microbubbles for ultrasound triggered drug delivery. *Int J Pharm* 2011; 414: 161-170. (PMID: 21609756) [\[Crossref\]](#)
6. Yan F, Li L, Deng Z, Jin Q, Chen J, Yang W, et al. Paclitaxel-liposome-microbubble complexes as ultrasound-triggered therapeutic drug delivery carriers. *J Control Release* 2013; 166: 246-255. (PMID: 23306023) [\[Crossref\]](#)
7. Vail DM, Amantea MA, Colbern GT, Martin FJ, Hilger RA, Working PK. Pegylated liposomal doxorubicin: proof of principle using preclinical animal models and pharmacokinetic studies. *Semin Oncol* 2004; 31: 16-35. (PMID: 15717736) [\[Crossref\]](#)
8. Harris L, Batist G, Belt R, Rovira D, Navari R, Azarnia N, et al. Liposome-encapsulated doxorubicin compared with conventional doxorubicin in a randomized multicenter trial as first-line therapy of metastatic breast carcinoma. *Cancer* 2002; 94: 25-36. (PMID: 11815957) [\[Crossref\]](#)
9. Bush N, Healey A, Shah A, Box G, Kirkin V, Eccles S, et al. Theranostic attributes of acoustic cluster therapy and its use for enhancing the effectiveness of liposomal doxorubicin treatment of human triple negative breast cancer in mice. *Front Pharmacol* 2020; 11: 75. (PMID: 32153400) [\[Crossref\]](#)
10. Pothuri B, Brodsky AL, Sparano JA, Blank SV, Kim M, Hershman DL, et al. Phase I and pharmacokinetic study of veliparib, a PARP inhibitor, and pegylated liposomal doxorubicin (PLD) in recurrent gynecologic cancer and triple negative breast cancer with long-term follow-up. *Cancer Chemother Pharmacol* 2020; 85: 741-751. (PMID: 32055930) [\[Crossref\]](#)
11. Zhao T, Zhou H, Lei L, Guo C, Yang Q, Gong T, et al. A new tandem peptide modified liposomal doxorubicin for tumor "ecological therapy". *Nanoscale* 2020; 12: 3359-3369. (PMID: 31984408) [\[Crossref\]](#)
12. Navashenaq JG, Zamani P, Nikpoor AR, Tavakkol-Afshari J, Jaafari MR. Doxil chemotherapy plus liposomal P5 immunotherapy decreased myeloid-derived suppressor cells in murine model of breast cancer. *Nanomedicine* 2020; 24: 102150. doi: 10.1016/j.nano.2020.102150 (PMID: 31931230) [\[Crossref\]](#)
13. Cao D, Zhang X, Akabar MD, Luo Y, Wu H, Ke X, et al. Liposomal doxorubicin loaded PLGA-PEG-PLGA based thermogel for sustained local drug delivery for the treatment of breast cancer. *Artif Cells Nanomed Biotechnol* 2019; 47: 181-191. (PMID: 30686051) [\[Crossref\]](#)
14. Lin CY, Li JR, Tseng HC. Enhancement of focused ultrasound with microbubbles on the treatments of anticancer nanodrug in mouse tumors. *Nanomedicine* 2012; 8: 900-907. (PMID: 22033084) [\[Crossref\]](#)
15. Tinkov S, Coester C, Serba S, Geis NA, Katus HA, Winter G, et al. New doxorubicin-loaded phospholipid microbubbles for targeted tumor therapy: in-vivo characterization. *J Control Release* 2010; 148: 368-372. (PMID: 20868711) [\[Crossref\]](#)
16. Onercan C. Development of ultrasound triggered drug delivery systems for cancer treatment. Izmir Institute of Technology, Master Thesis, Turkey, 2019. [\[Crossref\]](#)
17. Weigelt B, Ghajar CM, Bissell MJ. The need for complex 3D culture models to unravel novel pathways and identify accurate biomarkers in breast cancer. *Adv Drug Deliv Rev* 2014; 69-70: 42-51. (PMID: 24412474) [\[Crossref\]](#)
18. Imamura Y, Mukohara T, Shimono Y, Funakoshi Y, Chayahara N, Toyoda M, et al. Comparison of 2D- and 3D-culture models as drug-testing platforms in breast cancer. *Oncol Rep* 2015; 33: 1837-1843. (PMID: 25634491) [\[Crossref\]](#)
19. Lee JM, Mhawech-Fauceglia P, Lee N, Parsanian LC, Lin YG, Gayther SA, et al. A three-dimensional microenvironment alters protein expression and chemosensitivity of epithelial ovarian cancer cells in vitro. *Lab Invest* 2013; 93: 528-542. (PMID: 23459371) [\[Crossref\]](#)
20. Vinci M, Gowan S, Boxall F, Patterson L, Zimmermann M, Court W, et al. Advances in establishment and analysis of three-dimensional tumor spheroid-based functional assays for target validation and drug evaluation. *BMC Biol* 2012; 10: 29. (PMID: 22439642) [\[Crossref\]](#)



Treatment Results of Intralesional Steroid Injection and Topical Steroid Administration in Pregnant Women with Idiopathic Granulomatous Mastitis

Osman Toktas¹, Nurşen Toprak²

¹Department of Surgery, Van Yüzüncü Yıl University Faculty of Medicine, Van, Turkey

²Department of Radiology, Van Yüzüncü Yıl University Faculty of Medicine, Van, Turkey

ABSTRACT

Objective: Idiopathic granulomatous mastitis (IGM) is an inflammatory and chronic benign breast disease that has proven difficult to diagnose and treat. Since most treatment modalities cannot be used in pregnant patients, the choice of treatment is more difficult and the need for surgery is more pressing. In this first and innovative study, we assess the results of local corticosteroid therapy of IGM in pregnant women.

Materials and Methods: Pregnant women with IGM were evaluated between June 2017 and May 2019. The six pregnant women were treated using intralesional steroid injections and topical steroid administration. The treatment response was evaluated, both clinically and radiologically, at the end of 2 weeks and once more at the end of 1 month.

Results: The median patient age was 26 years. The mean duration of complaints was 4.3 months. The median number of children was 2, and the mean breastfeeding time was 41 months. The predominant complaints at onset were a breast mass or local pain and inflammation in four (66.7%) patients and a breast mass with pain and without signs of local skin inflammation in two (33.3%) patients. Diagnosis was made using a tru-cut biopsy in two patients, and with an incisional biopsy in four patients who had abscess drainage and fistulation to the skin. Five (83.3%) patients achieved a complete response, and one (16.7%) patient responded only partially after the first course of treatment. A second course of treatment was given to the patient with partial response. All patients achieved complete response at the end of the second course of treatment. The mean follow-up time was 19.5 months. During the follow-up period, one patient experienced a recurrence at 4 months after giving birth, and she then received a third course of treatment. Topical and systemic side effects of the corticosteroids were not observed in any patient.

Conclusion: While the state of pregnancy generally precludes the use of most drugs, the use of local corticosteroid in the treatment of IGM is effective in terms of treatment response, treatment duration, need for surgery, and reduced recurrence and side effects.

Keywords: Idiopathic granulomatous mastitis, pregnant women, steroid injection, topical steroid

Cite this article as: Toktas O, Toprak N. Treatment Results of Intralesional Steroid Injection and Topical Steroid Administration in Pregnant Women with Idiopathic Granulomatous Mastitis. Eur J Breast Health 2021; 17(3): 283-287

Key Points

- There is no consensus on the optimal treatment of IGM since its etiology is presently unknown due to insufficient case series and lack of prospective studies.
- Idiopathic granulomatous mastitis (IGM) is an inflammatory and chronic benign disease of the breast, which has long proven difficult to diagnose and treat. Since most treatment modalities cannot be used in pregnant patients, choice of treatment is more difficult.
- Pregnant women who were diagnosed with IGM and received treatment with local corticosteroids with at least 12 months of follow-up were included in the study. For patients treated with local steroids, protocol included an intralesional 40 mg methylprednisolone injection into the breast skin affected by mastitis and administration of topical 0.125% prednisolone twice a day, on alternate days, for 4 weeks.
- While pregnancy argues against the use of many drugs, the use of local corticosteroid in the treatment of IGM is effective in terms of response to treatment, duration of treatment, need for surgery, and reduced recurrence and side effects.

Introduction

Idiopathic granulomatous mastitis (IGM) is a benign inflammatory disorder and rare cause of chronic mastitis. There is no consensus on the optimal treatment of IGM, since its etiology is presently unknown given insufficient case series and lack of prospective studies (1). Antibiotic, corticosteroid, immunosuppressant, methotrexate, colchicine, and surgical treatment modalities have been previously used in IGM treatment. However, at present, since many medical treatments cannot be used in pregnant patients with IGM, corticosteroid and surgery are the most commonly used treatment modalities (2-4). Surgery carries with it cosmetic and healing problems; by contrast, long-term and high-dose use of corticosteroid has side effects (5, 6). Some recent studies have used steroids locally. These studies have shown that local corticosteroid was effective, better tolerated, and caused fewer side effects. In addition, studies have shown that steroid therapy results in faster recovery than expectant management and other systemic treatment (1, 4, 5). In this study, intralesional steroid injections with concomitant topical steroids are assessed in the treatment of IGM in pregnant women.

Materials and Methods

Data collected between June 2017 and May 2019 were analyzed retrospectively. Pregnant patients who visited the breast clinic with complaints of a breast mass, breast pain, and/or local erythema were evaluated clinically and radiologically. Patients with suspected IGM underwent core needle and incisional biopsy depending on their clinical presentation. The diagnosis of IGM was made histopathologically. In the histopathological diagnosis of each patient, infectious granulomatous mastitis agents were, excluded based on the results of Gram, periodic-acid-Schiff, Ehrlich-Ziehl-Neelsen, and Giemsa staining. Pregnant women who were diagnosed with IGM and received local corticosteroid treatment with at least 12 months of follow-up were included in the study. For patients treated with local steroids, the protocol included intralesional injection of 40 mg methylprednisolone (Prednol-L 40 mg ampule; Mustafa Nevzat Pharmaceuticals, İstanbul, Turkey) into the breast skin affected by mastitis and topical administration of 0.125% prednisolone (Prednol-a30 gr pomade; Mustafa Nevzat Pharmaceuticals, İstanbul, Turkey) twice a day, on alternate days, for 4 weeks. Patients who have diffuse disease, by which lesions cover more than two quadrants of the breast, received injection at different points at 5 cm intervals. In patients with multiple lesions, if lesions were more than 5 cm apart, lesions were injected separately, and if the lesions were less than 5 cm apart, the larger one was injected.

Patients with recurrent disease, patients for whom use of corticosteroids was contraindicated, and patients aged <18 years were excluded from the study. Patients were followed up to assess treatment results. Treatment responses were evaluated both clinically and radiologically after 2 weeks and again after 1 month. The responses were categorized as "complete response," "partial response," "no response," or "worsening disease." Patients with "complete response" were assigned follow-up, while patients with "partial response," "no response," or "worsening disease" received the second and, if necessary, third courses of treatment with monthly check-ups until the disease completely resolved (Figures 1a and b). Surgical treatment was a second option for all patients who clinically required or preferred surgery during follow-up.

This study was approved by the Local Ethics Committee of Yüzüncü Yıl University, Van, Turkey, with the registration number of 2020/04-33. Informed consent was received from each patient.

Results

Six women in their third trimester of pregnancy were included in the study. The disease localized bilaterally in one patient, in the left breast in three patients, and in the right breast in two patients. The mean patient age was 26 (range: 23–33) years. None of the patients had comorbid medical condition, but one patient had a history of smoking. The mean duration of complaints was 4.3 months. While the mean number of children was 2 (range: 2–5), the mean breastfeeding time was 41 (range, 24–72) months. Predominant complaints at onset were a breast mass with local pain and inflammation in four (66.7%) patients and a breast mass with pain and without signs of local skin inflammation in two (33.3%) patients. Diagnosis was made by using core biopsy in two (33.3%) patients and by an incisional biopsy in four (66.7%) patients. Abscess drainage was performed in four (66.7%) patients, and these patients had fistulation to the skin. All patients had used antibiotics. While ultrasonography (USG) was used in all patients, both USG and magnetic resonance imaging were employed in two patients.

Five (83.3%) patients achieved a complete response, and one patient (16.7%) achieved a partial response after the first course of the treatment. A second course of treatment was given to the patient with

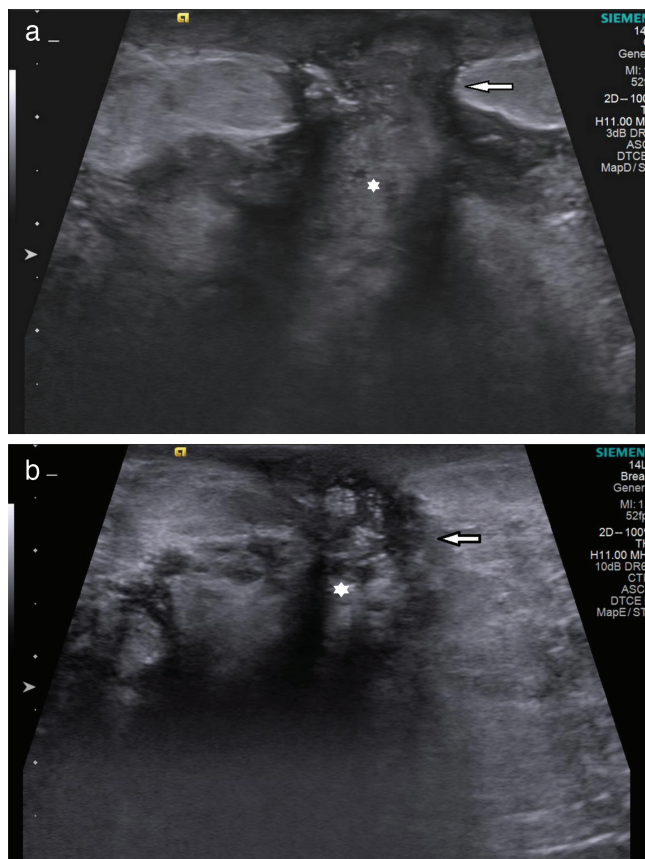


Figure 1. Fistula tract (white arrow) and abscess associated with fistula (white star) before treatment (a), significant regression in the fistula tract (white arrow) and abscess (white star) after treatment (b). (B-mode USG)

USG: Ultrasonography

partial response. Complete response was achieved by all patients at the end of the second course of treatment (Figures 2a and b). One patient had a recurrence during follow-up at 4 months after delivery, and a third course was administered to this patient. The mean follow-up time was 19.5 months. Neither topical nor systemic side effects of corticosteroids were observed in any patient. Patients and their clinical characteristics are shown in the accompanying table (Table 1).

Discussion and Conclusion

IGM is characterized by non-caseating chronic granulomatous lobules in which microorganisms are absent. Causes include local trauma, extravasated secretions, underlying auto-immune process, or damage to the ductal epithelium of an unknown infective etiology. This process is thought to induce a localized immune response that may elicit a local granulomatous response. (4, 7) Uncertainty over the exact cause

of IGM leads to a lack of clear consensus in its treatment. Research on the treatment of IGM indicates that corticosteroids and surgery are predominantly used in IGM treatment (8-10). Since the literature indicates that the number of pregnant women with IGM is low, there is little information about the effectiveness of IGM treatment in pregnant women. A few case reports described pregnant women with IGM who received oral prednisone (4, 11, 12). By contrast, the present study focused on the assessment of the effect of topical corticosteroid on IGM in pregnant women.

Recurrence rates would likely be higher after limited excision; by contrast, wide local excision may lead to poor cosmetic results. Therefore, surgery should be reserved for recurrent disease or disease unresponsive to medical therapy (4). Many medical treatment modalities cannot be used during pregnancy, with the result that surgery is used more frequently in these patients (11-14). Among the six patients, abscess drainage and incisional biopsy were performed in four patients. In these patients, postoperative wound healing required considerable time; in three patients with abscess drainage, recovery took approximately 4 weeks.

Corticosteroids cause significant regression in breast mass and skin lesions, but high-dose and long-term use of corticosteroids has side effects. Topical corticosteroids are used because of their anti-inflammatory, vasoconstrictor, antiproliferative, and immunosuppressive properties in treating various skin diseases. In addition, corticosteroid has been used in pregnant women for rheumatoid arthritis, lupus, antiphospholipid syndrome, and risk of miscarriage (15, 16). In our study, which compared the results of treatment with topical and systemic steroids as described in the literature, patients treated with topical steroids had a shorter duration of treatment, had fewer steroid-related side effects, had less need for surgery, and had lower recurrence rates than systemic steroids (1).

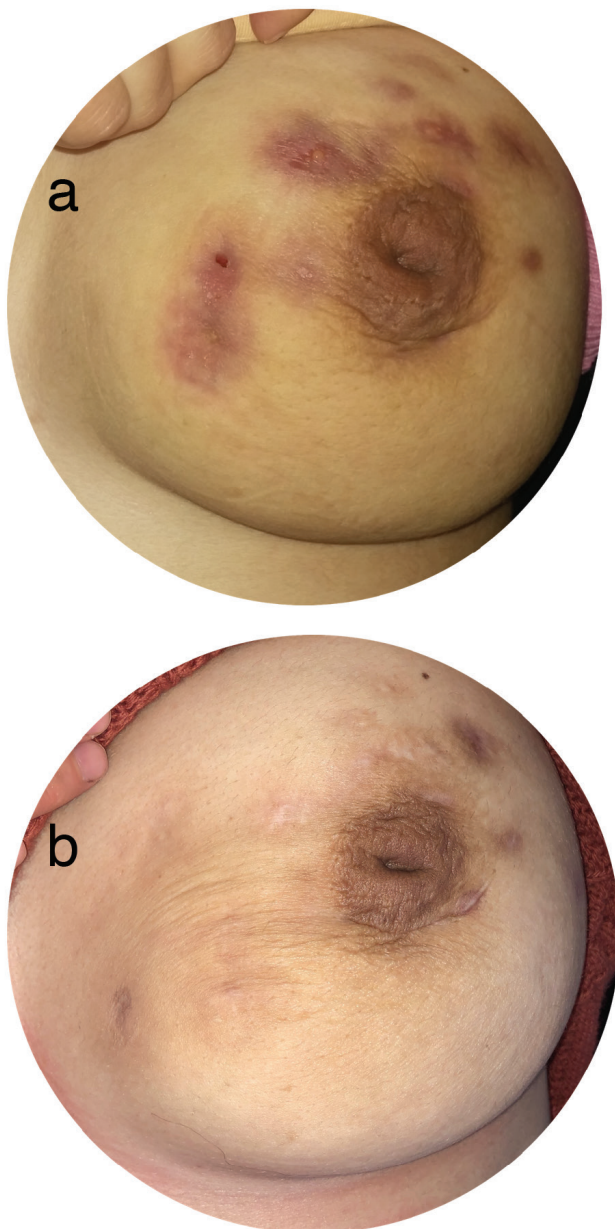


Figure 2. Widespread inflammation in the upper and inner quadrants of the left breast and multiple fistula orifices on the skin, before treatment (a), after treatment (b)

Table 1. Descriptive properties

	n (%/range)	
Mean age	26 (23–33)	
Mean duration of complaints (month)	4.3 (2–6)	
Mean number of children	2 (2–5)	
Mean breast-feeding time (month)	41 (24–72)	
Localization	Left	3 (50)
	Right	2 (33.4)
	Bilateral	1 (16.6)
Main complaint at onset	Breast mass with local pain and inflammation	4 (66.7)
	Breast mass and pain without inflammation	2 (33.3)
Diagnosis	Tru-cut	2 (33.3)
	Incisional	4 (66.7)
Treatment response	Complete	5 (83.3)
	Partial	1 (16.7)
Mean follow-up time (month)	19.5 (14–28)	

n: Number

Use of topical steroid in the treatment of IGM was also assessed in other studies (8, 11, 17-19). Cetin et al. (8) showed no significant difference between the efficacy rates of topical and systemic steroid treatment. Altintoprak et al. (17) showed that clinical improvement occurred within an average of 8.2 weeks in IGM treated with topical steroids, with a long-term success rate of >90% during a mean follow-up duration of 37.2 months. No topical steroid-related side effects were reported during the treatment period.

Goldberg et al. (11) reported that pregnant women with IGM did not respond to 5-week antibiotic treatment and low-dose oral corticosteroid treatment, and the breast mass remained stable until delivery. Breast lesions improved within 2 months with 60 mg corticosteroid prescribed daily postpartum.

Goulabchand et al. (20) treated a 32-week pregnant woman with IGM with antibiotics, but the symptoms persisted until delivery. After 1 month of breastfeeding, breast inflammation aggravated. Breastfeeding was stopped, and corticosteroid treatment was started. After a few months, complete resolution of wounds was achieved, and corticosteroids were tapered and ultimately stopped. Complete remission was observed during early follow-up. Boukaidi et al. (21) used a number of treatment modalities in treating pregnant patients with IGM, including antibiotherapy with nonsteroidal anti-inflammatory drugs, progestogens, vein tonicity drugs, and bromocriptine. Notwithstanding, they could not cure the disease, short of terminating the pregnancy, and used corticosteroids.

Garcia-Rodriguez et al. (2) reported the case of a patient in her 11th week of pregnancy. At the time, the patient's breast mass measured 3 cm, but measured 12 cm after 10 days. As the patient's pain became intolerable, she was hospitalized twice over 1.5 months. The patient also consulted with other clinics, among them internal medicine, emergency medicine, general surgery, gynecology, and infectious diseases. The patient was treated sequentially with clindamycin, cefazolin, vancomycin, piperacillin-tazobactam combination, ceftriaxone, and metronidazole. She showed no improvement, and narcotics were required to control her pain. After the first dose of vancomycin, the patient developed symptoms of the "red man" syndrome. She also had an allergic reaction to clindamycin. Further bacterial cultures, fungal cultures, and tuberculosis cultures and stains proved negative. After the diagnosis of IGM, the woman was treated with 20 mg prednisone four times daily, and symptoms were improved subsequently. Because of worsening symptoms, treatment options were re-evaluated by a multidisciplinary team, and mastectomy was recommended 1 month after delivery, but the patient did not accept the decision.

All the aforementioned studies show clearly the challenge of treating pregnant patients with IGM. In our study, we used intralesional injection of 40 mg methylprednisolone and topical administration of 0.125% prednisolone pomade. Within 2 months after treatment, complete remission was apparent in all our patients. Treating patients with topical corticosteroid has the following advantages: stress reduction, increased patient compliance, and a reduction in the cost of treatment. No side effects related to steroids were observed in either the mother or baby. Patients showed no problems with breastfeeding after birth. Moreover, no negative cosmetic results, which are common in repeated surgeries, were observed. Our patients' compliance and satisfaction with this topical steroid treatment, in which only two drugs were used for a short time, were highly encouraging.

In conclusion, the treatment discussed should be considered the first course of action to the treatment of IGM in pregnant women due to the relative ease in delivering a steroid injection and applying topical steroid pomade, more positive response seen in a relatively short time, high patient compliance with treatment, and lower rates of side effects and recurrence.

Ethics Committee Approval: This study was approved by the Local Ethics Committee of Yüzüncü Yıl University, Van, Turkey, with the registration number of 2020/04-33.

Informed Consent: Informed consent was received from each patient.

Peer-review: Externally and internally peer-reviewed.

Conflict of Interest: The authors declare that there are no potential conflicts of interest with respect to the research, authorship, and/or publication of this article.

Financial Disclosure: The authors received no financial support for the research, authorship, and/or publication of this article.

Authorship Contributions

Surgical and Medical Practices: O.T.; Conception: O.T., N.T.; Design: O.T., N.T.; Data Collection and/or Processing: O.T., N.T.; Analysis and/or Interpretation: O.T., N.T.; Literature Search: O.T.; Writing: O.T., N.T.

References

1. Toktas O, Konca C, Trabulus DC, Soyder A, Koksall H, Karanlik H. et al. A novel first-line treatment alternative for noncomplicated idiopathic granulomatous mastitis: combined intralesional steroid injection with topical steroid administration. *Breast Care* 2021; 16: 181-187. [[Crossref](#)]
2. Garcia-Rodriguez JA, Pattullo A. Idiopathic granulomatous mastitis: a mimicking disease in a pregnant woman: a case report. *BMC Research Notes* 2013; 6: 95. (PMID: 23497626) [[Crossref](#)]
3. Ocal K, Dag A, Turkmenoglu O, Kara T, Seyit H, Konca K. Granulomatous mastitis: clinical, pathological features, and management. *Breast J* 2010; 16: 176-182. (PMID: 20030652) [[Crossref](#)]
4. Gunduz Y, Altintoprak F, Ayhan TL, Kivilcim T, Celebi F. Effect of topical steroid treatment on idiopathic granulomatous mastitis: clinical and radiologic evaluation. *Breast J* 2014; 20: 586-591. (PMID: 25228089) [[Crossref](#)]
5. Alper F, Karadeniz E, Guven F, Cenkaya BY, Ozden K, Akcay MN. The evaluation of the efficacy of local steroid administration in idiopathic granulomatous mastitis: The preliminary results. *Breast J* 2020; 26: 309-311. (PMID: 31495032) [[Crossref](#)]
6. Mizrakli T, Velidedeoglu M, Yemisen M, Mete B, Kilic F, Yilmaz H. et al. Corticosteroid treatment in the management of idiopathic granulomatous mastitis to avoid unnecessary surgery. *Surg Today* 2015; 45: 457-465. (PMID: 24993812) [[Crossref](#)]
7. Bani-Hani KE, Yaghan RJ, Matalka I, Shatnawi NJ. Idiopathic granulomatous mastitis: time to avoid unnecessary mastectomies. *Breast J* 2004; 10: 318-322. (PMID: 15239790) [[Crossref](#)]
8. Cetin K, Sikar HE, Goret NE, Rona G, Barisik ON, Kucuk HF. et al. Comparison of topical, systemic, and combined therapy with steroids on idiopathic granulomatous mastitis: a prospective randomized study. *World J Surg* 2019; 43: 2865-2873. (PMID: 31297582) [[Crossref](#)]
9. Barreto DS, Sedgwick EL, Nagi CS, Benveniste AP. Granulomatous mastitis: etiology, imaging, pathology, treatment, and clinical findings. *Breast Cancer Res Treat* 2018; 171: 527-534. (PMID: 29971624) [[Crossref](#)]

10. Lei X, Chen K, Zhu L, Song E, Su F, Li S. Treatment for idiopathic granulomatous mastitis: systemic review and meta-analysis. *Breastfeed Med* 2017; 12: 415-421. (PMID: 28731822) [\[Crossref\]](#)
11. Goldberg J, Baute L, Storey L, Park P. Granulomatous mastitis in pregnancy. *Obstet Gynecol* 2000; 96: 813-815. (PMID: 11094217) [\[Crossref\]](#)
12. Destek S, Gul OV. Idiopathic granulomatous mastitis: a disease mimics breast cancer appearing in pregnancy. *Gen Surg: Open Access* 2018; 1: 7-10. [\[Crossref\]](#)
13. Yabanoglu H, Colakoglu T, Belli S, Aytac HO, Bolat FA, Pourbager A. et al. A comparative study of conservative versus surgical treatment protocols for 77 patients with idiopathic granulomatous mastitis. *Breast J* 2015; 21: 363-369. (PMID: 25858348) [\[Crossref\]](#)
14. Skandarajah A, Marley L. Idiopathic granulomatous mastitis: a medical or surgical disease of the breast? *ANZ J Surg* 2015; 85: 979-982. (PMID: 25424519) [\[Crossref\]](#)
15. Palmsten K, Rolland M, Hebert MF, Clowse MEB, Schatz M, Xu R. et al. Patterns of prednisone use during pregnancy in women with rheumatoid arthritis: Daily and cumulative dose. *Pharmacoepidemiol Drug Saf* 2018; 27: 430-438. (PMID: 29488292) [\[Crossref\]](#)
16. Empson MB, Lassere M, Craig JC, Scott JR. Prevention of recurrent miscarriage for women with antiphospholipid antibody or lupus anticoagulant. *Cochrane Database Syst Rev* 2005; 2005: CD002859. doi: 10.1002/14651858.CD002859.pub2 (PMID: 15846641) [\[Crossref\]](#)
17. Altintoprak F, Kivilcim T, Yalkin O, Uzunoglu Y, Kahyaoglu Z, Dilek ON. Topical steroids are effective in the treatment of idiopathic granulomatous Mastitis. *World J Surg* 2015; 39: 2718-2723. (PMID: 26148520) [\[Crossref\]](#)
18. Altintoprak, F, Kivilcim T, Ozkan OV. Aetiology of idiopathic granulomatous mastitis. *World J Clin Cases* 2014; 2: 852-858. (PMID: 25516860) [\[Crossref\]](#)
19. Karanlik H, Ozgur I, Simsek S, Fathalizadeh A, Tukenmez M, Sahin D. et al. Can steroids plus surgery become a first-line treatment of idiopathic granulomatous mastitis? *Breast Care (Basel)* 2014; 9: 338-342. (PMID: 25759614) [\[Crossref\]](#)
20. Goulabchand R, Perrochia H, Aubert-Bringer E, Do Trinh P, Guilpain P. Idiopathic granulomatous mastitis responding to oral prednisone. *Breast J* 2020; 26: 281-283. (PMID: 31686425) [\[Crossref\]](#)
21. Boukaidi ML, Ghazli M, Bennani O, Hermas S, Soummani A, Bouhya S. et al. [Granulomatous recurrent mastitis during pregnancy.] *Gynecol Obstet Biol Reprod (Paris)* 2000; 29: 102-104. (PMID: 10675840) [\[Crossref\]](#)



Fibroepithelial Breast Tumors in a Teenager with Beckwith-Wiedemann Syndrome: A Case Report and Review of Literature

Ayşenur Oktay¹, Habib Ahmad Esmat², Özge Aslan¹

¹Department of Radiology, Ege University, İzmir, Turkey

²Department of Radiology, Kabul University of Medical Sciences, Kabul, Afghanistan

ABSTRACT

Beckwith-Wiedemann syndrome (BWS) is a human genomic imprinting disorder that presents with a wide spectrum of clinical features, including overgrowth, abdominal wall defects, macroglossia, neonatal hypoglycemia, and predisposition to embryonal tumors. Its diagnosis is based on molecular tests or clinical signs. However, in children with features of BWS who do not fulfill the clinical diagnostic criteria, the molecular tests may play an important role in the diagnosis. There is an increased risk of embryonal tumors in patients with BWS, but few case reports have been reported on benign breast tumors in female adolescents with this syndrome. To our knowledge, this is the first case report in the literature that describes the imaging findings of fibroepithelial breast tumors (phyllodes tumor and fibroadenomas) in a 13-year-old female with BWS, highlighting the need for lifelong tumor surveillance in this patient population.

Keywords: Beckwith-Wiedemann syndrome, tumorigenesis, fibroepithelial breast tumors

Cite this article as: Oktay A, Esmat HA, Aslan Ö. Fibroepithelial Breast Tumors in a Teenager with Beckwith-Wiedemann Syndrome: A Case Report and Review of Literature. Eur J Breast Health 2021; 17(3): 288-291

Key Points

- Benign breast tumors can accompany to Beckwith-Wiedemann syndrome (BWS).
- Fibroepithelial tumor of the breast is a spectrum of lesions ranging from fibroadenoma to malignant phyllodes tumor.
- Lifelong tumor surveillance in patients with fibroepithelial tumor of breast in BWS is recommended.

Introduction

Beckwith-Wiedemann syndrome (BWS) is a human genomic imprinting disorder that presents with a wide spectrum of clinical features, including overgrowth, abdominal wall defects, macroglossia, neonatal hypoglycemia, and predisposition to embryonal tumors (1). It is a panethnic syndrome with a 1:1 sex ratio and approximate incidence of one in 10,000–13,700 births. Such incidence may be underestimated in mild phenotypes and most likely increases due to a positive correlation with assisted reproductive techniques. This syndrome is caused by diverse genetic and epigenetic disorders that usually affect the regulation of genes imprinted on chromosome 11p15.5 (2). The relevant imprinted chromosomal region in 11p15.5 and uniparental disomy (UPD) of chromosome 11p15 is a risk factor for BWS-associated tumorigenicity. Chromosome 11p15.5 consists of imprinting domains of IGF2, the expression of which is associated with the tumorigenesis of various breast cancers (3). To date, there have been only a few reports on benign breast tumors in patients with BWS. Here, the authors present a case of fibroepithelial breast tumors (phyllodes tumor and fibroadenomas) in a 13-year-old female with a known history of BWS to increase awareness about this rare and unusual presentation.

Case Presentation

A 13-year-old female with a known history of BWS presented to our hospital with a right breast mass in 2016. On physical examination, there were a right-sided hemihypertrophy (Figure 1), which she had since birth, and a nontender palpable large mass on the left breast, mobile over the underlying tissues, with no lymph nodes enlargement detected. Other findings were unremarkable. On an ultrasound, a giant solid mass measuring 7 cm in diameter was observed in her right breast. The mass was surgically excised, and the pathology result showed a juvenile

fibroadenoma (Figure 2). In 2017, on a controlled ultrasound exam, no cystic or solid mass was detected in her breasts.

In 2018, on the breast ultrasound, it was found that she had multiple masses in the lower inner quadrant of the right breast (Figure 3). On magnetic resonance imaging images, multiple masses were observed in the lower quadrant of her right breast, with the largest one about 3 cm in diameter (Figure 4a and b). The fine needle biopsy and cytology result of this lesion showed a benign entity. As this patient had a high risk of tumorigenesis and childhood cancers, following a multidisciplinary consultation, complex literature review, and evaluation of risks and



Figure 1. Plain X-ray image of lower extremities showing a right femoral hemihypertrophy

R: Right

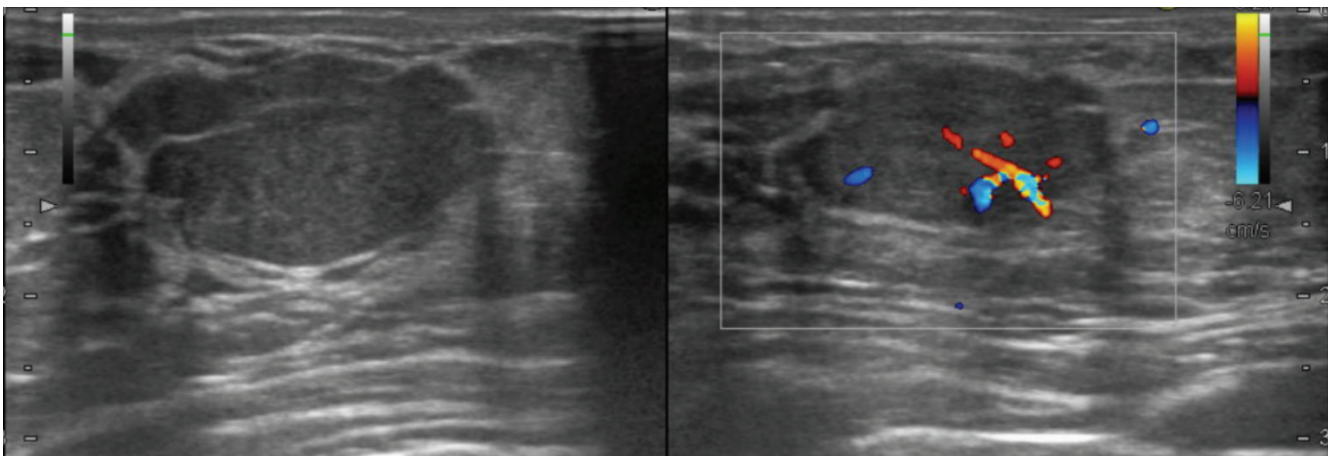


Figure 2. Ultrasound images of the right breast showing a well-defined, hypoechoic, lobulated mass with some vascularity, consisting of a fibroadenoma

benefits, a right breast lumpectomy was performed using a free nipple graft technique. The pathology examination of this lesion revealed a benign phyllodes tumor and fibroadenoma, but there were no signs of malignancy.

Discussion and Conclusion

BWS is the most common overgrowth syndrome. The condition was named after American pediatric pathologist John Bruce Beckwith in 1963, and German pediatrician Hans-Rudolf Wiedemann in 1964, reported the syndrome independently (4). This syndrome is caused by diverse genetic and epigenetic disorders that usually affect the regulation of genes imprinted on chromosome 11p15.5 (2). It presents with a wide and varied clinical spectrum, including hemihyperplasia, macroglossia, prominent eyes with infraorbital creases, facial nevus flammeus, and midfacial hypoplasia, but the BWS facies often normalizes across childhood. Hyperinsulinemia, hypoglycemia, abdominal wall defects, visceromegaly, fetal adrenocortical cytomegaly, and renal and cardiac malformations are the important signs of this syndrome (4, 5).

The diagnosis is based on molecular tests or clinical signs. However, in children with features of BWS who do not fulfill clinical diagnostic criteria, the molecular tests may play an important role in diagnosis (2, 5). Our patient had BWS with a positive family history and characteristic right hemihypertrophy.

There is an increased risk of embryonal tumors in BWS, but few case reports have been published on benign breast tumors in female adolescents with this syndrome. These tumors were often asymmetric, and the applied medical strategy was their surgical removal (6).

To our knowledge, this is the first case report in the literature to describe asymmetric fibroepithelial breast tumors (phyllodes tumor and fibroadenomas) in a teenager with BWS. Fibroepithelial tumor of the breast is a heterogeneous group of lesions ranging from fibroadenoma at the benign end of the spectrum to malignant phyllodes tumor. There are overlapping histologic features among various subtypes, and transformation and progression to a more malignant phenotype may also occur (7). Fibroadenomas and phyllodes tumors share many common features. However, phyllodes tumors tend to show a more rapid growth and tend to recur if incompletely excised. Moreover, borderline and malignant phyllodes tumors may metastasize. In

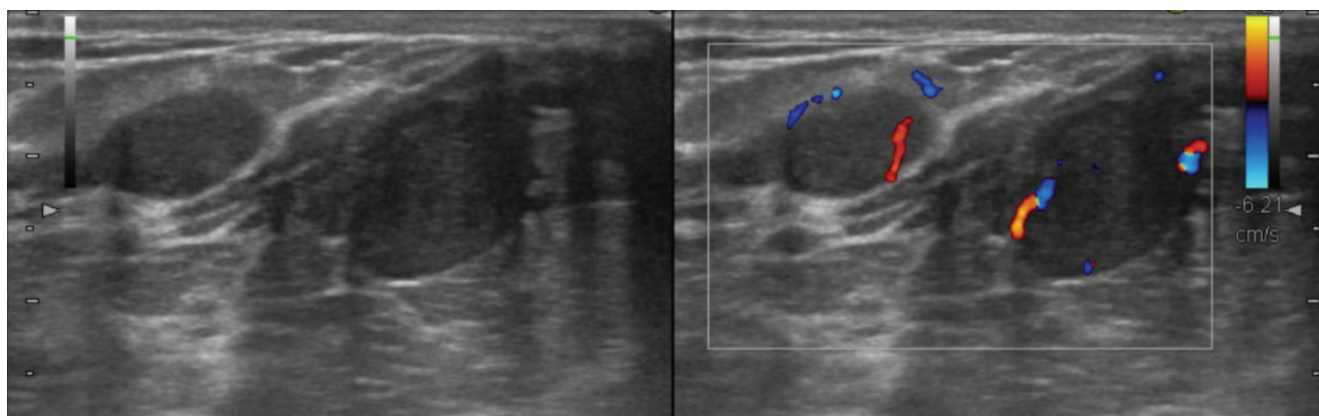


Figure 3. Ultrasound images of the right breast showing multiple well-defined, hypoechoic, lobulated masses with some vascularity, consisting of fibroepithelial breast tumors

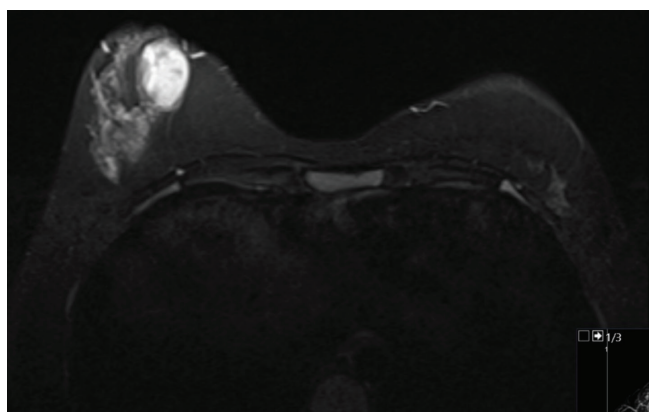


Figure 4a. Axial T2 weighted image demonstrates a high signal intensity mass with well-defined margins in the right breast

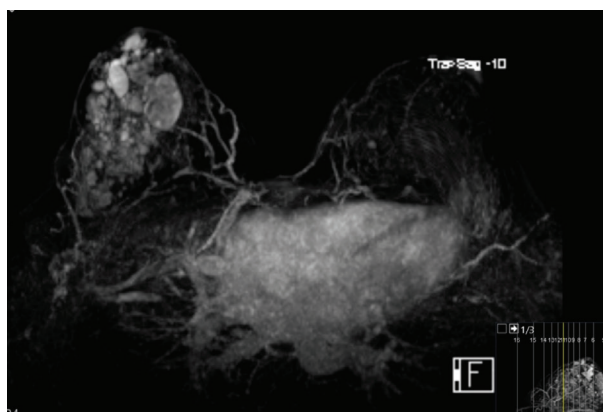


Figure 4b. 3D, maximum intensity projection (MIP), dynamic contrast-enhanced subtracted MRI image showing multiple, well-defined masses in the right breast

MRI: Magnetic resonance imaging

contrast, fibroadenomas usually need not be removed, and even when surgery is needed, enucleation is sufficient (8). In the patient described herein, a surgical reduction of giant breast lesion was performed using a free nipple graft technique, but the risk of recurrence may be the main lifelong concern Mishra et al. (9) in 2013. The relevant imprinted chromosomal region in 11p15.5 and UPD of chromosome 11p15 is a risk factor for BWS-associated tumorigenicity. Chromosome 11p15.5 consists of imprinting domains of IGF2, the expression of which is associated with the tumorigenesis of various breast cancers. However, it remains unclear whether BWS imposes an increased risk of breast lesions or a yet unknown molecular defect is responsible for the rare occurrence of this tumor in BWS (3-10).

This is the first case report in the literature to describe phyllodes tumor in a teenager with BWS. However, a wide range of both malignant and benign neoplasms has been reported in patients with BWS. This case report describes a case of fibroepithelial breast tumors (phyllodes tumor and fibroadenomas) in a 13-year-old female with BWS, highlighting the need for lifelong tumor surveillance in this patient population.

Informed Consent: Written informed consent was obtained from the patient's parents for publication of this case report.

Authorship Contributions

Conception: A.O.; Design: H.A.E.; Supervision: A.O.; Materials: Ö.A.; Data Collection and/or Processing: A.O., Ö.A.; Analysis and/or Interpretation: A.O.; Literature Search: Ö.A.; Writing: H.A.E.; Critical Review: A.O.

Conflict of Interest: The authors have no conflicts of interest to declare.

Financial Disclosure: The authors declare that this study received no financial support.

References

1. Wang KH, Kupa J, Duffy KA, Kalish JM. Diagnosis and Management of Beckwith-Wiedemann Syndrome. *Front Pediatr* 2020; 7: 562. (PMID: 32039119) [\[Crossref\]](#)
2. Cammarata-Scalisi F, Avendaño A, Stock F, Callea M, Sparago A, Riccio A. Beckwith-Wiedemann syndrome: clinical and etiopathogenic aspects of a model genomic imprinting entity. *Síndrome de Beckwith-Wiedemann: aspectos clínicos y etiopatogénicos de una entidad ejemplo de impronta genómica. Arch Argent Pediatr* 2018; 116: 368-373. (PMID: 30204990) [\[Crossref\]](#)
3. Takama Y, Kubota A, Nakayama M, Higashimoto K, Jozaki K, Soejima H. Fibroadenoma in Beckwith-Wiedemann syndrome with paternal uniparental disomy of chromosome 11p15.5. *Pediatr Int* 2014; 56: 931-934. (PMID: 25521982) [\[Crossref\]](#)

4. Borjas Mendoza PA, Mendez MD. Beckwith Wiedemann Syndrome. (Updated 2020 Oct 1). In: StatPearls (Internet). Treasure Island (FL): StatPearls Publishing; 2020 Jan. (PMID: 32644419)
5. Weksberg R, Shuman C, Beckwith JB. Beckwith-Wiedemann syndrome. *Eur J Hum Genet* 2010; 18: 8-14. (PMID: 19550435) [\[Crossref\]](#)
6. Szymańska E, Moszczyńska E, Polnik D, Szymańska S, Jurkiewicz E, Pylzak M, et al. Virginal breast hypertrophy in a patient with Beckwith-Wiedemann syndrome. *Clin Case Rep* 2018; 6: 484-489. (PMID: 29531723) [\[Crossref\]](#)
7. Yang X, Kandil D, Cosar EF, Khan A. Fibroepithelial tumors of the breast: pathologic and immunohistochemical features and molecular mechanisms. *Arch Pathol Lab Med* 2014; 138: 25-36. (PMID: 24377809) [\[Crossref\]](#)
8. Wiratkapun C, Piyapan P, Lertsithichai P, Larbcharoensub N. Fibroadenoma versus phyllodes tumor: distinguishing factors in patients diagnosed with fibroepithelial lesions after a core needle biopsy. *Diagn Interv Radiol* 2014; 20: 27-33. (PMID: 24356293) [\[Crossref\]](#)
9. Mishra SP, Tiwary SK, Mishra M, Khanna AK. Phyllodes tumor of breast: a review article. *ISRN Surg*. 2013; 2013: 361469. doi:10.1155/2013/361469 (PMID: 23577269) [\[Crossref\]](#)
10. Cappuccio G, De Crescenzo A, Ciancia G, Canta L, Moio M, Mataro I, et al. Giant breast tumors in a patient with Beckwith-Wiedemann syndrome. *Am J Med Genet A* 2014; 164A: 182-185. (PMID: 24214456) [\[Crossref\]](#)



Breast Recurrence of Acute Myeloid Leukemia After Bone Marrow Transplantation: A Case Report About Myeloid Sarcoma of the Breast

Ecenur Varol¹, Umay Kiraz², Sertaç Ata Güler¹, Çiğdem Vural², Zafer Gülbaş³, Nihat Zafer Utkan¹

¹Department of General Surgery, Kocaeli University School of Medicine, Kocaeli, Turkey

²Department of Pathology, Kocaeli University School of Medicine, Kocaeli, Turkey

³Department of Bone Marrow Transplantation, Anadolu Medical Center Hospital, Kocaeli, Turkey

ABSTRACT

Myeloid sarcoma of the breast is a rare malignancy, can be seen after bone marrow transplantation. Although there are no specific features for this malignancy which is difficult to diagnose, some common features draw attention in the published case reports. Since there is no consensus on the treatment of myeloid sarcoma of the breast, we aimed to explain our own diagnosis and treatment methods in this case report.

Keywords: Breast, myeloid sarcoma, breast sarcoma, bone marrow transplantation

Cite this article as: Varol E, Kiraz U, Güler SA, Vural Ç, Gülbaş Z, Utkan NZ. Breast Recurrence of Acute Myeloid Leukemia After Bone Marrow Transplantation: A Case Report About Myeloid Sarcoma of the Breast. Eur J Breast Health 2021; 17(3): 292-295

Key Points

- Myeloid sarcoma (MS) is an aggressive tumor.
- Breast tissue is a rare region for MS development.
- The development of MS of the breast tissue after bone marrow transplantation (BMT) in patients with acute myeloid leukemia (AML) is remarkable.
- If a breast mass is detected, the diagnosis should be supported by immunohistochemistry and biopsy.
- Systemic treatment should be started as soon as possible.

Introduction

Myeloid sarcoma (MS) is an aggressive tumor characterized by leukemic proliferation with or without mature myeloid cells, which can be seen anywhere in the body except bone marrow (1). MS is a hematological malignancy, rarely encountered as a soft tissue mass in the extramedullary system called granulocytic sarcoma or chloroma (2-4). Although MS can develop in any part of the body, it is frequently seen in bone, lymph nodes, soft tissue, and skin (1, 5). Breast tissue is a rare region for MS development, and only 3% of cases with MS in breast tissue were reported in the Mayo Clinic series (6, 7). The development of MS of the breast tissue after bone marrow transplantation (BMT) in patients with acute myeloid leukemia (AML) is remarkable (8).

Case Presentation

A 31-year-old female presented to the General Surgery Department Breast and Endocrine Unit with the complaint of a palpable mass in both breasts. Seventeen years ago, the patient underwent surgery and chemotherapy due to osteosarcoma in the left ankle. Six years ago, she underwent a bilateral breast fibroadenoma excision, and four years ago, she underwent an excision due to phyllodes tumor in the right breast. Four years ago, bone marrow biopsy, peripheral smears, and hematological tests during postoperative controls were performed and they showed abnormal findings. After she was diagnosed with AML, BMT was performed. One month ago, she had a total thyroidectomy due to a malignant tumor in the left thyroid lobe. She experienced a postoperative pathology of papillary thyroid carcinoma with AML infiltration and follicular variant. During that period, she had masses in both breasts. On physical examination, 4–5 cm masses were palpated on the bilateral breasts. On the recent breast ultrasonography (USG), it was observed that the patient had masses in the lower outer quadrant of the right breast, whose borders were

ambiguous. A 2.5 cm residual phyllodes tumor with a heterogeneous structure and an approximately 1 cm fibroadenoma with a slightly faint border at 3 o'clock were noted in the left breast. In the same period, fluorodeoxyglucose-18 (FDG-18) [FDG- positron emission tomography/computed tomography (PET)/CT] imaging showed that the mass in the right breast maximum standardized uptake values [(SUV_{max}) = 3.9] had activity involvement. There were no other positive findings in the PET/CT scan of the patient. Since the patient had a systemic disease, PET/CT imaging was performed after breast USG. This does not normally fit the breast imaging sequence and it is an exception for this patient. Due to the coronavirus disease 2019 (COVID-19) pandemic, there was a disruption in the follow-up. The control PET/CT imaging was performed after six months showing massive lesions of 4 cm in the right breast and 5 cm and 1.5 cm in the left breast (SUV_{max} = 9) and a 1 cm (SUV_{max} = 3.7) increase in the metabolism areas in both axilla (Figure 1). It was decided to perform a breast and axilla Tru-Cut biopsy. The results of the biopsies were interpreted MS containing diffuse blastic cell infiltration. Microscopic images of diffuse blastic cell infiltration in breast tissue with haematoxylin and eosin stain (H&E) are shown in Figure 2. When the blastic cells were examined immunohistochemically, they showed diffuse strong cytoplasmic staining with cluster of differentiation-45 (CD45), CD34, CD117, and human leukocyte antigen-DR (HLA-

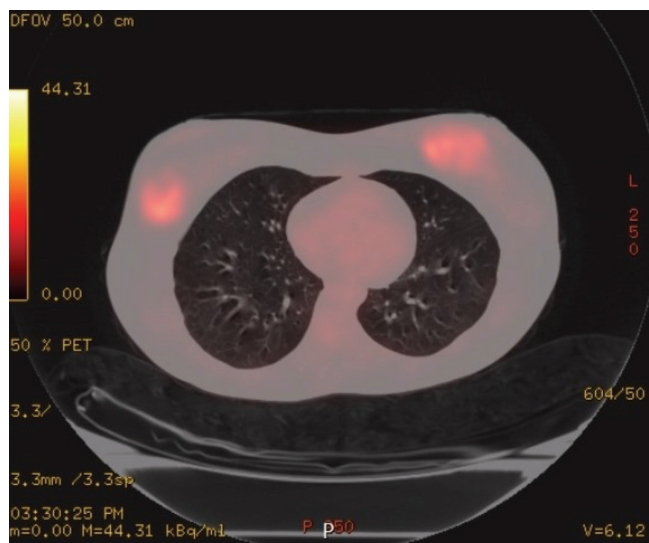


Figure 1. Axial paranchimal fused PET/CT image showing massive lesions of 4 cm in the right breast and 5 cm and 1.5 cm in the left breast (SUV_{max} = 9) and 1 cm (SUV_{max} = 3.7) increase in metabolism areas in both axilla

PET/CT: Positron emission tomography/computed tomography

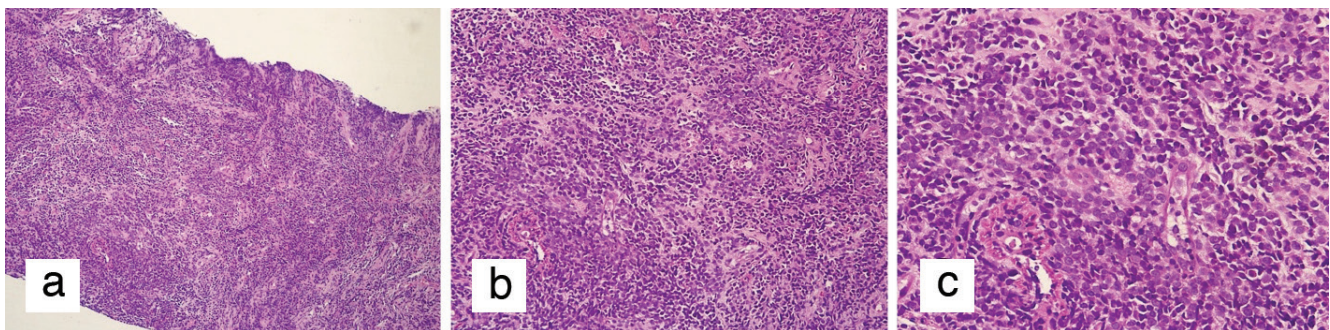


Figure 2. Microscopic images of diffuse blastic cell infiltration in breast tissue with haematoxylin and eosin stain (H&E). **a)** Diffuse blastic cell infiltration in breast tissue (H&E x100). **b)** Diffuse blastic cell infiltration in breast tissue (H&E x200). **c)** Diffuse blastic cell infiltration in breast tissue (H&E x400)

DR) and focal strong cytoplasmic staining with myeloperoxidase (MPO). Immunohistochemical staining images of breast tissue showing blast cells positive for CD45, CD34, CD117, HLA-DR, and MPO are shown in Figure 3.

The patient was evaluated in the oncology council. Due to the aggressive spread, a BMT and systemic chemotherapy were planned. The mass in the patient's breast did not need a palliative resection. The patient was followed up after the planned therapies.

Discussion and Conclusion

Although MS is an extramedullary hematological malignancy, in which myeloid cells show various degrees of maturation, it is frequently seen in patients with previously diagnosed myeloid leukemia (9, 10). According to the World Health Organization, MS is diagnosed based on three classes: blastic (consisting of myeloblasts), immature (consisting of myeloblasts and promyelocytes), and differentiated (consisting of promyelocytes and more mature neutrophils) (8). Although MS can develop in any part of the body, the development of MS of the breast is extremely rare. For this reason, patients with MS in the breast are often misdiagnosed as having lobular breast carcinoma, non-Hodgkin lymphoma, or small-round-blue-cell tumor (11). The first area where extramedullary relapse occurs after stem cell transplantation is the breast, and relapse can occur 2–73 months after transplantation (average 17 months) (8). MS may occur as a unilateral or bilateral breast mass, but it usually does not cause nipple retraction (2, 12–14). Although there was no specific finding of MS in the breast when examining the studies, case reports emphasize the findings of irregular, spiculated, angular or unclear margins, and posterior shadowing (7, 15). MS diagnosis can be supported by MPO, CD34, CD 43, CD 117, and CD 68 (12). Specific CD markers can be very useful in diagnosis. CD 117, CD 68, and CD 43 are positive in most cases, and CD 45 is reactive in 75% of the cases (12).

There is no consensus on the treatment of MS of the breast, but surgical resection (lumpectomy or mastectomy) with systemic chemotherapy is generally recommended (7, 8). Simultaneous radiotherapy is controversial (8). Disease-free survival is predicted between three and twelve years with systemic chemotherapy (8). In light of the literature, the diagnosis was supported by MPO, CD 34, and CD 117 staining in our patient, who developed bilateral breast MS four years after BMT for AML treatment. Considering the patient's diagnosis of MS in both breasts and the inclusion of AML infiltration of the cancerous tissue in the thyroidectomy material, it was decided that the patient undergoes BMT and receive systemic treatment again. Moreover, systemic chemotherapy was planned after the transplantation.

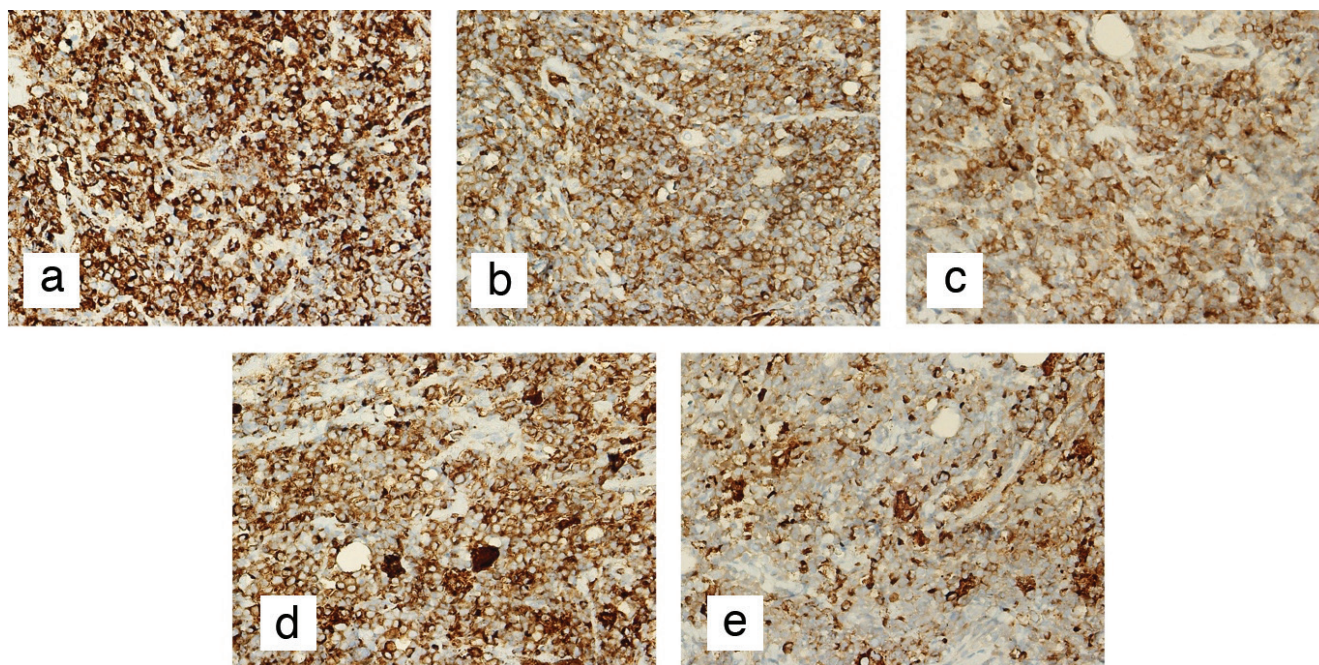


Figure 3. Immunohistochemical staining images of breast tissue. **a)** Immunohistochemical staining of blast cells showing diffuse strong cytoplasmic positivity for CD45 (CD45 x400). **b)** Immunohistochemical staining of blast cells showing diffuse strong cytoplasmic positivity for CD34 (CD34 x400). **c)** Immunohistochemical staining of blast cells showing diffuse strong cytoplasmic positivity for CD117 (CD117 x400). **d)** Immunohistochemical staining of blast cells showing diffuse strong cytoplasmic positivity for HLA-DR (HLA-DR x400). **e)** Immunohistochemical staining of blast cells showing focal strong cytoplasmic positivity for MPO (MPO x400)

CD: Cluster of differentiation; HLA-DR: Human leukocyte antigen-DR isotype; MPO: Myeloperoxidase

In this case report, we described the management of a patient with MS of the breast, which is a rare tumor. It should be kept in mind that MS may develop in the breast after BMT in patients with AML and those patients should be followed up using breast ultrasound. If a mass is detected, the diagnosis should be supported by immunohistochemistry and biopsy, and systemic treatment should be started as soon as possible.

Informed Consent: Written informed consent was obtained from the patient before participation in this study.

Peer-review: Externally peer-reviewed.

Author Contributions

Conception: E.V.; Design: E.V.; Supervision: S.A.G., N.Z.U.; Materials: U.K., Ç.V., Z.G., N.Z.U.; Data Collection and/or Processing: U.K., Ç.V., Z.G.; Analysis and/or Interpretation: E.V., S.A.G, N.Z.U.; Literature Search: E.V.; Writing: E.V.; Critical Review: S.A.G.

Conflict of Interest: The authors have no conflicts of interest to declare.

Financial Disclosure: The authors declare that this study received no financial support.

References

- Pileri SA, Ascani S, Cox MC, Campidelli C, Bacci F, Piccioli M, et al. Myeloid sarcoma: clinicopathologic, phenotypic and cytogenetic analysis of 92 adult patients. *Leukemia* 2007; 21: 340-350. (PMID: 17170724) [\[Crossref\]](#)
- Valbuena JR, Admirand JH, Gualco G, Medeiros LJ. Myeloid Sarcoma Involving the Breast. *Arch Pathol Lab Med* 2005; 129: 32-38. (PMID: 15628906) [\[Crossref\]](#)
- Roth MJ, Medeiros LJ, Elenitoba-Johnson K, Kuchnio M, Jaffe ES, Stetler-Stevenson M. Extramedullary myeloid cell tumors. An immunohistochemical study of 29 cases using routinely fixed and processed paraffin-embedded tissue sections. *Arch Pathol Lab Med* 1995; 119: 790-798. (PMID: 7668936) [\[Crossref\]](#)
- Avni B, Koren-Michowitz M. Myeloid sarcoma: current approach and therapeutic options. *Ther Adv Hematol* 2011; 2: 309-316. (PMID: 23556098) [\[Crossref\]](#)
- Vardiman JW. The World Health Organization (WHO) classification of tumors of the hematopoietic and lymphoid tissues: an overview with emphasis on the myeloid neoplasms. *Chem Biol Interact* 2010; 184: 16-20. (PMID: 19857474) [\[Crossref\]](#)
- Bubulac L, Bardaş A, Popa DC, Vasilache ED, Ionescu BO, Coriu D, et al. Breast myeloid sarcoma after allogeneic stem cell transplantation for acute myelomonocytic leukemia - case report. *Rom J Morphol Embryol* 2019; 60: 707-711. (PMID: 31658348) [\[Crossref\]](#)
- Zhai J, Kong X, Yang X, Gao J, Xuan L, Wang X, et al. An uncommon granulocytic sarcoma of the breast: a case report and literature review. *Onco Targets Ther* 2018; 11: 3685-3690. (PMID: 29983576) [\[Crossref\]](#)
- Toumeh A, Phinney R, Kobalka P, Mohamed I. Bilateral myeloid sarcoma of the breast and cerebrospinal fluid as a relapse of acute myeloid leukemia after stem-cell transplantation: A case report. *J Clin Oncol* 2012; 30: e199-e201. doi: 10.1200/JCO.2011.40.2255 (PMID: 22734027) [\[Crossref\]](#)
- Stewart RL, Dell CM, Samayoa L. Myeloid sarcoma of the breast misdiagnosed as poorly differentiated mammary carcinoma with lobular features. *Breast J* 2015; 21: 192-193. (PMID: 25583284) [\[Crossref\]](#)
- Ozsoy A, Akdal Dolek B, Barca N, Aktas H, Araz L, Kulacoglu S. Ultrasound findings in a case of myeloid sarcoma of the breast. *J Belg Soc Radiol* 2016; 100: 15. (PMID: 30151441) [\[Crossref\]](#)

11. Goma W, Ghanim A, Emam E, Bayoumi K, Ghanim A. Primary myeloid sarcoma of the breast: a case report and review of literature. *J Microsc Ultrastruct* 2018; 6: 212-214. (PMID: 30464895) [[Crossref](#)]
12. Wu HY, Liu L, Gu L, Luo YH. Clinical characteristics and management of primary granulocytic sarcoma of the breast: A case report. *Medicine (Baltimore)* 2019; 98: e16648. doi: 10.1097/MD.00000000000016648 (PMID: 31464900) [[Crossref](#)]
13. Cunningham I. A clinical review of breast involvement in acute leukemia. *Leuk Lymphoma*. 2006; 47: 2517-2526. (PMID: 17169796) [[Crossref](#)]
14. Thachil J, Richards RM, Copeland G. Granulocytic sarcoma—a rare presentation of a breast lump. *Ann R Coll Surg Engl* 2007; 89: W7-W9. doi: 10.1308/147870807X227827 (PMID: 17958995) [[Crossref](#)]
15. Kinoshita T, Yokokawa M, Yashiro N. Multicentric granulocytic sarcoma of the breast: mammographic, sonographic, and MR findings of granulocytic sarcoma of the breasts. *Clin Imaging* 2006; 30: 271-274. (PMID: 16814144) [[Crossref](#)]



In the article by Mathelin et al., entitled “**Breast Cancer Management During the COVID-19 Pandemic: The Senologic International Society Survey**” (Eur J Breast Health 2021; 17: 188-196. DOI: 10.4274/ejbh.galenos.2021.2021-1-4) that was published in the 2021/2 (April) issue of European Journal of Breast Health, the surname of the thirty fourth author had mistyped. Upon the written request from the authors, the correction was implemented.

Mathelin C, Ame S, Anyanwu S, Avisar E, Boubnider WM, Breitling K, Anie HA, Conceição JC, Dupont V, Elder E, Elfgen C, Elonge T, Iglesias E, Imoto S, Ioannidou-Mouzaka L, Kappos EA, Kaufmann M, Knauer M, Luzuy F, Margaritoni M, Mbodj M, Munding A, Orda R, Ostapenko V, Özbaş S, Özmen V, Pagani O, Pieńkowski T, Schneebaum S, Shmalts E, Selim A, Pavel Z, Lodi M, Maghales-Costa M. Breast Cancer Management During the COVID-19 Pandemic: The Senologic International Society Survey. Eur J Breast Health 2021; 17(2): 188-196

The aforementioned manuscript can be accessed through the following link:

10.4274/ejbh.galenos.2021.2021-1-4

The error and the correction in the article have been demonstrated in the following list:

Error

Carole Mathelin^{1,2}, Shanti Ame¹, Stanley Anyanwu³, Eli Avisar⁴, Wahib Mohcen Boubnider⁵, Katrin Breitling⁶, Hannah Ayettey Anie⁷, José Carlos Conceição⁸, Veronique Dupont⁹, Elisabeth Elder¹⁰, Constanze Elfgen¹¹, Tony Elonge¹², Edelmiro Iglesias¹³, Shigeru Imoto¹⁴, Lydia Ioannidou-Mouzaka¹⁵, Elisabeth A Kappos¹⁶, Martin Kaufmann¹⁷, Michael Knauer¹⁸, Franck Luzuy¹⁹, Marko Margaritoni²⁰, Mamadou Mbodj²¹, Alexander Munding²², Ruben Orda²³, Valerijus Ostapenko²⁴, Serdar Özbaş²⁵, Vahit Özmen²⁶, Olivia Pagani²⁷, Tadeusz Pieńkowski²⁸, Schlomo Schneebaum²⁹, Ekaterina Shmalts³⁰, Ashraf Selim³¹, Zotov Pavel³², Massimo Lodi¹, Maurício Maghales-Costa³³

Correction

Carole Mathelin^{1,2}, Shanti Ame¹, Stanley Anyanwu³, Eli Avisar⁴, Wahib Mohcen Boubnider⁵, Katrin Breitling⁶, Hannah Ayettey Anie⁷, José Carlos Conceição⁸, Veronique Dupont⁹, Elisabeth Elder¹⁰, Constanze Elfgen¹¹, Tony Elonge¹², Edelmiro Iglesias¹³, Shigeru Imoto¹⁴, Lydia Ioannidou-Mouzaka¹⁵, Elisabeth A Kappos¹⁶, Martin Kaufmann¹⁷, Michael Knauer¹⁸, Franck Luzuy¹⁹, Marko Margaritoni²⁰, Mamadou Mbodj²¹, Alexander Munding²², Ruben Orda²³, Valerijus Ostapenko²⁴, Serdar Özbaş²⁵, Vahit Özmen²⁶, Olivia Pagani²⁷, Tadeusz Pieńkowski²⁸, Schlomo Schneebaum²⁹, Ekaterina Shmalts³⁰, Ashraf Selim³¹, Zotov Pavel³², Massimo Lodi¹, Maurício Magalhaes Costa³³

Error

Cite this article as: Mathelin C, Ame S, Anyanwu S, Avisar E, Boubnider WM, Breitling K, Anie HA, Conceição JC, Dupont V, Elder E, Elfgen C, Elonge T, Iglesias E, Imoto S, Ioannidou-Mouzaka L, Kappos EA, Kaufmann M, Knauer M, Luzuy F, Margaritoni M, Mbodj M, Munding A, Orda R, Ostapenko V, Özbaş S, Özmen V, Pagani O, Pieńkowski T, Schneebaum S, Shmalts E, Selim A, Pavel Z, Lodi M, Maghales-Costa M. Breast Cancer Management During the COVID-19 Pandemic: The Senologic International Society Survey. Eur J Breast Health 2021; 17(2): 188-196

Correction

Cite this article as: Mathelin C, Ame S, Anyanwu S, Avisar E, Boubnider WM, Breitling K, Anie HA, Conceição JC, Dupont V, Elder E, Elfgen C, Elonge T, Iglesias E, Imoto S, Ioannidou-Mouzaka L, Kappos EA, Kaufmann M, Knauer M, Luzuy F, Margaritoni M, Mbodj M, Munding A, Orda R, Ostapenko V, Özbaş S, Özmen V, Pagani O, Pieńkowski T, Schneebaum S, Shmalts E, Selim A, Pavel Z, Lodi M, Costa MM. Breast Cancer Management During the COVID-19 Pandemic: The Senologic International Society Survey. Eur J Breast Health 2021; 17(2): 188-196